INACTIVATION OF HEPATITIS B VIRUS CCCDNA USING ENGINEERED TRANSCRIPTION ACTIVATOR-LIKE EFFECTOR NUCLEASES

Kristie Michelle Bloom

A thesis submitted to the Faculty of Health Science, University of the Witwatersrand, Johannesburg, in fulfilment of the requirements for the degree of Doctor of Philosophy in Molecular Medicine.

Johannesburg, 2013

DECLARATION

I declare that this thesis is my own, unaided work. It is being submitted for the Degree of Doctor of Philosophy in the University of the Witwatersrand, Johannesburg. It has not been submitted before for any degree or examination in any other University.

_____

Kristie Michelle Bloom

_____ day of _____ 2013

PUBLICATIONS AND PRESENTATIONS

Publications:

KRISTIE BLOOM, ABDULLAH ELY , CLAUDIO MUSSOLINO , TONI CATHOMEN, PATRICK ARBUTHNOT. **Inactivation of hepatitis B virus replication in cultured cells and in vivo with engineered TALENs**. (accepted for publication in Molecular Therapy)

MUSA MARIMANI, JUSTIN HEAN, KRISTIE BLOOM, ABDULLAH ELY AND PATRICK ARBUTHNOT. **Recent advances in developing nucleic acid based hepatitis B virus therapy.** (Invited review)

JUSTIN HEAN, CAROL CROWTHER, ABDULLAH ELY, RAFIQUE UL ISLAM, SAMANTHA BARICHIEVY, KRISTIE BLOOM, MARC S. WEINBERG, WILLEM A.L. VAN OTTERLO, CHARLES B. DE KONING, FELIX SALAZAR, PATRICIA MARION, ERIC B. ROESCH, MARC LEMAITRE, PIET HERDEWIJN AND PATRICK ARBUTHNOT. **Inhibition of hepatitis B virus replication in vivo using lipoplexes containing altritol-modified antiviral siRNAs (2010),** *Artificial DNA: PNA & XNA*; [Published by Landes Bioscience], Volume 1, Issue 1, Pages 1-10. Published online ahead of print: http://www.landesbioscience.com/journals/artificialdna/article/HeanADNA1-1.pdf

VICTORIA DYER, ABDULLAH ELY, KRISTIE BLOOM, MARC WEINBERG AND PATRICK ARBUTHNOT. **tRNA^{Lys3} promoter cassettes that efficiently express RNAi-activating**

antihepatitis B virus short hairpin RNAs (2010), *Biochemical and Biophysical Research Communications* [Published by Academic Press], Volume 398, Issue 4, Pages 640-646

SAKET CHATTOPADHYAY, ABDULLAH ELY, KRISTIE BLOOM, MARC S. WEINBERG AND PATRICK ARBUTHNOT. **Inhibition of hepatitis B virus replication with linear DNA sequences expressing antiviral micro-RNA shuttles (2009),** *Biochemical and Biophysical Research Communications* [Published by Academic Press], Volume 389, Issue 3, Pages 484-489. doi:10.1016/j.bbrc.2009.09.004

Presentations:

XIX. Annual Meeting of the German Society for Gene Therapy. Feb 28 February – 02 March 2013, Universitätsklinikum, Hamburg-Eppendorf, Germany *[INVITED LECTURE: Kristie Bloom, Abdullah Ely, Claudio Mussolino, Toni Cathomen, Patrick Arbuthnot.* Using engineered TALE nucleases and repressor TALEs to achieve effective inactivation of hepatitis B virus replication in vivo *(INV17)]*

The European Society of Gene and Cell Therapy (ESGCT) and French Society of Gene and Cell Therapy Collaborative Congress. 25 - 29 October 2012, Palais des Congrès de Versailles, Versailles, France. *[ORAL PRESENTATION: Kristie Bloom, Abdullah Ely, Claudio Mussolino, Toni Cathomen, Patrick Arbuthnot. Transcription Activator-like Effector Nucleases (TALENs) for targeted inactivation of Hepatitis B virus cccDNA (O86)]*

Wits Faculty of Health Sciences Research Day and Postgraduate Expo. 19 September 2012, University of the Witwatersrand, Parktown, Johannesburg, South Africa. *[ORAL PRESENTATION: Kristie Bloom, Abdullah Ely, Patrick Arbuthnot. Targeted inactivation of Hepatitis B virus with designer nucleases (ID-O-9)]*

South African Society of Biochemistry and Molecular Biology (SASBMB). 30 September – 1 February 2012, Champagne Sports Resort, Drakensburg, South Africa. *[POSTER PRESENTATION: Kristie Bloom, Abdullah Ely, Patrick Arbuthnot. Engineering zinc finger nucleases to disable cccDNA produced during chronic Hepatitis B virus infection]*

The European Society of Gene and Cell Therapy (ESGCT) and British Society of Gene Therapy (BSGT) Collaborative Congress. 27 - 31 October 2011, Brighton Convention Centre, Brighton, United Kingdom. *[POSTER PRESENTATION: Kristie Bloom, Patrick Arbuthnot. Targeted inactivation of Hepatitis B virus cccDNA using engineered Zinc Finger Nucleases (P60)]*

University of the Witwatersrand 3rd Postgraduate cross-faculty symposium. 25 – 29 October 2010. University of the Witwatersrand, Senate House, Johannesburg. *[ORAL PRESENTATION: Kristie Bloom, Abdullah Ely, Marc Weinberg, Patrick Arbuthnot. The design and application of a real time PCR assay to assess rcDNA and cccDNA produced by HBV during infection]*

South African Society of Biochemistry and Molecular Biology (SASBMB). 18 – 20 January 2010, Ilanga Estate, Bloemfontein, South Africa. *[POSTER PRESENTATION: Kristie*

Bloom, Abdullah Ely, Marc Weinberg, Patrick Arbuthnot. The design and application of a real time PCR assay to assess rcDNA and cccDNA produced by HBV during infection)]

Wits Faculty of Health Sciences Research Day and Postgraduate Expo. 20 August 2008, University of the Witwatersrand, Parktown, Johannesburg, South Africa. *[POSTER PRESENTATION: Kristie Bloom, Abdullah Ely, Marc Weinberg, Patrick Arbuthnot. The design and application of a real time PCR assay to assess rcDNA and cccDNA produced by HBV during infection (ID-P-21)]*

ABSTRACT

Hepatitis B virus (HBV) is a major global public health burden, with over 350 million people chronically infected. This results in approximately 600,000 liver cancer-related deaths annually. Chronic HBV infections are normally managed with long-term anti-HBV therapeutics, such as reverse transcription inhibitors, which target post-transcriptional viral processes without affecting the cccDNA. Treatment failure however is largely as a result of the stability of this episomal viral DNA. The cccDNA minichromosome serves as a reservoir of HBV DNA and is capable of re-establishing viral replication following withdrawal of treatment. Designer nucleases, like transcription activator-like effector nucleases (TALENs), have recently been used to create double stranded breaks (DSBs) at target-specific endogenous DNA loci. These nucleases are designed as pairs, which upon dimerisation cleave double-stranded DNA. Subsequent activation of the cellular non-homologous end-joining (NHEJ) pathway often results in targeted mutagenesis at the DSB site. As TALENs may be designed to bind to any DNA sequence, they are commonly used as genetic engineering agents. Inactivation of HBV cccDNA, using these engineered TALENs, presents a unique approach to disabling viral replication permanently. To investigate this, a panel of TALENs targeting the *core* (C), *surface* (S) and two different *polymerase* (P1 and P2) regions of HBV cccDNA were generated using a Golden gate modular assembly approach. TALENs were initially tested in two liver-derived cell lines. Firstly as transient co-transfections in Huh7 cells using a HBV replication competent plasmid, followed by long term investigations in HepG2.2.15 cells which model HBV replication *in vitro*. Inactivation of HBV was determined by measuring markers of viral replication, whilst TALEN-mediated targeted disruption was verified by T7 endonuclease 1 (T7E1) or CELI endonuclease assays

and sequencing. *In vitro*, the S TALEN inhibited HBsAg secretion by 80% in Huh7 cells and 60% in HepG2.2.15 cells. Furthermore, S TALEN-mediated targeted disruption occurred in 35-47% of cccDNA copies, whilst the C TALEN resulted in 11% targeted disruption of cccDNA in without inhibition of HBsAg expression. The P2 TALEN showed no anti-HBV efficacy, however the P1 TALEN inhibited HBsAg expression by up to 60% without any evidence of site-directed cleavage. As this TALEN binding site spans the HBV Enhancer I sequence, knock-down of HBsAg expression is most likely to occur as a result of transient transcriptional repression. To confirm whether permanent repression of HBV transcription could be achieved, a KRAB-based transcription activator-like repressor (rTALE) targeting the HBV pre-S2 promoter was generated. Using an *in vitro* reporter gene assay, the pre-S2 rTALE inhibited luciferase expression by up to 90%. However this was only achieved using high molar concentrations of the repressor, suggesting multiple rTALEs may improve HBV transcriptional repression. As the S and C TALENs displayed significant anti-HBV efficiency *in vitro*, they were tested in a murine hydrodynamic injection model of HBV replication. *In vivo*, the S TALEN inhibited HBsAg secretion by 95% and induced disruption in 77–87% of HBV DNA targets. In addition the C TALEN inhibited HBcAg expression and induced disruption in 78-93% of HBV DNA targets. Additionally, serological analysis showed a reduction in circulating virions and no apparent liver toxicity, as determined by real-time PCR (qPCR) and aspartate transaminase (AST)/ alanine aminotransferase (ALT) liver function tests respectively. Deep sequencing at the S and C TALEN binding sites showed targeted mutagenesis of HBV DNA in samples extracted from murine hepatocytes transfected with TALENs, however wild-type sequences were exclusively detected in mice that had not been treated with anti-HBV TALENs. Furthermore, frameshift deletions were predominantly detected indicating major disruptions in the HBV *surface* and *core* sequences. These results indicate that TALENs designed to disable and silence HBV cccDNA

are effective both *in vitro* and *in vivo* and as such provide a promising therapeutic approach to treat this serious infection.

AKNOWLEDGEMENTS

1. I would like to sincerely thank my supervisors, Prof. P Arbuthnot and Dr A Ely, for all their support, assistance and encouragement throughout my post-graduate studies.

2. I would like to thank Professor Toni Cathomen and Dr Claudio Mussolino for hosting me at the Institute of Experimental Haematology (Medizinischen Hochschule Hannover (MHH) in Germany) and providing all the necessary components for the generation of the anti-HBV TALENs.

3. Moreover, I would like to thank the following individuals for providing reagents or plasmids used during my PhD: Dr W Prinz (CelI single stranded nuclease); Dr M Nassal (pCH 9/3091), Dr H Nakabayashi (Huh7 cell line), Dr D. Kremsdorf (HepG2.2.15 cell line).

4. I would like to thank the following organisations for their financial assistance during my degree: The University of the Witwatersrand (Merit Award), The Poliomyelitis Research Foundation (PRF), Deutscher Akademischer Austausch Dienst (DAAD), The National Research Foundation (NRF), and The Stella and Paul Lowenstein Charitable and Educational Trust.

5. Finally I would like to thank my family, Juan, Martin, Denise and Michelle for their endless love and support.

TABLE OF CONTENTS

LIST OF FIGURES

LIST OF TABLES

LIST OF ABBREVIATIONS

5mC – 5-methylated cytosine

A1AT - alpha-1-antitrypsin

AAV - adeno-associated virus

AIDS - acquired immunodeficiency syndrome

ALT - Alanine aminotransferase

AP1 - activator protein 1

ATF/CREB - activating transcription factor/cAMP response element binding protein

BCP - basic core promoter

BLAST - basic local alignment search tool

bp - base pair

Cas9 - CRISPR-associated protein 9

CBF - CCAAT binding factor.

cccDNA - covalently closed circular DNA

C/EBP - CCAAT-enhancer-binding protein

CMV - Cytomegalovirus

CRE - cAMP response element

CRISPR - clustered regulatory interspaced short palindromic repeats

C TALEN - core TALEN

DAB - 3 3'-diaminobenzidine

ddH_2O - double distilled water

DHBV - Duck hepatitis B virus

DMEM - Dulbecco's Modified Eagle Medium

DNA - Deoxyribonucleic Acid

DMSO - dimethyl sulfoxide

dNTP - Deoxynucleotide triphosphate

DR1 - Direct Repeat 1

DR2 - Direct Repeat 2

DSB - double stranded break

dsDNA - double stranded DNA

dTALE - designer TALE

E. coli - Escherichia coli

ELISA - Enzyme-linked immunosorbant assay

ESC - embryonic stem cell

FCS - Foetal calf serum

FLASH - fast ligation based automatable solid-phase high-throughput

Fluc - Firefly luciferase

fmol - femtomole

GFP - green fluorescent protein

H&E - haematoxylin and eosin

HA - haemagglutinin epitope

HBV - Hepatitis B virus

HBcAg - Hepatitis B core antigen

HBeAg - Hepatitis B e antigen

HBIG - hepatitis B immune globulin

HBsAg - Hepatitis B surface antigen

HBx - Hepatitis B virus X protein

HCC - Hepatocellular carcinoma

HDI - hydrodynamic injection

HDR - homology directed repair

HIV - Human immunodeficiency virus

HNF-1 - hepatocyte nuclear factor 1

HNF-3 - hepatocyte nuclear factor 3

HNF-4 - hepatocyte nuclear factor 4

HR - homologous recombination

HSV - herpes simplex virus

ICA - iterative capped assembly

INFα - interferon alpha

iPSC - induced pluripotent stem cell

kb - kilobase

KRAB - Krüppel associated box

LIC - ligation-independent cloning

mGAPDH - Murine Glyceraldehyde-3-phosphate dehydrogenase

MID - multiplex identifier

miRNA - micro RNA

ml - millilitre

MMEJ - microhomology-mediated end joining

mRNA - Messenger RNA

MTT - 3-(4,5-Dimethylthiazol-2-yl)-2,5-diphenyl tetrazolium bromide

MW - molecular weight marker

NF1 - nuclear factor 1

ng - nanogram

NHEJ - non-homologous end joining

NLS - nuclear localisation signal

NMRI - Naval Medical Research Institute

nt - nucleotide

OD - optical density

ORF - Open reading frame

P1 TALEN - polymerase 1 TALEN

P2 TALEN - polymerase 2 TALEN

PBS - Phosphate buffered saline

PCR - Polymerase chain reaction

PEG-INFα - pegylated interferon alpha

PEI - polyethylenimine

pmol - picomole

pgRNA - pregenomic RNA

qPCR - Real-time quantitative PCR

RARE - retinoic acid response element

rcDNA - relaxed circular DNA

RFX1 - regulatory factor X 1

RGEN - RNA-guided endonuclease

RNA - Ribonucleic acid

RNAi - RNA interference

ROI - region of interest

rpm - revolutions per minute

rTALE - repressor TALE

RVD - repeat variable diresidue

RXRα/PPAR - retinoid X receptor alpha/peroxisome proliferator-activated receptor heterodimer

RT-PCR - Reverse transcription PCR

SCID - severe combined immunodeficiency

SEM - standard error of the mean

SID - mSin interaction domain

siRNA - small interfering RNA

SSA - single stranded annealing

ssDNA - single stranded DNA

S TALEN - surface TALEN

STAT3 - signal transducer and activator of transcription 3

T7E1 - T7 endonuclease 1

TA - transcriptional activator

Taq - *Thermus aquaticus*

TALE - transcription activator-like effector

TALEN - TALE nuclease

TBP - TATA binding protein

TR - transcriptional repressor

TRE - transcription regulatory element

U/L - units per litre

uPA SCID - urokinase plasminogen activator SCID

VPE - viral particle equivalent

WHB - woodchuck hepatitis virus

WHO - World Health Organisation

ZF - zinc finger

ZFN - zinc finger nuclease

ZFP - zinc finger protein

ε - epsilon

µl - microlitre

µM - micromolar

CHAPTER 1 – Hepatitis B virus pathogenesis, current treatment and novel therapeutic approaches

1.1 Hepatitis B virus

1.1.1 HBV epidemiology

Hepatitis B virus (HBV) is an enveloped partially double-stranded DNA virus that primarily infects hepatocytes, leading to acute or chronic infections (Seeger and Mason, 2000). Despite the availability of a universal recombinant anti-HBV DNA vaccine, there are 387 million people who are chronically infected (de Franchis et al., 2003; Perz et al., 2006). Most healthy adults, with uncompromised immune systems, readily clear acute infections by eliciting an immune response to antigenic epitopes present on the viral envelope or the surface of infected hepatocytes (Jung and Pape, 2002). Vaccine-naïve children and immunocompromised adults are more likely to develop chronic infections as their immune systems are un-primed and immature, or vulnerable (Fattovich et al., 2008; Seeger and Mason, 2000). Approximately 1-5% of adults, 50% of children, and 90% of neonates develop chronic infections following HBV exposure (Block et al., 2007; Dandri and Locarnini, 2012). Patients with chronic HBV are at greater risk for developing cirrhosis, hepatic decompensation, and primary hepatocellular carcinomas (HCCs), which typically only emerge decades after the initial infection (Di Bisceglie, 2009). Although the virus is not directly cytopathic, persistent infections result in immune-mediated necroinflammation and liver damage (Chisari and Ferrari, 1995). Annually these complications cause approximately 600,000 deaths, and account for between 60 to 80% of all

HCC incidences worldwide (Lavanchy, 2004). HBV infection therefore remains an important global public health problem.

Eight predominant HBV genotypes have evolved according to geographical location (Kurbanov et al., 2010). Each different genotype is identified as having more than 7.5% sequence variation when performing whole genome alignments, whilst intra-genotype variations between 4 - 8% denote viral subtypes. In Sub-Saharan Africa genotypes A and D predominate, whilst genotypes E and A are more commonly found in Central and North African regions. Genotypes B and C are found almost exclusively in Southeast Asia and China, although B and C have also been detected along with genotype D in Australia. Genotype D is found in the rest of Asia and Europe. In both South and North America a combination of genotypes F, A and D, and A, C, B, D and G have been primarily detected. In Central America genotypes F and H predominate. More recently, an additional HBV genotype 'I' has been identified Southeast Asia (Olinger et al., 2008; Tran et al., 2008). The clinical progression of chronic HBV infection has been shown to differ between genotypes (reviewed by Kramvis and Kew, 2007; Lin and Kao, 2011), although more comprehensive analysis across all genotypes and sub-genotypes is needed.

HBV infection is hyper-endemic to sub-Saharan and Central Africa, Southeast Asia, and certain regions of South America, where more than 8% of the population are chronically infected (Lavanchy, 2004). The virus is transmitted though percutaneous exposure to infected blood or body fluids. In Southeast Asia, perinatal transmission of HBV predominantly occurs. This has been attributed to a high rate of viral replication, associated with seroprevalence of HBV e (HBeAg) and surface antigen (HBsAg), detected in women from this region (Ott et al., 2012). However in Africa, the majority of HBV transmissions occur horizontally. In some rural areas of

South Africa, prior HBV infection has been detected in 98% of the population (Custer et al., 2004). This is generally as a result of interfamilial exposure to index carriers (Kramvis and Kew, 2007). The high prevalence of chronic HBV infection in these regions accounts for a large incidence of clinically observed cirrhosis and HCC (de Martel et al., 2012; Parkin, 2006). In sub-Saharan Africa, the risk of developing HCC is further exacerbated by the exposure of HBV infected individuals to the carcinogenic aflatoxin, as well as Human Immunodeficiency Virus (HIV) co-infections (Hainaut and Boyle, 2008). In South Africa alone, it is estimated that there are 5.6 million people living with HIV (UNAIDS, 2012), of which 5 to 25% of these individuals additionally harbour chronic HBV infections (Hoffmann and Thio, 2007; Modi and Feld, 2007). Reactivation of HBV replication is associated with acquired immunodeficiency syndrome (AIDS) progression, increasing the likelihood of HBV-related liver damage (Hoffmann and Thio, 2007). In addition, a high incidence of occult HBV infection has been observed in HIV positive patients who have not yet progressed to AIDS (Firnhaber et al., 2009; Hoffmann and Thio, 2007). With an estimated 3 – 4 million people already chronically infected with HBV in South Africa (Kew, 2008), increasing HBV/HIV co-infections are expected to increase morbidity and mortality dramatically, further burdening the limited medical and economic standings of the country (Hainaut and Boyle, 2008). As such, it remains a global priority to identify novel therapeutics that may eliminate chronic HBV infections.

1.1.2 HBV infection and replication in hepatocytes

Human HBV is a member of the *Hepadnaviridae* family, and forms part of the mammalian specific *Orthohepadnavirus* genus. During active infection, two different viral DNA configurations, the relaxed circular DNA (rcDNA) and the covalently closed circular DNA (cccDNA), are detected. The infectious virion contains the rcDNA genome, which is partially double stranded and contains a gap region. As rcDNA is reverse transcribed from viral pregenomic RNA (pgRNA), artefacts of this process, including a polymerase at the 5' end of the negative strand, and an RNA oligomer at the 5' end of the positive strand, can be found (Robinson et al., 1974; Summers et al., 1975). This form of encapsidated HBV DNA, initially referred to as the Dane particle, is primarily located within circulating viral particles isolated from the serum and livers of chronically infected patients (Dane et al., 1970; Huang et al., 1972). The cccDNA however is found in the nucleus of infected hepatocytes as an episomal minichromosome (Newbold et al., 1995; Tuttleman et al., 1986). During infection, the rcDNA translocates to the nucleus of hepatocytes where it is repaired, forming the cccDNA. This cccDNA drives the expression of viral proteins and pgRNA, which are required for the reverse transcription of new rcDNA. As the fundamental viral transcription intermediate, the cccDNA is essential for viral replication and new virion assembly.

The episomal cccDNA is extremely compact, at approximately 3200 base pairs (bp), and comprises four overlapping open reading frames (ORFs) (Figure 1.1). These encode the *precore/core* (*C*), *polymerase* (*P*), *surface* or *envelope* (*S*) and *X* genes (Robinson, 1977; Seeger and Mason, 2000; Tiollais et al., 1985). HBV gene expression is regulated by four

individual promoter sequences, the basic core promoter (BCP), pre-S1, pre-S2, and X promoters. The *P* ORF encodes the polymerase protein, which is the enzyme responsible for reverse transcription of the 3.5 kb pgRNA. This pgRNA is transcribed from the *precore/core* ORF. The core proteins or HBV core antigens (HBcAg) as well as the HBeAg, are translated from different initiation codons in the *precore/core* transcript. The core proteins are important for new virion assembly as they make up the viral nucleocapsid. HBeAg, which is used clinically as a marker of active viral replication, is not involved in virion assembly but is detected in the serum. Although the function of HBeAg has not yet been confirmed, recent investigations suggest that it acts predominantly as an innate and adaptive immunomodulator by inhibiting Toll-like receptor cascades and T-cell activation (reviewed by Revill and Yuan, 2013). The *surface* or *envelope* ORFs includes the *pre-S1*, *pre-S2* and *S* regions which the large (L), middle (M) and major (S) envelope surface antigens (HBsAgs) respectively (Heermann et al., 1984). Transcription from the *pre-S1* ORF results in a 2.4 kb subgenomic mRNA encoding the L surface protein, whilst transcription from the *pre-S2* ORF results in a 2.1 kb subgenomic mRNA encoding the M and S surface proteins. All three surface proteins are essential in the formation of new viral envelopes which surround the nucleocapsid. Finally the *X* ORF is transcribed into a 0.8 kb subgenomic mRNA which encodes the transactivator protein HBx. The function of HBx is still elusive however it is thought to be important in maintaining viral replication in primary hepatocytes by regulating transcription of cellular genes (Gearhart and Bouchard, 2011), and may possibly facilitate the integration of HBV DNA into the host genome (Arbuthnot et al., 2000; Feitelson, 1998; Robinson, 1977). Although viral mRNAs are transcribed from separate ORFs, a common viral protein polyadenylation signal is located downstream of the BCP (Nassal, 2008). In addition to the encoded viral transcripts, HBV splice variants have been identified. The HBV splice-generated protein (HBSP) is encoded by a 2.2 kb version of the pgRNA transcript and,

like the HBeAg, it is produced during viral replication (Soussan et al., 2003). However it has been shown to activate the adaptive immune response, most likely accelerating liver disease progression (Mancini-Bourgine et al., 2007). This suggests that HBV viral proteins and splice variants are not only essential for replication but also regulate the host's immune response.

Together with the four promoter regions, viral transcription is further regulated by three additional *cis*-elements, the negative regulatory element, Enhancer I, and Enhancer II domains. The negative regulatory element, which is located upstream of the BCP region, acts as an inhibitor of BCP function (Chen and Ou, 1995). The Enhancer I is located between the S ORF and the X promoter region, and activates viral transcription in a hepatocyte-dependant manner through the recruitment of liver specific transcription factors (Antonucci and Rutter, 1989; Guo et al., 1991). Finally, the Enhancer II domain overlaps the BCP sequence, and works synergistically with Enhancer I to promote viral gene transcription, particularly in differentiated hepatocytes (Su and Yee, 1992). Overall, HBV transcription and translation is a highly regulated process which occurs through an exceptionally compact genome arrangement.

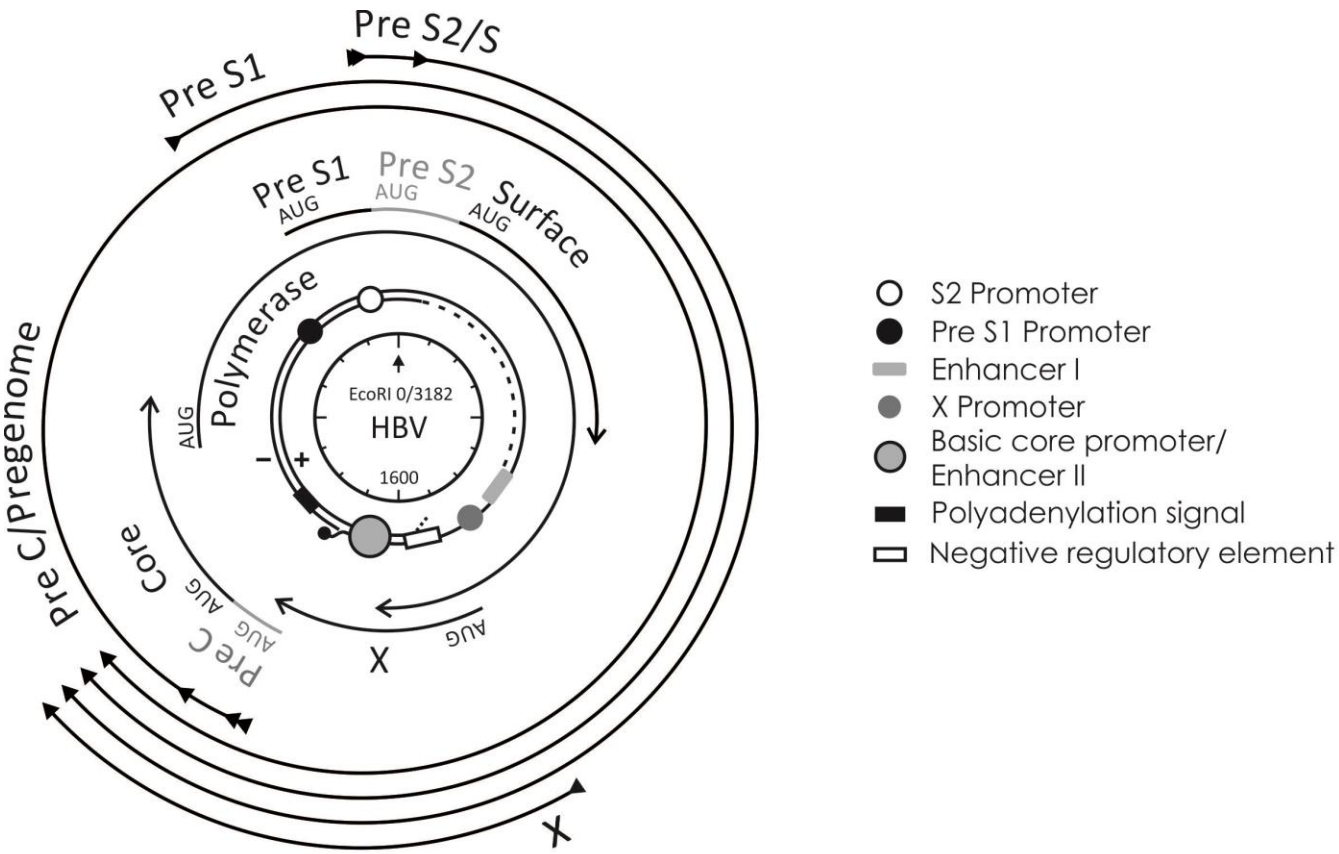

Figure 1.1: Genomic organisation of HBV. The rcDNA, schematically indicated in the centre of the circular genome map, has a partially double stranded positive sense (+) and negative sense (-) strand. This rcDNA is converted to cccDNA in the nucleus of hepatocytes. The cccDNA encodes the four viral ORFs: *precore/core*, *polymerase*, *surface*, and *X*, which are shown as arrows immediately surrounding the genome. The approximate location of the promoters is shown as circles and additional regulatory elements are shown as rectangles. Nucleotide co-ordinates are calculated clockwise from the unique *Eco*RI site that occurs in both rcDNA and cccDNA genomes.

HBV is primarily hepatotropic, however the virus has been isolated from peripheral blood mononuclear cells (Neurath et al., 1992; Trippler et al., 1999). The circulating viral particles, which contain the rcDNA genome, are responsible for viral transmission and new HBV infections (Figure 1.2). This rcDNA is encapsidated within an icosahedral core or nucleocapsid comprising HBV core proteins. The capsid is subsequently enclosed within an envelope involving an arrangement of L, M, and S surface proteins, which confers hepatocyte specificity (Blum et al., 1989; Nassal, 2008). These circulating viral particles initiate infection and replication within hepatocytes (Figure 1.2), a process which has been extensively researched but not yet fully elucidated (Glebe and Urban, 2007; Nassal, 2008; Seeger and Mason, 2000). The circulating virion initially attaches to the hepatocyte through associations with the envelope proteins and the cell membrane, following which the capsid is internalised, most likely through clathrin-mediated endocytosis (Cooper and Shaul, 2006). In the cytoplasm the capsid, which contains the rcDNA genome, interacts with the nucleoporin 153 protein found in the nuclear membrane (Schmitz et al., 2010). Interaction with the nuclear pore complex facilitates the dissociation of the capsid and the translocation of the rcDNA into the nucleus. Here the partially synthesised positive DNA strand of the rcDNA is repaired, generating episomal cccDNA. To achieve this, the polymerase and RNA oligomers found at the 5' ends of the negative and positive rcDNA strands respectively, are removed before positive strand synthesis and ligation of the gap region (Blum et al., 1989). The episomal cccDNA is the transcriptional intermediate which drives the expression of viral proteins required for new virion assembly.

With the aid of host transcription factors, the pgRNA and subgenomic mRNAs are transcribed from the cccDNA (as previously described). These viral RNAs are transported to the cytoplasm where they are translated into core, polymerase, surface (L, M, S), and X proteins. Here the

greater than genome length pgRNA associates with viral polymerase and core proteins to drive nucleocapsid formation. During pgRNA encapsidatation, reverse transcription of the viral RNA is initiated. A comprehensive account of the complex reverse transcription strategy employed by HBV has previously been described (Nassal, 2008). As such only a brief summary of these events will be described. HBV reverse transcription is initiated through an interaction between the polymerase and a stem-loop epsilon (ε) structure created at the 5' end of the pgRNA. This interaction results in the transcription of a 3 to 4 base DNA oligonucleotide. Following this initial transcription event, the polymerase moves to the 3' end of the pgRNA, facilitating the binding of the newly synthesised oligonucleotide to a complementary sequence at the proximal direct repeat 1 (DR1). This oligonucleotide acts as a primer which triggers reverse transcription of the negative DNA strand. At the same time the polymerase, which has inherent RNaseH activity, degrades the majority of the pgRNA template, leaving only a short residual 5' capped oligonucleotide. This oligonucleotide has a complementary binding site at the direct repeat 2 (DR2) sequence located at the 3' end of the newly synthesised negative DNA strand. This oligonucleotide primes the initial stage of positive DNA strand synthesis. However as positive DNA strand synthesis is discontinuous, a template switch is required. Using the terminal redundancy found at the 5' and 3' ends of the negative strand, the small positive strand is able to switch to the 3' end of the negative strand and resume elongation. This results in newly synthesised rcDNA, which is simultaneously enclosed in the new viral capsid. This capsid is either recycled to the nucleus, which expands or maintains the cccDNA pool, or enters the secretory pathway, where it associated with surface proteins and buds out of the cell as a new virion (Nassal, 2008; Zoulim, 2005). Additional cccDNA copies will enhance viral replication whilst new circulating virions may infect other hepatocytes, thereby increasing serum viraemia and facilitating liver specific dissemination of HBV.

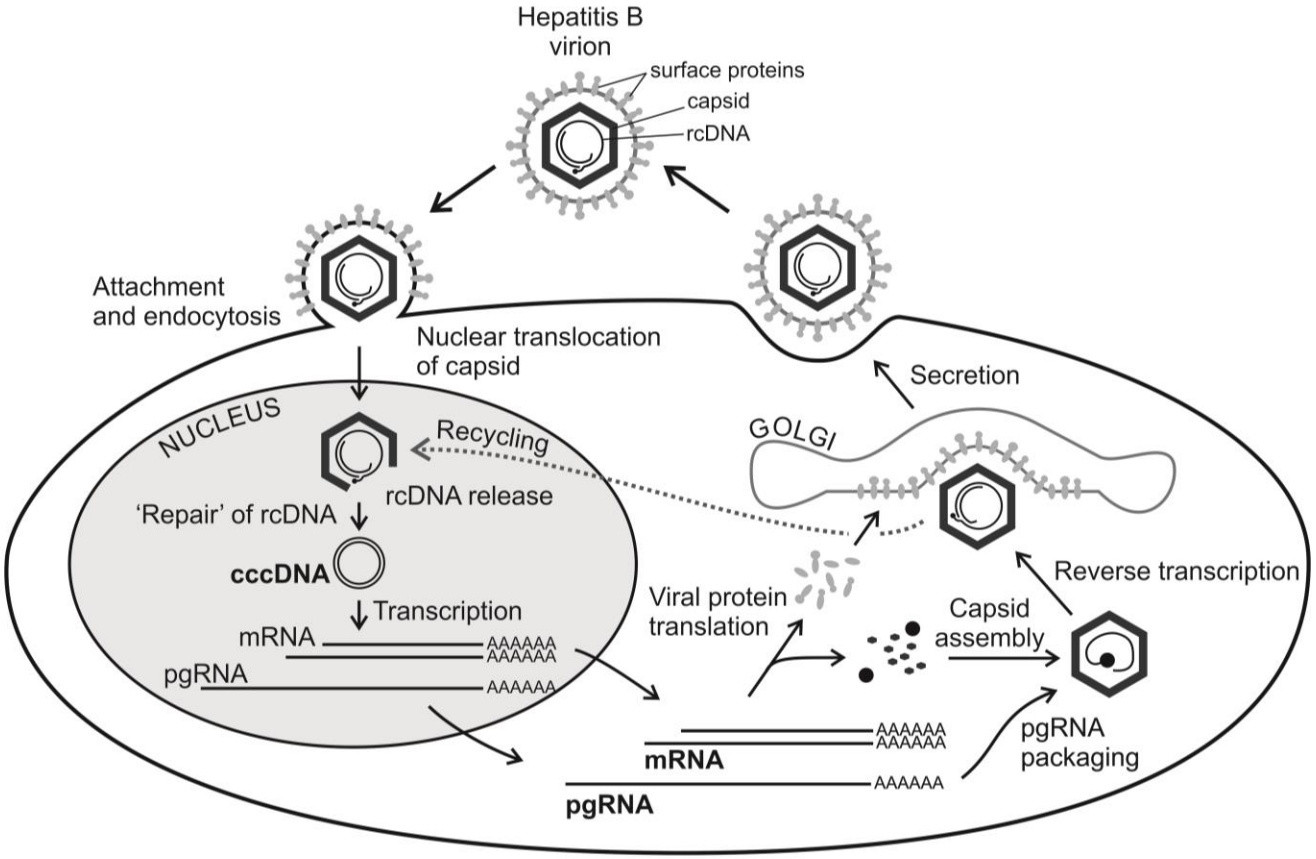

Figure 1.2: Hepatitis B virus replication cycle. Following attachment to the hepatocyte cell membrane, the capsid is released into the cytoplasm where it translocates to the nucleus. Here the rcDNA viral genome is released and repaired to form cccDNA. The cccDNA acts as the primary replication intermediate from which the pgRNA and viral subgenomic mRNAs are transcribed. These viral RNAs are transported to the cytoplasm where the subgenomic mRNAs are translated into proteins required for virion packaging and assembly. The pgRNA associates with polymerase and the new core proteins to assemble the new capsid. Within the capsid, the pgRNA is reverse transcribed to form rcDNA. Finally inside the endoplasmic reticulum, surface proteins surround the new virion allowing the virus to bud out of the cell.

1.1.3 Commercially available therapeutics

As the universal recombinant vaccine confers protection against HBV infection in 90-95% of vaccinated individuals (Margolis, 1998), the WHO has embarked on a global campaign to introduce the vaccine into national infant immunisation schemes, focussing specifically on endemic countries (Franceschi and Raza, 2008). In addition to offering protective immunity, the vaccine can also be used prophylactically following exposure to infected blood or body fluids. In conjunction with hepatitis B immune globulin (HBIG), the HBV vaccine has been used extensively to prevent perinatal transmission (reviewed by Chen, 2009). However, as prophylactic vaccination cannot confer protection once chronic HBV infection is established, long-term therapeutics have been developed to inhibit viral replication.

There are currently seven licenced therapeutics available for the treatment of chronic HBV infection (EASL, 2009), which can be divided into two major groups: the immunomodulators and nucleotide/side analogues. The immunomodulators, interferon alpha (INFα) and pegylated INFα (PEG-INFα) assist the host's adaptive immune response in eliminating infected hepatocytes. Both INFα and PEG-INFα have been successfully used as short-term therapeutics which achieve a sustained virological response in chronically infected patients (Cooksley et al., 2003; Marcellin et al., 2004; Perrillo et al., 1990; Wong et al., 1993). However, in addition to causing side-effects, interferon efficacy varies greatly depending on initial HBV viremia, liver damage, HBV genotype, and the host immune response. Clinically, INFα appears to have moderately improved therapeutic potential for patients infected with HBV genotype A versus C, D, or E (Erhardt et al., 2000; Janssen et al., 2005; Zhang et al., 1996). Nonetheless the overall anti-

HBV efficacy of interferon is still considered to be low, and therapy is contraindicated in patients with cirrhosis or HIV co-infection (Krastev, 2006).

While immunomodulators activate host immune responses, the nucleotide/side analogues act directly on viral replication by inhibiting HBV reverse transcription. Drugs in this group include lamivudine, adefovir dipivoxil, entecavir, telbivudine, and tenofovir (EASL, 2009; Zoulim and Locarnini, 2012). Although these nucleotide/side analogues have fewer side-effects, long-term therapy is required to maintain viral suppression. As HBV reverse transcription is error prone, viral escape mutants may arise following long-term monotherapy. Lamivudine, the first licensed nucleoside analogue, efficiently reduces HBV DNA levels, inhibits the establishment of new cccDNA, and reverses liver damage (Dienstag et al., 2003; Lai et al., 1998; Yuen et al., 2005). As the first commercially available therapy, lamivudine quickly became the 'gold standard' for the treatment of chronic HBV infections. However long-term lamivudine monotherapy frequently results in tyrosine-methionine-aspartate-aspartate (YMDD) escape mutants within the viral polymerase, which leads to reactivation of HBV replication (reviewed by Fischer et al., 2001). Furthermore, the number of viral escape mutants increases in a time-course dependant manner (Lai et al., 2003). In comparison to lamivudine, adefovir dipivoxil has shown only moderate anti-HBV efficacy, as nephrotoxicity has been associated with high doses of this nucleotide analogue (Fisher et al., 2001; Marcellin et al., 2008). Although low doses may reduce therapeutic efficiency, adefovir dipivoxil is effective against lamivudine resistant strains (Lee et al., 2009; Ono-Nita et al., 1999), and viral escape mutants occur infrequently (Hadziyannis et al., 2005). Unlike adenfovir dipivoxil, entecavir shows superior antiviral activity when compared to lamivudine (Chang et al., 2006; Lai et al., 2006). In addition, long-term entecavir treatment improves liver histology (Chang et al., 2010b; Hosaka et al., 2012) and viral escape is virtually

negligible (Chang et al., 2010a; Tenney et al., 2009). The latest nucleoside and nucleotide analogues approved for chronic HBV treatment, telbivudine and tenofovir (Delaney et al., 2006; Osborn, 2009), also exhibit anti-HIV activity (Fung et al., 2002; Low et al., 2009) and may therefore be used to treat HBV/HIV co-infections (Soriano et al., 2008). Telbivudine has shown improved antiviral activity when compared to lamivudine (Hou et al., 2008; Lai et al., 2007) and adefovir dipivoxil (Chan et al., 2007). However, HBV escape mutants and drug-induced myopathy and myalgia have been reported (Gane et al., 2011; Zhang et al., 2008). Tenofovir has recently been identified as the most efficient anti-HBV monotherapy (Wiens et al., 2013), without any evidence of viral escape. However as this nucleotide analogue was only approved for the treatment of chronic HBV in 2008, long-term mutational analysis is not yet available.

As entecavir and tenofovir display high antiviral activity with minimal HBV resistance, they are both currently recommended as first-line monotherapies, thereby replacing lamivudine, for the treatment of chronic HBV infection. Although these nucleotide/side analogues improve liver histology and inhibit viral replication, they have no effect on established cccDNA pools. In addition, long-term therapy may result in viral mutagenesis and cessation of therapy often leads to HBV reactivation. Chronic HBV treatment failure has predominantly been attributed the persistence of episomal cccDNA (Caruntu and Molagic, 2005; Zoulim, 2004). Although nucleotide/side therapeutics may inhibit disease progression, there is still no cure for chronic HBV infection.

1.1.4 Persistence of cccDNA

The persistence of episomal cccDNA presents a major hurdle in the management and treatment of chronic HBV. During chronic infection, multiple cccDNA copies are established as stable minichromosomes in the nucleus of hepatocytes (Newbold et al., 1995; Tuttleman et al., 1986) and, since current therapeutics only target cytoplasmic replication events, these episomal cccDNA pools remain unaffected. In addition, as cccDNA is epigenetically regulated (Pollicino et al., 2006), it is able to remain dormant in the nucleus of hepatocytes, establishing a latent or occult infection (Mulrooney-Cousins and Michalak, 2007; Rehermann et al., 1996). This occult infection may lead to a spontaneous *de novo* reactivation of HBV replication. Alternatively, reactivation may also occur as a result of host immune suppression or a disruption in anti-viral therapeutic regimes. Regulation of intrahepatic cccDNA is important for viral replication, minichromosome formation, and the maintenance of occult infections. This involves complex interactions between host transcription factors and adaptive immune response, viral proteins, as well as epigenetic factors (reviewed by Levrero et al., 2009).

In the nucleus of hepatocytes the cccDNA is organised into minichromosomes through the association of both histone and non-histone proteins (Bock et al., 2001; Newbold et al., 1995). The acetylation and methylation status of key histones facilitates chromatin-like transcriptional regulation of viral replication (Pollicino et al., 2006). Binding of histone actyltransferases, host transcription factors, and HBV X proteins to the cccDNA promote viral transcription (Belloni et al., 2009; Bock et al., 2001; Pollicino et al., 2006), whilst histone deacetylases and methyltransferases promote a heterochromatin-like structure during occult infection

(Vivekanandan et al., 2008). It is estimated that on average, a human hepatocytes retains 1.5 cccDNA copies per cell (Laras et al., 2006), however copy numbers between 0.03 and 173.1 have also been observed in clinical specimens (Chen et al., 2004). The hosts' innate and adaptive immune responses contribute to the dilution and clearance of cccDNA, particularly when acute infections are resolved. Non-cytolytic inflammatory cytokines and cytotoxic T cells inhibit viral replication and destroy infected hepatocytes (Fisicaro et al., 2009; Guidotti et al., 1999; Thimme et al., 2003), whilst constant hepatocyte proliferation dilutes established cccDNA pools (Mason et al., 2007; Summers et al., 2003). However as hepatocytes have a relatively long half-life, immune-mediated clearance of cccDNA remains inefficient during chronic infection, and as hepatocytes have a relatively long half-life, cell division is not sufficient to eliminate cccDNA. In addition, occult infections may evade the immune system, allowing spontaneous reactivation of HBV replication. As a result, new therapeutic approaches that result in the direct inactivation of HBV cccDNA would contribute significantly to the treatment of chronic HBV.

1.1.5 An anti-HBV gene therapy approach

With continuous advances in the manipulation of DNA and RNA for therapeutic gain, a number of promising anti-viral gene therapies are currently under investigation. In particular, RNA interference (RNAi) based therapeutics designed to target HBV have been studied extensively (Ely and Arbuthnot, 2010). The RNAi pathway, which results in the silencing of gene expression in an RNA-dependant manner, occurs naturally in mammalian cells (Hammond et al., 2001). This post-transcriptional gene silencing approach has been manipulated for therapeutic

application (Aagaard and Rossi, 2007). Single and multiple RNAi effectors, like short interfering RNAs (siRNAs) and artificial microRNAs (miRNAs), have shown efficient knock-down of HBV by inhibiting reverse transcription and translation of pgRNA and sub-viral mRNAs (Carmona et al., 2006; Chattopadhyay et al., 2009; Ely et al., 2008; Kayhan et al., 2007; Konishi et al., 2003; Li et al., 2007; Liu et al., 2004; Wu et al., 2007). However as they inhibit viral replication post-transcriptionally, akin to nucleoside/tide analogues, RNAi activators have no effect on established episomal cccDNA (Starkey et al., 2009). To target the cccDNA directly, a therapeutic capable of eliciting an antiviral effect in the nucleus of infected cells is necessary. To achieve this, an alternative gene therapy approach using DNA-binding proteins to control and manipulate gene expression, has recently been explored (Zimmerman et al., 2008).

Zinc finger proteins (ZFPs), which bind to specific DNA sequences, occur naturally as eukaryotic transcription factors. Each zinc finger is capable of binding a specific nucleotide triplet. Therefore sequentially arranged ZFPs can be designed to bind to a sequence of up to 18 nucleotides (Klug, 2010). These polydactyl ZFP arrays can be engineered using modular cloning techniques (Bhakta and Segal, 2010) to alter DNA transcription of endogenous genes (Jamieson et al., 2003). Several ZFPs designed to target a 9 or 18 bp sequence in the enhancer region of Duck Hepatitis B virus (DHBV) cccDNA, were shown to reduce pgRNA and viral protein expression (Zimmerman et al., 2008). These ZFPs were most likely obstructing transcription of the cccDNA through competitive binding inhibition at the target site. However, as it is likely that these ZFPs do not permanently alter cccDNA, the anti-HBV effect is likely to be transient. Designer nucleases on the other hand, are engineered DNA binding proteins with endonuclease activity. They are capable of binding and cleaving discrete DNA sequences, leading to permanent genome modifications. Binding of the nuclease to the target site results in

a DNA double stranded break (DSB) which are repaired by either non-homologous end-joining (NHEJ) or homologous recombination (HR) (reviewed by Bernstein and Rothstein, 2009; Lieber, 2010). The NHEJ pathway is intrinsically error prone whereas HR uses homologous DNA sequences to repair chromosomal breaks. By exploiting these cellular repair pathways, nucleases can be used for site-directed mutation or repair of endogenous genes. There are currently four different types of designer nucleases developed specifically for DNA engineering. These are the meganucleases, zinc finger nucleases (ZFNs), transcription activator-like effector nucleases (TALENs), and RNA-guided endonucleases (RGENs) (Figure 1.3). Whilst meganucleases and RGENs have natural endonuclease activity, ZFPs and TALENs are created by fusing nuclease domains to DNA binding proteins.

Meganucleases, otherwise known as homing endonucleases, were the first DNA-specific cleavage proteins identified within mobile genetic elements of yeast (Jacquier and Dujon, 1985; Kostriken et al., 1983). They were shown to trigger homologous recombination events in both yeast and eukaryotic cells by binding to specific DNA sequences, usually between 12 and 40 nucleotides in length (Thierry and Dujon, 1992). Meganucleases can be artificially engineered to cleave defined DNA targets (Chevalier et al., 2002; Epinat et al., 2003; Grizot et al., 2009; Rosen et al., 2006; Seligman et al., 2002; Smith et al., 2006) and have shown therapeutic potential for herpes simplex virus (HSV) infections (Grosse et al., 2011). The company responsible for the HSV meganuclease, Cellectis Bioresearch (Paris, France), have also patented anti-HBV meganucleases (WO/2010/136981 and US2012/0171191A1) however results of these investigations have yet to be published. Although artificial meganucleases can be engineered to target certain sequences, pre-existing DNA binding constraints limit the number of possible binding sites. Unlike the meganuclease, RGENs are based on a bacterial

RNA-guide CRISPR (clustered regularly interspaced short palindromic repeats) which recruit Cas9 (CRISPR-associated protein) to facilitate DNA cleavage (Jinek et al., 2012; Wiedenheft et al., 2012). These naturally occurring endonucleases have recently been exploited for genome engineering (Cho et al., 2013; Cong et al., 2013; Hwang et al., 2013; Jinek et al., 2013; Mali et al., 2013; Qi et al., 2013). As the RNA-guide can be manipulated to target any 20 bp DNA sequence, the potential for RGEN-mediated site-directed cleavage is immense. As these designer nucleases have only recently been described, further investigation into activity and specificity is still needed.

In contrast to meganucleases and RGENs, ZFNs and TALENs are engineered by fusing *Fok*I endonuclease domains to DNA binding domains (Christian et al., 2010; Kim et al., 1996). The *Fok*I enzyme is an obligate dimer, which requires interactions between the catalytic domains to facilitate cleavage of double stranded DNA (Bitinaite et al., 1998; Wah et al., 1997). For this reason, ZFNs and TALENs are designed in pairs, each with a left and right subunit (Figure 1.3). As *Fok*I endonuclease cleavage is sequence independent, the DNA binding domains are used to confer sequence specificity. ZFNs are engineered using polydactyl ZFPs (Klug, 2010), and over the past 10 years they have been extensively explored as potential human gene therapy agents (Rahman et al., 2011). An array of three to four ZFPs, targeting DNA sequences between 9 and 12 bp, is typically used to generate left and right ZFNs. A spacer region of 6 bp separates each left and right subunit enabling *Fok*I dimerisation and cleavage. As ZFNs are designed as pairs, the complete DNA target site is approximately 30 nucleotides long. Although ZFNs are most commonly designed to target endogenous human genes (Porteus, 2006), Thomas Cradick and colleagues (Cradick et al., 2010) have investigated the ability of modularly assembled ZFNs to cleave and disrupt HBV DNA targets. Using a replication competent HBV

expression plasmid, they showed that ZFNs cleaved episomal DNA targets *in vitro*. Furthermore, this site-directed targeted mutagenesis inhibited pgRNA transcription. Although the activity of these ZFNs on cccDNA has not yet been determined, this is the first study to describe targeted disruption of HBV as a potential gene therapy. However the major drawback of ZFN engineering is the intricate arrangement of specific context-dependent subunits (Ramirez et al., 2008; Sander et al., 2010a), which are required for efficient DNA binding. Although each ZFP is capable of binding a specific pre-defined nucleotide triplet, the position of each protein within the array can either reduce or enhance its affinity for the target sequence. To circumvent this, a library of ZFPs may be used to create multiple ZF arrays that could potentially bind to a specific DNA sequence (Maeder et al., 2009). Nonetheless, as several selection steps are required to isolate superior context-dependent ZF arrays this process is time consuming. Recently the traditional ZFPs have been substituted for an alternative DNA binding domain, the bacterial transcription activator-like effector (TALE). TALEs were first discovered in the *Xanthomonas* plant pathogens as transcriptional activators of avirulence genes (Boch and Bonas, 2009). Unlike ZFPs, a single monomer within the TALE DNA binding domain confers individual nucleotide specificity (Boch et al., 2009; Moscou and Bogdanove, 2009). As a result of this, TALE monomers have been conveniently concatamerised into sequence-specific DNA-binding domains that can be fused to *Fok*I endonucleases (Figure 1.3) (Cermak et al., 2011; Hockemeyer et al., 2011; Li et al., 2010; Li et al., 2011b; Miller et al., 2011; Morbitzer et al., 2011; Mussolino et al., 2011). As the left and right TALEN subunits are designed to target 19 bp sequences, they confer higher sequence specificity than ZFNs, which may account for their improved activity *in vitro* (Mussolino et al., 2011). TALENs have successfully been used to target multiple endogenous genes (Ding et al., 2013; Hockemeyer et al., 2011; Huang et al., 2011; Li et al., 2011b; Li et al., 2012; Liu et al., 2012; Sander et al., 2011; Sun et al., 2012;

Tesson et al., 2011) however the anti-viral efficacy of TALENs has not yet been determined (Schiffer et al., 2012).

Nuclease-mediated targeted mutagenesis of the episomal cccDNA established during chronic HBV infections, may lead to a permanent inactivation of viral replication and the subsequent elimination of persistent cccDNA pools. Recent investigations have shown that TALENs designed to target endogenous chromosomal loci have improved activity and are less cytotoxic than corresponding ZFNs. As the cccDNA is established as a minichromosome, engineered TALENs provide a unique approach to disabling both active and latent HBV infections. The work described in this thesis aimed to investigate the anti-viral potential of modularly assembled TALENs designed specifically to inactivate HBV-encoding DNA and cccDNA in both liver derived cells and *in vivo*. Examination of the effect of TALENs on viral protein expression and replication was determined by measuring cell culture, serum, and intrahepatic markers of viral replication. In addition, the direct application of TALENs in an adult murine model of HBV replication was explored. Successfully using TALENs to inactivate cccDNA in hepatocytes of HBV carriers should contribute significantly to advancing the treatment of this serious infection, especially since chronic HBV infection remains endemic to sub-Saharan Africa.

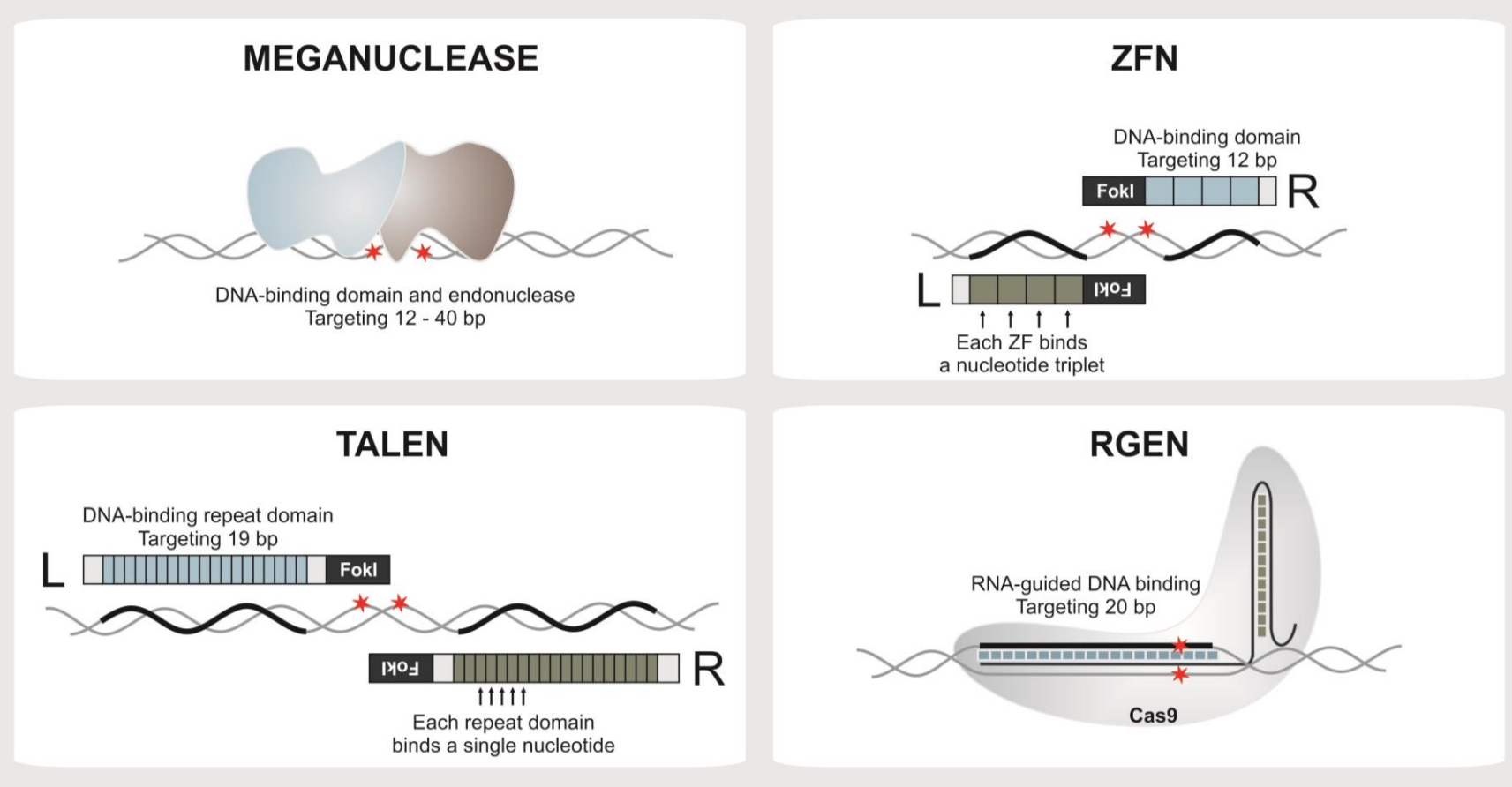

Figure 1.3: Designer nucleases for genome engineering. Four different engineered nucleases are illustrated schematically. Meganucleases are found naturally as endonucleases which target DNA sequences between 12 and 40 bp in length. ZFNs are engineered as pairs with each ZF in the array binding a specific nucleotide triplet. When a polydactyl ZFP array consists of four ZF, each left or right subunit targets a 12 bp sequence. TALENs are engineered as pairs with each left and right subunit DNA-binding domain targeting a 19 bp sequence. Each subunit is assembled from single TALE repeats which confer single nucleotide specificity. Both ZFNs and TALENs cleave target DNA with *Fok*I endonuclease domains. RGENs are RNA-guided endonucleases that bind to 20 bp target sequences. The Cas9 endonuclease facilitates double stranded DNA cleavage.

CHAPTER 2 – Engineering HBV TALENs

2.1 Introduction

Since the discovery of the *Xanthomonas* TALEs, and their inherent DNA binding capabilities, various research groups have focused on improving array propagation for the most convenient and rapid TALE assembly. Unlike the engineering of ZFNs, which requires the arrangement of specific context-dependent subunits for effective DNA binding (Ramirez et al., 2008; Sander et al., 2010a), TALE arrays can easily be assembled by modular cloning techniques without context-dependent selection (Moscou and Bogdanove, 2009). Individual TALE monomers comprise of approximately 34 amino acid polypeptide chains. TALE arrays are made up of tandem repeats of these monomers, which vary only at amino acid positions 12 and 13, referred to as the repeat variable diresidues (RVDs). The majority of these polymorphic RVDs bind to a single nucleotide, based on each diresidue's pre-defined affinity (Boch et al., 2009; Mak et al., 2012; Moscou and Bogdanove, 2009). All characterised RVDs, and their preferred nucleotide binding sites, are shown in Table 2.1. The four most commonly used RVDs are NI, HD, NK, and NG which bind to adenine, cytosine, guanine and thymine respectively. Alternative RVD's, such as NN and NS, are capable of binding to multiple nucleotides, whilst N* efficiently binds to 5-methylated cytosines (5mC) (Valton et al., 2012). Recently the NN diresidue, which is capable of binding guanine or adenine, has been shown to have a higher affinity for guanine than the NK RVD (Christian et al., 2012). As each RVD's binding affinity has been characterised, TALE arrays can be assembled to target specific DNA sequences. These arrays are created by joining

TALE monomers together in a distinct order, using RVDs that correspond to the intended DNA binding site.

Table 2.1: RVDs with established nucleotide binding affinities

RVD	Target Nucleotide/s
NI	A
HD	C
NK	G
NG	T
NS	A/C/G/T
NN	G/A
N*	C/A/T (5mC)
HG	T/C
H*	T
IG	T
HA	C/A/G
ND	C
HI	C
HN	G
NA	G

There are a number of commercial and publically available techniques currently used to assemble designer TALE (dTALE) arrays. These dTALEs may be fused to different effector domains to generate transcriptional activators, repressors, or nucleases. Two commercial companies, Cellectis Bioresearch (Paris, France) and Life Technologies (New York, USA), offer design and synthesis services. Cellectis Bioresearch mainly deals with pre-validated and custom TALENs whilst Life Technologies supplies GeneArt® Precision TALs. There are also several publically available methods of generating TALE arrays which include: 1) PCR amplification (Li et al., 2010; Miller et al., 2011; Zhang et al., 2011); 2) Modular assembly involving Golden Gate cloning (Cermak et al., 2011; Geissler et al., 2011; Li et al., 2011b; Morbitzer et al., 2011; Weber et al., 2011; Zhang et al., 2011); 3) Fast ligation-based automatable solid-phase high-throughput (FLASH) systems (Reyon et al., 2012); 4) Iterative capped assembly (ICA) (Briggs et al., 2012); and 5) Ligation-independent cloning (LIC)-based multiple-fragment assembly (Schmid-Burgk et al., 2012). Initially, TALEs were generated by amplifying TALE-encoding *Xanthomonas* genomic DNA. This PCR assembly method used primers that incorporated 5' restriction sites into amplicons, so that they could be ligated into various plasmid backbones. Amplicons contained either single RVD-encoding sequences or multiple TALE arrays. While this is the simplest method of generating TALEs, performing multiple PCR amplification steps increases the likelihood of incorporating single base mutations into the TALE array sequence. Nevertheless the entire dTALE assembly field was pioneered by this PCR approach, as it enabled the synthesis of single RVD-encoding TALE plasmid libraries, and in doing so, facilitated modular assembly techniques.

The most common method of generating TALEs is by modular assembly, using Golden Gate cloning in conjunction with a pre-assembled TALE module plasmid library. Each TALE-encoding

DNA module contains a unique RVD-encoding sequence with flanking type IIS restriction sites which, when cleaved, generates unique 4 nt 5' overhangs (Engler et al., 2009; Engler et al., 2008). These unique overhangs can then ligate with complementary overhangs from other TALE modules in the library. As the type IIS restriction enzymes cleave downstream of their recognition sites to create these unique overhangs, cut-ligation reactions occur simultaneously without restoration of the recognition site. As a result of this, ligated modules will not be susceptible to another round of restriction digestions with the same type IIS enzyme. Although this method has been used by many different research groups to generate TALEs successfully, a number of screening steps are required during assembly. This is to ensure that cut-ligations have resulted in the complete and precise arrangement of all RVD-encoding sequences within the dTALE. To accelerate modular TALE assembly, the FLASH, ICA, and LIC-based approaches have recently been developed. These three methods use a solid-phase platform to anchor the first TALE-encoding module before propagating the dTALE array. FLASH assembly can be automated and uses plasmids encoding between one and four RVDs, whilst ICA prevents imprecise dTALE arrangements by using capped oligonucleotides to inhibit the ligation of redundant TALE modules. Finally, unlike the 4 nt 5' overhangs used during Golden Gate cloning, LIC-based assembly relies on longer single-stranded DNA overhangs of between 10 and 30 bp, thereby improving the binding specificity of RVD-encoding sequences with complementary overhangs. Even though these three sold-phase assembly techniques allow faster dTALE synthesis, they are relatively new and require further validation. Only the modular assembly technique, by means of Golden gate cloning, has been extensively used and has been shown to be a reliable means of assembling dTALEs and generating TALENs.

The TALE repeat assembly procedure devised by Morbitzer and colleagues uses a pre-assembled TALE-encoding DNA module library with a two-step cut-ligation protocol to generate sequence specific TALENs (Morbitzer et al., 2011). This pre-assembled library, which comes standard with the kit, includes individual TALE-encoding DNA modules with sequences for the NI, NG, NK, HD, NN, and NS RVDs (Table 2.2). These were originally amplified by PCR from the *avrBs3* gene, before cloning into level 1 destination vectors (Figure 2.1) to create the DNA module library. Destination vectors are used throughout this TALE repeat assembly procedure to accommodate sequences encoding either individual RVDs or multiple TALE arrays in plasmids that are amenable to Golden gate cloning. In addition to the level 1 destination vectors, which comprise the TALE-encoding DNA module library, level 2 and 3 destination vectors are required for dTALE assembly. Level 2 destination vectors, pUC57-AB-DESTINATION (pUC-AB) and pUC57-BC-DESTINATION (pUC-BC) are required during dTALE assembly, whilst four separate level 3 destination vectors (pVAX-NI-*Fok*I, pVAX-NG-*Fok*I, pVAX-NK-*Fok*I pVAX-HD-*Fok*I) are required for final TALEN assembly (Mussolino et al., 2011).

All destination vectors contain Golden gate cloning-specific restriction sites, which are compatible with simultaneous cut-ligations reactions. Level 1 destination vectors include a DNA recognition site for the type IIS restriction enzyme *Bsa*I, which is used to create unique 5' overhangs. These pre-assembled libraries contain all RVD TALE-encoding modules that, upon digestion with *Bsa*I, yields unique position-specific 4 nt 5' overhangs, such that the DNA modules will only ligate in a structured collation (Figure 2.2). Therefore a TALE-encoding DNA module with a 5' antisense strand overhang at position 1 (#1) will only ligate to a TALE-encoding DNA module that has the corresponding 5' sense strand overhang. That same module, with the #1 sense strand overhang, will have a 5' antisense strand overhang for

position 2 (#2). Accordingly, only a module with a 5' sense strand overhang for #2 will ligate. In this way, by selecting the correct TALE-encoding modules from the library for each position in the final array, a DNA target specific dTALE can be assembled. In addition, the level 2 and level 3 destination vectors used during the cut-ligation reactions contain the necessary 5' and 3' adaptor sequences required to ligate to the first and last modules of each array. The degeneracy of the genetic code and the positioning of tandem amino acid repeats within TALE-encoding sequences were used to create unique overhangs for all DNA-encoding RVDs in every possible dTALE position. As the DNA encoding amino acid repeat sequences were used to shift junction sites and create unique overhangs, some variation in the length of TALE-encoding sequences within the library can be found. However these differences do not affect the final dTALE array.

Table 2.2: TALE monomers for engineering sequence specific HBV TALENs

Amino acid sequences of TALE monomers targeting individual bases	Target nucleotide	RVD
LTPDQVVAIAS**NI**GGKQALETVQRLLPVLCQAHG	A	NI
LIPQQVVAIAS**NG**GGKQALETVQRLLPVLCQDHG	T	NG
LTPEQVVAIAS**NK**GGKQALETVQRLLPVLCQAHG	G	NK
LTPEQVVAIAS**HD**GGKQALETVQALLPVLCQAHG	C	HD
LTPQQVVAIAS**NN**GGKQALETVQRLLPVLCQAHG	G/A	NN

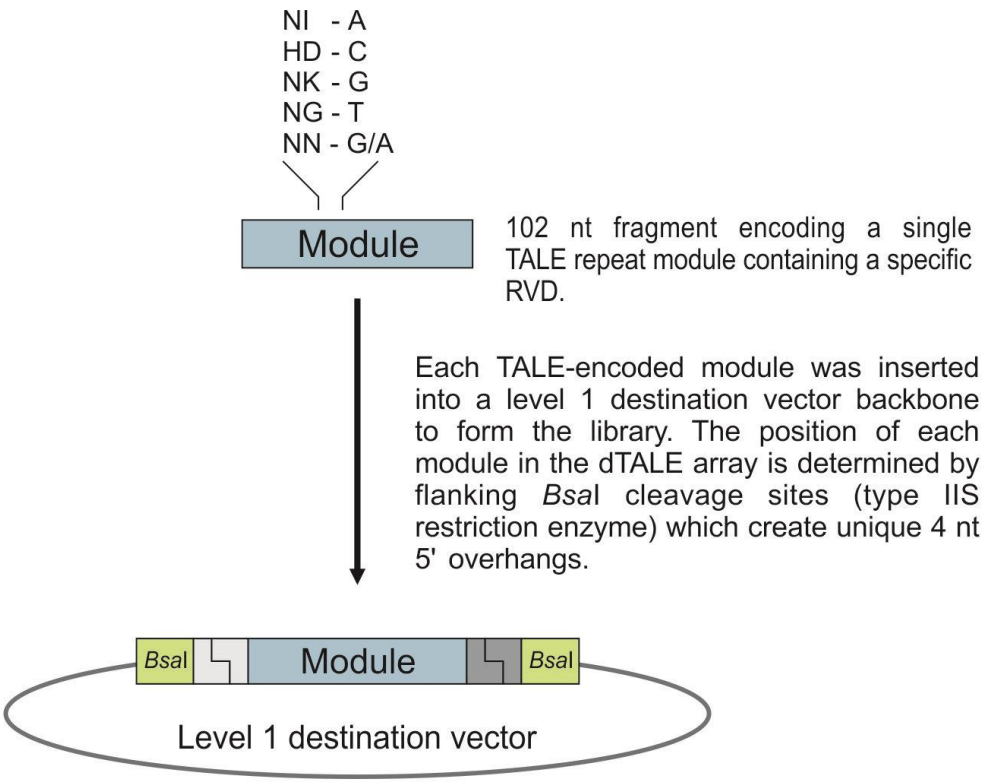

Figure 2.1: Pre-assembled TALE module libraries. Sequences encoding specific RVDs give rise to five different TALE-encoding modules. Each translated diresidue protein sequence recognises a different nucleotide in the target DNA site. The DNA encoding each TALE module is PCR amplified and inserted into a level 1 destination plasmid, with *Bsa*I restriction sites and position-specific adaptor sequences on either side. As *Bsa*I is a type IIS restriction enzyme the TALE module library can be used for Golden gate cloning.

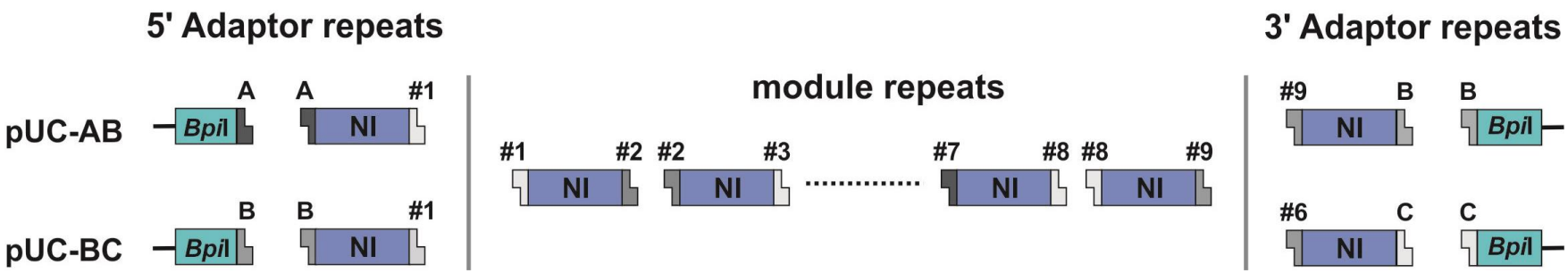

Figure 2.2: Golden Gate cloning position-specific overhangs for dTALE assembly. The level 2 destination vectors (pUC-AB and pUC-BC) and the NI RVD module library are illustrated. After type IIS restriction digestion, the pUC-AB vector has a 5' overhang (designated 'A') and a 3' overhang (designated B), which are required for AB fragment ligations. The first NI module will have a complementary overhang, designated 'A', at the 5' sense strand which will ligate with the pUC-AB vector. All subsequent modules are ligated based on 5' overhang #1 – #9. The final module required for pUC-AB assembly has a B overhang at the 5' antisense strand allowing ligation to the vector's 3' adaptor. The pUC-BC ligations are carried out in the same manner however the vector has a different 5' and 3' adaptor overhangs, designated 'B' and 'C'. The first TALE module contains a 'B' overhang on the 5' sense strand and 5' overhang #1 at the antisense strand. The same module repeats, but only using 5' overhangs #1 – #6, are used during pUC-BC ligations. The final module has a 5' antisense strand overhang that ligates to the C adaptor in the destination vector. A total of 10 modules are ligated into pUC-AB, and 7 modules are ligated into pUC-BC. The pre-assembled TALE library has position-specific modules for NI, NG, NK, HD, NN and NS diresidues.

This Golden gate cloning-based assembly procedure uses a two-step cut-ligation approach. The first is the simultaneous restriction digestion and ligation of selected TALE-encoding DNA modules into the level 2 destination vectors pUC-AB and pUC-BC as shown in Figure 2.3. As Golden gate cloning requires the precise ligation of complementary overhangs to generate a sequence specific array, the assembly of the 17 module dTALE-encoding sequence is divided into two separate fragments (AB and BC) which are ligated into two different level 2 destination vectors. This should improve the efficiency of simultaneous cut-ligation reactions. The AB fragment begins at the 'A' 5' adaptor repeat of the first TALE-encoding module and ends at the 'B' 3' adaptor repeat of the tenth TALE-encoding module, whilst the BC fragment begins and the 'B' 5' adaptor of the first TALE-encoding module and ends at the 'C' 3' adaptor of the seventh TALE-encoding module (Figure 2.2). The first 10 modules (AB fragments) of the dTALE are ligated into pUC-AB whilst the remaining 7 modules (BC fragments) are ligated into pUC-BC, using the appropriate 5' and 3' adaptor repeats (Figure 2.2). Both level 2 destination vectors have the type IIS restriction enzyme, *Bpi*I flanking the AB and BC fragment ligation sites. This is required for the second cut-ligation reaction, where AB and BC fragments are inserted into a level 3 destination vector (Figure 2.4). The level 3 destination vectors used to generate the anti-HBV TALENs, pVAX-NI-*Fok*I, pVAX-NG-*Fok*I, pVAX-NK-*Fok*I, and pVAX-HD-*Fok*I, were revised by Mussolino and colleagues, to improve cleavage efficiency (Mussolino et al., 2011). These level 3 destination vector sequences encode the upstream immediate early CMV promoter/enhancer, nuclear localisation signal (NLS), and haemagglutinin epitope (HA) as well as the downstream the *Fok*I nuclease domain. Additionally they include the DNA encoding the initial 'T' binding site and the terminal half-binding site (position 19 of the TALEN) at the 5' and 3' adaptor ends respectively. As each TALEN has a specific terminal binding site corresponding to one of the four base pairs, there are four separate destination vectors with NI, NG, NK and

HD diresidues. Since *Fok*I is an obligate heterodimer, left and right TALEN subunits are required to produce a DSB at the target site. To generate TALENs against HBV, the modular cloning TALE repeat assembly kit (Morbitzer et al., 2011) was used in conjunction with the modified *Fok*I nuclease vectors (Mussolino et al., 2011) (Figures 2.1 – 2.4). Four sets of TALENs targeting the *polymerase*, *core* and *surface* genes were synthesised using this TALE Golden Gate modular cloning system. All TALENs were designed in pairs to promote double stranded DNA cleavage by dimerisation of the *Fok*I endonuclease domains. Each left and right TALEN subunit was engineered to target a 19 bp DNA sequence beginning with a thymine. For optimal nuclease cleavage, a 13 bp spacer region was chosen to separate TALEN subunits.

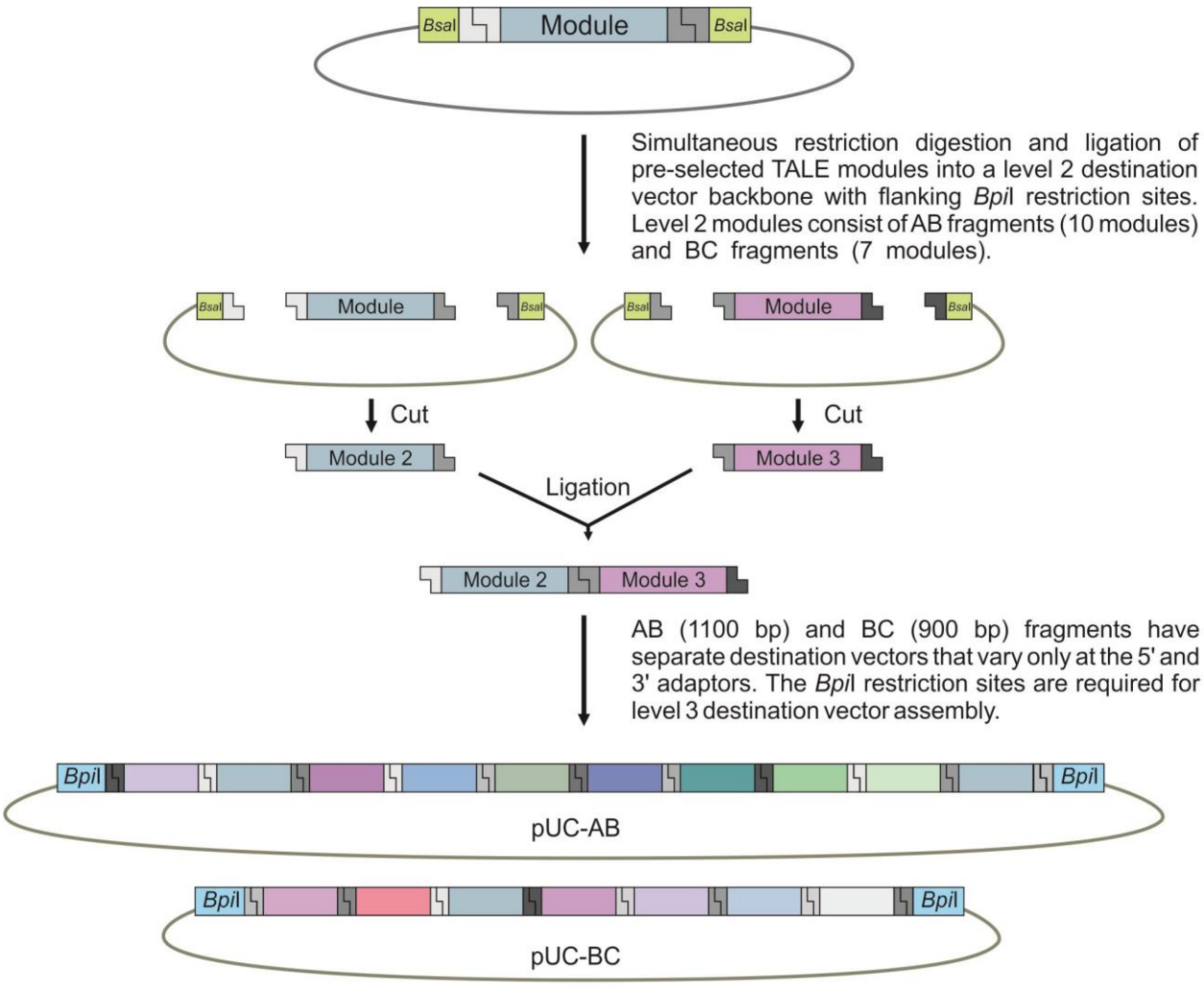

Figure 2.3: Assembly of AB and BC TALE fragments. The pre-assembled TALE module library is used to assemble AB and BC fragments using a simultaneous cut-ligation reaction. The first 10 TALE modules are cloned into pUC-AB whilst the remaining 7 modules are cloned into pUC-BC. Both AB and BC fragments are flanked by *Bpi*I restriction sites required for the second cut-ligation reaction and cloning of the complete TALE array into the level 3 destination vector.

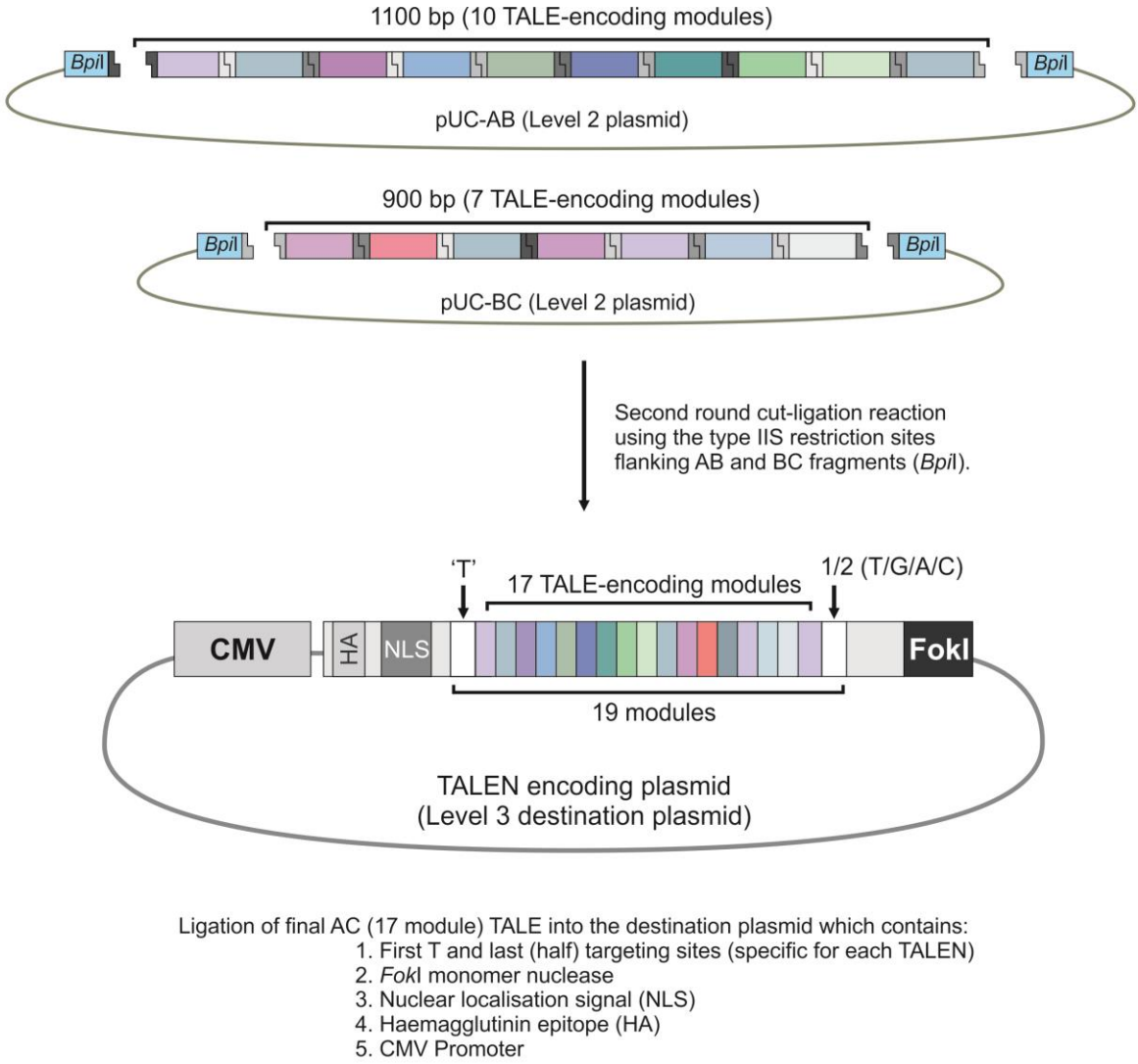

Ligation of final AC (17 module) TALE into the destination plasmid which contains:
1. First T and last (half) targeting sites (specific for each TALEN)
2. *Fok*I monomer nuclease
3. Nuclear localisation signal (NLS)
4. Haemagglutinin epitope (HA)
5. CMV Promoter

Figure 2.4: Assembly of a complete TALEN subunit. The type IIS restriction enzyme, *Bpi*I, was used to cut the AB and BC fragments before ligation, to form the 17 module AC TALE. Subsequently this TALE was cloned into a TALEN subunit-specific level 3 destination vector, which encodes all the necessary upstream and downstream sequences required to synthesise a fully functioning TALEN. These include DNA sequences for: the CMV promoter region to drive TALEN transcription; the nuclear localisation signal (NLS) which is required to traffic the protein into the cell nucleus; and the *Fok*I nuclease domain to enable DNA cleavage. Additionally a haemagglutinin epitope (HA) sequence is included at the N-terminal, which acts as a protein tag for TALEN expression.

2.2 Results

2.2.1 Targeting HBV cccDNA

TALEN target sites were identified by following basic design rules. These included: 1) Each TALEN subunit should comprise of a 19 bp binding site; 2) A 12 - 21 bp spacer between TALEN pair subunits is required for optimal nuclease activity; 3) Each subunit binding site must begin with a 'T'; and 4) The initial 'T' binding site should not be followed by a 'T' at position 2 and an 'A' at position 3. That is, avoid 5' – TTA NNN NNN NNN NNN NNN N – 3' sites. Four potential viral DNA binding sites were selected for targeting. By taking advantage of the compact HBV genome arrangement and overlapping reading frames, the selected anti-HBV TALENs target more than one genomic feature (Figure 2.5). The *surface* (S) and *core* (C) TALENs will cleave the overlapping *polymerase* ORF, whilst the two *polymerase* TALENs (P1 and P2) bind to sequences encoding transcriptional regulatory elements. DNA sequences targeted by each of the selected left and right subunit binding sites are given in Table 2.3. The left subunit is designed to bind to the sense strand whilst the right subunit is designed to bind to the antisense strand. The complete cccDNA target site for each TALEN pair, including the spacer region, is 51 bp. Multiple alignments of twenty six different viral genotypes and sub-genotypes showed high sequence homology at the selected TALEN target sites (Appendix 8.2). This is particularly true for the S TALEN, and suggests that the HBV-targeting nucleases generated here may be effective across HBV genotypes.

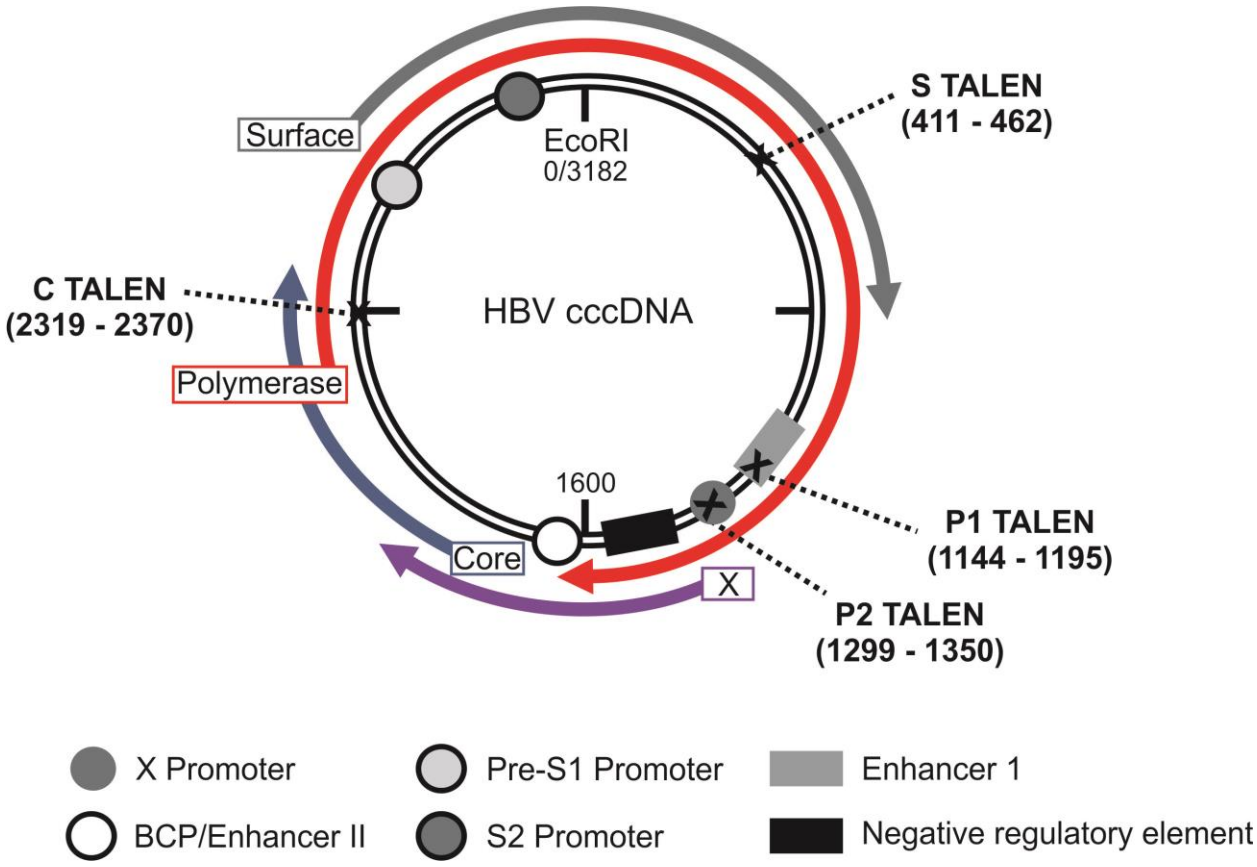

Figure 2.5: HBV cccDNA TALEN binding sites. TALENs were designed to bind to three of the four overlapping ORFs of HBV. In addition to targeting the *surface* and *core* ORFs the S and C TALENs also target the HBV *polymerase* ORF. The P1 TALEN binds the *polymerase* ORF and Enhancer I, whilst the P2 TALEN binds the *polymerase* ORF as well as the *HBx* promoter region. The HBV genome coordinates of each complete TALEN binding site are shown in parentheses, and follow the same HBV genome orientation shown in Figure 1.1.

Table 2.3: HBV TALEN target sites

HBV targets	TALEN binding sites (5' to 3')	
	Left subunit (L) **Sense strand site**	**Right subunit (R)** **Antisense strand site**
Surface (S)	TCCTGCTGCTATGCCTCAT	TACCTTGATAGTCCAGAAG
Core (C)	TATCAACACTTCCGGAGAC	TAGGGGACCTGCCTCGTCG
Polymerase 1 (P1)	TACCCCGTTGCCCGGCAAC	TGCGTCAGCAAACACTTGG
Polymerase 2 (P2)	TCGCAGCAGGTCTGGAGCA	TAGGACAACAGAGTTATCA

2.2.2 Modular assembled TALENs

Position-specific modules were chosen for dTALE assembly of the left (L) and right (R) subunits to synthesise S, C, P1 and P2 target-specific TALENs. Simultaneous cut-ligation reactions were employed to generate AB and BC fragments, which were subsequently verified by colony PCR, restriction digestion and sequencing. Representations of these colony PCR reactions are shown in Figure 2.6. The NI, NK, NG and HD RVDs were exclusively used to generate S and P2 dTALE arrays whilst the NK RVD was substituted for the NN module during C and P1 dTALE assembly, at all TALE array positions except for the final half-site. The level 3 destination vector encoding the NN RVD at the terminal half-site was not available during anti-HBV TALEN synthesis. Consequently, the NK RVD encoding level 3 destination plasmid vector was used to generate SR, CR and P1R TALEN subunits. The TALE repeat assembly library also included plasmids encoding the NS RVD, however this module was not used in anti-HBV TALEN assembly. On average a total of 50 colonies were screened for each AB fragment assembly whilst only 25 colonies were screened for BC fragments. This is primarily because the AB fragments are longer, with a total of 10 modules, versus the BC fragments with only 7 modules, making the cut-ligation reaction somewhat less efficient. Colony PCR reactions identified a number of potential AB and BC fragment clones for each TALE subunit. These were subsequently analysed by *Bpi*I restriction digestion (Figure 2.7) and sequencing to verify position-specific assembly. As shown in Figure 2.7, colony PCR amplification may only be used to identify potential positive clones, as further verification by restriction digestion is necessary to confirm complete assembly. Colonies 373 and 378 contain complete BC fragments of approximately 900 bp each, whilst colony 385 has a BC fragment of 800 bp. This smaller BC

fragment is likely to be lacking a single module as a result of an incomplete cut-ligation reaction. Both colonies 186 and 187 represent complete AB fragments. This was based on restriction digestion analysis that showed a distinct band, of approximately 1100 bp, which represents a ten module assembly. Positive AB and BC clones were subjected to confirmatory sequencing.

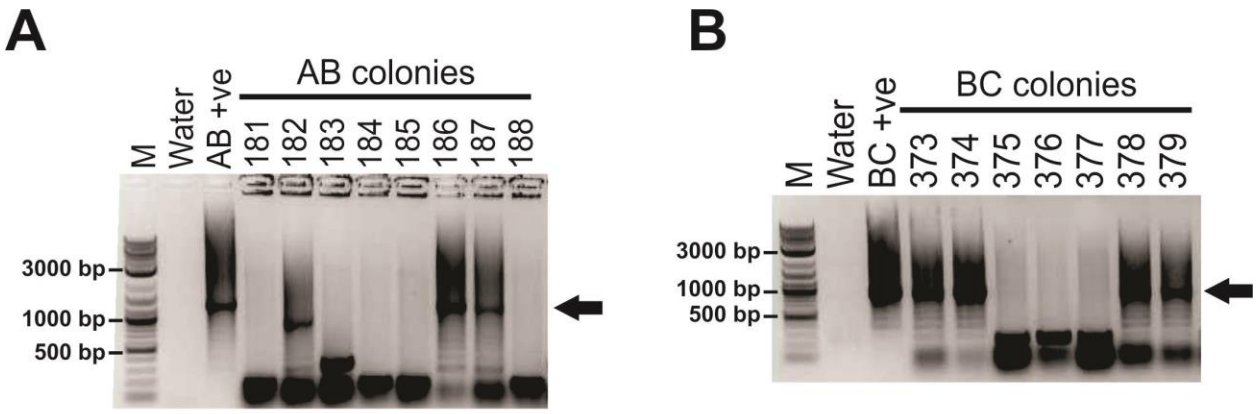

Figure 2.6: Initial identification of complete cut-ligation reactions. Representative colony PCR products for SL dTALE AB fragments (**A**) and BC fragments (**B**) are shown. Each lane represents an individual colony picked from a bacterial plate. Arrows indicate the correct sizes of 10 module and 7 module PCR products at approximately 1100 bp and 900 bp respectively. Incomplete cut-ligation reactions result in smaller banding patterns showing only partial synthesis of the fragments. Positive (AB +ve and BC +ve) and negative (water) PCR controls were included.

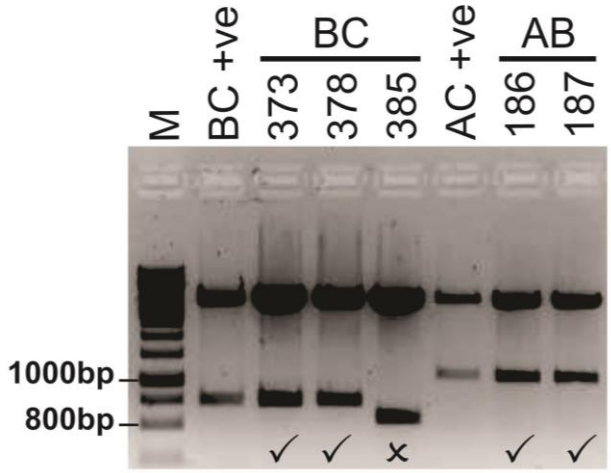

Figure 2.7: Confirmation of AB and BC fragment assembly from colony PCR selected plasmid extractions. Restriction digestion with *Bpi*I was used to identify complete 10 module and 7 module clones. The correct band migration patterns of BC fragments are ~ 4500 bp and 900 bp whilst AB fragments are ~ 4500 bp and 1100 bp. Colonies 373 and 378 represent complete BC fragments and colonies 186 and 187 represent complete AB fragments. AB +ve and BC +ve were included as restriction digestion guides.

Sequence-verified AB and BC fragments were used to generate complete TALEN subunits. This was achieved through a second cut-ligation reaction where corresponding AB and BC arrays were cloned into the level 3 destination vector as a 17 module dTALE. These destination vectors were selected specifically for each TALEN subunit, as the final half-site, which is located at the 3' end of the vector cloning site, is unique to each array. This second assembly is far more efficient than the first reaction and only 10 - 15 colonies were screened for each TALEN subunit. As shown in Figure 2.8, colony PCR analysis was used to identify potentially positive clones, where seven out of eight SL TALEN subunit plasmids have complete AC fragments. Two different restriction digestions (*Pvu*II-HF and *Pvu*II-HF/*Hinc*II), were required to confirm complete AC ligations. Figure 2.9 shows two potential P1R TALEN subunit clones 578 and 593. Although both clones appear to have the correct band migration pattern for *Pvu*II-HF/*Hinc*II double digestion (2000 bp, 1700 bp, 1200 bp, 950 bp, and 350 bp), the 578 clone has additional bands in the *Pvu*II-HF single digestion and was therefore excluded. Completeness of the AC fragments was verified by sequencing. The final amino acid sequences of each 18 repeat module dTALE are shown in Table 2.4. In addition to the final half-site, all level 3 destination vectors contain the initial 'T' binding module at the 5' ligation end, making the final TALEN binding site 19 nucleotides. The DNA sequences encoding the early CMV promoter, HA tag and NLS signal are upstream of the initial 'T' module, whilst the sequence encoding the *Fok*I nuclease domain is downstream of the half-site.

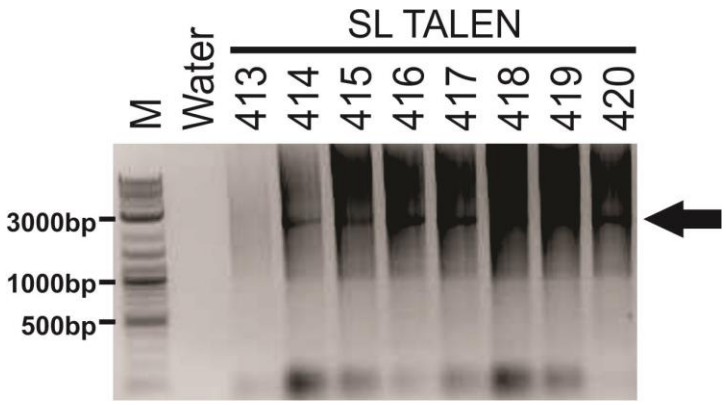

Figure 2.8: Identification of complete AC cut-ligations. Eight different colony PCR products for the SL TALEN subunit's AC ligations are shown. Bands corresponding to approximately 2800 bp indicate complete 17 module AC fragments (shown by the arrow). AC cut-ligation reactions are more efficient than AB and BC. Negative water controls were included during PCR reactions.

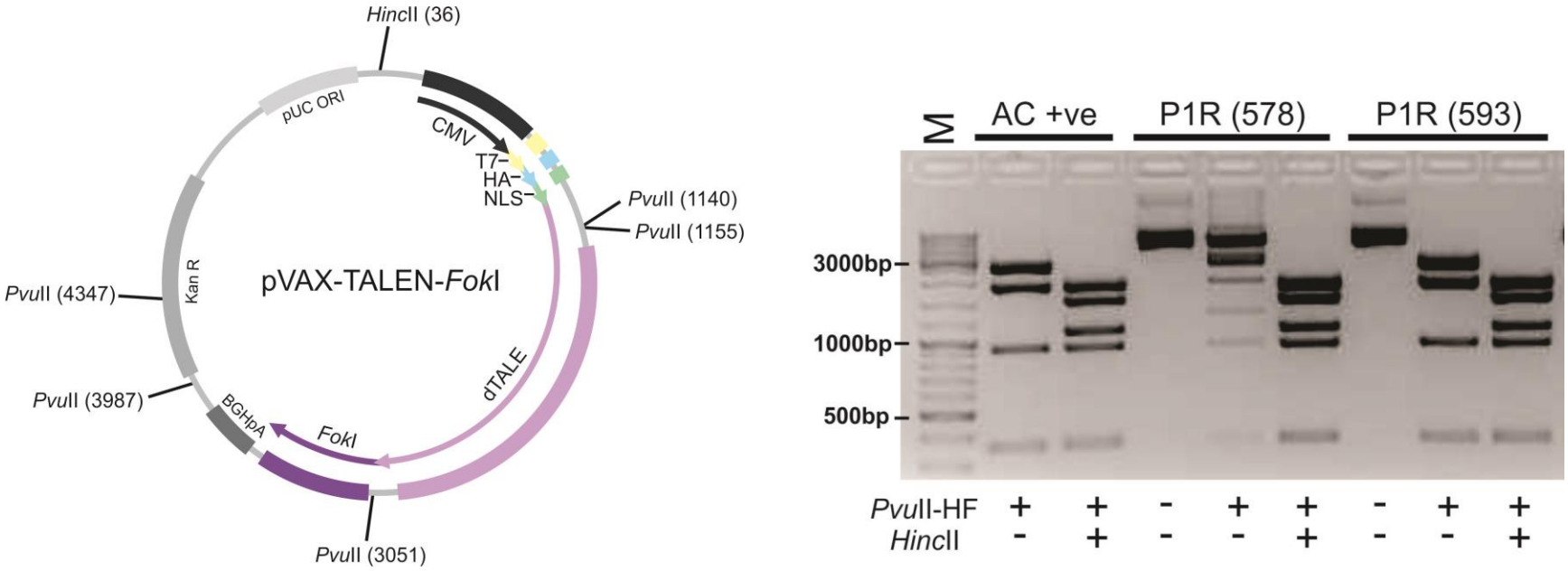

Figure 2.9: Confirmation of complete dTALE assembly. Two different restriction digestions were used to verify complete 17 module AC cut-ligation reactions. The final TALEN plasmid map with *Pvu*II and *Hinc*II restriction sites is shown on the left and agarose gel electrophoresis restriction digestion migration patterns of selected TALEN clones is shown on the right. The P1R TALEN clones 578 and 593 are represented, with a positive AC control to validate band migration patterns. Complete AC ligations will result in 2800 bp, 2000 bp, 950 bp, and 350 bp products with *Pvu*II-HF digestion, and 2000 bp, 1700 bp, 1200 bp, 950 bp, and 350 bp products with *Pvu*II-HF/*Hinc*II double digestion. The 593 clone migration pattern matches that of the positive control whilst the 578 clone contains additional bands in the *Pvu*II-HF digestion. A single positive dTALE clone for each TALEN subunit was selected.

Table 2.4: Final amino acid sequences of all eight HBV-targeting TALEN subunits*

	d-TALE‡	Left subunit (L)	DNA target	d-TALE‡	Right subunit (R)	DNA target
S TALEN	2	LTPEQVVAIAS**HD**GGKQALETVQALLPVLCQAHG	**C**	2	LTPDQVVAIAS**NI**GGKQALETVQRLLPVLCQAHG	**A**
	3	LTPEQVVAIAS**HD**GGKQALETVQALLPVLCQAHG	**C**	3	LTPEQVVAIAS**HD**GGKQALETVQALLPVLCQAHG	**C**
	4	LIPQQVVAIAS**NG**GGKQALETVQRLLPVLCQDHG	**T**	4	LTPEQVVAIAS**HD**GGKQALETVQALLPVLCQAHG	**C**
	5	LTPEQVVAIAS**NK**GGKQALETVQRLLPVLCQAHG	**G**	5	LIPQQVVAIAS**NG**GGKQALETVQRLLPVLCQDHG	**T**
	6	LTPEQVVAIAS**HD**GGKQALETVQALLPVLCQAHG	**C**	6	LIPQQVVAIAS**NG**GGKQALETVQRLLPVLCQDHG	**T**
	7	LIPQQVVAIAS**NG**GGKQALETVQRLLPVLCQDHG	**T**	7	LTPEQVVAIAS**NK**GGKQALETVQRLLPVLCQAHG	**G**
	8	LTPEQVVAIAS**NK**GGKQALETVQRLLPVLCQAHG	**G**	8	LTPDQVVAIAS**NI**GGKQALETVQRLLPVLCQAHG	**A**
	9	LTPEQVVAIAS**HD**GGKQALETVQALLPVLCQAHG	**C**	9	LIPQQVVAIAS**NG**GGKQALETVQRLLPVLCQDHG	**T**
	10	LIPQQVVAIAS**NG**GGKQALETVQRLLPVLCQDHG	**T**	10	LTPDQVVAIAS**NI**GGKQALETVQRLLPVLCQAHG	**A**
	11	LTPDQVVAIAS**NI**GGKQALETVQRLLPVLCQAHG	**A**	11	LTPEQVVAIAS**NK**GGKQALETVQRLLPVLCQAHG	**G**
	12	LIPQQVVAIAS**NG**GGKQALETVQRLLPVLCQDHG	**T**	12	LIPQQVVAIAS**NG**GGKQALETVQRLLPVLCQDHG	**T**
	13	LTPEQVVAIAS**NK**GGKQALETVQRLLPVLCQAHG	**G**	13	LTPEQVVAIAS**HD**GGKQALETVQALLPVLCQAHG	**C**
	14	LTPEQVVAIAS**HD**GGKQALETVQALLPVLCQAHG	**C**	14	LTPEQVVAIAS**HD**GGKQALETVQALLPVLCQAHG	**C**
	15	LTPEQVVAIAS**HD**GGKQALETVQALLPVLCQAHG	**C**	15	LTPDQVVAIAS**NI**GGKQALETVQRLLPVLCQAHG	**A**
	16	LIPQQVVAIAS**NG**GGKQALETVQRLLPVLCQDHG	**T**	16	LTPEQVVAIAS**NK**GGKQALETVQRLLPVLCQAHG	**G**
	17	LTPEQVVAIAS**HD**GGKQALETVQALLPVLCQAHG	**C**	17	LTPDQVVAIAS**NI**GGKQALETVQRLLPVLCQAHG	**A**
	18	LTPDQVVAIAS**NI**GGKQALETVQRLLPVLCQAHG	**A**	18	LTPDQVVAIAS**NI**GGKQALETVQRLLPVLCQAHG	**A**
	19	LIPQQVVAIAS**NG**GGKQALETVQRLLPVLCQDHG	**T**	19	LTPEQVVAIAS**NK**GGKQALETVQRLLPVLCQAHG	**G**

	d-TALE‡	Left subunit (L)	DNA target	d-TALE‡	Right subunit (R)	DNA target
C TALEN	2	LTPDQVVAIAS**NI**GGKQALETVQRLLPVLCQAHG	**A**	2	LTPDQVVAIAS**NI**GGKQALETVQRLLPVLCQAHG	**A**
	3	LIPQQVVAIAS**NG**GGKQALETVQRLLPVLCQDHG	**T**	3	LTPEQVVAIAS**NN**GGKQALETVQRLLPVLCQAHG	**G**
	4	LTPEQVVAIAS**HD**GGKQALETVQALLPVLCQAHG	**C**	4	LTPEQVVAIAS**NN**GGKQALETVQRLLPVLCQAHG	**G**
	5	LTPDQVVAIAS**NI**GGKQALETVQRLLPVLCQAHG	**A**	5	LTPEQVVAIAS**NN**GGKQALETVQRLLPVLCQAHG	**G**
	6	LTPDQVVAIAS**NI**GGKQALETVQRLLPVLCQAHG	**A**	6	LTPEQVVAIAS**NN**GGKQALETVQRLLPVLCQAHG	**G**
	7	LTPEQVVAIAS**HD**GGKQALETVQALLPVLCQAHG	**C**	7	LTPDQVVAIAS**NI**GGKQALETVQRLLPVLCQAHG	**A**
	8	LTPDQVVAIAS**NI**GGKQALETVQRLLPVLCQAHG	**A**	8	LTPEQVVAIAS**HD**GGKQALETVQALLPVLCQAHG	**C**
	9	LTPEQVVAIAS**HD**GGKQALETVQALLPVLCQAHG	**C**	9	LTPEQVVAIAS**HD**GGKQALETVQALLPVLCQAHG	**C**
	10	LIPQQVVAIAS**NG**GGKQALETVQRLLPVLCQDHG	**T**	10	LIPQQVVAIAS**NG**GGKQALETVQRLLPVLCQDHG	**T**
	11	LIPQQVVAIAS**NG**GGKQALETVQRLLPVLCQDHG	**T**	11	LTPEQVVAIAS**NN**GGKQALETVQRLLPVLCQAHG	**G**
	12	LTPEQVVAIAS**HD**GGKQALETVQALLPVLCQAHG	**C**	12	LTPEQVVAIAS**HD**GGKQALETVQALLPVLCQAHG	**C**
	13	LTPEQVVAIAS**HD**GGKQALETVQALLPVLCQAHG	**C**	13	LTPEQVVAIAS**HD**GGKQALETVQALLPVLCQAHG	**C**
	14	LTPEQVVAIAS**NN**GGKQALETVQRLLPVLCQAHG	**G**	14	LIPQQVVAIAS**NG**GGKQALETVQRLLPVLCQDHG	**T**
	15	LTPEQVVAIAS**NN**GGKQALETVQRLLPVLCQAHG	**G**	15	LTPEQVVAIAS**HD**GGKQALETVQALLPVLCQAHG	**C**
	16	LTPDQVVAIAS**NI**GGKQALETVQRLLPVLCQAHG	**A**	16	LTPEQVVAIAS**NN**GGKQALETVQRLLPVLCQAHG	**G**
	17	LTPEQVVAIAS**NN**GGKQALETVQRLLPVLCQAHG	**G**	17	LIPQQVVAIAS**NG**GGKQALETVQRLLPVLCQDHG	**T**
	18	LTPDQVVAIAS**NI**GGKQALETVQRLLPVLCQAHG	**A**	18	LTPEQVVAIAS**HD**GGKQALETVQALLPVLCQAHG	**C**
	19	LTPEQVVAIAS**HD**GGKQALETVQALLPVLCQAHG	**C**	19	LTPEQVVAIAS**NK**GGKQALETVQRLLPVLCQAHG	**G**

	d-TALE‡	Left subunit (L)	DNA target	d-TALE‡	Right subunit (R)	DNA target
P1 TALEN	2	LTPDQVVAIAS**NI**GGKQALETVQRLLPVLCQAHG	**A**	2	LTPEQVVAIAS**NN**GGKQALETVQRLLPVLCQAHG	**G**
	3	LTPEQVVAIAS**HD**GGKQALETVQALLPVLCQAHG	**C**	3	LTPEQVVAIAS**HD**GGKQALETVQALLPVLCQAHG	**C**
	4	LTPEQVVAIAS**HD**GGKQALETVQALLPVLCQAHG	**C**	4	LTPEQVVAIAS**NN**GGKQALETVQRLLPVLCQAHG	**G**
	5	LTPEQVVAIAS**HD**GGKQALETVQALLPVLCQAHG	**C**	5	LIPQQVVAIAS**NG**GGKQALETVQRLLPVLCQDHG	**T**
	6	LTPEQVVAIAS**HD**GGKQALETVQALLPVLCQAHG	**C**	6	LTPEQVVAIAS**HD**GGKQALETVQALLPVLCQAHG	**C**
	7	LTPEQVVAIAS**NN**GGKQALETVQRLLPVLCQAHG	**G**	7	LTPDQVVAIAS**NI**GGKQALETVQRLLPVLCQAHG	**A**
	8	LIPQQVVAIAS**NG**GGKQALETVQRLLPVLCQDHG	**T**	8	LTPEQVVAIAS**NN**GGKQALETVQRLLPVLCQAHG	**G**
	9	LIPQQVVAIAS**NG**GGKQALETVQRLLPVLCQDHG	**T**	9	LTPEQVVAIAS**HD**GGKQALETVQALLPVLCQAHG	**C**
	10	LTPEQVVAIAS**NN**GGKQALETVQRLLPVLCQAHG	**G**	10	LTPDQVVAIAS**NI**GGKQALETVQRLLPVLCQAHG	**A**
	11	LTPEQVVAIAS**HD**GGKQALETVQALLPVLCQAHG	**C**	11	LTPDQVVAIAS**NI**GGKQALETVQRLLPVLCQAHG	**A**
	12	LTPEQVVAIAS**HD**GGKQALETVQALLPVLCQAHG	**C**	12	LTPDQVVAIAS**NI**GGKQALETVQRLLPVLCQAHG	**A**
	13	LTPEQVVAIAS**HD**GGKQALETVQALLPVLCQAHG	**C**	13	LTPEQVVAIAS**HD**GGKQALETVQALLPVLCQAHG	**C**
	14	LTPEQVVAIAS**NN**GGKQALETVQRLLPVLCQAHG	**G**	14	LTPDQVVAIAS**NI**GGKQALETVQRLLPVLCQAHG	**A**
	15	LTPEQVVAIAS**NN**GGKQALETVQRLLPVLCQAHG	**G**	15	LTPEQVVAIAS**HD**GGKQALETVQALLPVLCQAHG	**C**
	16	LTPEQVVAIAS**HD**GGKQALETVQALLPVLCQAHG	**C**	16	LIPQQVVAIAS**NG**GGKQALETVQRLLPVLCQDHG	**T**
	17	LTPDQVVAIAS**NI**GGKQALETVQRLLPVLCQAHG	**A**	17	LIPQQVVAIAS**NG**GGKQALETVQRLLPVLCQDHG	**T**
	18	LTPDQVVAIAS**NI**GGKQALETVQRLLPVLCQAHG	**A**	18	LTPEQVVAIAS**NN**GGKQALETVQRLLPVLCQAHG	**G**
	19	LTPEQVVAIAS**HD**GGKQALETVQALLPVLCQAHG	**C**	19	LTPEQVVAIAS**NK**GGKQALETVQRLLPVLCQAHG	**G**

	d-TALE‡	Left subunit (L)	DNA target	d-TALE‡	Right subunit (R)	DNA target
P2 TALEN	2	LTPEQVVAIAS**HD**GGKQALETVQALLPVLCQAHG	**C**	2	LTPDQVVAIAS**NI**GGKQALETVQRLLPVLCQAHG	**A**
	3	LTPEQVVAIAS**NK**GGKQALETVQRLLPVLCQAHG	**G**	3	LTPEQVVAIAS**NK**GGKQALETVQRLLPVLCQAHG	**G**
	4	LTPEQVVAIAS**HD**GGKQALETVQALLPVLCQAHG	**C**	4	LTPEQVVAIAS**NK**GGKQALETVQRLLPVLCQAHG	**G**
	5	LTPDQVVAIAS**NI**GGKQALETVQRLLPVLCQAHG	**A**	5	LTPDQVVAIAS**NI**GGKQALETVQRLLPVLCQAHG	**A**
	6	LTPEQVVAIAS**NK**GGKQALETVQRLLPVLCQAHG	**G**	6	LTPEQVVAIAS**HD**GGKQALETVQALLPVLCQAHG	**C**
	7	LTPEQVVAIAS**HD**GGKQALETVQALLPVLCQAHG	**C**	7	LTPDQVVAIAS**NI**GGKQALETVQRLLPVLCQAHG	**A**
	8	LTPDQVVAIAS**NI**GGKQALETVQRLLPVLCQAHG	**A**	8	LTPDQVVAIAS**NI**GGKQALETVQRLLPVLCQAHG	**A**
	9	LTPEQVVAIAS**NK**GGKQALETVQRLLPVLCQAHG	**G**	9	LTPEQVVAIAS**HD**GGKQALETVQALLPVLCQAHG	**C**
	10	LTPEQVVAIAS**NK**GGKQALETVQRLLPVLCQAHG	**G**	10	LTPDQVVAIAS**NI**GGKQALETVQRLLPVLCQAHG	**A**
	11	LIPQQVVAIAS**NG**GGKQALETVQRLLPVLCQDHG	**T**	11	LTPEQVVAIAS**NK**GGKQALETVQRLLPVLCQAHG	**G**
	12	LTPEQVVAIAS**HD**GGKQALETVQALLPVLCQAHG	**C**	12	LTPDQVVAIAS**NI**GGKQALETVQRLLPVLCQAHG	**A**
	13	LIPQQVVAIAS**NG**GGKQALETVQRLLPVLCQDHG	**T**	13	LTPEQVVAIAS**NK**GGKQALETVQRLLPVLCQAHG	**G**
	14	LTPEQVVAIAS**NK**GGKQALETVQRLLPVLCQAHG	**G**	14	LIPQQVVAIAS**NG**GGKQALETVQRLLPVLCQDHG	**T**
	15	LTPEQVVAIAS**NK**GGKQALETVQRLLPVLCQAHG	**G**	15	LIPQQVVAIAS**NG**GGKQALETVQRLLPVLCQDHG	**T**
	16	LTPDQVVAIAS**NI**GGKQALETVQRLLPVLCQAHG	**A**	16	LTPDQVVAIAS**NI**GGKQALETVQRLLPVLCQAHG	**A**
	17	LTPEQVVAIAS**NK**GGKQALETVQRLLPVLCQAHG	**G**	17	LIPQQVVAIAS**NG**GGKQALETVQRLLPVLCQDHG	**T**
	18	LTPEQVVAIAS**HD**GGKQALETVQALLPVLCQAHG	**C**	18	LTPEQVVAIAS**HD**GGKQALETVQALLPVLCQAHG	**C**
	19	LTPDQVVAIAS**NI**GGKQALETVQRLLPVLCQAHG	**A**	19	LTPDQVVAIAS**NI**GGKQALETVQRLLPVLCQAHG	**A**

* Initial ‘T’ binding modules have been excluded from these sequences

‡ Indicating module position, with full amino acid sequence, in the final dTALE array (initial T at position 1)

2.3 Discussion

HBV cccDNA targeting TALENs were successfully generated using the TALE repeat assembly method. The position-specific module library and two-step cut-ligation protocol made it relatively simple to construct these dTALEs. The first cut-ligation reaction, to create AB and BC fragments, can easily be accomplished in 4 – 6 days, whilst the second AC assembly, can be completed in 4 days. The major rate limiting step in this Golden Gate cloning strategy is identification of complete AB fragments. As there are 10 modules in this particular array, the cut-ligation reactions are sometimes less efficient and a number of additional colonies need to be screened. An alternative is to split the AB ligation into two 5-module arrays. The AC cut-ligation reactions will then consist of three fragments, two 5 module and one 7 module, to make up the complete dTALE-encoding sequences. Although this would improve AB fragment assembly, it reduces the efficiency of AC cut-ligations, which are normally very proficient. Because of this, all HBV TALENs were rather assembled using the AB and BC fragments.

Although the S, C, P1 and P2 TALEN binding sites were selected by manually searching the viral genome for appropriate targets, the process was very laborious and identifying potentially suitable sites was difficult. This is mainly because these sites require an initial thymine on both the left and right subunits and an optimal spacer region, which restricts the number of potential targets. Most naturally occurring TALEs require the initial ‘T’ binding site for efficient DNA targeting (Boch et al., 2009; Moscou and Bogdanove, 2009), which has also been shown for TALENs (Miller et al., 2011; Mussolino et al., 2011; Zhang et al., 2011). Additionally, adjusting the spacer region affects TALEN cleavage efficacy (Christian et al., 2012; Mussolino et al.,

2011). As the final level 3 destination vectors were synthesised by Mussolino and colleagues (Mussolino et al., 2011), an optimal spacer region of 13 bp was selected. However spacer regions of 12, 14 or 21 bp would have been acceptable. Recently there have been a number of online TAL effector and TALEN design tools to assist with finding potential target sites. These include the TAL Effector Nucleotide Targeter 2.0 (Doyle et al., 2012), TALEN™ Hit software (Cellectis Bioresearch, France), idTALE (King Abdullah University of Science and Technology, Saudi Arabia) and Mojo Hand (Neff et al., 2013). The ZiFiT software (Sander et al., 2010b; Sander et al., 2007) which was originally used to design ZFNs has also been adapted to identify TALEN target sites. Although these software tools may be used to design potential TALEN sites, they have only recently become available and more detailed comparisons between the different platforms still needs to be established. Nevertheless, as input values may be adjusted automatically, such as the selection of RVDs and assignment of specific spacer regions, these computer-based programs should make it easier to find other potential anti-HBV TALEN binding sites.

CHAPTER 3 – Use of TALENs to achieve targeted inactivation of HBV cccDNA

3.1 Introduction

TALENs have recently been designed to create DSBs at endogenous human DNA target sites resulting in permanent gene alterations. This occurs through activation of the host cell's DNA repair pathways, to initiate either NHEJ or HR repair (reviewed by Bernstein and Rothstein, 2009; Lieber, 2010). As NHEJ is error-prone, TALEN cleavage may be used to introduce mutations at the target site (Figure 3.1). These mutations could be insertions, deletions, substitutions or a combination of all three. This type of targeted mutagenesis is useful when gene disruption or knock-out mutations are desired.

To establish targeted mutagenesis of human genes, mammalian cells have been transfected with various site-specific TALENs (Cermak et al., 2011; Ding et al., 2013; Kim et al., 2013a; Miller et al., 2011; Mussolino et al., 2011; Reyon et al., 2012; Stroud et al., 2013). The initial *in vitro* cleavage efficacy of these TALENs is often determined using plasmid target binding sites in conjunction with reporter gene systems. These initial investigations are often preferred over direct endogenous gene targeting, as it is easier to measure the amount of TALEN cleavage with a reporter system. Additionally, as TALEN transfection efficiencies and NHEJ events are not universally conserved throughout a cell population, it is possible to select individual cells that have the desired TALEN-mediated targeted disruption. Once TALEN efficiency has been established, the endogenous DNA targets may then be investigated. To facilitate the selection

of successfully mutated endogenous genes, a surrogate reporter system may be included during TALEN transfections (Kim et al., 2011). Although the exogenous surrogate reporter has its own nuclease cleavage site to activate fluorescent protein expression, the likelihood of selecting a cell with both exogenous and endogenous gene disruption is higher than without any selection. As a number of these TALEN target genes are involved in monogenic disorders or disease progression, selected single clones with a defined mutation can be expanded into a stable cell line. These cells can be generated from immortalised cultures, induced pluripotent stem cells (iPSC), or embryonic stem cells (ESC) (Ding et al., 2013).

Although TALEN-mediated targeted mutagenesis of human genes could provide a unique therapeutic approach to disabling unwanted gene expression permanently, NHEJ tends to be an indiscriminate repair process. Consequently, a more controlled approach to gene manipulation is necessary. TALEN directed HR would be a valuable tool for restoring mutated genes, however this repair process occurs infrequently. To improve this, donor sequences may be included to trigger homology directed repair (HDR) following nuclease cleavage (Figure 3.1) (Porteus and Baltimore, 2003; Urnov et al., 2005). These donors have flanking DNA sequences that are homologous to the nuclease binding sites and are able to induce HR repair at the target site following cleavage. HDR can also be used to add specific DNA sequences or repair gene mutations (Hockemeyer et al., 2009; Moehle et al., 2007). TALENs have successfully been used in combination with donor sequences to induce HDR in zebrafish (Bedell et al., 2012; Zu et al., 2013), and mammalian cells (Hockemeyer et al., 2011; Miller et al., 2011; Sun et al., 2012; Valton et al., 2012).

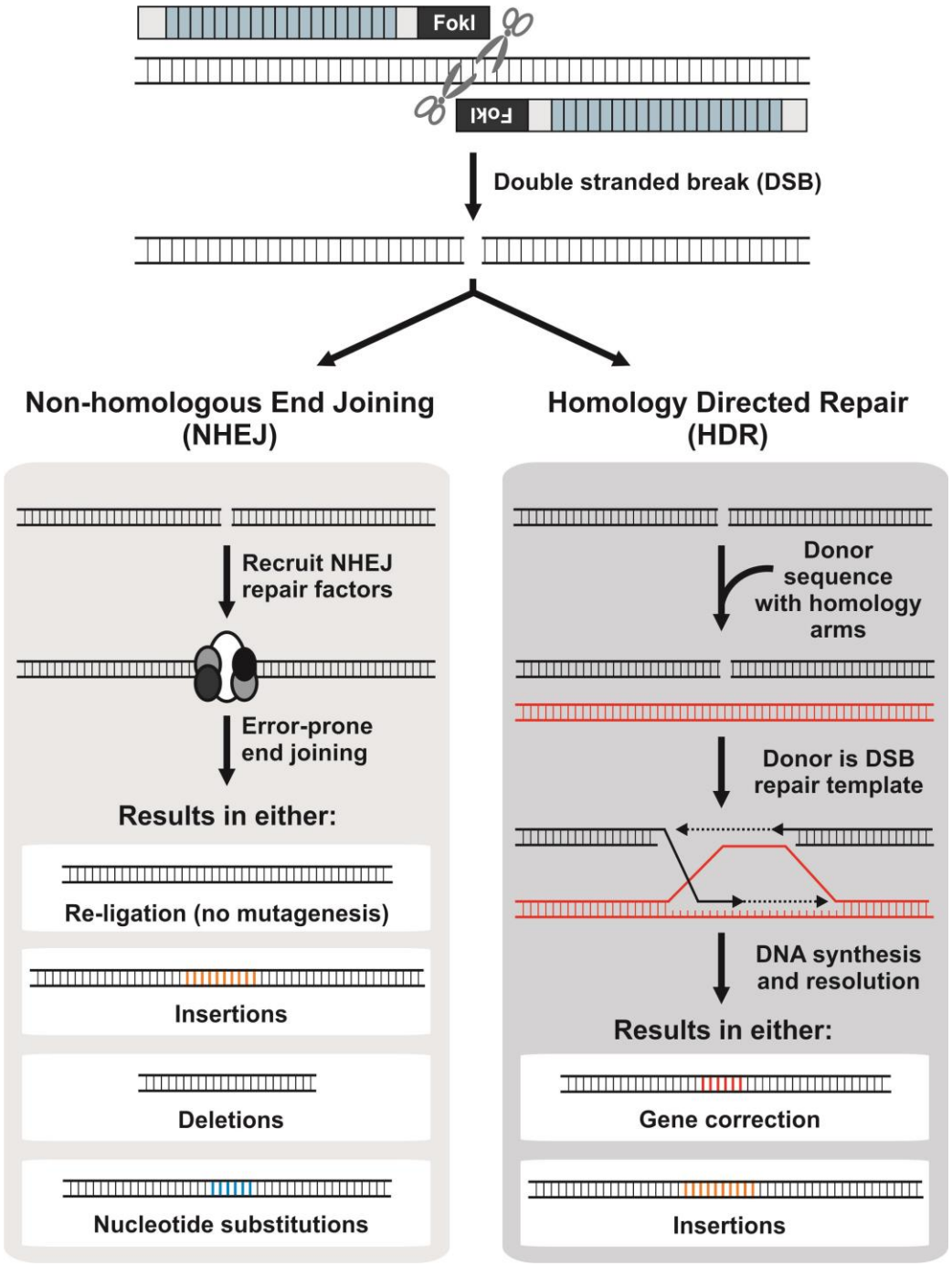

Figure 3.1: Cellular repair pathways used during TALEN-mediated mutagenesis or gene correction. TALEN dimerisation and cleavage at the DNA target sites result in a DSB which is most often repaired by NHEJ or HDR. When NHEJ is triggered, DSB repair factors are recruited to the site resulting in either re-ligation of the two strands or mutagenic events (insertions, deletions or substitutions). If a donor sequence is used, the HDR pathway can be triggered to either repair or insert a gene of interest at the DSB site. As the donor sequence has homologous arms, it can act as a repair template.

Whether a NHEJ or HDR TALEN-mediated gene therapy approach is used, DNA cleavage is not always easily achieved. A high percentage of targeted disruption in a plasmid reporter does not always translate to efficient cleavage at the endogenous gene locus (Sun et al., 2012). Nuclease cleavage efficiency has been shown to differ between cell lines, target sites, and donor sequences (Hockemeyer et al., 2011). This seems to be a multi-factorial phenomenon which is not completely understood but may be influenced by chromosomal methylation (Kim et al., 2013a; Valton et al., 2012), subunit spacer length (Li et al., 2011b; Miller et al., 2011; Mussolino et al., 2011), or the incorporation of specific 'strong' RVDs, such as HD and NN (Christian et al., 2012; Streubel et al., 2012).

To date, TALEN research has focused on creating transgenic animal models or correcting endogenous human genes. Although on-going investigations into creating HIV-resistant T-cells are promising, the latent pro-viral DNA has not been targeted. Instead, Δ32-like mutations are generated within the endogenous human CCR5 receptor-encoding sequence to inhibit viral entry (Miller et al., 2011; Mussolino et al., 2011). Engineering TALENs to directly target DNA viruses however, provides a unique approach to antiviral gene therapy. Viruses that are capable of establishing a latent infection, such as HIV and HBV, are prime candidates for TALEN-mediated targeted disruption, as current therapeutics may not eliminate these persistent infections. But as HIV is a highly mutagenic virus (Richman et al., 2004), escape mutants and genomic rearrangements could easily arise following TALEN cleavage. Conversely, HBV has a small compact genome arrangement and infection results in an episomal cccDNA pool. As HBV has overlapping reading frames, mutations within the genome are likely to affect viral fitness. In addition, during chronic infection the virus is predominantly maintained episomally, with integration only occurring decades after viral persistence. Therefore nuclease mediated

cleavage and NHEJ repair of the HBV cccDNA may permanently disable the virus. For this reason, TALEN-directed targeted disruption of an HBV replication competent plasmid as well as cccDNA was examined *in vitro*.

3.2 Results

3.2.1 Expression of TALENs and knockdown of HBV replication markers in liver-derived cells

Initially, TALEN expression and anti-HBV efficacy was determined in cultured liver-derived Huh7 cells. Transient transfections with either the left or right S, C, P1 and P2 TALEN subunit expressing plasmids were used to confirm TALEN expression and nuclear localisation. The HA epitope, included at the N-terminal of each TALEN subunit, was used as a tag for immunohistochemical detection. The SL, SR, CL, CR, P1L, P1R, P2L and P2R subunits were identified in both the nucleus and the cytoplasm of TALEN transfected cells (Figure 3.2). Although TALEN subunits were efficiently expressed in a liver-derived cell line, transfection efficiencies were low. This resulted in the detection of only a small number of positive cells per well. Despite this, distinct nuclear localisation of expressed TALENs was established in these cells. As TALENs are protein-based designer nucleases, they need to be translated in the cytoplasm and transported back to the nucleus before they can cleave their intended targets. The detection of these TALENs in the nucleus, suggests that these proteins are being expressed, translated and transported back to the nucleus efficiently.

To determine whether these TALENs were capable of knocking down markers of viral replication, without affecting cell viability, TALEN encoding plasmids were co-transfected with the pCH-9/3091 HBV replication-competent plasmid (Nassal, 1992). This plasmid encodes a greater-than-genome-length HBV sequence which actively expresses the viral pgRNA and

subgenomic mRNAs required for HBV replication. When an MTT cell viability assay was performed, there was no change in mitochondrial metabolic activity in either the no DNA or mock DNA transfections when compared to TALEN transfected cells (Figure 3.3A, Supplementary Table 8.3.1). This indicates that there was no TALEN-induced cytotoxicity detected. However, when measuring markers of HBV replication, both the S and P1 TALENs significantly knocked-down HBV surface protein concentrations in cell culture supernatants at days 2 and 3 post-transfection (Figure 3.3B, Supplementary Table 8.3.2). The S TALEN showed significant knock-down on both days 2 ($p = 0.0279$) and day 3 ($p = 0.0037$) post-transfection, when compared to no TALEN controls. The P1 TALEN also showed significant knock-down of HBsAg concentrations at days 2 ($p = 0.0268$) and 3 ($p = 0.0029$). This suggests that both these TALENs are inhibiting HBV surface protein expression, particularly the S TALEN which showed a sustained knock-down efficiency of over 80% at both time points.

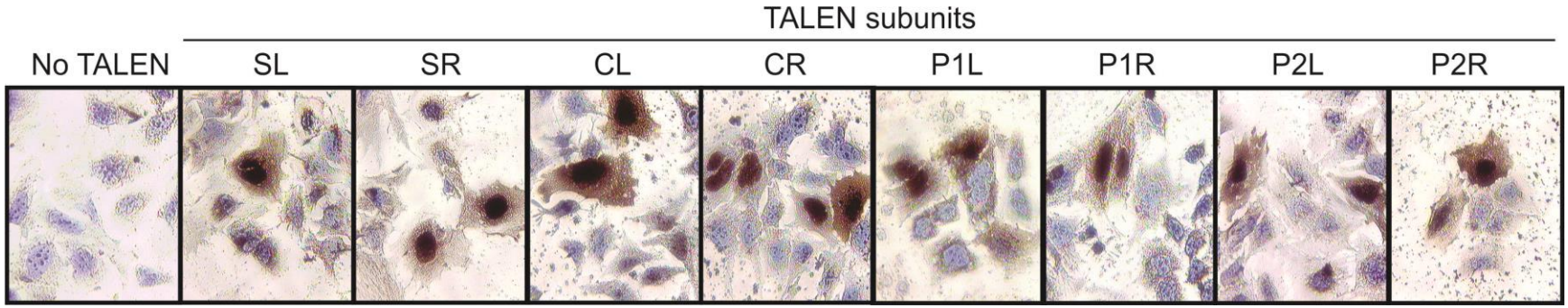

Figure 3.2: Immunohistochemical detection of TALENs *in vitro*. Plasmid transfected Huh7 cells were fixed and stained with DAB (brown). A primary antibody against the haemagglutinin epitope was used to detect TALENs. Haematoxylin (blue) was used as a counterstain. Each of the left (L) and right (R) subunits of the S, C, P1 and P2 TALEN pairs are shown. All TALEN subunits are detected in both the nucleus and the cytoplasm of TALEN transfected cells. Cells were visualised under a light microscope at 400 × magnification.

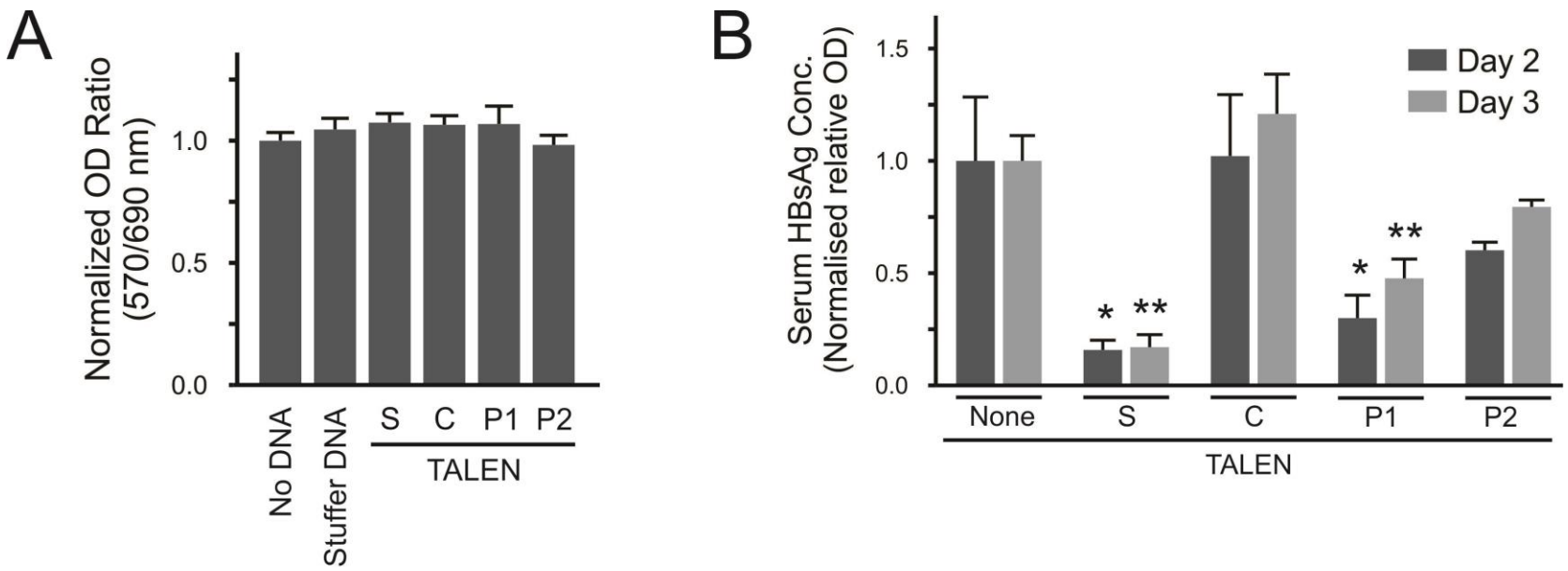

Figure 3.3: TALEN associated cytotoxicity and knockdown of HBV. A) An MTT cell viability assay was used to measure TALEN-associated cytotoxicity at 48 hours post-transfection. Data is represented as the mean (n = 5) ±SEM. **B)** HBsAg concentrations were measured by ELISA in Huh7 cell culture supernatants at days 2 and 3 post transfection to determine anti-HBV TALEN efficacy. Data is represented as the mean (n = 3) ±SEM. Statistical significance is shown by * ($p \leq 0.05$) and ** ($p \leq 0.001$).

3.2.2 Direct targeted disruption of cccDNA

Although the knock-down of HBV replication intermediates in Huh7 cells suggests that the TALENs were cleaving their cognate pCH-9/3091 episomal plasmid DNA targets and disrupting protein expression, their ability to target cccDNA still needed to be determined. To examine this, transfection of the liver-derived HepG2.2.15 cell line (Sells et al., 1988) was carried out. As HepG2.2.15 cells contain a stable greater-than genome length HBV integrant, they constitutively produce new virions and are capable of maintaining a cccDNA pool. As such, this cell line is frequently used to assess the efficiency of anti-HBV therapeutics, as changes in cccDNA copy numbers can be monitored (Li et al., 2011a; Shi et al., 2012; Wu et al., 2012; Xin et al., 2008). However this cccDNA pool, of approximately 10 copies per cell (Rabe et al., 2006; Sells et al., 1988), is higher than the estimated 1.5 copies found in the hepatocytes of chronically infected patients (Laras et al., 2006). These HepG2.2.15 cell cultures are also difficult to transfect, with reported efficiencies of only 20% (Guo et al., 2005). As a result of the elevated cccDNA pools and poor transfection efficiencies, multiple transfections and mildly hypothermic conditions were used in an attempt to enhance TALEN-mediated targeted disruption of cccDNA. Previous reports have shown by culturing transfected cells under mildly hypothermic conditions at 30 °C instead of the normal 37 °C, nuclease cleavage is improved (Doyon et al., 2010). HepG2.2.15 cells were transfected one to three times with S, C, P1 and P2 TALEN pair-expressing plasmids and maintained at either 37 °C or 30 °C. Initial transfections showed no knockdown of HBsAg concentrations in cell culture supernatants by any of the four TALEN pairs at either of the incubation temperatures. However the S TALEN showed an increasingly significant reduction in HBsAg concentrations after transfections 2 ($p = 0.0195$) and 3 ($p = 0.0102$) under mildly

hypothermic conditions (Figure 3.4, Table 3.1). A maximum knockdown efficiency, of over 60%, was measured after the third S TALEN transfection. This trend was not observed in cultures incubated at 37 °C, or with the C and P2 TALENs.

To confirm that TALEN cleavage was occurring at the intended DNA target site, cccDNA was extracted from transfected cells maintained at mildly hypothermic conditions. A modified plasmid DNA extraction protocol was used to purify HBV cccDNA from contaminating HepG2.2.15 genomic DNA. As the HepG2.2.15 cells contain multiple integrated HBV DNA copies, it is important to remove residual genomic DNA to prevent amplification of these viral integrants during T7 endonuclease assays. A PCR-based analysis of HepG2.2.15 genomic DNA and cccDNA extracts was performed using primer sets specific for the endogenous alpha-1-antitrypsin (A1AT) gene and the HBV *core* ORF (Figure 3.5A). When using the A1AT gene primers, only the HepG2.2.15 genomic DNA was efficiently amplified, as indicated by the presence of a 1224 bp PCR product. However the HBV *core* primers amplified a 125 bp PCR product in both the HepG2.2.15 genomic DNA and cccDNA extracts, although the amplification efficiency was considerably higher with the cccDNA. This indicates that the modified plasmid DNA extraction protocol results in concentrated HBV cccDNA without significant genomic DNA contamination.

Site-specific TALEN-mediated cleavage of cccDNA was examined using a T7 endonuclease 1 (T7E1) assay. As the T7E1 enzyme cuts single stranded mismatches present in DNA heteroduplexes, any NHEJ events resulting in targeted disruption at the DSB site can be measured. If heteroduplexes were formed, the T7E1 cleaved in the middle of the DNA amplicon (~520 bp), to yield an additional, smaller DNA product (~280 bp). HBV cccDNA was isolated

from triple transfected mock and S TALEN HepG2.2.15 cell cultures and analysed (Figure 3.5B). The episomal cccDNA was separated from HepG2.2.15 genomic DNA to exclude integrated HBV DNA copies from this analysis. This allowed a direct assessment of TALEN-mediated cccDNA cleavage, mimicking chronic infection without integration. There was no detectable targeted disruption observed after mock transfections, however the S TALEN resulted in 49% targeted disruption of cccDNA. This suggests that the S TALEN was binding and cleaving its cognate DNA target site. When performing a T7E1 assay on the cccDNA isolated from single, double and triple transfected cells (Figure 3.5C) a gradual increase in the percentage of targeted cleavage, from <1% to 35% was achieved after three S TALEN transfections. Therefore the number of S TALEN transfections directly correlates with the amount of targeted disruption achieved. These results correlate with the improved reduction in HBV surface protein expression after the second and third S TALEN transfections under mildly hypothermic conditions. This suggests that the S TALEN cleaved HBV cccDNA at the intended target site to result in NHEJ-based targeted disruption. By directly disrupting the cccDNA, which is the transcriptional template and viral replication intermediate, wild-type HBV surface protein production has, most likely, been permanently disrupted. Although the C TALEN did not result in any measurable reduction in HBsAg concentrations, even when cultured under mildly hypothermic conditions (Figure 3.6A, Table 3.1), a T7E1 assay of the *C* ORF binding site revealed that targeted disruption occurred in 11% of cccDNA isolates (Figure 3.6B). This suggests that both the S and C TALENs are specific for their cognate binding sites and disrupt the synthesis of HBV proteins encoded at these sites.

During transient co-transfections of Huh7 cells with TALEN-encoding plasmids and pCH-9/3091, the P1 TALEN efficiently knocked down HBsAg concentrations, by 69% and 51%, on both days

2 and 3 post-transfection (Figure 3.3). In HepG2.2.15 cells, the same P1 TALEN was examined for anti-HBV efficacy. After multiple transfections at mildly hypothermic conditions there again was a reduction in HBsAg concentrations, by 32% and 40% after transfections 2 and 3 (Table 3.1). To confirm that the P1 TALEN was capable of cleaving its cognate plasmid-based or cccDNA binding site, a T7E1 assay was performed on Huh7 co-transfected cells and mildly hypothermic HepG2.2.15 triple transfected cells (Figures 3.7A and 3.7B). There was no detectable targeted disruption in either of the liver-derived cell lines suggesting that the P1 TALEN is not cleaving at its cognate site. This was further corroborated by the absence of targeted disruption when using the CelI single-stranded specific endonuclease instead of T7E1 (Figure 3.7A). As the P1 TALEN failed to cleave its cognate binding site, the reduction in HBsAg expression is not a result of targeted disruption.

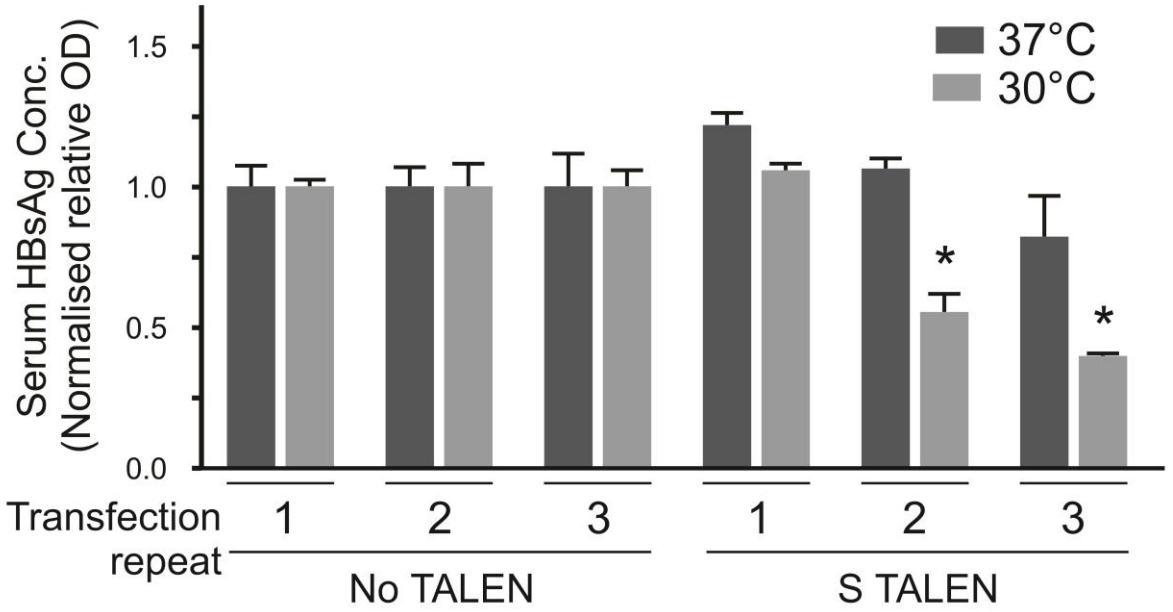

Figure 3.4: S TALEN mediated knockdown of HBsAg in HepG2.2.15 cells. Both mock (no TALEN) and S TALEN HepG2.2.15 cell cultures were subjected to repeat plasmid transfections and maintained in hypothermic (30 °C) or normal (37 °C) incubation conditions. HBsAg concentrations were measured in cell culture supernatants. Data is represented as the mean (n = 3) ±SEM.

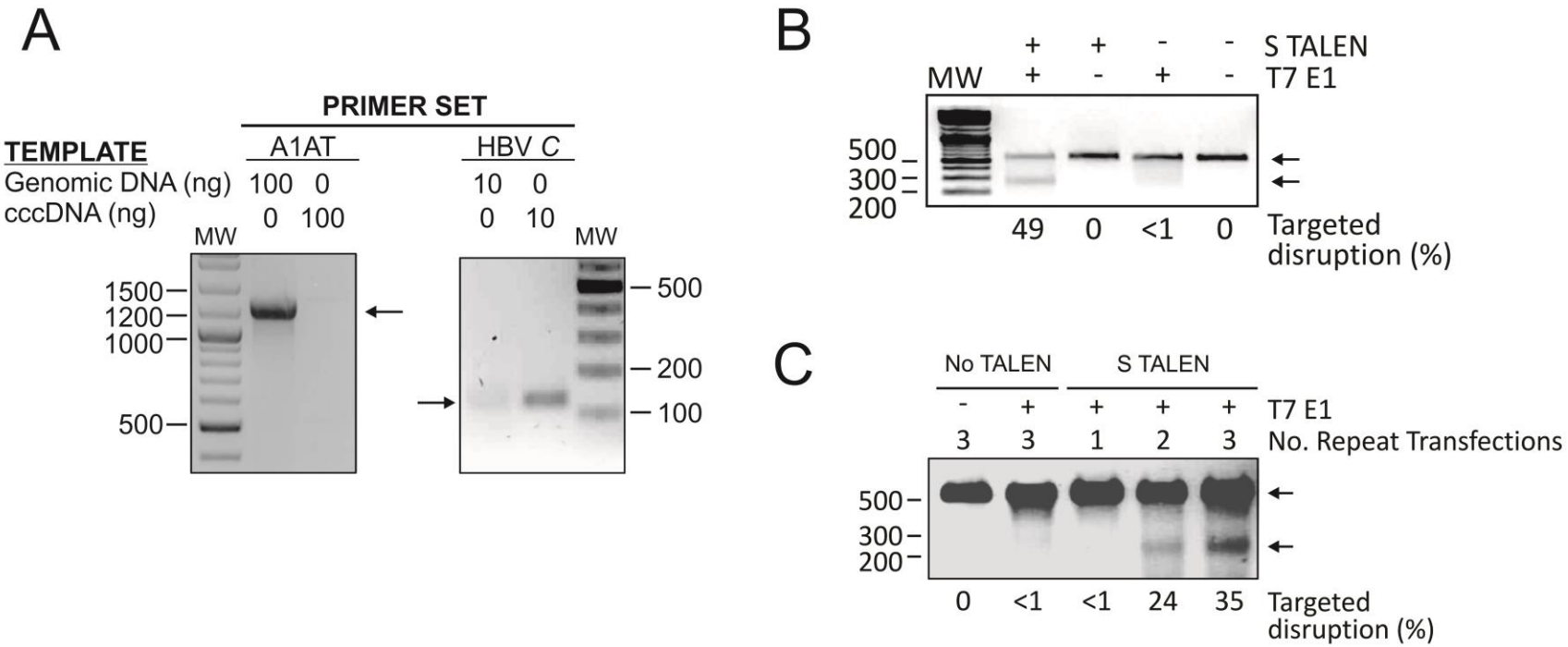

Figure 3.5: S TALEN-mediated cleavage of cccDNA isolated from HepG2.2.15 cells. A) PCR analysis of total genomic DNA or cccDNA isolated from HepG2.2.15 cell cultures, using A1AT or HBV *core* (C) gene primer sets. Arrows indicate the A1AT and C gene amplicons of expected sizes of 1224 bp and 125 bp respectively. The sizes of DNA fragments (bp) in the molecular weight marker lane (MW) are shown on the left and right. **B)** T7E1 assay of cccDNA extracted from mock and S TALEN triple transfected cells maintained under hypothermic conditions. The arrows indicate the T7E1 undigested (~520 bp) and digested (~280 bp) PCR products. The measured percentage of targeted disruption is indicated below each sample. The sizes of DNA fragments (bp) in the molecular weight marker lane (MW) are shown on the left. **C)** T7E1 assay was repeated as described in **B)** but on cccDNA fragments isolated from single, double or triple transfected cells.

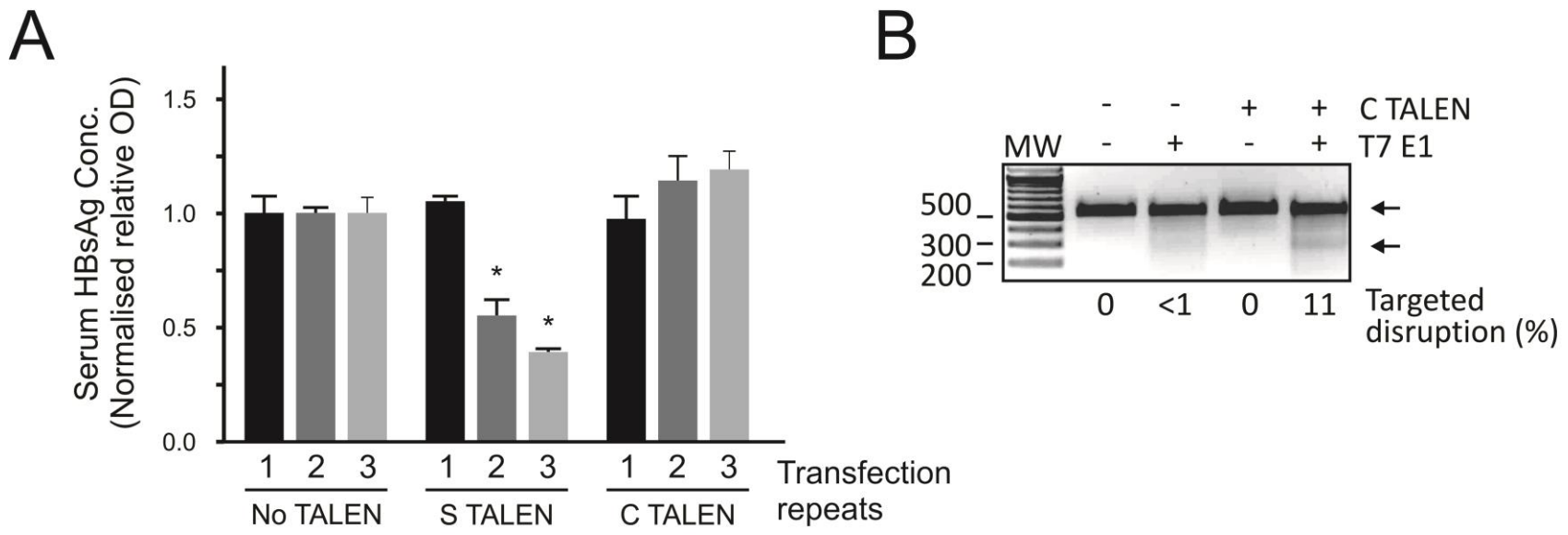

Figure 3.6: C TALEN mediated cleavage of cccDNA in HepG2.2.15 cells. A) HBsAg concentrations from supernatants of mock (no TALEN), S TALEN and C TALEN plasmid transfected HepG2.2.15 cells maintained at mildly hypothermic conditions. Data is represented as the mean (n = 3) ±SEM. **B)** T7E1 assay of cccDNA extracted from mock and C TALEN triple transfections. The arrows indicate undigested (~520 bp) and digested (~280 bp) PCR products, and the percentage of targeted disruption is indicated below each sample. The sizes of DNA fragments (bp) in the molecular weight marker lane (mw) are shown on the left.

Table 3.1: Quantification of HBsAg concentrations in HepG2.2.15 cells following multiple transfections

	HBsAg normalised relative OD ratio of 450/620 nm (±SEM, n = 3)					
	Incubation at 37°C			Incubation at 30°C		
	Transfection repeat			Transfection repeat		
	T1	T2	T3	T1	T2	T3
No TALEN	1.000 (± 0.0870)	1.000 (± 0.0727)	1.000 (± 0.1234)	1.000 (± 0.0181)	1.000 (± 0.0721)	1.000 (± 0.0594)
S TALEN	1.225 (± 0.0444)	1.072 (± 0.0341)	0.817 (± 0.1450)	1.060 (± 0.0115)	0.546 (± 0.0672)	0.388 (± 0.0070)
C TALEN	1.269 (± 0.0665)	0.952 (± 0.0622)	1.080 (± 0.0016)	0.979 (± 0.0881)	1.145 (± 0.1017)	1.199 (± 0.0704)
P1 TALEN	1.283 (± 0.0359)	0.970 (± 0.0295)	0.982 (± 0.0327)	1.047 (± 0.0640)	0.676 (± 0.0513)	0.599 (± 0.0371)
P2 TALEN	1.129 (± 0.0591)	1.040 (± 0.0136)	1.075 (± 0.0821)	1.032 (± 0.0425)	0.930 (± 0.1380)	0.888 (± 0.1484)

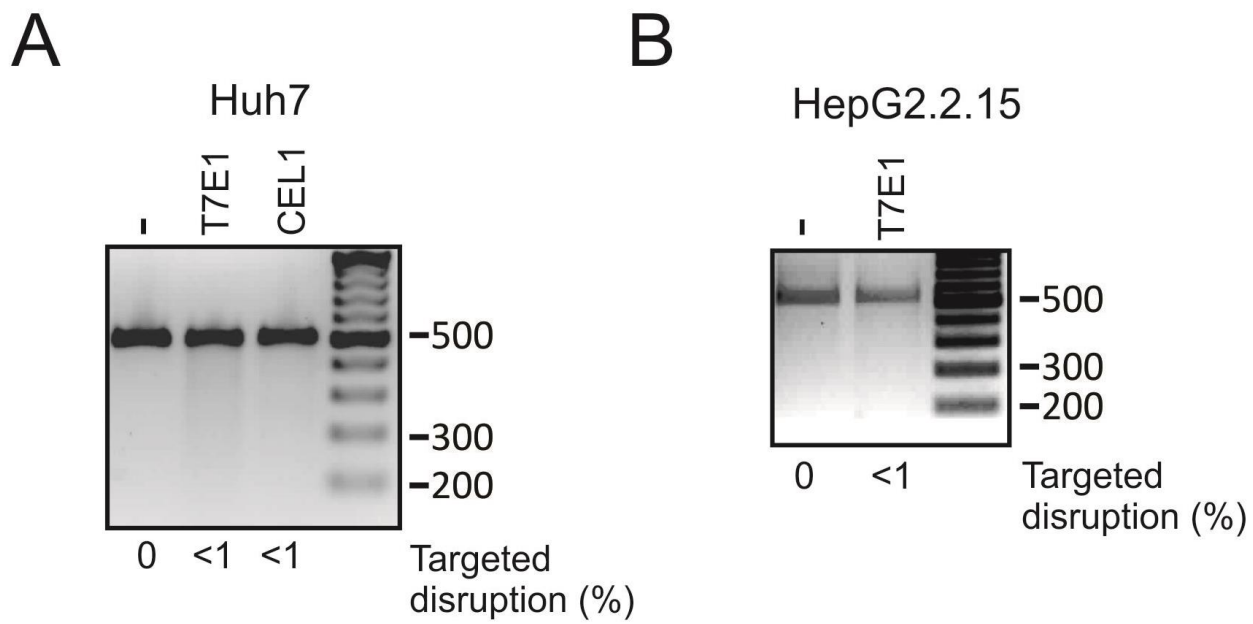

Figure 3.7: Inefficient cleavage of HBV target DNA with the P1 TALEN. A) A T7E1 or CelI assay of HBV target DNA extracted from Huh7 cells transiently co-transfected with P1 TALEN-encoding plasmids. The percentage of targeted disruption is indicated below each sample. **B)** T7E1 assay on cccDNA isolated from triple P1 TALEN plasmid transfected HepG2.2.15 cells maintained at mildly hypothermic conditions. The sizes of DNA fragments (bp) are shown on the right of **A)** and **B)**.

3.3 Discussion

TALENs provide a unique approach to editing or disrupting specific DNA sequences. However when targeting endogenous human genes, multiple selection steps are required to isolate successfully mutated or repaired target sites. Furthermore, low cleavage efficiencies and TALEN associated cytotoxicity has been observed during endogenous gene targeting investigations. This is most likely a result of cellular repair pathways being triggered in response to the formation of chromatin induced DSB, which is essentially a genotoxic event that may result in apoptosis (Bree et al., 2004; Roos and Kaina, 2006). Conversely, anti-HBV TALENs act on the episomal viral replication intermediate. This is likely to account for the absence of measurable cytotoxic events, as endogenous genes are not the targets of these virus-specific TALEN pairs.

Of the four anti-HBV TALENs investigated, site-directed cleavage of episomal cccDNA was achieved using the S and C TALENs. Targeted disruption of the HBV *surface* and *core* ORFs was found in 49% and 11% of cccDNA isolates from HepG2.2.15 cell cultures respectively. In the same S TALEN triple transfected cells, HBsAg concentrations were diminished by approximately 60%. This suggests that the S TALEN is cleaving and disrupting the *surface* ORF, resulting in truncated or aberrant viral proteins. A previous study, assessing the activity of ZFNs against an HBV replication competent plasmid *in vitro*, demonstrated 36% disruption at the cognate binding site (Cradick et al., 2010). Although the cleavage efficiency of the TALENs was not established during transient co-transfections with the HBV pCH-9/3091 replication competent plasmid, the S TALEN shows superior targeted disruption of cccDNA when

compared to these ZFNs. Furthermore, as ZFN-mediated cleavage of HBV cccDNA has not been demonstrated, the S and C TALENs are the first example of nuclease-mediated targeted disruption of episomal cccDNA in an HBV cell culture model system. Even though the activity of these TALENs *in vitro* suggests that HBV replication is permanently disrupted, there are limitations associated with these cell cultures models. To further verify the anti-HBV efficacy of these S and C TALENs, essential *in vivo* studies are still required.

Analogous to the S TALEN, the P1 TALEN reduced the concentration of detectable HBsAg during transient co-transfections in Huh7 cells, as well as triple transfected HepG2.2.15 cells maintained at mildly hypothermic conditions. Although the TALEN-mediated knock-down of HBV viral proteins is expected to occur through direct targeted disruption of the cognate DNA target site, the P1 TALEN consistently inhibited HBsAg expression without any measurable targeted disruption. This suggests that the P1 TALEN is inhibiting viral protein expression by another mechanism. As both the *polymerase* ORF as well as the HBV Enhancer I encoding sequences are targets of this P1 TALEN, it is most likely binding to HBV DNA and obstructing viral transcription rather than disrupting protein expression. Such transcriptional inhibition has previously been studied using several ZFPs designed to inhibit DHBV cccDNA (Zimmerman et al., 2008). These ZFPs are predicted to prevent cccDNA transcription by competitively inhibiting binding of key transcription factors to the target site. TALEN subunits designed to bind to HBV promoter and enhancer sequences, are likely to confer the same transcriptional repression.

CHAPTER 4 – Transcriptional gene silencing with rTALEs

4.1 Introduction

TALE DNA-binding modules are not the only amendable regions of these versatile proteins. The effector domain may also be substituted to facilitate transcriptional regulation of a particular gene (Figure 4.1). In the case of *Xanthomonas* TALEs, the effector is an activation domain which binds to plant promoter regions in order to stimulate transcription of otherwise silent genes. During infection, the bacteria synthesise these TALEs to manipulate plant gene expression, and ultimately promote survival (Boch and Bonas, 2009; Buttner and Bonas, 2010; Kay et al., 2007; Romer et al., 2007). As the TALE array can be engineered to bind to any target sequence, these transcriptional activators have recently been used in mammalian cells to trigger human gene expression (Bultmann et al., 2012; Cong et al., 2012; Garg et al., 2012; Geissler et al., 2011; Miller et al., 2011; Tremblay et al., 2012; Zhang et al., 2011). Although individual TALEs are capable of stimulating gene transcription *in vitro*, a combined approach, using multiple TALEs targeting a single promoter region was shown to be the most effective method of activating human genes (Perez-Pinera et al., 2013).

In addition to transcriptional activation, TALE DNA binding arrays may be fused to effectors that promote gene repression. These repressor TALEs (rTALEs) have recently been shown to be potent inhibitors of endogenous mammalian gene transcription (Cong et al., 2012; Garg et al., 2012). Here the effector is a naturally occurring transcriptional repressor domain which is fused to the TALE DNA binding domain (Figure 4.1). There are a large number of different repressor

domains that have been investigated in combination with DNA-binding dTALEs, however the mSin interaction domain (SID) and Krüppel associated box (KRAB) domain showed the most efficient gene silencing activity (Cong et al., 2012). In mammalian cells, the SID region is located at the N-terminal of Mad proteins, which themselves are naturally occurring composite repressors (Hurlin et al., 1996). As these Mad proteins have limited, pre-defined DNA targets, the SID repressor region may be isolated and fused to a DNA binding domain to create designer transcriptional repressors (Ayer et al., 1996). On the other hand, multiple KRAB repressors occur naturally as zinc finger (ZF) fusions (Bellefroid et al., 1991). The KRAB-ZF proteins are the largest group of mammalian transcriptional regulators, accounting for 290 of the 799 ZF proteins discovered. As each ZF array is capable of binding to a different DNA target site, these KRAB-ZF proteins are capable of silencing a variety of genes. The exact mechanism of KRAB transcriptional repression has not been completely elucidated, however KRAB-ZF protein binding results in the recruitment of heterochromatin forming complexes, which seem to facilitate gene silencing (Schultz et al., 2002).

In one study, the TALE-based SID repressors were shown to be slightly more efficient at transcriptional gene silencing of the endogenous *SOX2* locus than the equivalent KRAB repressor (Cong et al., 2012). However, these TALEs were constructed using the NH RVD to enrich for guanine binding, which is less frequently used than the NK or NN. Garg and colleagues did not investigate the SID repressor, however they showed between 36- and 97-fold transcriptional gene silencing, across multiple target sites, using the KRAB domain (Garg et al., 2012). In this case, the rTALEs encompassed more commonly used RVDs like NI, HD and NG. Both these studies replaced the natural activation domain, located at the C terminus of the TALE, with a SID or KRAB repressor. Although these repressors showed potent targeted gene

silencing, the naturally occurring SID and KRAB domains occur at the N-terminus of their protein arrays.

We have already demonstrated that TALENs, where the effector domain is replaced with the *Fok*I nuclease (Figure 4.1), provide a promising approach to anti-HBV gene therapy by creating DSBs at designated target sites. Although S and C TALENs mediated cleavage of cccDNA, which is likely to result in permanent modifications of the viral genome, the P1 TALEN showed reduced HBsAg expression without cleavage. This may be a result of the P1 TALEN interacting with the HBV Enhancer 1 sequence, which is situated at the binding site. As TALENs induce DSBs at target DNA sites, they present a genotoxic threat which may possibly elicit unwanted mutations and genomic translocations (Richardson and Jasin, 2000). By using transcriptional repression instead of targeted inactivation as a potential HBV gene therapy, the likelihood of introducing undesirable mutagenic events may be diminished. In the same way that ZFPs are able to inhibit DHBV transcription (Zimmerman et al., 2008), transient transcriptional repression with TALENs most likely requires competitive binding at the target site without any endonuclease cleavage. To investigate this, each P1 TALEN subunit was individually assessed for HBsAg knock-down efficiency. To further explore the anti-HBV potential of rTALEs, a KRAB-repressor domain fused to a dTALE targeting the pre-S2 promoter, was assessed *in vitro*. Analogous to the naturally occurring repressor proteins, the KRAB-rTALE was designed with the repressor domain at the N-terminus.

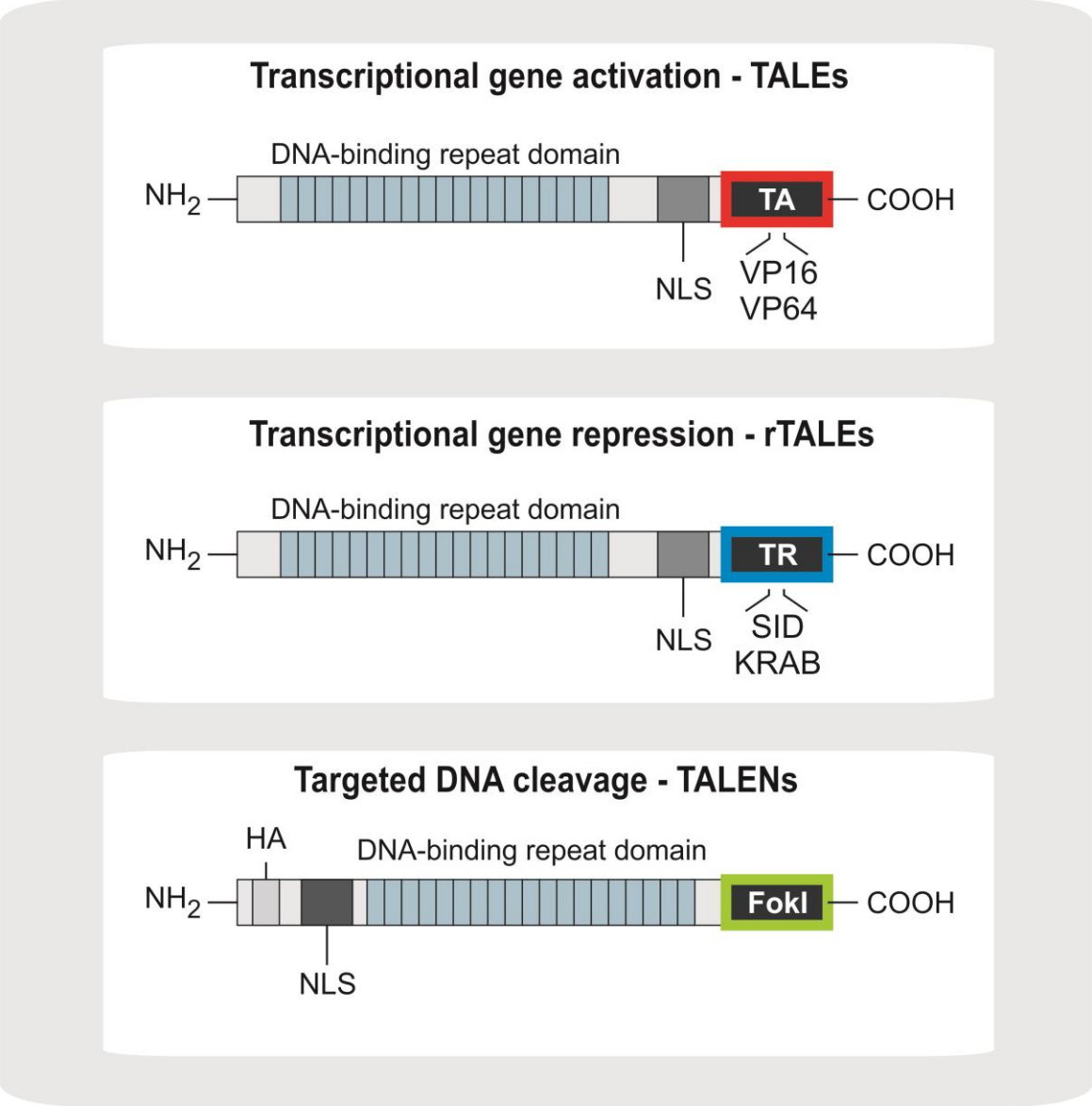

Figure 4.1: Effector domains used for TALE-mediated human gene manipulation. Transcriptional gene activation and silencing is achieved using TALEs which contain C-terminal (-COOH) transcriptional activator (TA) or transcriptional repressor (TR) domains respectively. Activators (e.g. VP16 and VP64) and repressors (e.g. SID and KRAB) are commonly used during human gene targeting. DNA cleavage is typically carried out by a pair of TALENs which have *Fok*I endonuclease domains at the C-terminal. The NLS is found at the C-terminal in TALEs and rTALEs, and at the N-terminal (NH_2) for TALENs. DNA-binding repeat domains typically consist of between 15.5 and 19 TALE modules.

4.2 Results

4.2.1 P1L and P1R TALEN subunits inhibit HBsAg expression

To determine whether individual TALEN subunits were inhibiting HBsAg secretion by mechanisms other than site-directed targeted mutagenesis, liver-derived Huh7 cells were transfected with pCH-9/3091 and either the S or P1 TALEN subunit-encoding plasmids, or the complete TALEN pair. An HBsAg ELISA was performed on cell culture supernatants at day 2 post-transfection. A 60% knockdown of measurable HBsAg was only observed when both the SL and SR TALEN subunits were transfected (Figure 4.2A). Although the P1 TALEN pair showed efficient knockdown of 54% of HBsAg, both the P1L and P1R TALEN subunits were each, individually, capable of reducing surface expression by 40% and 57% respectively (Figure 4.2B). This suggests that the P1 TALEN was inhibiting HBsAg secretion by an alternative manner, which is most likely to be a result of transcriptional gene repression. As the P1 TALEN binding site is located within the HBV enhancer I sequence, competitive binding of the TALEN subunits may inhibit transcription.

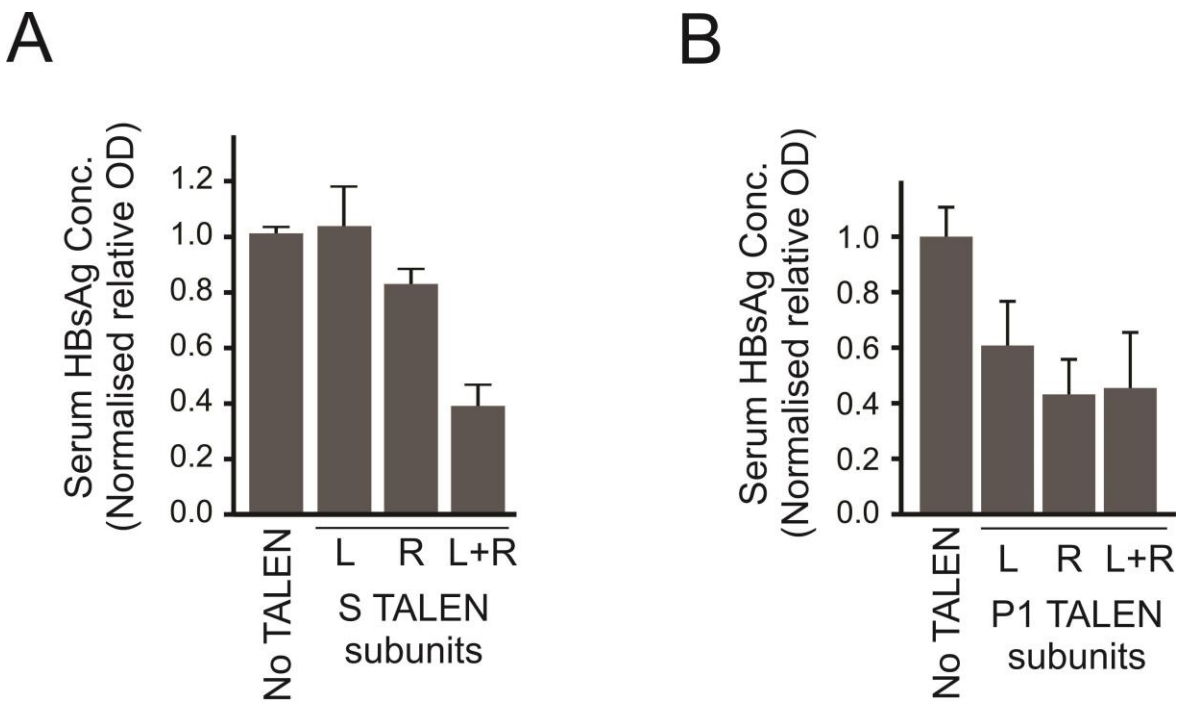

Figure 4.2: Assessment of S and P1 TALEN subunit-mediated knockdown of HBsAg. Transient co-transfections were performed in Huh7 cells with pCH9/3091 and individual left (L) and right (R) S and P1 TALEN subunits as well as TALEN pairs. HBsAg concentrations were measured by ELISA on day 2 post transfection. Knock-down of HBsAg by S TALEN subunits (**A**) and P1 TALEN subunits (**B**) relative to mock transfections (no TALEN) is shown. Data is represented as the mean (n = 3) ±SEM.

4.2.2 Propagation of the HBV pre-S2 promoter rTALE

A single rTALE target site in the pre-S2 promoter region was selected to examine transcriptional gene silencing efficiency (Figure 4.3). This promoter sequence coincides with the *pre-S1* ORF, and drives the expression of both the middle (M) and major (S) surface proteins. Transcriptional regulation of HBV surface gene expression has been well characterised (reviewed by Bar-Yishay et al., 2011; Moolla et al., 2002; Quasdorff and Protzer, 2010). The pre-S2 promoter is regulated by nuclear factor 1 (NF1) and Sp1 transcription factor binding (Cattaneo et al., 1983). Additionally the CCAAT motif, which recruits additional transcription factors NF-Y and CCAAT binding factor (CBF), is essential for M and S protein expression (Bock et al., 1999; Zhou and Yen, 1991). The rTALE was designed to target a 19 bp HBV sequence, located between nucleotides 3129 and 3148. This pre-S2 rTALE should competitively inhibit Sp1, NF-Y, and CBF binding as well as induce KRAB-based heterochromatin formation.

Initially, the complete 19 bp dTALE array was assembled as a single TALEN subunit using the Golden Gate modular assembly kit (Morbitzer et al., 2011; Mussolino et al., 2011), as previously described in Section 2.2.2. This subunit was constructed using the NI, HD, NG and NN RVD-encoding plasmids, which were used to confer A, C, T and G nucleotide binding specificities respectively. The dTALE array was initially constructed as a TALEN, as the level 3 destination vectors used during TALEN assembly encode the initial ‘T’ binding site and terminal half-binding sites required to assemble a complete dTALE (Figure 2.4). This pre-S2 promoter targeting dTALE was extracted from the TALEN before cloning into the KRAB repressor plasmid (pRK5-HA-KRAB-NLS-TAL) (Figure 4.4). *BamH*I and *Nhe*I restriction sites, which flank the dTALE

array in the TALEN level 3 destination vectors, were used to excise the 2325 bp dTALE encoding sequence (Figure 4.5). Identical restriction sites were used to clone the dTALE-encoding array into the pRK5-HA-KRAB-NLS-TAL repressor vector (Figure 4.5). Unlike the rTALEs previously investigated, the KRAB domain is located at the N-terminal of the pRK5-HA-KRAB-NLS-TAL repressor vector, therefore mimicking the assembly of the naturally occurring mammalian KRAB-ZF proteins. The HA tag and NLS signal are also located at the N-terminal, which corresponds with the TALEN destination vector. The amino acid sequence of the HBV pre-S2 rTALE DNA-binding subunit was confirmed using conventional sequencing (Table 4.1) prior to testing *in vitro*.

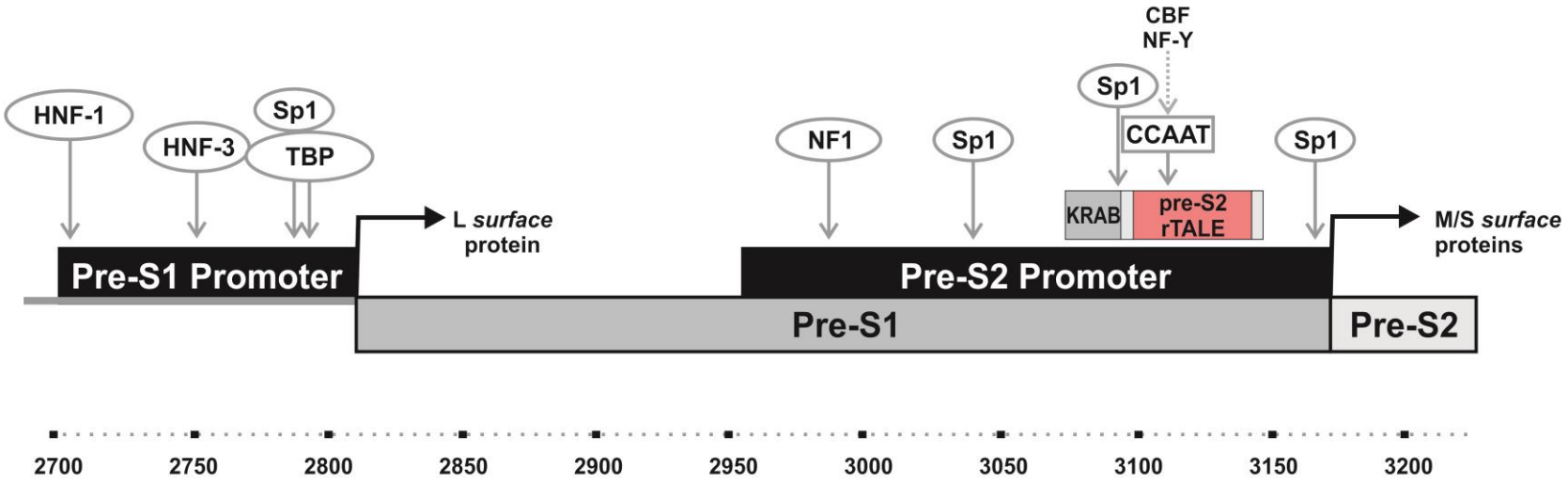

Figure 4.3: Transcriptional regulation of HBV surface protein expression. Two separate viral promoters, pre-S1 and pre-S2, are required for surface protein expression. The pre-S1 promoter drives expression of mRNA encoding the large (L) surface protein transcript, while the pre-S2 promoter drives expression of mRNAs encoding the middle (M) and major (S) surface protein transcripts. The pre-S2 promoter region overlaps with the *pre-S1* ORF. Transcription factor binding either up regulates or down regulates pre-S1 and pre-S2 promoter activity. The pre-S1 rTALE binds to the pre-S2 promoter region at the same location as the Sp1, NF-Y and CBF transcription factors. The nucleotide coordinates are shown below as a dotted line, and follow the same HBV genome orientation shown in Figure 1.1. HNF-1, hepatocyte nuclear factor 1; HNF-3, hepatocyte nuclear factor 3; TBP, TATA binding protein; NF1, nuclear factor 1; CBF, CCAAT binding factor.

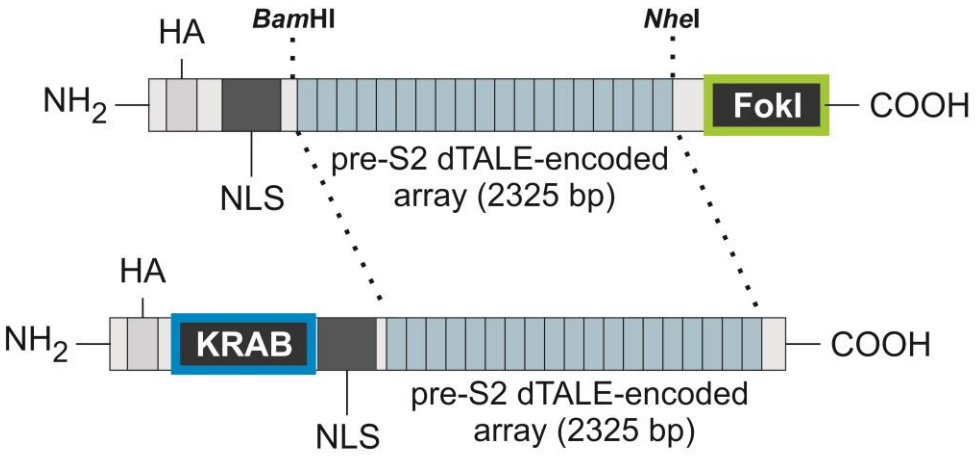

Figure 4.4: Construction of the pre-S2 rTALE from the TALEN. The pre-S2 dTALE array was initially assembled as a TALEN subunit using the Golden gate assembly kit. The *Bam*HI and *Nhe*I restriction sites, which flank the final dTALE array, were used to excise the pre-S2 dTALE from the TALEN. The KRAB repressor domain is located at the N-terminal of the pRK5-HA-KRAB-NLS-TAL vector (KRAB repressor plasmid). Corresponding *Bam*HI and *Nhe*I restriction sites within the KRAB repressor plasmid were used to transfer the dTALE array and assemble the pre-S2 rTALE.

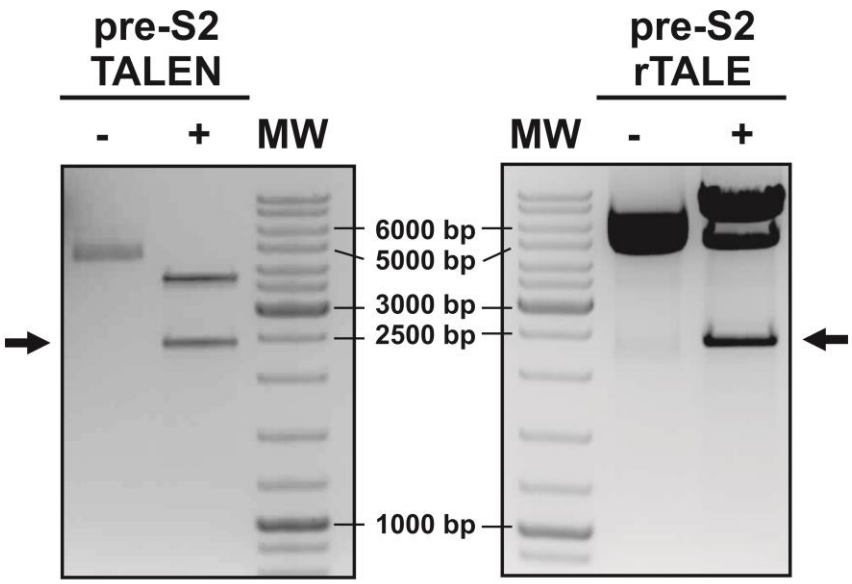

Figure 4.5: Cloning and verification of pre-S2 rTALE by double restriction digestion. TALEN and rTALE clones were subjected to either no digestion (-) or *Bam*HI/*Nhe*I double restriction digestion (+) followed by agarose gel electrophoresis. The complete pre-S2 dTALE array, which migrates to ~ 2400 bp, is found in both TALEN and rTALE clones, as indicated by the arrows. The sizes of the DNA fragments (bp) in the molecular weight marker lanes (MW) are shown in the centre.

Table 4.1: Amino acid sequence of the pre-S2 rTALE DNA binding subunit*

	d-TALE‡	dTALE subunit	DNA target
***pre-S2* rTALE**	2	LTPDQVVAIAS**NI**GGKQALETVQRLLPVLCQAHG	**A**
	3	LTPEQVVAIAS**HD**GGKQALETVQALLPVLCQAHG	**C**
	4	LTPEQVVAIAS**HD**GGKQALETVQALLPVLCQAHG	**C**
	5	LTPEQVVAIAS**HD**GGKQALETVQALLPVLCQAHG	**C**
	6	LTPEQVVAIAS**HD**GGKQALETVQALLPVLCQAHG	**C**
	7	LTPEQVVAIAS**NN**GGKQALETVQRLLPVLCQAHG	**G**
	8	LTPEQVVAIAS**HD**GGKQALETVQALLPVLCQAHG	**C**
	9	LIPQQVVAIAS**NG**GGKQALETVQRLLPVLCQDHG	**T**
	10	LTPEQVVAIAS**NN**GGKQALETVQRLLPVLCQAHG	**G**
	11	LIPQQVVAIAS**NG**GGKQALETVQRLLPVLCQDHG	**T**
	12	LTPEQVVAIAS**HD**GGKQALETVQALLPVLCQAHG	**C**
	13	LIPQQVVAIAS**NG**GGKQALETVQRLLPVLCQDHG	**T**
	14	LTPEQVVAIAS**HD**GGKQALETVQALLPVLCQAHG	**C**
	15	LTPEQVVAIAS**HD**GGKQALETVQALLPVLCQAHG	**C**
	16	LTPDQVVAIAS**NI**GGKQALETVQRLLPVLCQAHG	**C**
	17	LTPEQVVAIAS**HD**GGKQALETVQALLPVLCQAHG	**A**
	18	LTPEQVVAIAS**HD**GGKQALETVQALLPVLCQAHG	**C**
	19	LIPQQVVAIAS**NG**GGKQALETVQRLLPVLCQDHG	**C**
			T

* Initial ‘T’ binding modules have been excluded from these sequences

‡ Indicating module position, with full amino acid sequence, in the final dTALE array (initial T at position 1)

4.2.3. *In vitro* targeted gene silencing of the pre-S2 promoter

A reporter gene construct, which contains the HBV pre-S2 promoter region controlling the expression of Firefly Luciferase (FLuc) protein (Figure 4.6A), was used to determine the transcriptional gene silencing efficiency of the pre-S2 rTALE. Transient co-transfections were performed in liver-derived Huh7 cells with increasing concentrations of the rTALE-encoding sequences relative to the reporter plasmid. A pre-S2 rTALE concentration dependent reduction in detectable FLuc protein activity, determined by measuring the relative light units, was observed at day 2 post-transfection (Figure 4.6B). No significant decrease in FLuc expression was detected after a 1-, 2- and 3-fold molar increase in repressor to reporter plasmid concentration. However significant reductions of approximately 30% and 50% were detected after 4- and 5-fold molar increases in the pre-S2 rTALE. Maximum gene silencing activity was reached when a 10-fold molar increase was investigated. This resulted in a 90% reduction in luciferase expression. Although higher concentrations of pre-S2 rTALE are required for efficient reporter gene silencing, the N-terminal KRAB domain was capable of inhibiting transcription from the pre-S2 promoter. This effect is most likely to result from induction of heterochromatin formation. Binding of this pre-S2 rTALE to its target site may result in long-lasting transcriptional silencing of the HBV large surface protein.

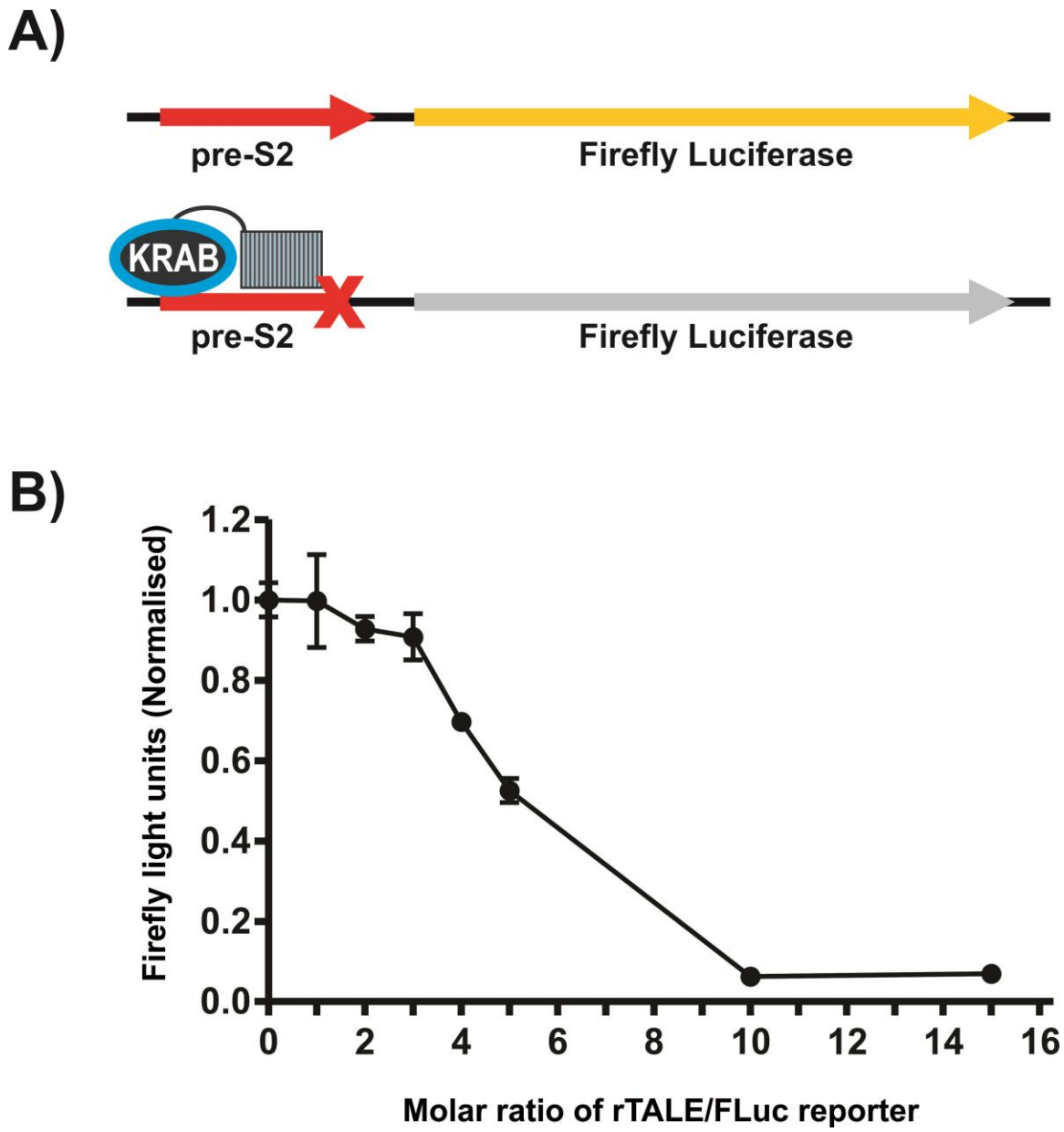

Figure 4.6: Transcriptional gene repression of the pre-S2 promoter by the rTALE. A) The HBV pre-S2 promoter was used to drive the expression of Firefly luciferase in the reporter construct. The pre-S2 TALE facilitates target-specific DNA binding whilst the N-terminal KRAB repressor domain recruits heterochromatin forming complexes to silence FLuc gene expression. **B)** Firefly luciferase light units were measured in liver-derived Huh7 cells on day 2 post-transfection. A molar ratio concentration gradient, of pre-S2 rTALE plasmid to FLuc reporter plasmid, was measured. Results are normalised to mock Firefly luciferase light unit measurements. Data is represented as the mean ±SEM (n = 3).

4.3 Discussion

The HBV Enhancer I sequence is able to regulate viral protein expression through the binding of key transcription factors (reviewed by Bar-Yishay et al., 2011; Moolla et al., 2002; Quasdorff and Protzer, 2010). However both the P1L and P1R TALENs localise at typical transcription factor binding sites located on the *cis*-acting Enhancer I core domain and LSR element (Figure 4.7). The P1L TALEN is likely to inhibit the binding of retinoic acid response element (RARE) or regulatory factor X 1 (RFX1) competitively, which in turn may prevent the cooperative binding of hepatocyte nuclear factor 4 (HNF-4) and retinoid X receptor alpha/peroxisome proliferator-activated receptor (RXRα/PPAR) heterodimers. The P1R TALEN subunit however, is most likely to bind to a region of the LSR element which is involved in the regulation of the Enhancer I motif as well as *HBx* gene expression (Fukai et al., 1997). These transcription factors are essential for promoting HBV gene expression, particularly in liver-derived cell lines like Huh7 and HepG2.2.15 cultures, where the Enhancer I motif has been shown to work in conjunction with Enhancer II, to increase surface protein expression (Su and Yee, 1992). As both the P1L and P1R TALEN subunits inhibit HBsAg expression, it is likely that these proteins are obstructing RARE and RFX1 binding or LSR regulation, ultimately inactivating the Enhancer I motif. Like the anti-HBV ZFPs (Zimmerman et al., 2008), these TALENs appear to be repressing viral gene expression by means of competitive inhibition. Nonetheless, these P1 TALEN subunits still contain C-terminal endonuclease domains, which could potentially dimerise and cleave unintended DNA target sites. To generate safer anti-HBV competitive inhibitors, this nuclease domain needs to be removed or substituted with a repressor domain.

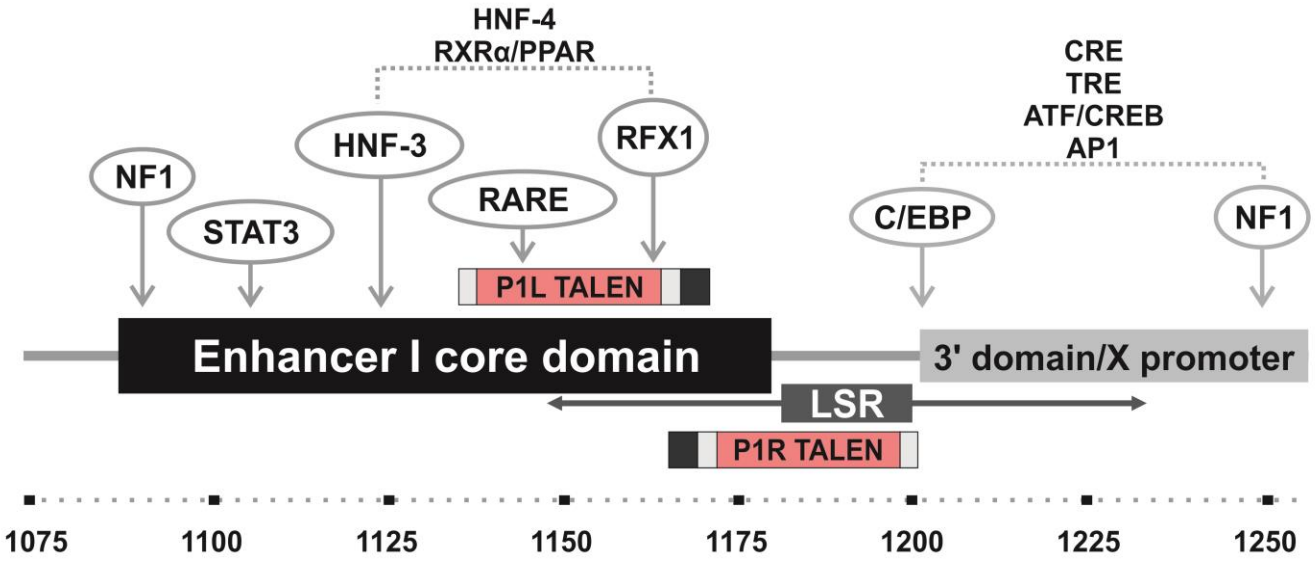

Figure 4.7: Transcription factor binding arrangements at HBV Enhancer I and LSR elements. The Enhancer I core domain is located upstream of the 3' domain/X promoter region. The LSR element overlaps with the 3' region of Enhancer I and the 5' region of the X promoter. The P1L TALEN binds exclusively to the Enhancer I core domain. The P1R TALEN binds to the LSR element and the Enhancer I core domain. Vertical arrows indicate known transcription factor binding sites. The nucleotide coordinates are shown below as a dotted line, and follow the same HBV genome orientation shown in Figure 1.1. NF1, nuclear factor 1; STAT3, signal transducer and activator of transcription 3; HNF-3, hepatocyte nuclear factor 3; RARE, retinoic acid response element; RFX1, regulatory factor X 1; C/EBP, CCAAT-enhancer-binding protein; HNF-4, hepatocyte nuclear factor 4, RXRα/PPAR, retinoid X receptor alpha/peroxisome proliferator-activated receptor heterodimer; CRE, cAMP response element; TRE, transcription regulatory element; ATF/CREB, activating transcription factor/cAMP response element binding protein; AP1, activator protein 1.

Transcriptional gene silencing using KRAB repressor domains fused to target specific dTALEs provides a unique approach to controlling HBV gene expression. The pre-S2 rTALE showed effective silencing of transgene expression in human liver-derived Huh7 cells, particularly when a 5- to 10-fold saturation of the repressor expression plasmid was employed. This correlates with *in vitro* data from KRAB rTALEs designed to target endogenous human promoter regions, which also used a 10-fold excess of TALE repressor plasmid to achieve a 36 to 97-fold decrease in reporter gene expression (Garg et al., 2012). Previous studies using only ZFPs designed to bind to sequence specific targets in DHBV showed up to 41.6% reduction in pgRNA expression (Zimmerman et al., 2008). However, as KRAB-ZF proteins occur naturally in mammalian cells, fusing a repressor domain to these ZFPs may enhance the cccDNA transcriptional gene silencing efficiency of these DNA binding proteins. This would also allow for a more comprehensive comparison between designer repressors with ZFP and TALE DNA binding arrays.

While the anti-HBV efficiency of this pre-S2 rTALE is promising, this was a proof-of-concept investigation. As with the combinatorial TALEs designed to activate endogenous human genes (Perez-Pinera et al., 2013), multiple rTALEs designed to target each of the HBV promoter regions are likely to enable complete transcriptional gene silencing of the entire viral genome. To investigate this further, rTALEs targeting the pre-S1, Enhancer I, and X promoter are currently being developed. As HBV promoter and *cis*-regulatory elements rely on the binding of multiple host transcription factors to stimulate viral gene expression, these KRAB-based rTALEs may permanently inhibit cccDNA transcription. However as these rTALEs are still under development, their direct anti-HBV activity has not yet been established. The S and C TALENs on the other hand, have already demonstrated site-directed cleavage and disruption in HBV

cccDNA. Additionally the S TALEN knocked down HBsAg concentrations in the HepG2.2.15 cell line, suggesting that cleavage of the cccDNA influences viral protein expression. Although these liver-derived cell culture systems provide a good foundation for therapeutic investigations, an *in vivo* model of HBV replication will present a more compelling evaluation of TALEN activity. For this reason, both the S and C TALENs were selected for further investigation using an *in vivo* murine disease model.

CHAPTER 5 – Targeted disruption of HBV-encoding DNA *in vivo*

5.1 Introduction

As HBV infection is hepatotropic, it is important to test the efficacy of the anti-HBV TALENs in an *in vivo* model system. Recently, designer nuclease-mediated mutagenesis or repair of endogenous loci has been extended from cell culture-based studies to create both knock-out and transgenic animal models. TALENs have successfully induced site-directed mutagenesis or HDR in the genomes of nematodes (Wood et al., 2011), insects (Liu et al., 2012; Sajwan et al., 2012; Watanabe et al., 2012), fish (Ansai et al., 2013; Bedell et al., 2012; Cade et al., 2012; Huang et al., 2011; Sander et al., 2011), amphibians (Ishibashi et al., 2013; Lei et al., 2012), rodents (Sung et al., 2013; Tesson et al., 2011; Tong et al., 2012), and livestock (Carlson et al., 2012). To generate knock-out or transgenic mammalian animal models, TALENs are introduced into pre-selected cells *ex vivo*. This is normally achieved either by direct micro-injection of TALEN mRNA into isolated embryos and zygotes, or by transfection of TALEN-encoding DNA or mRNA into primary fibroblasts, ESCs, or iPSCs. As the TALEN-encoding sequences are usually linked to reporter constructs, cells that efficiently express the reporter may be selected. This is to increase the likelihood of selecting TALEN modified cells before re-implantation. Embryos and zygotes are then implanted into surrogate females whilst primary fibroblasts, ESCs and iPSCs may be used as donor cells for chromatin transfer. The genetically engineered offspring are then selected for subsequent breeding and expansion of the animal model. These endogenous gene alterations may be either heterozygous or homozygous, depending on whether mono-allelic or bi-allelic TALEN cleavage was achieved.

Although an *ex vivo* approach to human gene manipulation has yet to be established for TALENs, a clinical trial using ZFN-modified CD4+ T-cells is currently underway (Maier et al., 2013). In this trial, CD4+ T-cells were isolated from patients before implementing ZFN-mediated disruption of the CCR5-encoding sequence to confer HIV resistance. These HIV resistant CD4+ T-cells are then expanded *ex vivo*, before transplanting these cells into HIV-positive patients. A number of ZFNs and TALENs have already been used in somatic, ESC and iPSC cultures to repair genes associated with monogenic disorders like severe combined immunodeficiency (SCID) (Urnov et al., 2005), X-linked chronic granulomatous disease (X-CGD) (Zou et al., 2011), sickle cell disease (Sun et al., 2012), and cystic fibrosis (Lee et al., 2013). Therefore, as these mutated genes have already been successfully repaired using designer nucleases in cell cultures, an *ex vivo* gene editing approach could potentially be used to treat these monogenic disorders.

Whilst efficient cleavage of the designated target site is important, potential off-target cleavage sites also need to be considered. As these designer nucleases are initiating cellular DNA-damage response pathways, often resulting in mutagenesis of endogenous genes, they are ultimately genotoxic. Unintended off-target cleavage events could permanently alter vital genetic components leading to cell death or malignancies (Pattanayak et al., 2011). Investigations into the specificity of TALE arrays for their designated DNA targets suggest that a single mismatch in the nucleotide recognition site may be enough to impede dTALE binding, but that 3 - 4 mismatches within a target sequence will prevent binding (Morbitzer et al., 2010). The high specificity of this dTALE array for its cognate binding site decreases the likelihood of TALEN off-target cleavage. Furthermore, TALENs have recently been shown to be less cytotoxic than

ZFNs (Geurts et al., 2009; Mussolino et al., 2011; Tesson et al., 2011). This may be a result of improved TALEN target specificity when compared to ZFNs, which have been shown to trigger more off-target cleavage events (Mussolino et al., 2011). Either way, potential off-target sites need to be identified, and designer nucleases should be optimised to prevent unsolicited mutagenesis.

Although an *ex vivo* genome editing approach may be practical for the treatment of monogenic disorders, where the mutated or repaired gene is endogenous, this method would be ineffective as an anti-HBV gene therapy. This is because persistent episomal cccDNA pools maintain chronic HBV infection in hepatocytes, and as such, targeted disruption of this viral DNA is not a heritable trait. Consequently, anti-HBV TALENs need to be delivered throughout the liver to mediate efficient cccDNA cleavage. To establish whether the S and C TALENs are capable of inactivating hepatotropic HBV replication *in vivo*, they were tested in a murine model system. As these TALENs were administered directly to adult mice, a genome wide analysis was additionally performed to determine if any potential off-target binding sites are found in either the *Mus musculus* or human genomes.

5.2 Results

5.2.1 TALEN-mediated knock-down of markers of HBV replication *in vivo*

Of the four engineered TALENs tested in liver-derived cell culture models of HBV infection, both the S and C TALENs displayed the most efficient targeted disruption of cccDNA. For this reason, they were chosen to assess the anti-HBV efficacy of TALENs in a murine hydrodynamic tail vein injection (HDI) model of HBV replication (Liu et al., 1999; Yang et al., 2002). Plasmids expressing either the S or C TALENs were injected together with the pCH-9/3091 replication competent plasmid (Nassal, 1992) into the tail vein of NMRI mice (as described in section 7.4). In addition, a Firefly luciferase reporter plasmid was included in the bolus injectate to monitor delivery efficiency. Serological and intrahepatic markers of HBV viral replication, TALEN-associated liver toxicity, and HBV targeted mutagenesis assays were used to determine the anti-HBV efficiency of the S and C TALENs (Figures 5.1 – 5.8). A compilation of this data is represented in Table 5.1.

To confirm that equivalent transfection efficiencies occurred in the livers of mock, S TALEN, and C TALEN injected mice, bioluminescence imaging was used to measure Firefly luciferase expression on day 3 post-HDI (Figure 5.1A). Plasmid delivery efficiencies were determined by calculating the amount of luciferase radiance, measured as emitted relative light units, in each region of interest (ROI) (Figure 5.1B). For the six mice selected in each of the mock, S TALEN and C TALEN groups, bioluminescence was exclusively detected in the livers, and, although small variances were observed, equivalent mean luciferase radiance was detected across the

groupings. It is important to select for comparable delivery efficacies as HBV replication and TALEN expression is dependent on the efficient transfection of hepatocytes.

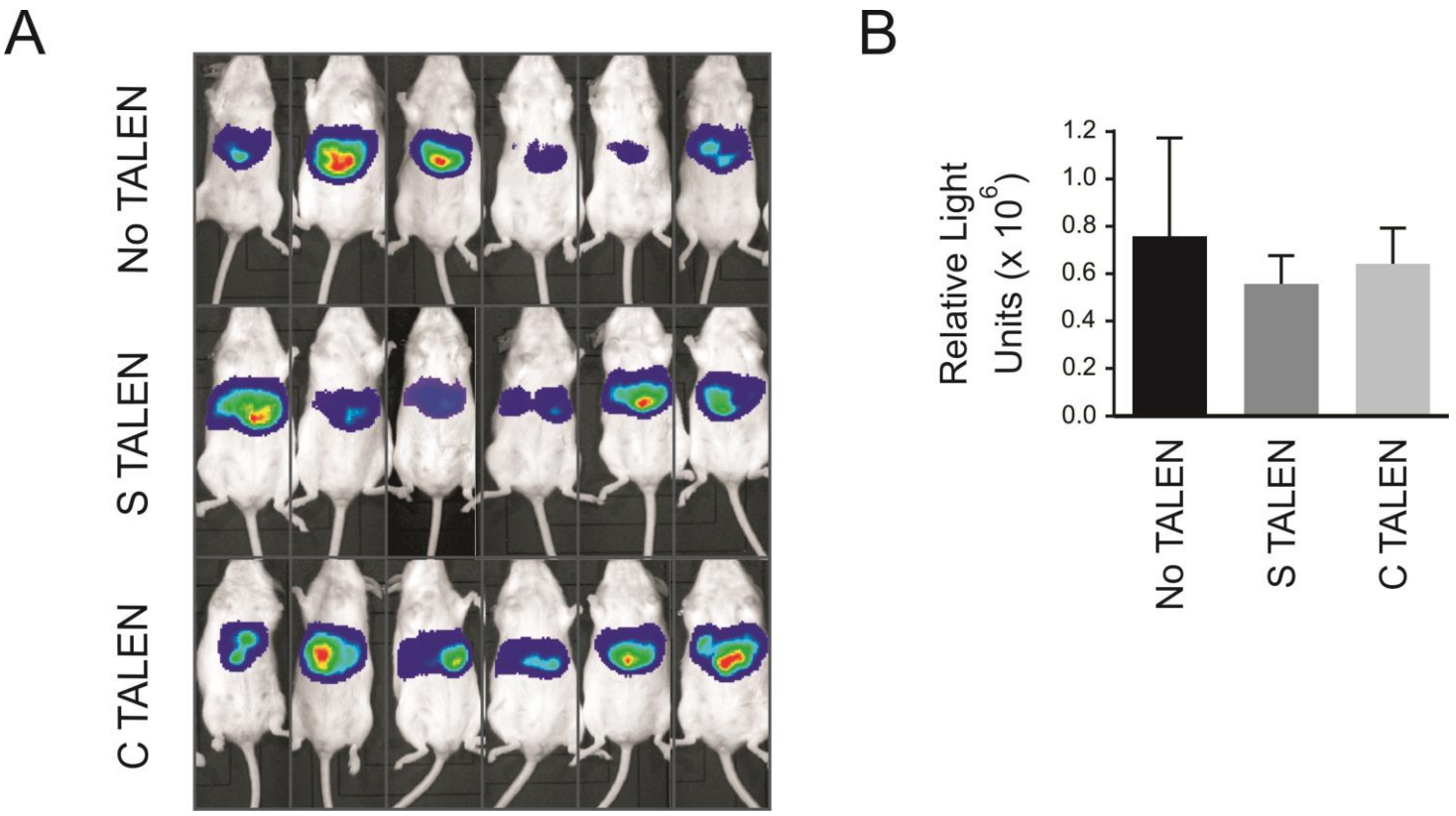

Figure 5.1: Bioluminescence imaging of *in vivo* reporter gene expression. A) At day 3 post-HDI, live imaging of Firefly luciferase expression was performed on mice from each of the mock, S TALEN and C TALEN groups. Liver specific plasmid delivery was detected in all injected mice. **B)** The number of relative light units emitted from the livers of injected mice was calculated. Equivalent delivery efficiencies were observed across the groups. Data is represented as the mean ±SEM (n = 6).

To determine the anti-HBV effects of S and C TALENs on viral replication, blood samples were collected on days 3 and 5 post-injection. Serum HBsAg concentrations and circulating viral particle equivalents (VPEs) were measured in these samples. When compared to mock treated mice, the S TALEN showed >90% reduction in serum HBsAg concentrations (Figure 5.2). This significant knockdown was sustained in all mice within the S TALEN group, at both days 3 and 5 post-HDI ($p<0.0001$ and $p = 0.0005$ respectively). The C TALEN showed approximately 30% knockdown in HBsAg expression, however this is at a much lower efficiency when compared to the S TALEN. To establish whether the S and C TALENs have a direct effect on HBV virion secretion, circulating VPEs were extracted from serum samples and rcDNA was quantified using real-time PCR (qPCR). The number of circulating VPEs decreased by approximately 70% at day 3 in both the S and C TALEN samples (Figure 5.3). By day 5 there were significantly less circulating VPEs detected in the S TALEN group ($p = 0.0284$), and both TALENs maintained between 50 – 70% fewer VPEs when compared to the mock. This suggests that these TALENs were affecting HBV replication and subsequently new virion production. As the S TALEN showed a marked decrease in both HBsAg concentrations and VPEs, it is most likely cleaving its cognate DNA binding site and interrupting surface protein production. During HBV replication these surface proteins are important for coating and budding on new virions (as shown in Figure 1.2). Although the C TALEN binding site is distinct from the *surface* ORF, the slight reduction in HBsAg concentration is more likely a result of this TALEN inhibiting new virion assembly, as shown by the decreased circulating VPEs.

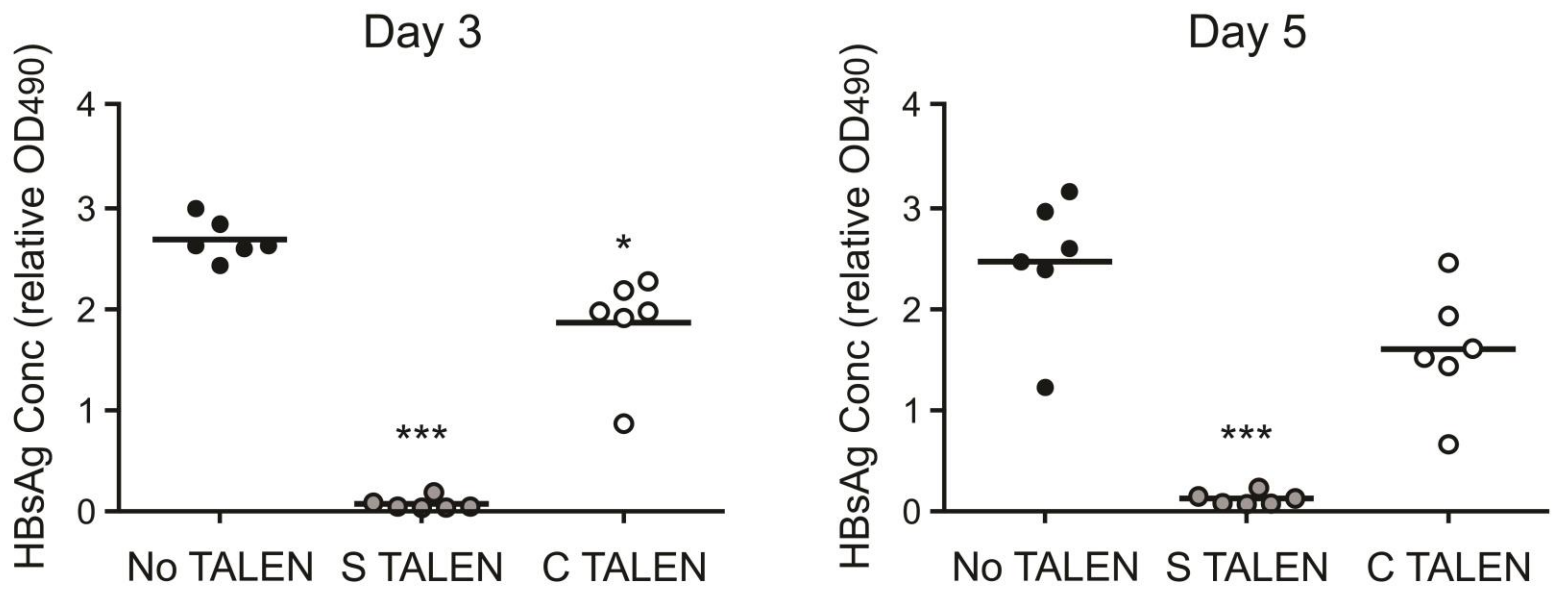

Figure 5.2: TALEN-mediated inhibition of serum markers of HBV replication. HBsAg concentrations were measured in serum samples collected from mice subjected to hydrodynamic injection of mock, S or C TALEN-expressing plasmids at days 3 (left panel) and 5 (right panel) post-injection. Data from individual samples are represented (n = 6).

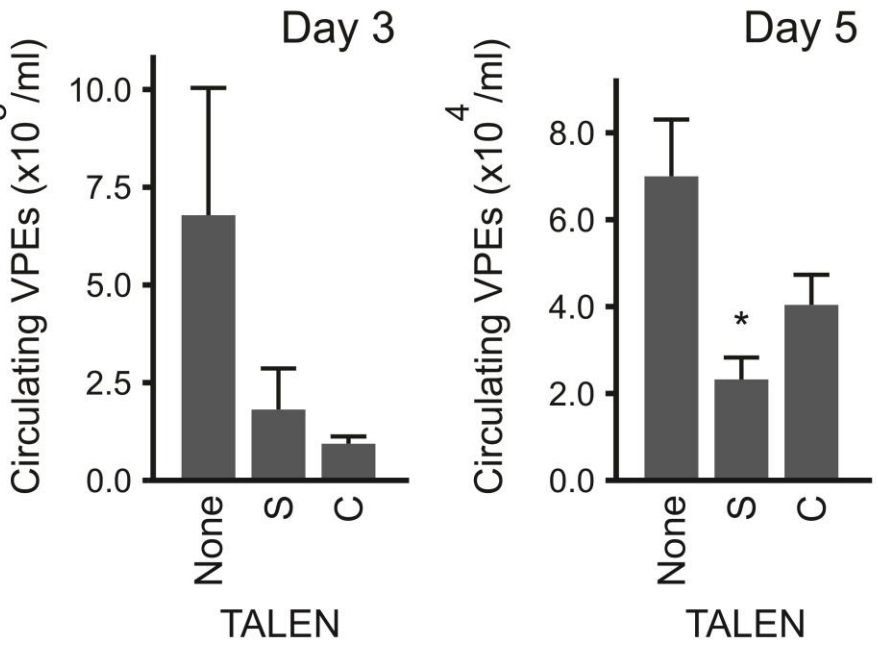

Figure 5.3: Inhibition of HBV replication by TALENs. Circulating VPEs were quantified by using qPCR to measure HBV DNA in serum samples collected on days 3 (left panel) and 5 (right panel) after HDI. Data is represented as the mean ±SEM where n = 6.

To confirm that TALENs were acting directly on HBV expression plasmids, intrahepatic analysis was subsequently performed. Mice were sacrificed five days after HDI and livers harvested for HBcAg detection and pgRNA quantification. Liver sections were subjected to immunohistochemical staining to detect intrahepatic HBcAg expression of mock, S, and C TALEN transfected murine hepatocytes. Visualisation under a light microscope at 100× (low) and 1000× (high) power fields showed distinct nuclear and cytoplasmic HBcAg staining in mock- and S TALEN-treated mice (Figure 5.4). In contrast, the C TALEN liver samples showed a marked decrease in HBcAg expression, with only a small number of hepatocytes showing nuclear staining when visualised under high power fields. As the *surface* and *core* ORFs are distinct from each other, the S TALEN should not affect core protein expression and the C TALEN should not interfere with surface protein expression. Since it has been shown that the S TALEN significantly reduced HBsAg expression (Figure 5.2) without affecting HBcAg production, and the C TALEN markedly decreased HBcAg expression, it can be concluded that both TALENs are specific for their cognate HBV DNA binding sites. In addition, the S and C TALENs independently inhibit VPE production, suggesting that disruptions in either the *surface* or *core* ORFs affect viral replication.

To establish whether these TALENs inhibited HBV mRNA expression, reverse transcription qPCR (RT-qPCR) was performed on RNA extracted from homogenised liver samples. HBV mRNA concentrations were quantified relative to the murine *glyceraldehyde-3-phosphate dehydrogenase* (*mGAPDH*) housekeeping gene. Despite a reduction in viral surface and core protein levels, there was no difference in intrahepatic HBV mRNA concentrations between the mock and TALEN treated hepatocytes (Figure 5.5). This suggests that these TALENs are not

inhibiting transcription of the HBV DNA, but instead inducing mutations at the target sites resulting in truncated or aberrant protein production.

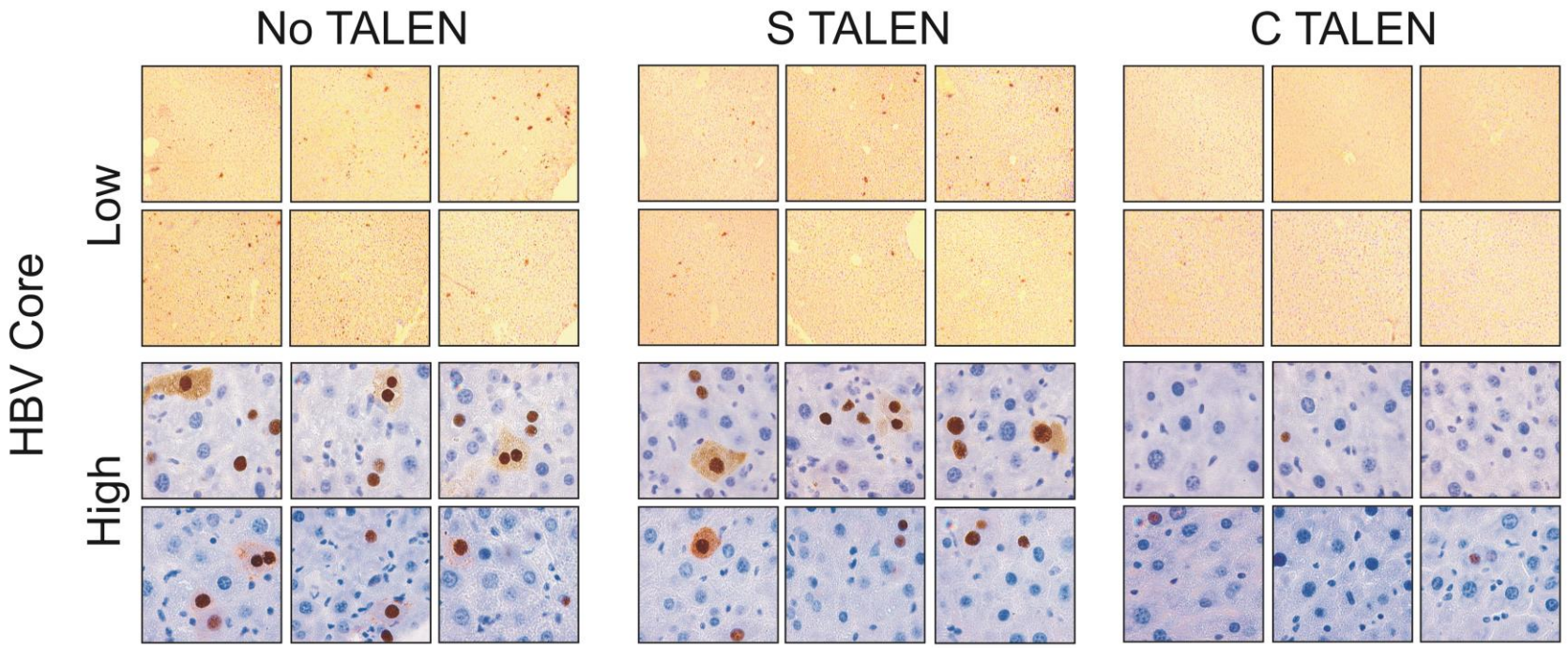

Figure 5.4: C TALEN mediated inhibition of HBcAg expression. Core antigen was detected in hepatocytes of mock (no TALEN), S, and C TALEN plasmid injected mice by immunoperoxidase staining (brown). The nuclei of cells were counterstained with haematoxylin (blue). A representative section from all six mice in each group is shown. The mock and S TALEN treated livers display both nuclear and cytoplasmic HBcAg expression, whilst the C TALEN hepatocytes shown little or no HBcAg expression. Low (100×) and high (1000×) power fields are shown.

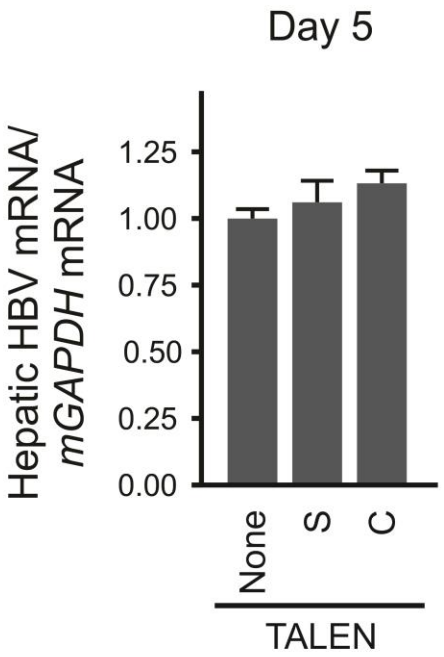

Figure 5.5: S and C TALENs do not affect hepatic HBV mRNA concentrations. RT-qPCR was used to measure intrahepatic HBV mRNA concentrations relative to *mGAPDH*, on day 5 following HDI. No variance in HBV mRNA expression was observed between mock and TALEN treated samples. Data is represented as the mean ±SEM, where n = 6.

A major concern regarding the administration of ZFNs and TALENs either *in vitro*, *ex vivo* or *in vivo* is nuclease-mediated cytotoxicity, which is most often associated with the induction of DSBs at both target and off-target binding sites. As this is the first direct *in vivo* administration of TALENs in a murine model, TALEN-associated liver toxicity was investigated. Serum transaminase activities and liver histology was performed on blood and liver samples collected from mock, S, and C TALEN treated mice on day 5 following HDI. Serum alanine transaminase (ALT) and aspartate transaminase (AST) levels were consistent between mock and TALEN treated samples, suggesting that there is no measurable TALEN associated toxicity (Figure 5.6A). Histological assessment using Haematoxylin and Eosin (H&E) staining showed no gross morphological changes between the mock, S TALEN, and C TALEN liver sections (Figure 5.6B). From these results it can be inferred that the S and C TALENs are not hepatotoxic.

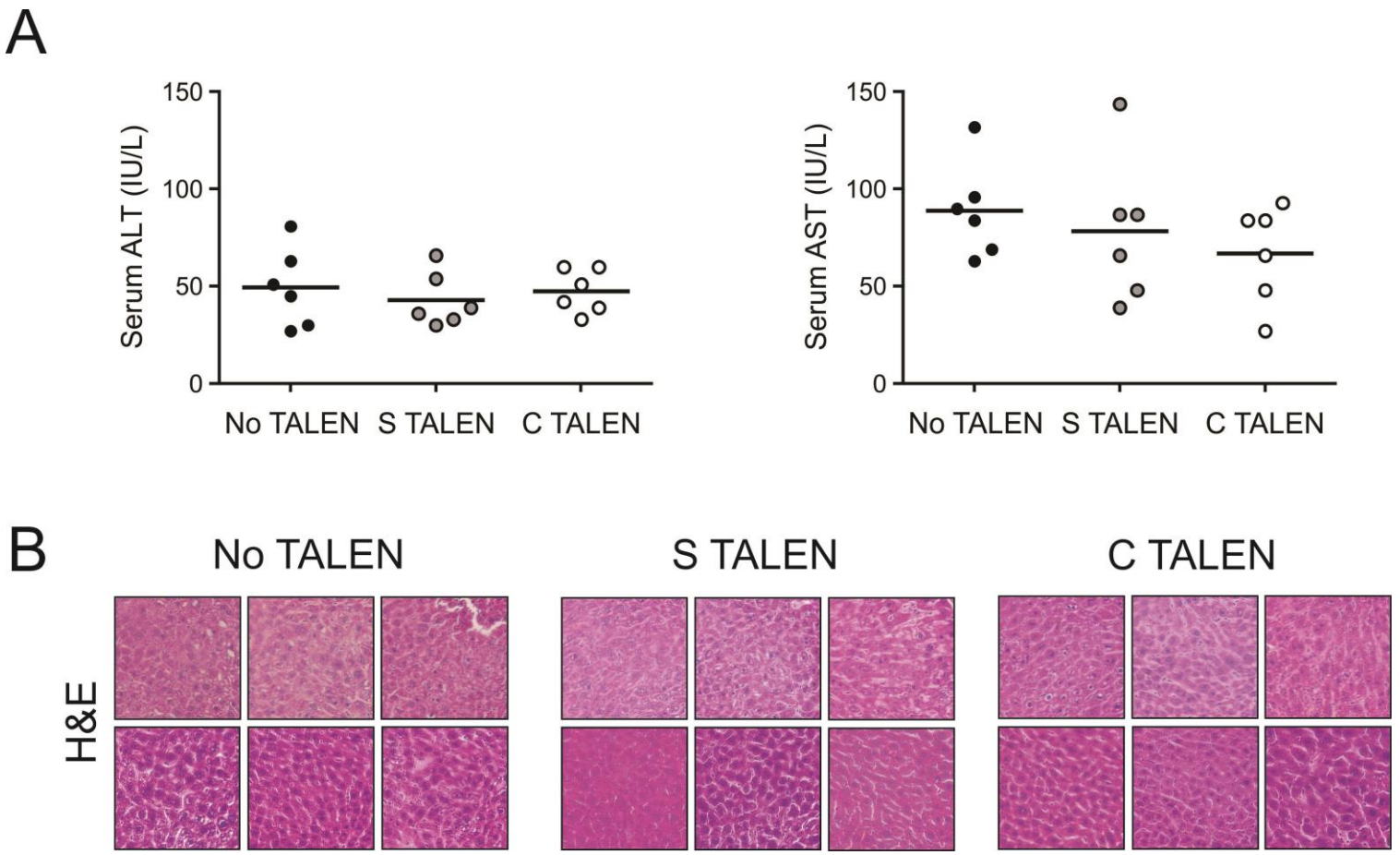

Figure 5.6: Absence of TALEN-associated liver toxicity. A) Serum alanine transaminase (ALT, left) and aspartate transaminase (AST, right) activity in mock, S, and C TALEN treated mice at day 5 post-HDI. No TALEN-associated toxicity was found in either the ALT or AST analysis. Data of serum samples from individual mice are shown (n = 6). **B)** Haematoxylin and Eosin staining (H&E) of liver sections recovered from mock and TALEN treated mice at day 5 following HDI. S and C TALEN treated liver sections showed similar gross morphology when compared to mock treated liver sections.

To confirm that S and C TALENs initiated target-specific mutagenesis, T7E1 assays and ultra-deep sequencing were performed on HBV-encoding DNA extracted from the livers of mock and TALEN treated mice. T7E1 analysis of HBV-encoded DNA isolated from S TALEN treated mice showed between 77% and 87% targeted disruption (Figure 5.7A). This site-directed cleavage was clearly demonstrated in DNA from the hepatocytes of all six mice in the S TALEN group, whilst mock treated mice consistently showed <1% targeted disruption. Deep sequencing was then used to define the mutagenic events occurring after TALEN-mediated cleavage. A large number of unique deletions were detected in S TALEN transfected liver samples whilst only wild-type sequences were detected in the mock (Figure 5.7B). Contig. 2 revealed an 83 nucleotide truncation, which was identified as the largest and most universal deletion detected. A single complex mutagenic event was identified in contig. 9, which included a 4 bp deletion as well as a 2 bp substitution. In addition, all the deletions identified displayed frameshift mutations, which would most likely result in the expression of severely truncated or aberrant surface proteins. When the C TALEN cleavage site was analysed using the T7E1 assay, targeted disruption occurred in 78 – 93% of HBV-encoding DNA from the six mice in the C TALEN treated group whilst no targeted disruption (<1%) was detected in mock treated animals (Figure 5.8A). Deep sequencing revealed that only wild-type sequences were detected in mock treated animals whilst seven distinct deletions were exclusively identified in C TALEN treated mice (Figure 5.8B). Two in-frame deletions were found in contigs. 3 (Δ3) and 8 (Δ93), whilst the remaining five contigs. contained frameshift mutations. Although there are both in-frame and frameshift mutations, these deletions will still result in aberrant core protein expression. Furthermore, as both the *S* and *C* ORFs overlaps with the *polymerase* encoding sequence, deletions at the S and C TALEN cleavage site would also disrupt polymerase protein conformations.

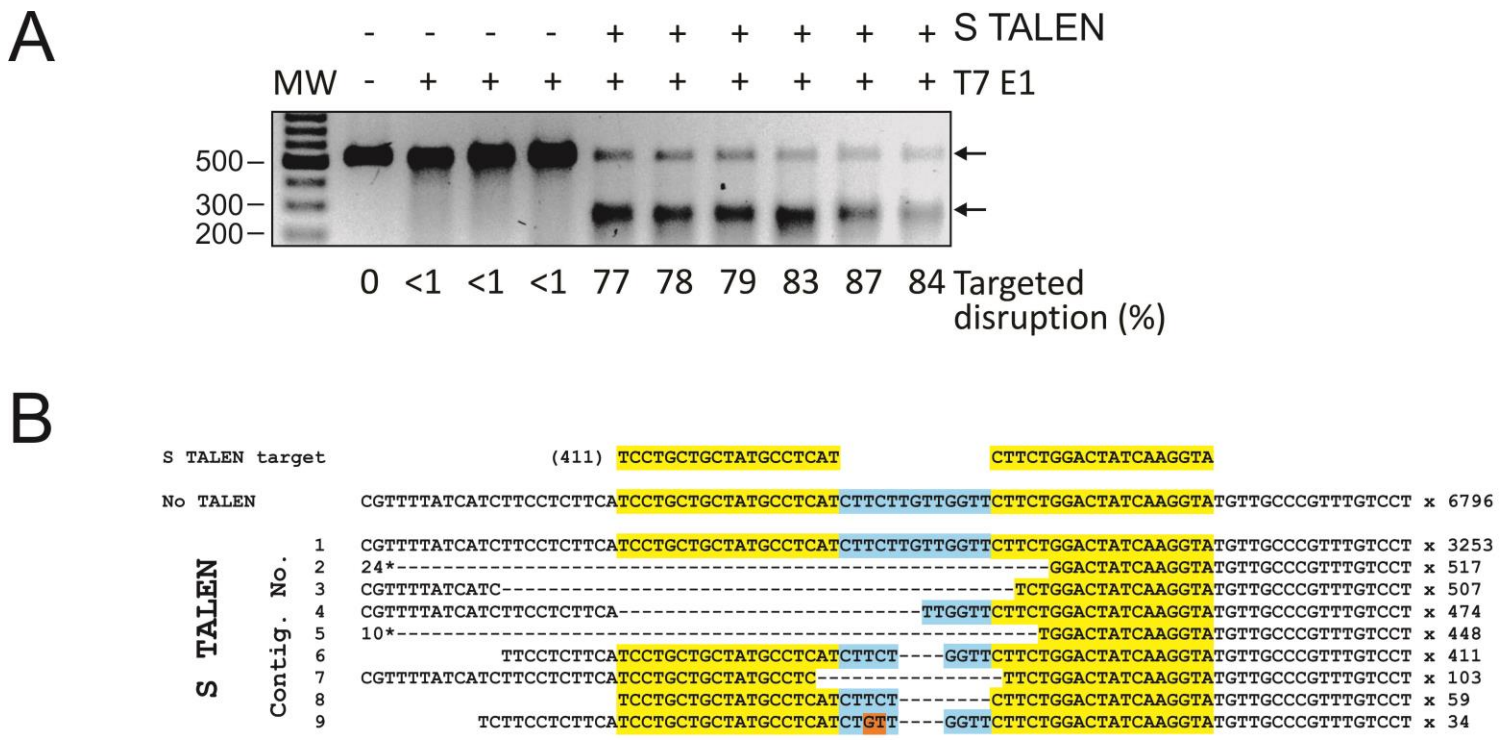

Figure 5.7: S TALEN-mediated *in vivo* site-directed mutagenesis. Intrahepatic HBV-encoding DNA was isolated from injected mice treated with either mock or S TALEN-expression plasmids in conjunction with an HBV expression plasmid. The region flanking the S TALEN cleavage site was amplified by PCR before T7E1 analysis and deep sequencing. **A)** Three mock treated mice (- S TALEN) and all six S TALEN treated mice (+ S TALEN) were assessed for targeted disruption. **B)** Deep sequencing performed on the S TALEN cleavage site. The SL and SR TALEN targets are highlighted in yellow with the wild-type spacer region in blue. All detected sequences are shown with the number of reads on the right. Wild-type sequences were detected in both the mock (no TALEN) and S TALEN samples. Deletions, shown as dashed lines, and substitutions, shown in red, were detected in the S TALEN treated samples. Additional deletions of 24 and 10 nucleotides were identified at the 5' ends of contigs 2 and 5.

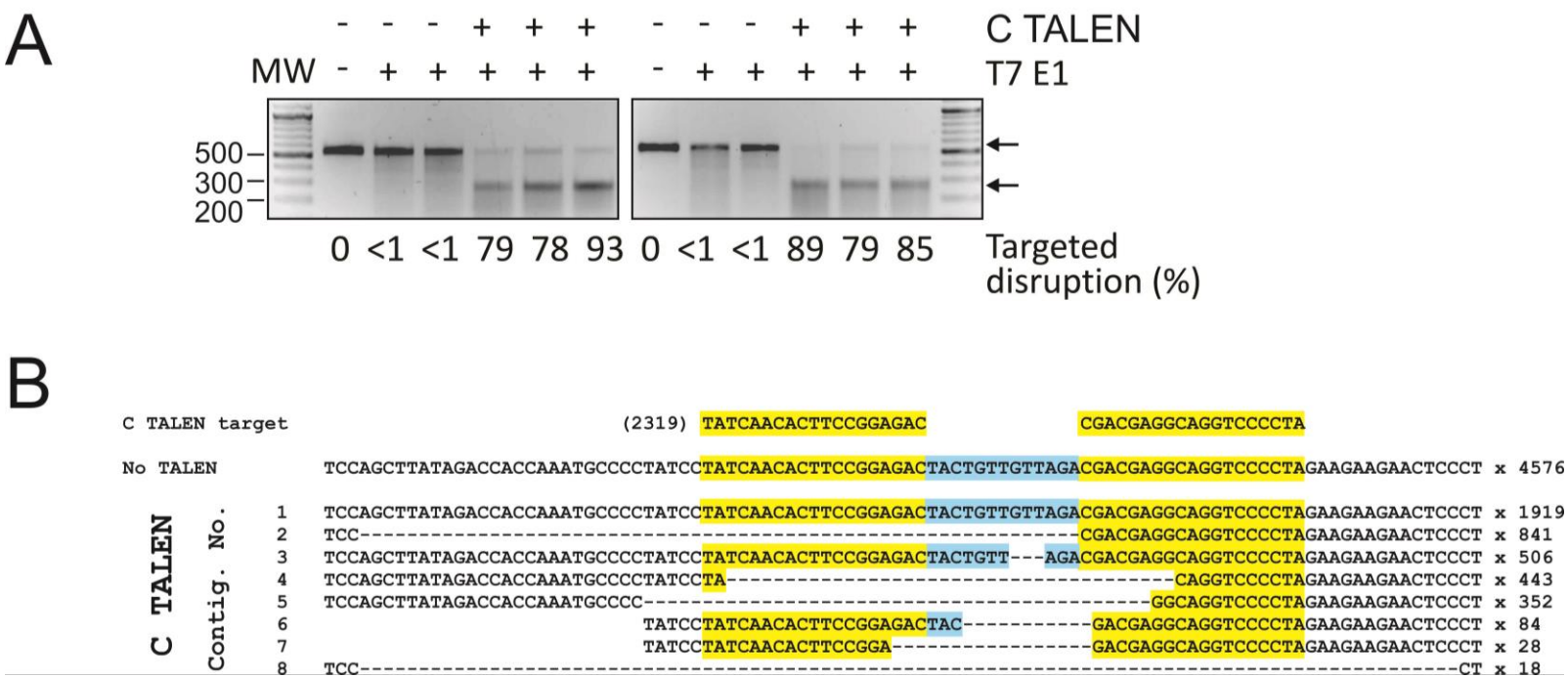

Figure 5.8: C TALEN-mediated *in vivo* site-directed mutagenesis. Intrahepatic HBV-encoding DNA was collected, amplified and analysed using T7E1 **(A)** and deep sequencing **(B)** as described in Figure 3.13, but for mock and C TALEN treated mice. **A)**. Four mock treated mice (- C TALEN) and all six C TALEN treated mice (+ C TALEN) were assessed for targeted disruption. **B)** Wild-type sequences were detected in both mock (no TALEN) and C TALEN HBV-encoding DNA samples. Seven different deletion events were detected in C TALEN treated samples but not in mock treated samples.

Table 5.1: *In vivo* analysis of anti-HBV TALENs

		No TALEN	S TALEN	C TALEN
Emitted relative Light units	Day 3	758500 (± 414561)	557167 (± 119802)	642833 (± 150703)
Serum HBsAg concentration (relative OD_{490})	Day 3	2.690 (± 0.0811)	0.077 (± 0.0240)	1.869 (± 0.2075)
	Day 5	2.476 (± 0.2772)	0.128 (± 0.0259)	1.609 (± 0.2423)
Circulating VPEs per ml	Day 3	1.000 (± 0.5913)	0.313 (± 0.1759)	0.159 (± 0.0131)
	Day 5	1.000 (± 0.1358)	0.404 (± 0.0943)	0.714 (± 0.1166)
Hepatic HBV mRNA /m*GAPDH* mRNA	Day 5	0.996 (± 0.0340)	1.061 (± 0.0750)	1.127 (± 0.0487)
Serum ALT (U/L)	Day 5	49.50 (± 8.334)	43.00 (± 5.727)	47.50 (± 4.610)
Serum AST (U/L)	Day 5	89.00 (± 10.00)	78.50 (± 15.36)	67.00 (± 10.35)
T7E1 Targeted Disruption	Day 5	<1% (± 0)	81.3% (± 3.93)	81.2% (± 4.22)

All data is represented as the mean (n = 6) ±SEM

5.2.2 Examining potential off-target cleavage sites

Potential for off-target cleavage presents a major risk for genotoxicity associated with using designer nucleases. To determine whether the anti-HBV S and C TALENs are capable of binding to any endogenous human or mouse genes, the TALENT 2.0 paired target finder (Doyle et al., 2012) and Basic Local Alignment Search Tool (BLAST) (Altschul et al., 1990), were used to identify additional TALEN binding sites. The TALENT 2.0 paired target finder may be used to identify potential off-target binding sites for a combination of any TALEN subunit pairs. This is particularly useful for the anti-HBV TALENs used in this study which contain wild-type *Fok*I domains. As a result, two left or two right TALEN subunits could potentially dimerise and cleave at an endogenous off-target site. To identify off-targets either the designed S and C TALEN pairs, or dual left and dual right TALEN subunits were examined. When searching the human and mouse genomes for potential off-target binding sites, with a predefined spacer region of between 10 – 15 bp, the TALENT 2.0 paired target finder was unable to detect any significant binding sites for either the S or C TALENs or their dual left and right subunits.

Although these results were promising, a standard nucleotide BLAST alignment was performed to map any individual TALEN subunit binding sites. The mouse genomic + transcript or human genomic + transcript databases were used during TALEN alignments. To include potential off-target binding sites with strong sequence homology as well as various nucleotide mismatches, BLAST searches were performed using both the 'highly similar sequences (megablast)' and 'somewhat similar sequences (blastn)' search optimisation algorithms. As it has been previously demonstrated that 3 – 4 mutations typically block TAL binding (Morbitzer et al., 2010), possible

off target sites were defined as having a minimum sequence identity of 15 out of a possible 19 nucleotides at each TALEN subunit DNA recognition site. This allowed for a maximum of four mismatches per subunit. A number of different potential binding sites were identified for SL and SR TALENs in both the mouse (Table 5.2) and human (Table 5.3) genomes. Additionally, multiple left or right subunit binding sites were identified on single chromosomes. Despite having detected a number of potential SL and SR TALEN subunit binding positions, no off-target cleavage sites could be identified since all prospective sites were intermittently dispersed across the genome. As none of the potential off-target binding sites were located within a close proximity of one another, no TALEN dimers, and therefore no DSB sites, could be identified. When the C TALEN subunits were investigated, CL and CR TALENs resulted in very few potential binding sites in the mouse (Table 5.4) and human (Table 5.5) genome. Again, potential multiple binding sites were located in certain chromosomes, but none were positioned within a close enough nucleotide range that would result in cleavage. The lack of possible off-target sites, especially when the C TALEN subunits were analysed, may be attributed to the fact that these TALENs were designed to target a viral DNA sequence and not an endogenous gene. This may also allude to the absence of cytotoxic events when these TALENs were investigated *in vitro* or *in vivo*, suggesting that the host cell's DNA is not targeted. Patients with long-term chronic HBV infections however, are at a greater risk for developing HCC, which has been linked to multiple viral DNA integrations (Murakami et al., 2005). If S and C TALEN binding sites are conserved within HBV integrants, both TALENs could potentially cleave these integrated transcripts. However as HBV integration may occur at multiple endogenous DNA target loci which also vary between different HBV-induced HCCs (Ding et al., 2012), it will be difficult to examine the global effect of anti-HBV TALENs on these integrated transcripts.

Table 5.2: BLAST analysis of the *Mus musculus* genome to identify potential binding sites of combined and individual left and right subunits (SL and SR) of the S TALEN.

	CH	Nucleotide Range	S TALEN Sites		ID[#]	S-Ref
			SL	SR		
			TCCTGCTGCTATGCCTCAT AGGACGACGATACGGAGTA	***CTTCTGGACTATCAAGGTA*** GAAGACCTGATAGTTCCAT		
Potential combined SL and SR sites	6	6830661 to 6830677 11962065 to 11962080 41232469 to 41232483	●CCTGCTGCTATGCCTCA●* TCCTGCTGCTATGCCT●●● 	 CTTCTGGACTATCAA●●●●	17/19 16/19 15/19	NW_001030820.1
	4	44188029 to 44188045 31532806 to 31532820 8318087 to 8318104 36732721 to 36732735	●●CTGCTGCTATGCCTCAT ●CCTGCTGCTATGCCT●●● ●CCTGCTGCTA●GCCTCAT 	 ●TTCTGGACTATCAAG●●●	17/19 15/19 15/19 17/19	NT_187032.1
	4	22544951 to 22544966 10954765 to 10954779	TCCTGCTGCTATGCCT●●● 	 ●●●●TGGACTATCAAGGTA	16/19 15/19	NT_187033.1
	8	9218161 to 9218176 26838227 to 26838244	TCCTGCTGCTATGCCT●●● 	 ●TTCTGGA●TATCAAGGTA	16/19 17/19	NT_078575.7
	9	3697632 to 3697647 44495841 to 44495855	TCCTGCTGCTATGCCT●●● 	 CTTCTGGACTATCAA●●●●	16/19 15/19	NT_039474.8
	13	1175041 to 1175059 4966540 to 4966554	TCCTGCTGCT●TGCCTCAT 	 ●●●●TGGACTATCAAGGTA	18/19 15/19	NW_001030529.1
	9	43318590 to 43318605 44102972 to 44102987 10709989 to 10710005	TCCTGCTGCTATGCCT●●● TCCTGCTGCTATGCCT●●● 	 CTTCTGGACTA●CAAGG●●	16/19 16/19 16/19	NW_001030907.1
	7	1111381 to 1111396 38299233 to 38299248 53113291 to 53113306 50396556 to 50396574 2339469 to 2339486 8016639 to 8016656 2033241 to 2033255	TCCTGCTGCTATGCCT●●● TCCTGCTGCTATGCCT●●● TCCTGCTGCTATGCCT●●● TCCTGCTGCT●TGCCTCAT TCCTGCTGCTATG●CTCA● TCCTGCTGCT●TGCCTCA● 	 CTTCTGGACTATCAA●●●●	16/19 16/19 16/19 18/19 17/19 17/19 15/19	NT_039433.8
	3	41300341 to 41300356 27971181 to 27971195 66053798 to 66053816	TCCTGCTGCTATGCCT●●● 	 ●TTCTGGACTATCAAG●●● CTTCTGG●CTATCAAGGTA	16/19 15/19 18/19	NT_039240.8
	17	69593674 to 69593692 30114485 to 30114500	TCCTGCT●CTATGCCTCAT 	 ●●TCTGGACTATCAAGGT●	18/19 16/19	NT_039649.8
Potential individual SL sites	13	17430998 to 17431014 2227826 to 2227841	TCCTGCTGCTATGCCTC●● TCCTGCTGCTATGCCT●●●		17/19 16/19	NW_001030517.1
	6	845523 to 845539 5969096 to 5969111	●CCTGCTGCTATGCCTCA● TCCTGCTGCTATGCCT●●●		17/19 16/19	NT_039360.8
	4	12854748 to 12854763 25385538 to 25385553	TCCTGCTGCTATGCCT●●● TCCTGCTGCTATGCCT●●●		16/19 16/19	NT_039264.7
	9	36145333 to 36145348 36938186 to 36938201	TCCTGCTGCTATGCCT●●● TCCTGCTGCTATGCCT●●●		16/19 16/19	NT_039472.8
	14	28926064 to 28926081 60263242 to 60263256	●CCTGCTGCTATGCCTCAT ●CCTGCTGCTATGCCT●●●		18/19 15/19	NT_039606.8
	19	49262317 to 49262333 2286312 to 2286326	TCCTGCTGCTATGCCTC●● ●●CTGCTGCTATGCCTC●●		17/19 15/19	NT_039687.8

		15839462 to 15839476	TCCTGCTGCTATGCC●●●●		15/19	
	7	22820518 to 22820533 37540231 to 37540246 34806807 to 34806825	TCCTGCTGCTATGCCT●●● TCCTGCTGCTATGCCT●●● TCCTGCTGCT●TGCCTCAT		16/19 16/19 18/19	NW_001030877.1
	11	55118539 to 55118554 60207885 to 60207900	TCCTGCTGCTATGCCT●●● TCCTGCTGCTATGCCT●●●		16/19 16/19	NT_096135.6
Potential individual SR sites	3	27971181 to 27971195 66053798 to 66053816		●TTCTGGACTATCAAG●●● CTTCTGG●CTATCAAGGTA	15/19 18/19	NT_039240.8
	11	8445188 to 8445204 12712726 to 12712742		CTTCTGG●CTATCAAGG●● ●TTCTG●ACTATCAAGGT●	16/19 16/19	NW_001030434.1
	2	16581880 to 16581894 25991220 to 25991236 68974756 to 68974772		CTTCTGGACTATCAA●●●● ●TTCTG●ACTATCAAGGT● CTTCTGGACT●TCAAGG●●	15/19 16/19 16/19	NT_039207.8
	16	61477073 to 61477087 36662006 to 36662022 71304901 to 71304917		●TTCTGGACTATCAAG●●● CTTCTGGACTA●CAAGG●● ●TTCTGGA●TATCAAGGT●	15/19 16/19 16/19	NW_001030584.1
	19	26586727 to 26586741 26777773 to 26777787 26955911 to 26955925		CTTCTGGACTATCAA●●●● CTTCTGGACTATCAA●●●● CTTCTGGACTATCAA●●●●	15/19 15/19 15/19	NT_039687.8

CH = chromosome; ID = identity; S-Ref = sequence reference accession number in GenBank

[#]A minimum sequence ID between TALEN subunit cognates and sites within the *Mus musculus* genome of 15 out of 19 sense or antisense nucleotides was used as a cut off.

*Mismatches between the TALEN subunit cognates and the aligned sequence in the *Mus musculus* genome are indicated by '●'.

Table 5.3: BLAST analysis of the human genome to identify potential binding sites of combined and individual left and right subunits (SL and SR) of the S TALEN.

	CH	Nucleotide Range	S TALEN Sites		ID[#]	S-Ref
			SL	SR		
			TCCTGCTGCTATGCCTCAT AGGACGACGATACGGAGTA	***CTTCTGGACTATCAAGGTA*** GAAGACCTGATAGTTCCAT		
Potential combined SL and SR sites	5	5316824 to 5316838 1348622 to 1348638	●●CTGCTGCTATGCCTC●●	●TTCTGGACTATC●AGGT●	15/19 16/19	NW_004078023.1
	6	16508260 to 16508274 36973928 to 36973944 28906310 to 28906326 66068358 to 66068374	●●CTGCTGCTATGCCTC●● ●●CTGCTGCTAT●CCTCAT	 ●TTCTGGACTAT●AAGGT● ●TTCTGGACTATC●AGGT●	15/19 16/19 16/19 16/19	NW_004078028.1
	3	52993974 to 52993988 81226837 to 81226851 9589025 to 9589042	TCCTGCTGCTATGCC●●●● ●●●TGCTGCTATGCCTCA●	 ●TTCTGGA●TATCAAGGTA	15/19 15/19 17/19	NT_005612.16
	17	28496793 to 28496807 35558057 to 35558074 13845926 to 13845940	●●●●GCTGCTATGCCTCAT ●CCTGCTGCT●TGCCTCAT	 ●●●●TGGACTATCAAGGTA	15/19 17/19 15/19	NT_010783.15
	16	9515596 to 9515610 10180724 to 10180741 20197304 to 20197318	●●●TGCTGCTATGCCTCA●	 CTTCTGGACTATCAAGGT● ●●●●TGGACTATCAAGGTA	15/19 18/19 15/19	NT_010393.16
	4	28481514 to 28481528 86675613 to 86675630 5401736 to 5401752 26630796 to 26630810 91203543 to 91203560 42836405 to 42836421	TCCTGCTGCTATGCC●●●● ●CCTGCTGCT●TGCCTCAT TCCTGCTGC●ATGCCTC●● 	 ●●●●TGGACTATCAAGGTA ●TTCTGGACTAT●AAGGTA CTTCTG●ACTATCAAGG●●	15/19 17/19 16/17 15/19 17/19 16/19	NT_016354.19
	19	8260049 to 8260063 5398156 to 5398173	TCCTGCTGCTATGCC●●●●	 CTTCT●GACTATCAAGGT●	15/19 17/19	NT_011109.16
	9	32244124 to 32244141 26866298 to 26866315	●CCTGCTGCTA●GCCTCAT	 CTTCTGGA●TATCAAGGT●	17/19 17/19	NT_008413.18
	1	61198693 to 61198710 11611961 to 11611975 47930542 to 47930556 66083096 to 66083110	TCCTGCTGCT●TGCCTCA●	 ●●TCTGGACTATCAAGG●● ●●●CTGGACTATCAAGGT● ●●●CTGGACTATCAAGGT●	17/19 15/19 15/19 15/19	NT_032977.9
	6	10893712 to 10893726 9894805 to 9894819 14658716 to 14658733	●CCTGCTGCTATGCCT●●●	 ●TTCTGGACTATCAAG●●● ●TTCTGGACT●TCAAGGTA	15/19 15/19 17/19	NT_007299.13
Potential individual SL sites	22	13395721 to 13395736 23229742 to 23229758 26356393 to 26356409 30107958 to 30107974	●CCTGCTGCTATGCCTC●● TCCTGCTGCTAT●CCTC●● TCCTGCTGCT●TGCCTC●● ●CCTGCTGCT●TGCCTCA		16/19 16/19 16/19 16/19	NW_004078112.1
	15	69598949 to 69598963 7011373 to 7011389 42322452 to 42322468	●CCTGCTGCTATGCCT●●● ●●CTGCTGCT●TGCCTCAT ●●CTGCTGCTAT●CCTCAT●		15/19 16/19 16/19	NW_004078084.1
	17	12292150 to 12292164 5230569 to 5230586	●●●●GCTGCTATGCCTCAT ●CCTGCTGCT●TGCCTCAT		15/19 17/19	NW_001838454.2
	3	11943588 to 11943602 20444778 to 20444795	●CCTGCTGCTATGCCT●●● TCCTGCTGCTAT●CCTCA●		15/19 17/19	NW_001838877.2

		1113755 to 1113771	●●CTGCTGCTATGC●TCAT		16/19	
	11	3402649 to 3402663 21709223 to 21709239	●●CTGCTGCTATGCCTC●● TCCTGCTGCT●TGCCTC●●		15/19 16/19	NT_033899.8
	6	16509724 to 16509738 36971717 to 36971733	●●CTGCTGCTATGCCTC●● ●●CTGCTGCTAT●CCTCAT		15/19 16/19	NT_025741.15
Potential individual SR sites	13	67246550 to 67246566 36698126 to 36698140 37005816 to 37005830 32823986 to 32824003		CTTCTGGACTATCAAGG●● CTTCTGGACTATCAA●●●● ●●●CTGGACTATCAAGGT● ●TTCTGGA●TATCAAGGTA	17/19 15/19 15/19 17/19	NT_024524.14
	21	8582147 to 8582162 26035956 to 26035973		●●●CTGGACTATCAAGGTA CTTCTGGACTATC●AGGT●	16/19 17/19	NT_011512.11
	12	2866821 to 2866835 485378 to 485394		●●●CTGGACTATCAAGGT● ●●TTCTGGACTATCCAGGT●	15/19 16/19	NW_001838060.2
	1	5704171 to 5704185 23791575 to 23791591		●●●CTGGACTATCAAGGT● CTTCTGGACTA●CAAGG●●	15/19 16/19	NW_001838579.2
	9	49639304 to 49639318 30386318 to 30386335		●TTCTGGACTATCAAG●●● ●TTCTGGACTA●CAAGGTA	15/19 17/19	NT_008470.19

CH = chromosome; ID = identity; S-Ref = sequence reference accession number in GenBank

#A minimum sequence identity (ID) between TALEN subunit cognates and sites within the human genome of 15 out of 19 sense or antisense nucleotides was used as a cut off.

*Mismatches between the TALEN subunit cognates and the aligned sequence in the human genome are indicated by '●'.

Table 5.4: BLAST analysis of the *Mus musculus* genome to identify potential binding sites of combined and individual left and right subunits (CL and CR) of the C TALEN.

	CH	Nucleotide Range	C TALEN Sites		ID#	S-Ref
			CL	CR		
			TATCAACACTTCCGGAGAC ATAGTTGTGAAGGCCTCTG	***CGACGAGGCAGGTCCCCTA*** GCTGCTCCGTCCAGGGGAT		
Potential combined CL and CR sites	5	18010816 to 18010830 19827052 to 19827066 16218494 to 16218508	●●TCAACACTTCCGGAG●● ●●TCAACACTTCCGGAG●●	 ●●●●GAGGCAGGTCCCCTA	15/19 15/19 15/19	NW_001030796.1
	9	47261339 to 47261354 7863713 to 7863727	TATCAA●ACTTCCGGA●●●	 ●●●●GAGGCAGGTCCCCTA	15/19 15/19	NT_039474.8
	17	38384398 to 38384414 43566525 to 43566540 70416673 to 70416687	●ATCAACACTTCC●GAGA● ●●●CAACACTTCCG●AGAC	 ●●●●GAGGCAGGTCCCCTA	16/19 15/19 15/19	NT_039649.8
Potential CL sites	3	38866300 to 38866314 53841380 to 53841397 34012433 to 34012449 59437720 to 59437735	●ATCAACACTTCCGGA●●● TATCA●CACTTCCGGAGA● ●●TCAA●ACTTCCGGAGAC TATCA●CACTTCCGGA●●●		15/19 17/19 16/19 15/19	NT_039240.8
	5	531836 to 531850 2348932 to 2348946	●●TCAACACTTCCGGAG●● ●●TCAACACTTCCGGAG●●		15/19 15/19	NT_078458.7
	14	6519500 to 6519514 6659119 to 6659133 6798768 to 6798782 26304835 to 26304850	●ATCAACACTTCCGGA●●● ●ATCAACACTTCCGGA●●● ●ATCAACACTTCCGGA●●● ●●●CAACACTTC●GGAGAC		15/19 15/19 15/19 15/19	NT_039606.8
	2	93924002 to 93924019 9619835 to 9619851 87013076 to 87013092	●ATCAACACTTCC●GAGAC TATCAACACTTC●GGAG●● ●●TCAACAC●TCCGGAGAC		17/19 16/19 16/19	NT_039207.8
Potential CR sites	Sequences in the *Mus musculus* genome with 15 or more nucleotide identities to the CR cognate were not found.					

CH = chromosome; ID = identity; S-Ref = sequence reference accession number in GenBank

#A minimum sequence identity (ID) between TALEN subunit cognates and sites within the *Mus musculus* genome of 15 out of 19 sense or antisense nucleotides was used as a cut off.

*Mismatches between the TALEN subunit cognates and the aligned sequence in the *Mus musculus* genome are indicated by '●'.

Table 5.5: BLAST analysis of the human genome to identify potential binding sites of combined and individual left and right subunits (CL and CR) of the C TALEN.

	CH	Nucleotide Range	C TALEN Sites		ID#	S-Ref
			CL	CR		
			TATCAACACTTCCGGAGAC ATAGTTGTGAAGGCCTCTG	***CGACGAGGCAGGTCCCCTA*** GCTGCTCCGTCCAGGGGAT		
Potential combined CL and CR sites	3	51696616 to 51696632 65720310 to 65720324	TATCAACACTTC●GGAG●●	●●●●GAGGCAGGTCCCCTA	16/17 15/19	NT_022517.18
	2	56850349 to 56850365 15604047 to 15604063	●●TCAACACTTC●GGAGAC	●GACGAGGCAGG●CCCCT●	16/19 16/19	NW_004078008.1
	21	4560786 to 4560802 30289322 to 30289338	●●TCAACACTTC●GGAGAC	CGAC●AGGCAGGTCCCC●●	16/19 16/19	NW_004078109.1
Potential CL sites	8	4869274 to 4869289 12795942 to 12795958	●●●CAACACTTCCGGAGAC ●●TCAACACTTC●GGAGAC		16/19 16/19	NT_167187.1
	7	30035998 to 30036012 36477879 to 36477895 42858728 to 42858744	●●TCAACACTTCCGGAG●● TATCAACACTTC●GGAG●● ●●TCAACACTTC●GGAGAC		15/19 16/19 16/19	NT_007819.17
	6	5016435 to 5016449 31733101 to 31733119	●●TCAACACTTCCGGAG●● TATCAACACTTCC●GAGAC		15/19 18/19	NT_007592.15
	3	30147609 to 30147625 55554086 to 55554102	TATCAACA●TTCCGGAG●● ●●TCAACACTTC●GGAGAC		16/19 16/19	NT_005612.16
Potential CR sites	2	553285 to 553301 830629 to 830645		●GACGAGGCAGG●CCCCT● ●GACGAGGCAGG●CCCCT●	16/17 16/17	NT_022135.16

CH = chromosome; ID = identity; S-Ref = sequence reference accession number in GenBank

#A minimum sequence identity (ID) between TALEN subunit cognates and sites within the human genome of 15 out of 19 sense or antisense nucleotides was used as a cut off.

*Mismatches between the TALEN subunit cognates and the aligned sequence in the human genome are indicated by '●'.

5.3 Discussion

Previous mammalian animal studies have used an *ex vivo* gene editing approach to disrupt or repair endogenous DNA sequences. Multiple selection steps are then required to isolate efficiently mutated or repaired target sites before re-implantation. Although this method is appropriate for generating knock-out or transgenic animal models, and treating certain human diseases, it is not suitable for TALEN-mediated inactivation of HBV. Since viral replication is driven by the transcription of episomal cccDNA, cleavage of this viral intermediate will not result in heritable mutations. Instead we implemented an alternative nuclease delivery approach, which facilitated the study of intrahepatic TALEN-mediated targeted disruption of episomal HBV DNA in a murine disease model.

This was achieved by hydrodynamic tail vein injection of both TALEN and HBV-encoding plasmids. TALEN-mediated targeted mutagenesis of intrahepatic HBV-encoding DNA was accomplished using either the S or C TALENs. The S TALEN efficiently knocked-down serum HBsAg expression, whilst the C TALEN reduced intrahepatic HBcAg levels showing that each TALEN is specific for its cognate binding site. Knock-down of HBV replication intermediates was shown to occur in a transcription-independent manner, as HBV mRNA levels remained unchanged. TALEN-mediated disruption of the cognate DNA target site inhibited *surface* and *core* protein production, ultimately impeding viral replication and virion secretion. This site-directed mutagenesis is likely to result in aberrant or truncated viral protein production, essentially reducing viral fitness. In addition, no nuclease associated toxicity was observed, suggesting that endogenous off-target cleavage did not occur. To our knowledge this is the first

direct administration of TALENs in an animal disease model system, as well as the only *in vivo* demonstration of nuclease-mediated disruption of HBV replication.

By characterising TALEN-mediated site-directional mutagenesis we confirmed that the S and C TALENs were indeed actively cleaving their designated HBV DNA target sites resulting mainly in frameshift mutations. This targeted disruption is most likely attributable to error-prone NHEJ events occurring after TALEN cleavage. Deletions were predominantly detected at both the S and C TALEN target sites, which corresponds with the recent discovery that ZFNs and TALENs stimulate different mutational events (Kim et al., 2013b). TALEN cleavage results almost exclusively in targeted deletions whereas ZFNs give rise to insertions and more combined mutational events. It has been hypothesised that the differences between ZFN and TALEN mutation signatures may result from the distinct lengths of the spacer regions used to initiate DSBs (Kim et al., 2013b). ZFNs are usually designed with at 5 or 6 bp spacer region, whilst TALENs have shown efficient cleavage with spacer lengths ranging from 12 to 21 bp (Christian et al., 2012; Mussolino et al., 2011). With a confined spacer region, the ZFNs are likely to create defined overhangs after cleavage. However the longer TALEN spacer regions may result in an assortment of overhangs, as the *Fok*I nuclease heterodimers cleave non-specifically. Although it has been predicted that TALEN mediated DSBs induce targeted mutagenesis through NHEJ events, alternative cellular repair mechanisms may also be employed. Two specific pathways, microhomology-mediated end joining (MMEJ) and single stranded annealing (SSA), resect DNA overhangs at the DSB site, and in doing so create deletions (Huertas, 2010; McVey and Lee, 2008). These alternative repair pathways may work in conjunction with NHEJ to repair DSBs generated by ZFN or TALEN cleavage.

Previous anti-HBV ZFN investigations were performed in liver-derived cell cultures (Cradick et al., 2010), whilst the S and C TALENs were assessed intrahepatically. However as this murine mouse model does not generate cccDNA, both studies used an HBV replication competent plasmid as an episomal target DNA sequence to determine nuclease-mediated cleavage. When comparing cleavage efficiencies, the ZFNs demonstrated 36% targeted disruption whilst the S and C TALENs displayed superior nuclease activity, with an average of 81% targeted disruption. Sequencing of the ZFN binding sites revealed mutagenic events in only 6% of HBV DNA targets, of which 81% were frameshift mutations as a result of a 4 bp insertion. Deep sequencing of the S and C TALEN target sites showed deletions in 44% and 54% of samples respectively, of which 89% were frameshift mutations. These results support the observation that ZFNs and TALENs have different mutation signatures, and suggest that the S and C TALENs are cleaving the episomal HBV DNA target more efficiently *in vivo*, than the anti-HBV ZFNs *in vitro*.

CHAPTER 6 – CONCLUSION

Chronic HBV treatment failure has predominantly been attributed to the persistence of episomal cccDNA, the fundamental viral transcription intermediate from which active replication is initiated. As the cccDNA minichromosome is epigenetically regulated, it is able to establish a dormant reservoir in the nucleus of hepatocytes leading to latent or occult infections. Current therapeutics include nucleoside/tide analogues which successfully inhibit reverse transcription of the cytoplasmic pre-genomic RNA, however chronic infections require constant therapeutic intervention as the cccDNA is not eliminated. Although RNAi effectors present a promising gene therapy approach, they too act solely through post-transcriptional mechanisms, by destroying HBV mRNA transcripts. The inability of both these therapeutics to directly target the cccDNA poses a major challenge in developing a cure for chronic HBV, as an occult infection may re-emerge after cessation of either therapy. This study is the first to demonstrate direct targeted inactivation of HBV replication through TALEN-mediated cleavage of cccDNA *in vitro* and HBV-encoding DNA *in vivo,* illustrating the therapeutic potential of these designer nucleases. In addition to showing that TALENs could potentially permanently disable chronic HBV infections, this is the first study to demonstrate the direct delivery of TALENs to an adult mammalian animal model.

Disabling HBV replication through TALEN-mediated targeted mutagenesis presents a unique approach to anti-HBV gene therapy, however several challenges still need to be addressed before these designer nucleases become clinically viable therapeutic agents. Some of these challenges include: 1) Determining TALEN-mediated cleavage of cccDNA in an *in vivo* model

system that unambiguously mimics human chronic HBV infection; 2) Selecting a safe and efficient liver-specific gene therapy delivery vector that will transiently express anti-HBV TALENs; and 3) Determining the effect of these TALENs on integrated viral sequences, particularly in HBV-related HCCs.

In this assessment of anti-HBV TALEN efficacy, two commonly used *in vitro* and *in vivo* HBV replication models were employed. However they displayed varying TALEN cleavage efficiencies. In HepG2.2.15 cell cultures, the S TALEN displayed a maximum targeted disruption of 49% in cccDNA isolates, whilst the same TALEN achieved an average of 81% targeted disruption of HBV-encoding DNA in mouse hepatocytes. Discrepancies between these *in vitro* and *in vivo* model systems could be attributed to a number of factors including target-specific structural variance, transfection efficiencies, cccDNA copy numbers, or integrated viral genomes. During HDIs, HBV-expression sequences are transfected into murine hepatocytes, but as the mice are not predisposed to HBV infection, cccDNA pools are not established. Instead, viral replication is initiated through transcription of the HBV-expression sequence, which results in the assembly and secretion of new virions and VPEs, but not active infection (Yang et al., 2002). As such, the episomal HBV TALEN target is plasmid DNA. HepG2.2.15 cells however, are susceptible to HBV infection, and harbour up to 10 fold more cccDNA copies per cell than normal chronically infected hepatocytes (Rabe et al., 2006; Sells et al., 1988). The configuration of these minichromosomes within cccDNA pools may result in fewer accessible TALEN-cleavage sites. As these cells are difficult to transfect, only approximately 60% of the cells will express TALENs after triple transfections. Furthermore, HepG2.2.15 cells also contain multiple integrated HBV genomes (Sells et al., 1988) which continuously produce new virus. Besides cccDNA mutagenesis, these integrated genomes would also require TALEN-mediated

targeted inactivation to prevent the formation of new wild-type pgRNA, which could ultimately re-populate the cccDNA pool. As HepG2.2.15 cells contain multiple integrated HBV genomes and retain considerable cccDNA pools, it is difficult to determine the TALEN therapeutic dose required to completely inhibit HBV replication. However, during HDIs in mice, a 2:1 ratio of TALEN to HBV-encoding plasmid was successfully used. It is likely that a combination of these factors contributed to the moderate TALEN efficiency observed when targeting cccDNA compared to *in vivo* HBV-encoding sequences.

Although both the HepG2.2.15 cell culture and the HDI mouse model are both useful when establishing initial TALEN therapeutic efficacy, alternative *in vivo* model systems, like the HBV transgenic mice (Guidotti et al., 1995), the woodchuck (Paronetto and Tennant, 1990), or the urokinase plasminogen activator SCID (uPA-SCID) mice (Meuleman et al., 2005) are more suited to future investigations. The transgenic mice have a HBV replication competent sequence integrated into the endogenous genome. This facilitates the continuous expression of new viral proteins, leading to virion assembly and secretion of circulating viral particles and VPEs. However, mouse hepatocytes are not susceptible to active infection and do not result in the formation of cccDNA. For this reason, the transgenic mouse model may be more appropriate for investigating TALEN-mediated targeted disruption of integrated HBV sequences, which most commonly occurs in patients with HBV-related HCC. Alternatively the woodchuck model, which has been extensively used to investigate the anti-viral potential of novel therapeutics (D'Ugo et al., 2010), may be employed to determine anti-HBV TALEN efficacy. Woodchuck hepatitis virus (WHB) infection mimics the immunological progression, persistence, morbidity, and mortality often associated with human chronic infections (Gerin et al., 1983; Menne and Cote, 2007; Roggendorf and Tolle, 1995). However as sequence variations occur between the WHB and

HBV genomes (Galibert et al., 1982), TALENs may have to be re-designed to facilitate WHB-targeted DNA binding. So far, the only *in vivo* model system capable of establishing active human HBV infection is the uPA-SCID mouse model (Meuleman and Leroux-Roels, 2008; Meuleman et al., 2005; Vanwolleghem et al., 2010). These mice, which express the thrombolytic *uPA* transgene, are born with compromised livers. As a result, primary human hepatocytes which are transplanted into uPA-SCID neonatal mice colonise the mouse liver and give rise to chimaeric livers that contain both mouse and human cells. As a large portion of human hepatocytes repopulate these livers, they are susceptible to human HBV infection. During infection, episomal cccDNA is established in the nucleus of the human hepatocytes, resulting in active viral replication. Therefore the uPA-SCID mice remain the definitive *in vivo* model system for which new anti-HBV therapeutics, such as the TALENs described here, should be tested.

Nevertheless, as hydrodynamic injections are not well tolerated by either the transgenic or uPA-SCID mice, TALEN-encoding sequences need to be incorporated into an appropriate delivery vector. This remains a major challenge in the gene therapy field as 'naked' DNA is easily degraded by extra- and intercellular nucleases and does not readily pass through the cell membrane, a result of its conformation, size, and negative charge (Schreier, 1994). Currently delivery vectors are divided into two major classes, non-viral vectors and viral vectors (reviewed by Giacca and Zacchigna, 2012; Kay et al., 2001; Robbins and Ghivizzani, 1998; Zhang et al., 2012). Non-viral vectors, such as cationic liposomes and DNA conjugates, are designed to coat and shield DNA sequences promoting cell-specific targeted delivery. Although these vectors are generally non-immunogenic, delivery efficiency is often inadequate. Viral vectors on the other hand are very efficient gene therapy delivery vehicles, although immunogenic epitopes on these capsids or envelopes are often modified to prevent immune stimulation. Retroviral, adenoviral,

lentiviral, and adeno-associated virus (AAV) vectors are most commonly investigated as potential delivery vehicles for human gene therapy. Integrating viruses, like the retroviral and lentiviral vectors, are used to establish stable expression of therapeutic genes, whilst AAVs and adenoviral vectors are more commonly used to promote long-term gene expression without integration. A recent study showed that packaging and delivery of individual TALEN subunits was achieved using serotype 5 adenoviral vectors, but not with an HIV type 1 lentivirus (Holkers et al., 2013). It is believed that recombination events occur between the TALE repeat domains within the lentiviral vector, resulting in scrambled and truncated TALE arrays. Since HBV integration events already occur unpredictably during chronic infection, integrating viral vectors may further compromise the integrity of the hepatocyte genome. Furthermore, the probability of generating non-specific off-target cleavage events would most likely increase if TALENs were continuously expressed. This would put the already infected hepatocyte under additional, unnecessary genotoxic stress. The non-integrating adenoviral and AAV vectors are therefore more suitable candidates, particularly as both vectors can be adapted for liver-specific transgene expression and/or delivery (Mowa et al., 2010; Wang et al., 2010). Including liver specific or inducible promoter systems to drive the expression of TALENs or rTALEs, may provide enhanced *in vivo* activity and diminish potential side effects (Jazwa et al., 2013). The AAVs however can only accommodate small transgene insertions and, as TALEN-encoding sequences are reasonably large, individual AAVs encoding each TALEN subunit would be required. A gutless adenoviral vector could single-handedly accommodate both the left and right TALEN subunits (Brunetti-Pierri and Ng, 2011), which may prove more convenient for future studies. Overall, adenoviral or AAV mediated delivery of transiently expressed TALENs directly to infected hepatocytes would be the most suitable anti-HBV gene therapy approach.

As both the S and C TALENs were designed to target a specific viral DNA sequence, achieving liver-specific delivery of these anti-HBV designer nucleases may result in targeted cleavage of both cccDNA replicative intermediates and integrated viral DNA. For decades HBV-related HCC has been associated with viral integration (Brechot et al., 1980; Hino et al., 1984; Koshy et al., 1983; Shafritz et al., 1981; Shaul et al., 1986; Tokino and Matsubara, 1991) however variations between integration sites as well as the viral DNA encoded at these sites suggest that this process is random. Recent improvements in molecular biology techniques, such as whole genome sequencing, have permitted a more in-depth analysis of viral integration patterns in patients with HBV-related HCC (Ding et al., 2012; Jiang et al., 2012; Sung et al., 2012; Toh et al., 2013). Between 255 and 399 different HBV integration sites have been detected in more than 173 different HCC liver samples and adjacent tissues, allowing potential 'hot spots' to be identified. These included the *human telomerase reverse transcriptase* (hTERT) and *fibronectin 1* (FN1) genes, the mixed lineage leukaemia (MLL), and platelet derived growth factor (PDGF) families, as well genes involved in the calcium signalling pathway. Although these sites have been identified in multiple patient samples, the majority of insertions are relatively unique. In addition, large variations in the number of predicted integration events per cell, ranging from 4.9 to 64, have been reported. Finally, Jiang and colleagues imply that HBV integrations do not predispose hepatocytes to HCC (Jiang et al., 2012a), whilst Sung and colleagues show that these integration events occur predominantly in HCC liver samples (Sung et al., 2012). However Ding, et al. (2013) showed only 14% of the HBV integrations identified were associated with cancerous cells, whilst the remaining 86% were found in adjacent tissues. These inconsistent reports confirm that the exact mechanism of HBV integration is still poorly understood. Although TALENs have successfully been used to target endogenous DNA sequences, it will be difficult

to investigate the holistic effect that TALENs may have on integrated viral DNAs, unless patient dependant HBV integration patterns are initially determined.

In conclusion, targeted inactivation of episomal cccDNA was achieved using the S and C TALENs in HepG2.2.15 cells. These TALENs also interrupted viral protein production, inhibiting HBV replication in a murine disease model. Furthermore, rTALEs designed to target HBV promoter regions may enable transcriptional gene silencing of the cccDNA. Finally, direct TALEN-mediated *in vivo* gene editing can be achieved without measurable hepatotoxicity. As HBV cccDNA is refractory to currently available therapeutics, these TALENs and rTALEs present a unique gene therapy approach to treat chronic HBV infections.

CHAPTER 7 – MATERIALS AND METHODS

7.1 Generating HBV-targeting TALENs

7.1.1 Selecting HBV target sites

TALEN pairs (Left and Right subunits) were designed to target the *surface* (S), *core* (C) and *polymerase* (P) ORFs of HBV, subtype D (Table 2.1). Basic TALEN design rules were followed when selecting suitable target sites (described in Section 2.2.1).

7.1.2 Assembling of TALENs

The publically available TALE repeat assembly kit (Morbitzer et al., 2011) was used to generate anti-HBV TALENs. This kit has a pre-assembled TALE repeat array library, alternatively referred to as the level one vectors. Golden Gate cloning, with specific type IIS restriction enzymes was used to generate level 2 and level 3 vectors in a two-step cut-ligation protocol. RVDs containing NI, HD, NK, or NG diresidues, which bind nucleotides A, C, G or T, respectively, were used to constitute the TALE DNA binding regions. Additionally the NN module (binding G or A) was used in C and P1 TALENs. The Golden Gate TALEN assembly method is divided into two separate cut-ligation reactions. The first is the assembly of AB and BC TALE fragments is achieved by selecting TALE modules that correspond to the chosen TALEN binding sites. The first 10 modules form the AB fragment and the remaining 7 modules form the BC fragment. Modules are selected from the TALE plasmid library, where each module is flanked on both

ends by a *Bsa*I restriction site. The cut-ligation reactions included 40 fmol of each level 1 vector (position specific TALE module), 15 U *Bsa*I (New England Biolabs, MA, USA), 1 × T4 DNA ligase buffer (Thermo Scientific, IL, USA), 2.5 U T4 DNA Ligase (Thermo Scientific), and 150 ng pUC level 2 vector (either pUC-AB or pUC-BC) in a final volume of 20 µl with ddH_2O. The cut-ligation reaction was performed in a thermocycler under the following conditions: 37 °C for 5 minutes, and 20 °C for 5 minutes. This was repeated 50 times before heating to 50 °C for 10 minutes, heating to 80 °C for 10 minutes and finally cooling to 4 °C. Ten microlitres of each ligation mix (AB and BC) were separately transformed into 50 µl of chemically competent DH5α *Escherichia coli* (*E*. *coli*) (Appendix 8.1.1). The transformations were incubated on ice for 25 minutes followed by heat shock at 42 °C for 90 seconds, then rescued on ice for 2 minutes. An additional rescue step was performed by adding 250 µl of fresh LB to each transformation and incubating at 37 °C for 40 min. Transformed bacteria were plated onto Luria-Bertani (LB) agar containing spectinomycin (100 µg/ml) and incubated at 37 °C overnight.

To identify clones containing complete TALE fragments, bacterial colonies were picked from plates containing AB and BC ligations, and analysed by colony PCR and gel electrophoresis. Individual colonies were picked using a ten microlitre pipette tip and smeared across the bottom of standard 0.2 ml PCR tubes. The tip was then aspirated in 500 µl of LB medium (100 µg/ml spectinomycin) in a 1.7 ml capped tube and kept at 37 °C until after PCR analysis. The colony PCR reaction mix included: 10 µM forward primer, 10 µM reverse primer, 0.6 mM of each dNTP, 1 × ThermoPol® buffer (New England Biolabs), and 0.75 U *Taq* DNA polymerase (New England Biolabs) to a final volume of 12.5 µl with ddH_2O. Primers used to amplify AB and BC clones were M13 #1524 Fw 5’ – CAG TCA CGA CGT TGT AAA ACG – 3’and M13 #1525 Rv 5’ – CGG ATA ACA ATT TCA CAC AGG – 3’. PCR reactions were performed in a standard

thermocycler using the following conditions: initial denaturation at 95 °C for 10 min to lyse the bacterial cells, followed by 30 cycles of 95 °C for 40 s, 60 °C for 40 s, and 72°C for 60 s. A final elongation at 72 °C for 10 min was completed before cooling to 4 °C. Samples were analysed by electrophoresis on a 1 × Tris-borate-EDTA (TAE) agarose gel containing 0.0025% Ethidium Bromide. The GeneRuler™ 1kb DNA ladder (Thermo Scientific) and 5 × Orange G (10 mg Orange G dye, 3 ml 50% glycerol, 0.6 ml of 0.5 M EDTA (pH 8.0), and 1.4 ml ddH_2O) were used as molecular weight markers and sample loading dyes. PCR band migration patterns were evaluated under UV transillumination. Bands corresponding to approximately 1100 bp represent complete 10 module AB fragments whilst bands corresponding to approximately 900 bp represent complete 7 module BC fragments. Colonies containing plasmids with complete AB and BC ligations were selected and their equivalent 500 µl LB cultures were grown (in a total volume of 5 ml of LB) at 37 °C in a shaking incubator overnight. Plasmids were purified using the QIAprep Spin Miniprep Kit (Qiagen) as per the manufacturer's instructions.

Plasmids containing AB and BC fragments were screened by restriction digest to confirm all 10 modules (AB) and 7 modules (BC) were inserted. Restriction digest reactions contained 1 µg of plasmid DNA (either pUC-AB or pUC-BC), 1 × Buffer G (Thermo Scientific), 2.5 U *Bpi*I (Thermo Scientific) and 16.75 µl ddH_2O. Reactions were incubated at 37 °C for 2 hours before analysis by agarose gel electrophoresis. Restriction digests of positive clones resulted in two distinct bands, 4500 bp and 1100 bp for pUC-AB, and 4500 bp and 900 bp for pUC-BC. Finally plasmids were sequenced and translated to confirm module positioning with regards to the TALE binding site. Five hundred nanograms of plasmid DNA was sequenced using 20 pmol of the following primer set: M13 #1517 Fw 5' – GTA AAA CGA CGG CCA G – 3'; M13 #1518 Rv 5' – CAG GAA ACA GCT ATG AC – 3'.

The second cut-ligation reaction is the assembly of the AC TALE array into the level 3 destination vector. The reaction mix included 150 ng of pUC-AB, 150 ng pUC-BC, 150 ng level 3 vector pVAX (pVAX-NI, pVAX-NK, pVAX-NG or pVAX-HD), 15 U *Bpi*I (Thermo Scientific), 1 × T4 DNA ligase buffer (Thermo Scientific), 2.5 U T4 DNA Ligase (Thermo Scientific), in a final volume of 20 µl with ddH_2O. Cut-ligations, transformations, colony PCRs and gel electrophoresis were performed as described above with kanamycin (40 µg/ml) as the selective antibiotic and the following AC specific primer set: VAX #1403 Fw 5' – TAA TAC GAC TCA CTA TAG GG – 3'and *Fok*I #733 Rv 5' – TCC TTG ATC CAC CCA AAT GT – 3'. Bands corresponding to approximately 2800 bp indicate complete AC fragment synthesis, resulting in a sequence encoding the Left or Right TALEN subunit. Bacterial colonies with complete TALEN plasmids were grown in 5 ml of LB (40 µg/ml kanamycin) overnight in a shaking incubator at 37 °C before plasmid purification with the QIAprep Spin Miniprep Kit (Qiagen) according to the manufacturer's instructions.

Plasmids containing AC TALEs were screened using two separate restriction digests. The first was a *Pvu*II-HF digest which included 1 µg pVAX-AC (TALEN encoding plasmid), 1 × NEB Buffer 4 (New England Biolabs), 5 U *Pvu*II-HF (New England Biolabs), and 12.25 µl ddH_2O. The second was a *Pvu*II-HF/*Hinc*II double digest which included 1 µg pVAX-AC (TALEN encoding plasmid), 1 × NEB Buffer 4 (New England Biolabs), 1 × BSA (New England Biolabs), 5 U *Pvu*II-HF (New England Biolabs), 5 U *Hinc*II (New England Biolabs), and 10.25 µl ddH_2O. Restriction digests were incubated at 37 °C for 90 minutes and analysed by agarose gel electrophoresis. The *Pvu*II-HF restriction digest pattern includes four bands at approximately 2800 bp, 2000 bp, 950 bp, and 350 bp. The *Pvu*II-HF/*Hinc*II double digest pattern comprises five bands at

approximately 2000 bp, 1700 bp, 1200 bp, 950 bp, and 350 bp. Positive clones were sequenced to confirm TALEN assembly. Five hundred nanograms of plasmid DNA was sequenced using 20 pmol of the following primer set VAX #1403 Fw 5' – TAA TAC GAC TCA CTA TAG GG – 3'and FokI #733 Rv 5' – TCC TTG ATC CAC CCA AAT GT – 3'.

7.2 *In vitro* transfection of TALENs and HBV knockdown analysis

Two different human liver-derived cell lines, Huh7 and HepG2.2.15, were used to determine the efficiency of TALENs against HBV in tissue culture. Cell lines were cultured in 75 cm^2 flasks using Dulbecco's Modified Eagle Medium (DMEM) (Lonza, Basel, Switzerland) supplemented with 10% foetal calf serum (FCS) (Gibco, BRL, UK), penicillin (100 000 U/ml), and streptomycin (100 000 µg/ml), and maintained in a humidified incubator at 37 °C and 5% CO_2 until confluent.

7.2.1 Transient co-transfection of Huh7 cells with plasmids expressing TALENs

An HBV replication competent plasmid, pCH-9/3091 (Nassal, 1992), was used in transient co-transfections of Huh7 cells with plasmids expressing TALENs. pCH-9/3091 is a greater-than-genome length construct, which is capable of replicating, and therefore producing new HBV virions when transfected *in vitro* or *in vivo*. Huh7 cells were seeded, in triplicate, in 12-well plates at 120 000 cells per well, one day prior to transfection. Polyethylenimine (PEI) was used to transfect cells with 200 ng pCH-9/3091, 200 ng pCMV-GFP, and either 800 ng of plasmid

expressing the Left TALEN (SL, CL, P1L, P2L) and 800 ng of plasmid expressing the corresponding Right TALEN (SR, CR, P1R, P2R), or 1600 ng of pUC118. As pUC118 does not express TALENs or HBV viral proteins it was used during mock transfections. Production of green fluorescent protein, from the pCMV-GFP vector, was used as an indicator of transfection efficiency. The transfection mix, per well, included 2 µg total DNA in a final volume of 50 µl NaCl (150 mM), which was subsequently added to 50 µl of 0.1 mg/ml PEI (150 mM NaCl, pH 7.0) and incubated at room temperature for 8 minutes. The DNA/PEI mix was added directly to the cell culture media with gentle mixing and incubated overnight. The medium was replaced the following morning, and GFP expression measured 24 hours post-transfection by fluorescence microscopy. GFP expression showed transfection efficiencies of between 40-50%. To determine viral knockdown, HBsAg concentrations were measured by ELISA on days 2 and 3 post-transfection, using the Monolisa™ HBs Ag ULTRA kit (Bio-Rad, CA, USA). One hundred microlitres of culture media was used per assay, which were performed in accordance with the manufacturer's instructions.

7.2.1.1. *In vitro* immunohistochemistry

To assess liver cell specific expression and nuclear localisation of TALENs, immunohistochemistry was performed. Transient co-transfections of Huh7 cells were performed with either the left or right TALEN subunit (SL, SR, CL, CR, P1L, P1R, P2L, or P2R) to confirm each separate TALEN is expressed. PEI was used to transfect cells with 100 ng pCH-9/3091, 100 ng pCMV-GFP, and 400 ng of plasmid expressing TALEN subunits. Immunohistochemistry was performed on day 3 post-transfection. The N-terminal hemagglutinin epitope was used as a

protein tag. Cells were washed with phosphate buffered saline (PBS) and fixed using ice cold methanol. Monoclonal mouse anti-HA primary antibodies (Sigma, MO, USA) were used in conjunction with the Ultra-Sensitive ABC Mouse IgG Staining Kit (Thermo Scientific) to detect TALENs, as per the manufacturer's instructions. Cells were stained with 3,3'-Diaminobenzidine (DAB) and counter-stained with haematoxylin before visualisation under a light microscope.

7.2.1.2. Co-transfection of plasmids expressing individual TALEN subunits

To confirm that HBV knock-down was a direct result of TALEN cleavage and not a consequence of transcriptional inhibition, the anti-HBV efficacy of individual Left and Right TALENs was investigated. Only TALEN pairs that resulted in a reduction in HBsAg expression during experiments described in section 6.2.1 were assessed for transcriptional inhibition. A day prior to transfection, Huh7 cells were seeded in triplicate, in 12-well plates at 120 000 cells per well. Fifty microlitres of 0.1 mg/ml PEI was used in combination with 200 ng pCH-9/3091, 200 ng pCMV-GFP, and either 1600 ng of plasmid expressing the Left TALEN (SL, P1L), 1600 ng of plasmid expressing the Right TALEN (SR, P1R), 1600 ng of an equal combination of each Left and Right TALEN (SL+SR, P1L+P1R) or 1600 ng of pUC118. Transfections were performed as described in section 6.2.1. HBsAg concentrations were measured 48 hours post-transfection using 100 µl of aspirated cell culture media, with the Monolisa™ HBs Ag ULTRA kit (Bio-Rad) as per the manufacturer's instructions.

7.2.2 Transfection of HepG2.2.15 cells with plasmids expressing TALENs

HepG2.2.15 cells contain a stably integrated greater-than-genome length HBV sequence (Sells et al., 1987). These cells constitutively produce HBV particles and are capable of maintaining cccDNA pools in the nucleus. As such, they simulate severe chronic HBV infection and were therefore used to determine the anti-HBV efficacy of TALENs in this model of persistent viral replication. HepG2.2.15 cells were seeded in 6-well plates at 140 000 cells per well, one day prior to transfection. Two hours before transfection, HBsAg concentrations were measured by ELISA to determine baseline expression. Fifty microlitres of culture medium was mixed with 50 µl 1 × PBS before using the Monolisa™ HBs Ag ULTRA kit (Bio-Rad) according to the manufacturer's instructions. One hundred microlitres of 0.1 mg/ml PEI (pH 7.0) was then used to transfect cells with 400 ng pCMV-GFP and either 2300 ng of plasmid expressing the Left TALEN (SL, CL, P1L, P2L) and 2300 ng of plasmid expressing the corresponding Right TALEN (SR, CR, P1R, P2R), or 4600 ng of pUC118. Two plates of each experimental and control groups were transfected. One plate was maintained at standard growth conditions (37 °C and 5% CO_2) whilst the second plate was maintained at mild hypothermic conditions (30 °C and 5% CO_2) (Doyon et al., 2010). Growth medium was replaced and HBsAg concentrations were measured on day 2 and day 3. On day 5 cells were harvested by trypsinisation, and a 1:5 cell dilution was re-seeded in a new 6-well plate. The remaining cells were stored in 1% PBS at -70 °C. This transfection procedure was repeated twice. An overview of the HepG2.2.15 cell transfection procedure is shown in Figure 6.1. Cells harvested from HepG2.2.15 cultures were used for T7E1 assays (section 7.5).

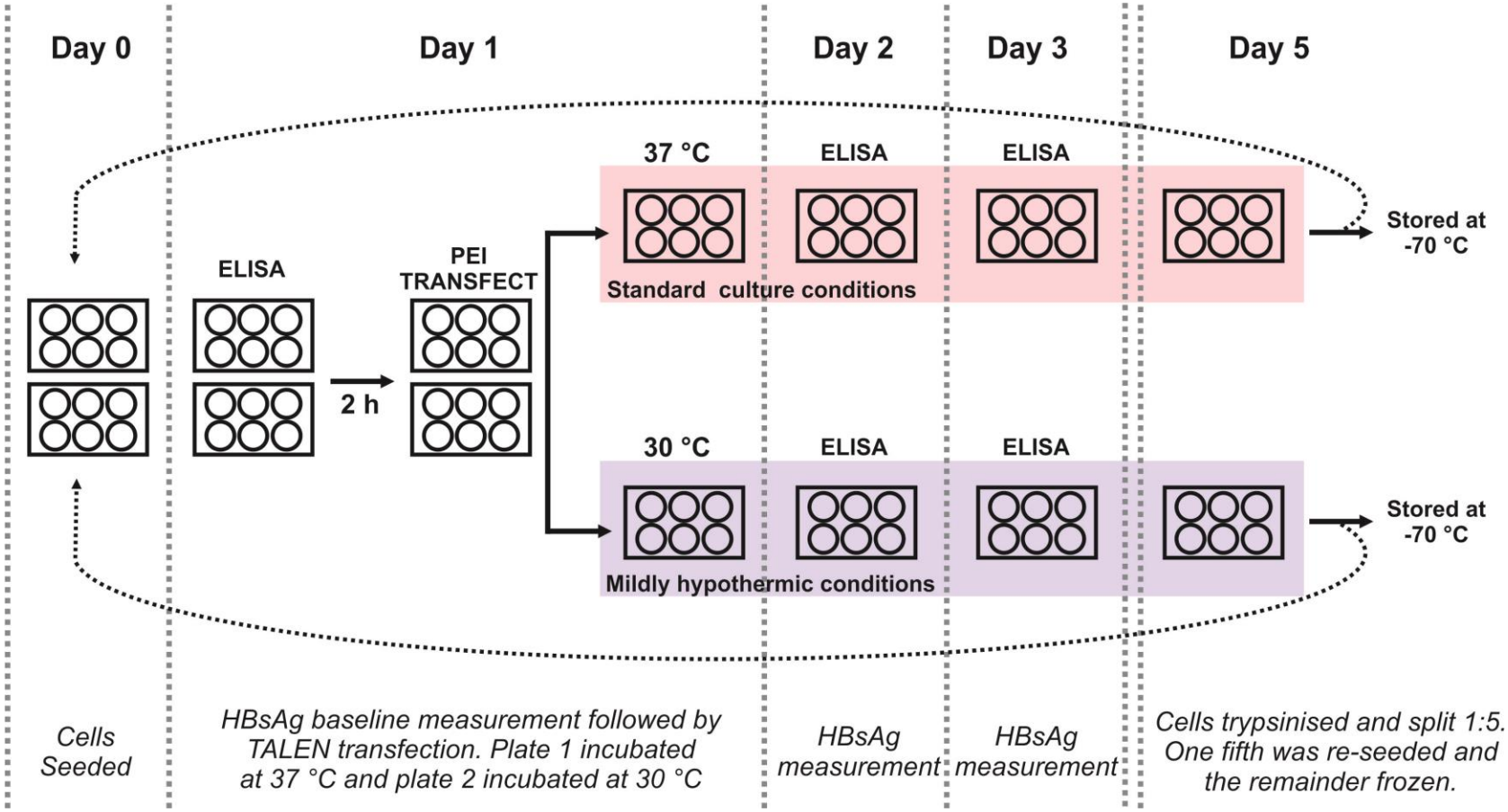

Figure 7.1: Multiple TALEN transfection protocol for HepG2.2.15 cells. On day 0, HepG2.2.15 cells were seeded into six well plates. Two plates were seeded for each of the four experimental and one control groups. HBsAg concentrations were measured two hours before transfection on day 1 to determine the baseline HBV expression profiles in each well. Cells were transfected with S, C, P1, P2 or mock TALEN plasmids before incubating at either standard culturing conditions at 37 °C or mildly hypothermic conditions (30 °C). HBsAg concentrations were measured on days 2 and 3. Cells were harvested on day 5 and re-seeded into new six well plates to repeat the transfection procedure. Remaining cell aliquots were stored at -70 °C. This TALEN transfection was repeated twice.

7.3 *In vitro* cell viability assay

The 3-(4,5-Dimethylthiazol-2-yl)-2,5-diphenyl tetrazolium bromide (MTT) colorimetric assay was used to determine cell viability and TALEN-associated toxicity. This test is routinely used to establish cell proliferation as only healthy mitochondria, in metabolically active cells, are capable of reducing the yellow MTT tetrazolium salt into an insoluble purple formazan by-product. Huh7 cells were seeded in 96-well plates at 15 000 cells per well a day prior to PEI transfection. Plates included 5 well replicates of each experimental and control group tested. These groups comprised cells that were untransfected, mock transfected (25 ng pCH-9/3091, 25 ng pCMV-GFP, 200 ng pUC118) or TALEN transfected (25 ng pCH 9/3091, 25 ng pCMV-GFP, 100 ng Left TALEN plasmid (SPL, CPL, XL, PL) and 100 ng Right TALEN plasmid (SPR, CPR, XR, PR)). Cell viability was assessed three days after transfection by adding 20 µl of 5 mg/ml MTT (in 1 × PBS) to each well, and incubating at 37 °C (5% CO_2) for one hour. Active metabolism of the MTT into the blue formazan by-product was measured by aspirating the growth medium and re-suspending the formazan in 200 µl of dimethyl sulfoxide (DMSO). Cell viability was determined spectrophotometrically by measuring the optical density at a wavelength of 570 nm, and subtracting it from the background optical density at 690 nm.

7.4 Murine hydrodynamic injection of TALEN-expressing plasmids

The silencing efficacy of TALENs *in vivo* was assessed using the murine hydrodynamic tail vein injection model of HBV replication (Liu et al., 1999; Yang et al., 2002). Five to six week old

female Naval Medical Research Institute (NMRI) mice, weighing between 25 and 30 g, were housed under standard husbandry conditions. All experiments on animals were conducted in accordance with protocols approved by the University of the Witwatersrand Animal Ethics Screening Committee. A copy of the animal ethics clearance certificate has been included in Appendix 8.4. Mice were divided into three groups: mock (no TALEN), S TALEN, and C TALEN. The bolus injectate contained 45 µg of plasmid DNA in a saline solution that comprised 10% of each mouse's body weight. The plasmid DNA solutions contained 8 µg HBV target DNA (pCH-9/3091), and either 32 µg of mock pUC118 or 16 µg of each corresponding Left and Right TALEN expressing plasmids (SL + SR or CL + CR). Additionally, 5 µg of luciferase reporter plasmid (pCMV-FLuc) was included to control for hepatic gene delivery. Blood samples were collected on days three and five post injection for HBV knockdown analysis and liver toxicity assays. On day 5, mice were sacrificed by CO_2 exposure and their livers removed to assess intrahepatic HBV DNA, RNA and protein levels.

7.4.1 Bioluminescence imaging

To determine hydrodynamic injection delivery efficacy, bioluminescence imaging was performed on day 3 post injection, using a CaliperLS IVIS® bioluminescence system (PerkinElmer, MA, USA). Mice were injected intraperitoneally with 150 mg/kg of D-luciferin (15 mg/ml) (Gold Biotechnology, MO, USA) immediately before imaging with 1% Isofor anaesthesia. The region of interest (ROI) was calculated for each mouse based on the liver-specific luminescence heat map obtained after measuring luciferase radiance (p/sec/cm^2/sr).

7.4.2 Measurement of HBsAg and transaminases in serum samples

To determine knockdown efficiency of TALENs on HBV circulating viral particles, blood samples were collected after retro-orbital puncture at days 3 and 5 post injection. Mice were anaesthetised using 5% Isofor, and approximately 200 µl of blood was collected. To separate the serum from cells and clotting factors, the blood was refrigerated at 4 °C in 1.5 ml microcentrifuge tubes for 1 hour. Once the blood had coagulated, samples were centrifuged for 6 minutes at 3000 rpm in an Eppendorf MiniSpin® microcentrifuge, rotor F45-12-11, GE 010 (Eppendorf, Hamburg, Germany). The serum was transferred into a new 1.7 ml microcentrifuge tube and an additional centrifugation was performed (6 minute, 3000 rpm). One hundred microlitres of serum was transferred to a new 1.7 ml microcentrifuge tube and diluted three-fold in 1% PBS before measuring serological markers of HBV replication and liver associated toxicity. The Monolisa™ HBs Ag ULTRA kit (Bio-Rad) was used to measure surface antigen expression using 100 µl of pre-diluted serum. DNA from circulating viral particles was extracted from 100 µl of the pre-diluted serum using the QIAamp® DNA Mini Kit blood spin protocol (Qiagen) according to the manufacturer's instructions, but without the use of carrier DNA. TALEN-related toxicity was determined by measuring liver secreted enzymes, specifically Aspartate Transaminase (AST) and Alanine Transaminase (ALT) levels. AST and ALT activities were measured in a routine chemistry laboratory (National Health Laboratory Service, Charlotte Maxeke Johannesburg Academic Hospital) using a kinetic assay with an automated photometric analyser (Roche Diagnostics, Rotkreuz, Switzerland). All serological results were adjusted accordingly, to account for the initial serum dilution.

7.4.2.1. Quantification of HBV viral particle equivalents

Real-time quantitative PCR (qPCR) was used to measure the number of HBV DNA copies in mock and TALEN injected mouse serum samples. Four-fold log serial dilutions of pCH-9/3901 were included in each qPCR run as positive controls, and to create standard curves. All reactions were performed using the SensiMix™ Capillary Kit (Bioline Reagents Ltd, UK), as per the manufacturer's instructions, with 10 picomoles (pmol) of each forward and reverse primer and 5 µl of template (water, pCH-9/3091 or circulating viral particle DNA) per reaction. The HBV *preS1* region was amplified using the following primer set: pre-S1 Fw 5' – TTA TTA TCC AGA ACA TGT AGT TAA TCA TTA CTT CC – 3', pre-S1 Rv 5' – TTG ATG GGA TTG AAG TCC CAA TCT GGA TT – 3'. All qPCR reactions were performed using the Bio-Rad CFX96™ Real-Time System (Bio-Rad) with the following cycling conditions: hot start at 95 °C for 10 min and 40 PCR cycles of denaturation at 95 °C for 15 s, annealing at 60 °C for 15 s and elongation at 72 °C for 15 s with a single SYBR® Green signal acquisition during elongation. Melting curve analysis was performed directly after qPCR by denaturing at 95 °C for 10 s, cooling to 65 °C for 1 min, and heating to 95°C at a ramp of 0.1 °C/s with continuous SYBR® Green signal acquisition. To quantify the number of HBV DNA copies per sample, the pCH-9/3091 serial dilutions were used to calculate plasmid copy number using the following equation: copy number = (mass × Avogadro's number) / (1 mol × length × 1 × 10^9 × 650 g/mol), where the mass is the amount of plasmid in nanograms, the length is the size of the plasmid in base pairs, and a single base pair has a molecular weight of 650 Da.

7.4.3 Analysis of intrahepatic anti-HBV efficacy of TALENs

To determine the effects of TALENs on HBV replication in hepatocytes, mice were sacrificed on day 5 post injection and livers were harvested. Total RNA was extracted from 100 mg of homogenised mouse liver using TRI Reagent (Sigma-Aldrich, MO, USA) followed by reverse transcription using the QuantiTect reverse transcription kit (Qiagen). Both the TRI Reagent RNA extraction and the reverse transcription were performed according to the manufacturer's instructions. HBV RNA was quantified relative to the *mGAPDH* housekeeping gene. qPCR reactions were performed as described in section 6.4.2.1, using the same HBV pre-S1 primer set for viral cDNA amplification and the following primer set for *m*GAPDH quantification: *m*GAPDH Fw 5' – TTC ACC ACC ATG GAG AAG GC – 3' and *m*GAPDH Rv 5' – GGC ATG GAC TGT GGT CAT GA – 3'.

In addition to RNA analysis, histology and immunohistochemistry were performed on formalin fixed liver sections to assess intrahepatic TALEN mediated toxicity and measure HBV core protein expression. Haematoxylin and Eosin (H&E) staining was used to evaluate general hepatocyte morphology and assess evidence of intrahepatic inflammation. Liver sections were analysed under a light microscope. Immunohistochemistry was used to determine intrahepatic HBV core expression using Novocastra™ Lyophilized HBcAg mouse monoclonal antibody (Leica biosystems, Wetzlar, Germany). Core antigen was detected by immunoperoxidase staining. Cells were counter-stained with haematoxylin before visualisation at 100 × magnification and 1000 × magnification (oil immersion) using a light microscope.

7.5 T7 endonuclease 1 assay

To confirm that TALEN cleavage and targeted sequence disruption occurred at the designated target site, a mismatch-sensitive T7E1 (New England BioLabs) was used (Mussolino et al., 2011). HBV cccDNA was extracted from HepG2.2.15 cells with a modified plasmid DNA extraction method (Wong et al., 2004) using an EconoSpin® plasmid extraction protocol (Epoch Life Sciences, TX, USA) followed by treatment with Plasmid-safe™ ATP-dependent DNase (Epicentre Biotechnologies, WI, USA) as per the manufacturer's instructions. To confirm that cccDNA was successfully isolated from HepG2.2.15 cells a PCR analysis was performed. The A1AT genomic DNA sequence and HBV *core* ORF were amplified using the following primer sets respectively: A1AT F 5' – TTC CCT GGT CTG AAT GTG TG – 3' and A1AT R 5' – ACT GTC CCA GGT CAG TGG TG – 3'; HBV C F 5' – ACC ACC AAA TGC CCC TAT – 3' and HBV C R 5' – TTC TGC GAC GCG GCG A – 3'. The A1AT PCR analysis was performed using 25 µl of the KAPA2G™ Robust HotStart ReadyMix (Kapa Biosystems, MA, USA) and 100 ng of either HepG2.2.15 genomic DNA or cccDNA preparations. HBV *core* ORF amplification was performed using 12.5 µl of the KAPA Taq ReadyMix (Kapa Biosystems, MA, USA) and 10 ng of either HepG2.2.15 genomic DNA or cccDNA preparations. PCR reactions were carried out in an Eppendorf Mastercycler gradient thermocycler (Eppendorf) under the following conditions: initial denaturation at 95 °C for 3 min followed by either 50 cycles or 30 cycles of 95 °C for 30 s, 60 °C for 30 s and 72 °C for 30 s for A1AT and HBV core PCR reactions respectively. Final elongation was performed at 72 °C for 5 min and samples were cooled to 4 °C. A fifteen microliter aliquot of each PCR product was mixed with 3 µl of 5 × Orange G loading dye before analysis using 1 × TAE agarose gel (0.0025% Ethidium Bromide) electrophoresis. PCR products were visualized

under UV transillumination using the Syngene G:BOX fluorescence imaging system with GeneSnap software V 7.01 (Syngene, Cambridge, UK).

Intrahepatic HBV DNA was extracted from homogenised mouse liver tissue using the QIAamp® DNA Blood Mini Kit as per the manufacturer's instructions. Both HepG2.2.15 cccDNA and intrahepatic HBV DNA extracts were analysed using the T7E1 assay. Sequences flanking the putative S and C TALEN binding sites were amplified with KAPA2G™ Robust HotStart ReadyMix (Kapa Biosystems, MA, USA) using the following primer sets, respectively: S Fw 5' – CCT AGG ACC CCT TCT CGT GT – 3'; S Rv 5' – ACT GAG CCA GGA GAA ACG GG – 3' and C Fw 5' – GAA CTA ATG ACT CTA GCT ACC T – 3'; C Rv 5' – CCT ACA AAC TGT TCA CAT TT – 3'. The PCR reaction mix included 12.5 µl KAPA2G™ Robust HotStart ReadyMix (Kapa Biosystems), 10 pmol of each forward and reverse primer (SFw + SRv or CFw + CRv), and 5 µl of DNA template (HepG2.2.15 cccDNA or murine hepatic DNA) in a total volume of 25 µl, made up with ddH_2O. PCR reactions were performed using the Eppendorf Mastercycler gradient thermocycler (Eppendorf) under the following conditions: initial denaturation at 95 °C for 2 min; 30 cycles of 95 °C for 15 s, 58 °C for 15 s, and 72 °C for 15 s; final elongation at 72 °C for 5 min and cooling to 4 °C. A three microlitre aliquot of each sample was mixed with 3 µl of 5 × Orange G loading dye before analysis using 1 × TAE agarose gel (0.0025% Ethidium Bromide) electrophoresis. Single band PCR products were visualised under UV transillumination using the Syngene G:BOX fluorescence imaging system with GeneSnap software V 7.01 (Syngene, Cambridge, UK). The remaining PCR products were purified using the EconoSpin® PCR cleanup protocol (Epoch Life Sciences) according to the manufacturer's instructions, and eluted in 50 µl of ddH_2O. For the T7E1 digestion, heteroduplex formation was achieved by denaturing 150 ng of PCR amplified DNA at 95 °C for 5 minutes followed by cooling to 35 °C at a rate of -

0.1 °C per second (Figure 7.2). Samples were cooled on ice for 5 minutes before adding 3 U of T7E1 and incubating in 1 × NEB buffer 2 (New England BioLabs). The reaction mix was incubated at 37 °C for 15 minutes and then resolved on a 2% agarose gel (1 × TAE, 0.0025% Ethidium Bromide). UV transillumination was used to assess band migration patterns using the Syngene G:BOX and GeneSnap software (Syngene). ImageJ (version 1.46)(Abramoff, 2004) was used to measure the integrated density of separated bands and determine percentage targeted disruption. This was achieved by initially subtracting the background from each band, followed by calculating the percentage of cleaved product to un-cleaved product, and finally subtracting the no T7E1 control, as explained in Figure 7.3. A second single stranded DNA endonuclease, CelI*,* was substituted for T7E1 to confirm either presence or lack of heteroduplex formation. The CelI enzyme, courtesy of Dr Wolfgang Prinz, was extracted directly from celery stalks.

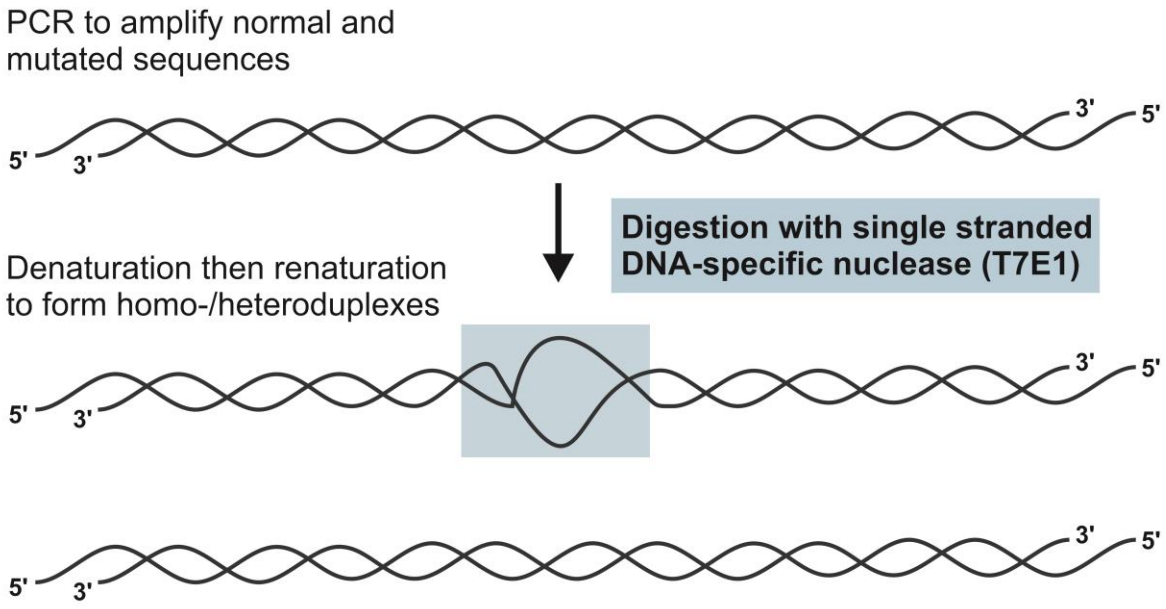

Figure 7.2: Heteroduplex formation for T7E1 single stranded nucleases cleavage. Sequences flanking the TALEN DNA binding sites were PCR amplified. dsDNA amplicons were subsequently denatured and renatured allowing homo- and heteroduplex formation. TALEN-mediated disruptions at the cleavage site will result in the formation of dsDNA heteroduplexes which are susceptible to digestion with a single stranded nuclease like T7E1.

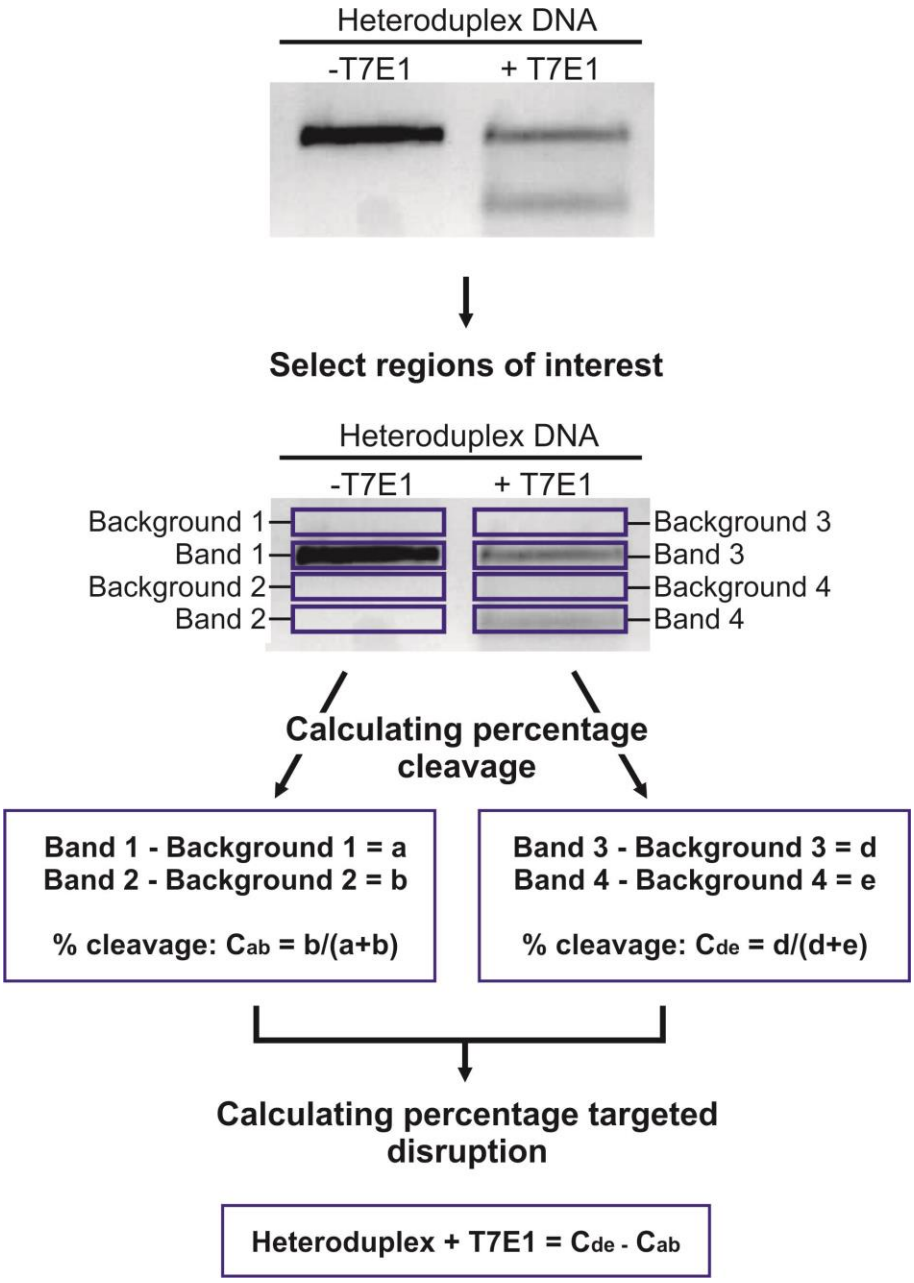

Figure 7.3: Calculating TALEN percentage targeted disruption. The T7E1 assay with gel electrophoresis was used to measure TALEN cleavage efficiency. A negative control (no T7E1) was used during each assay in conjunction with heteroduplexed samples (+T7E1). ImageJ software was used to calculate band density. This was achieved by measuring the raw integrated intensity of a defined area. A background density measurement, close to each region of interest, was subtracted before determining the percentage of cleaved product in each lane. Finally, the percentage of targeted disruption was ascertained by subtracting the negative control percentage cleavage from the heteroduplex percentage cleavage.

7.6 Ultra-deep sequencing

To map site-specific mutations induced by TALEN cleavage, the GS Junior System (Roche 454 Life Sciences, CI, USA) was used to perform ultra-deep sequencing of murine liver-derived DNA amplicons. Sequencing primers were designed to amplify a 450 bp region flanking the S and C TALEN binding sites. Multiplex Identifiers (MIDs) were included as 'barcodes' in each primer set to distinguish between amplicons from the different groups of mice. Primers for ultra-deep sequencing of mock, S and C TALEN hydrodynamic injections are shown in Table 6.1. Primers with different MIDs were used to amplify S and C flanking regions of mock DNA samples. The initial PCR amplicon library preparations were performed using KAPA HiFi™ HotStart ReadyMix (Kapa Biosystems, MA, USA). The PCR reaction mix included 12.5 µl KAPA HiFi™ HotStart ReadyMix, 15 pmol of each cognate forward and reverse primer, and 5 µl of intrahepatic murine DNA in a total volume of 25 µl, made up with ddH_2O. PCR reactions were performed using the Bio-Rad T100™ thermocycler (Bio-Rad) with the following cycling conditions: initial denaturation at 95 °C for 5 min; 5 cycles of 95 °C for 30 s, 62 °C for 30 s, and 72 °C for 60 s; 30 cycles of 95 °C for 30 s and 72 °C for 80 s, and finally elongation at 72 °C for 5 min followed by cooling to 4 °C. PCR products were resolved on a 1.5 % agarose gel (0.0025% Ethidium Bromide) using 1 X TAE and 5 µl of 5 x Orange G as a loading dye. DNA bands corresponding to the 450 bp region flanking the TALEN binding sites were excised and purified using the EconoSpin® Gel extraction protocol (Epoch Life Sciences) according to the manufacturer's instructions. Samples were eluted in 50 µl of ddH_2O and quantified spectrophotometrically. All subsequent steps, including library bead-purifications, library quantifications, emulsion-based clonal amplification (emPCR), DNA library bead enrichment, loading of the PicoTiterPlate, and the sequencing run

were completed according to the manufacturer's instructions. The 454 Sequencing System Software v. 2.5p1 (Roche) was used for data acquisition, processing and initial analysis. Initially sequences were grouped according to the MID used during PCR reactions. To determine if targeted mutagenesis occurred at S and C TALEN binding sites multiple alignments were performed. Sequencing results from mock and TALEN treated samples were analysed using the AlignX software from the Vector NTI suite 9.0.0 (Invitrogen, MD, USA).

Table 7.1: Ultra-deep sequencing primer sets

	MID primer sequences (5'- 3')*‡
Mock S Fw MID3	CGTATCGCCTCCCTCGCGCCATCAG**AGACGCACTC***TCTCAATTTTCTAGGGGGAACTACCGTG*
Mock S Rv MID3	CTATGCGCCTTGCCAGCCCGCTCAG**AGACGCACTC***CGTCCGAAGGTTTGGTACAGCAACAG*
S Fw MID4	CGTATCGCCTCCCTCGCGCCATCAG**AGCACTGTAG***TCTCAATTTTCTAGGGGGAACTACCGTG*
S Rv MID4	CTATGCGCCTTGCCAGCCCGCTCAG**AGCACTGTAG***CGTCCGAAGGTTTGGTACAGCAACAG*
Mock C Fw MID7	CGTATCGCCTCCCTCGCGCCATCAG**CGTGTCTCTA***GGGCCTAAAGTTCAGGCAACTCTTGTG*
Mock C Rv MID7	CTATGCGCCTTGCCAGCCCGCTCAG**CGTGTCTCTA***AGAATAAAGCCCAGTAAAGTTCCCCA*
C Fw MID8	CGTATCGCCTCCCTCGCGCCATCAG**CTCGCGTGTC***GGGCCTAAAGTTCAGGCAACTCTTGTG*
C Rv MID8	CTATGCGCCTTGCCAGCCCGCTCAG**CTCGCGTGTC***AGAATAAAGCCCAGTAAAGTTCCCCA*

* MID for each primer is underlined in bold
‡ HBV target sequence is italicised

7.7 Engineering repressor TALEs

To investigate whether other domains could be fused to TALE repeat arrays, an HBV promoter specific repressor TALE (rTALE) was generated. The pre-S2 promoter region, required for *surface* protein expression was selected for rTALE binding. The same design principles and cut-ligation protocols described in sections 2.1 were used to generate a single pre-S2 Right TALEN subunit with the following target site: 5' – TAC CCC GCT GTC TCC ACC T – 3'.

7.7.1 Replacing the nuclease domain with a KRAB repressor

To generate pre-S2 KRAB, the TALE subunit was isolated from the level 3 destination plasmid (containing the *Fok*I domain), and cloned into the pRK5-HA-KRAB-NLS-TAL repressor vector (plasmid courtesy of Prof. Toni Cathomen and Dr Claudio Mussolino). Both the pre-S2 TALEN subunit and repressor vector were subjected to a *Bam*HI/*Nhe*I double digest before cloning. Digestion reactions included 1 × Tango buffer (Thermo Scientific), 2.5 U *Bam*HI (Thermo Scientific), 2.5 U *Nhe*I (Thermo Scientific) and 1 µg of either pRK5-HA-KRAB-NLS-TAL or pre-S2 TALEN in a total volume of 20 µl in ddH_2O. Samples were incubated at 37 °C for one hour before analysis using agarose gel electrophoresis. Bands corresponding to the repressor vector backbone (which included the KRAB domain) at 5097 bp and the pre-S2 dTALE at 2325 bp were excised and purified using the EconoSpin® Gel extraction protocol (Epoch Life Sciences) as per the manufacturer's instructions. Purified DNA fragments were ligated using the Quick Ligation™ Kit (New England Biolabs) with 100 ng of repressor vector backbone and 150 ng of

pre-S2 TALE. Reactions were incubated at 24 °C for 10 minutes before transforming 50 µl of One Shot® TOP10 chemically competent *E. coli* (Invitrogen, MA, USA) with 2 µl of ligation mix. Transformations were performed as described in Section 6.1.2 using ampicillin (100 µg/ml) as a selective antibiotic. Four bacterial colonies were selected, inoculated into 5 ml of LB medium (100 µg/ml ampicillin) and placed in a shaking incubator overnight at 37 °C and 140 rpm. Cloned plasmids were extracted using the EconoSpin® plasmid extraction protocol and screened for positive pre-S2 KRAB clones following *Not*I/*Pst*I restriction digestion and gel electrophoresis. Digestion reactions included 1 × Tango buffer (Thermo Scientific), 2 U *Not*I (Thermo Scientific), 2 U *Pst*I (Thermo Scientific), and 200 ng of plasmid DNA in a total volume of 10 µl, made up with ddH_2O. Reactions were incubated at 37 °C for 1 hour before resolving by electrophoresis on a 1.5% agarose gel. Positive pre-S2 KRAB clones were sequenced on the ABI 3130xl Sequencer (Inqaba Biotec, PTA, South Africa).

7.7.2 *In vitro* transcriptional repression of pre-S2 KRAB rTALE

To determine the ability of the pre-S2 KRAB repressor to inhibit transcription at the target binding site, a luciferase reporter-based system was implemented. The pS2-luc reporter plasmid (courtesy of Dr Abdullah Ely) contains an HBV pre-S2 promoter which drives the expression of Firefly luciferase (FLuc). A day prior to transfection, liver derived Huh7 cells were seeded, in triplicate, in 12-well plates at 120 000 cells per well. PEI was used to transfect cells with 100 ng pS2-luc, 100 ng pCMV-GFP, and either 100, 200, 300, 400, 500, 1000, or 1500 ng of pRK5-HA-KRAB-NLS-pre-S2. pUC118 was included to total DNA transfected to 2.5 µg per well. FLuc expression was measured 48 hours post transfection using the Dual-Luciferase® Reporter

Assay (Promega, WI, USA), as per the manufacturer's instructions, but excluding the measurement of *Renilla* luciferase activity. Relative Firefly light units were measured on a DLReady™ validated luminometer.

7.8 Multiple alignments of HBV genotypes

To determine if TALEN binding sites were conserved between different HBV genotypes and sub-genotypes, multiple alignments were performed. The following genotypes and sub-genotypes were selected based on the WHO HBV reference panel (Chudy et al., 2012): A1 (AY233288); A2 (X70185); A3 (AB194950); B1 (AB073851); B2 (AF121245); B3 (EF473977); B4 (AB115551); B5 (AB219428); B6 (AB287316); C1 (DQ089760); C2 (AB365451); C3 (X75665); C4 (AB048704); C5 (EU410079); C6 (AB493837); D1 (AB246348); D2 (EU594416); D3 (EU594435); D4 (AB033559); E (AM494708); F1 (AY090458); F2 (AY311369); F3 (AB036909); F4 (AF223965); G (AB375168); H (AY090457). All GenBank nucleotide accession numbers (Benson et al., 2013) are shown in parenthesis. Alignments of sequences flanking the S, C, P1 and P2 TALEN binding sites were performed using AlignX (Vector NTI suite 9.0.0, Invitrogen).

7.9 TALEN off-target binding site analysis

Potential TALEN off-target binding sites in the *Mus musculus* and *Homo sapien* genomes were determined using the TALENT 2.0 paired target finder (Doyle et al., 2012) and Basic Local

Alignment Search Tool (BLAST) (Altschul et al., 1990). The TALENT 2.0 paired target finder, found at the following web link: https://tale-nt.cac.cornell.edu/node/add/talef-off-paired, was used to detect potential off-target sites for designated S and C TALEN pairs, or dual left and dual right subunits. The 'search a Genome/Promoterome' link was used to search the *Homo sapiens* (genome) or *Mus musculus* (genome) pre-loaded sequences. The RVD sequences of the following TALEN subunits were investigated: SL/SR, SL/SL, SR/SR, CL/CR, CL/CL, CR/CR. The minimum spacer unit was set to 10 bp and the maximum spacer unit to 15 bp. The recommended score cut-off limit of 3.0 was implemented, and upstream base of 'T only' was chosen for analysis. Data outputs were downloaded from the server.

BLAST alignments were performed using the nucleotide alignment tool, which can be accessed at the following web link: http://blast.ncbi.nlm.nih.gov/Blast.cgi. Individual SL, SR, CL, and CR TALEN subunit DNA binding sites were used to identify potential off-target binding sites in the mouse genomic + and the human genomic + databases. BLAST alignments were performed using two different algorithms: highly similar sequences (megablast) and somewhat similar sequences (blastn). Only binding sites with a minimum of 15 out of 19 base pair matches with either of the SL, SR, CL or CR TALEN-binding sites were selected as possible off-target DNA sequences.

7.10 Statistical analysis

All TALEN and rTALE *in vitro* experiments were performed in triplicate, except for the TALEN MTT assay which was performed in quintuplet. All *in vivo* studies contained six mice per each of

the mock, S TALEN and C TALEN groups. Data are represented as the mean (*in vitro*: n=3 or n=5, *in vivo*: n=6) ± the standard error of the mean (SEM). Two-tailed homoscedastic Student's t tests were performed using GraphPad Prism version 4.00 (GraphPad software, CA, USA). P values of < 0.05 were regarded as statistically significant.

CHAPTER 8 – APPENDIX

8.1 Laboratory protocols and reagents

8.1.1 Production of chemically competent cells

A 50 µl aliquot of DH5α *E. coli* was grown in 10 ml of LB medium (10 g tryptone, 5 g yeast extract, 7.5 g sodium chloride to a final volume of 1 litre in ddH_2O) by incubating overnight at 37 °C with gentle shaking. Two millilitres of the overnight culture was mixed with 40 ml of fresh LB and placed at 37 °C in a shaking incubator for two hours before centrifugation at 4000 × g for 15 minutes. The supernatant was removed and the bacterial cells were re-suspended in 1 ml of transformation buffer (100 mM calcium chloride, 10 mM PIPES, 15 % glycerol [pH 7.0]) following which an additional 19 ml of transformation buffer was added. The solution was mixed and placed on ice for 30 min followed by centrifugation at 4000 × *g* for 10 min. The supernatant was decanted and the bacterial culture re-suspended in 1.5 ml transformation buffer. Chemically competent cells were aliquoted into 50 µl working stocks and stored at -80 °C.

8.2 Anti-HBV TALEN genotype alignments

```
S TALE nuclease                    (411) TCCTGCTGCTATGCCTCAT            CTTCTGGACTATCAAGGTA
Genotype
A1 (AY233288)  (391) TTTTATCATATTCCTCTTCATCCTGCTGCTATGCCTCATCTTCTTATTGGTTCTTCTGGATTATCAAGGTATGTTGCCCGTTTGTCCTCTA
A2   (X70185)  (391) TTTTATCATATTCCTCTTCATCCTGCTGCTATGCCTCATCTTCTTGTTGGTTCTTCTGGATTATCAAGGTATGTTGCCCGTTTGTCCTCTA
A3 (AB194950)  (391) TTTTATCATATTCCTCTTCATCCTGCTGCTATGCCTCATCTTCTTATTGGTTCTTCTGGACTATCAAGGTATGTTGCCCGTTTGTCCTCTA
B1 (AB073851)  (391) TTTTATCATCTTCCTCTGCATCCTGCTGCTATGCCTCATCTTCTTGTTGGTTCTTCTGGACTATCAAGGTATGTTGCCCGTTTGTCCTCTA
B2 (AF121245)  (391) TTTTATCATCTTCCTCTGCATCCTGCTGCTATGCCTCATCTTCTTGTTGGTTCTTCTGGACTATCAAGGTATGTTGCCCGTTTGTCCTCTA
B3 (EF473977)  (391) TTTTATCATCTTCCTCTGCATCCTGCTGCTATGCCTCATCTTCTTGTTGGTTCTTCTGGACTATCAAGGTATGTTGCCCGTTTGTCCTCTA
B4 (AB115551)  (391) TTTTATCATCTTCCTCTGCATCCTGCTGCTATGCCTCATCTTCTTGTTGGTTCTTCTGGACTATCAAGGTATGTTGCCCGTTTGTCCTCTA
B5 (AB219428)  (391) TTTTATCATATTCCTCTGCATCCTGCTGCTATGCCTCATCTTCTTGTTGGTTCTTCTGGACTATCAAGGTATGTTGCCCGTTTGTCCTCTA
B6 (AB287316)  (391) TTTTATCATCTTCCTTTGCATCCTGCTGCTATGCCTCATCTTCTTGTTGGTTCTTCTGGACTATCAAGGTATGTTGCCCGTTTGTCCTCTA
C1 (DQ089760)  (391) TTTTATCATCTTCCTCTTCATCCTGCTGCTATGCCTCATCTTCTTGTTGGTTCTTCTGGACTGTCAAGGTATGTTGCCCGTTTGTCCTCTA
C2 (AB365451)  (391) TTTTATCATATTCCTCTTCATCCTGCTGCTATGCCTCATCTTCTTGTTGGTTCTTCTGGACTACCAAGGTATGTTGCCCGTTTGTCCTCTA
C3   (X75665)  (391) TTTTATCATCTTCCTCTTCATCCTGCTGCTATGCCTCATCTTCTTGTTGGTTCTTCTGGACTACCAAGGTATGTTGCCCGTTTGTCCTCTA
C4 (AB048704)  (391) TTTTATCATCTTCCTCTTCATCCTGCTGCTATGCCTCATCTTCTTGTTGGTTCTTCTGGACTATCAAGGTATGTTGCCCGTTTGTCCTCTA
C5 (EU410079)  (391) TTTTATCATATTCCTCTTCATCCTGCTGCTATGCCTCATCTTCTTGTTGGTTCTTCTGGACTACCAAGGTATGTTGCCCGTTTGTCCTCTA
C6 (AB493837)  (391) TTTTATCATCTTCCTCTTCATCCTGCTGCTATGCCTCATCTTCTTGTTGGTTCTTCTGGATTACCAAGGTATGTTGCCCGTTTGTCCTCTA
D1 (AB246348)  (391) TTTTATCATCTTCCTCTTCATCCTGCTGCTATGCCTCATCTTCTTGTTGGTTCTTCTGGACTATCAAGGTATGTTGCCCGTTTGTCCTCTA
D2 (EU594416)  (391) TTTTATCATCTTCCTCTTCATCCTGCTGCTATGCCTCATCTTCTTGTTGGTTCTTCTGGACTATCAAGGTATGTTGCCCGTCTGTCCTCTA
D3 (EU594435)  (391) TTTTATCATCTTCCTCTTCATCCTGCTGCTATGCCTCATCTTCTTGTTGGTTCTTCTGGACTATCAAGGTATGTTGCCCGTTTGTCCTCTA
D4 (AB033559)  (391) TTTTATCATCTTCCTCTTCATCCTGCTGCTATGCCTCATCTTCTTGTTGGTTCTTCTGGACTATCAAGGTATGTTGCCCGTTTGTCCTCTA
 E (AM494708)  (391) TTTTATCATCTTCCTCTTCATCCTGCTGCTATGCCTCATCTTCTTGTTGGTTCTTCTGGACTATCAAGGTATGTTGCCCGTTTGTCCTCTA
F1 (AY090458)  (384) TTTTATCATATTCCTCTTCATCCTGCTGCTATGCCTCATCTTCTTGTTGGTTCTTCTGGACTATCAAGGTATGTTGCCCGTCTGTCCTCTA
F2 (AY311369)  (391) TTTTATCATCTTCCTCTTCATCCTGCTGCTATGCCTCATCTTCTTGTTGGTTCTTCTGGACTATCAAGGTATGTTGCCCGTTTGTCCTCTA
F3 (AB036909)  (391) TTTTATCATCTTCCTCTTCATCCTGCTGCTATGCCTCATCTTCTTGTTGGTTCTTCTGGACTATCAAGGTATGTTGCCCGTTTGTCCTCTA
F4 (AF223965)  (391) TTTTATCATCTTCCTCTTCATCCTGCTGCTATGCCTCATCTTCTTGTTGGTTCTTCTGGACTATCAAGGTATGTTGCCCGTTTGTCCTCTA
 G (AB375168)  (391) TTTTATCATATTCCTCTTCATCCTGCTGCTATGCCTCATCTTCTTGTTGGTTCTTCTGGACTATCAAGGTATGTTGCCCGTTTGTCCTCTG
 H (AY090457)  (394) TTTTATCATCTTCCTCTTCATCCTGCTGCTATGCCTCATCTTCTTGTTGGTTCTTCTGGACTATCAAGGTATGTTGCCCGTGTGTCCTCTA
pCH-9/3091   (1673) TTTTATCATCTTCCTCTTCATCCTGCTGCTATGCCTCATCTTCTTGTTGGTTCTTCTGGACTATCAAGGTATGTTGCCCGTTTGTCCTCTA
           Surface   F  I  I  F  L  F  I  L  L  L  C  L  I  F  L  L  V  L  L  D  Y  Q  G  M  L  P  V  C  P  L
        Polymerase   F  Y  H  L  P  L  H  P  A  A  M  P  H  L  L  V  G  S  S  G  L  S  R  Y  V  A  R  L  S  S
```

Figure 8.2.1 Comparison of HBV genotype sequences in the region targeted by the S TALEN. On the top row, the two 19 nucleotide sequences in the HBV plus strand that are targeted by each of the SL and SR TALEN subunits are highlighted in yellow. HBV genome coordinate of the first T residue of the left subunit target is underlined in parentheses. Cognates from HBV isolates, with 20 nt flanking on either side, are shown below. HBV genotypes, subgenotypes, accession numbers, pCH-9/3091 and first nucleotide coordinate of each sequence are provided on the left in bold. Sequences within the S TALEN targets that are conserved in each of the genotypes are also highlighted in yellow. Adjacent amino

acid sequences of Surface and Polymerase, by the pCH-9/3091 plasmid, are shown on the bottom two rows. Individual amino acids are aligned to the first nucleotide of each codon.

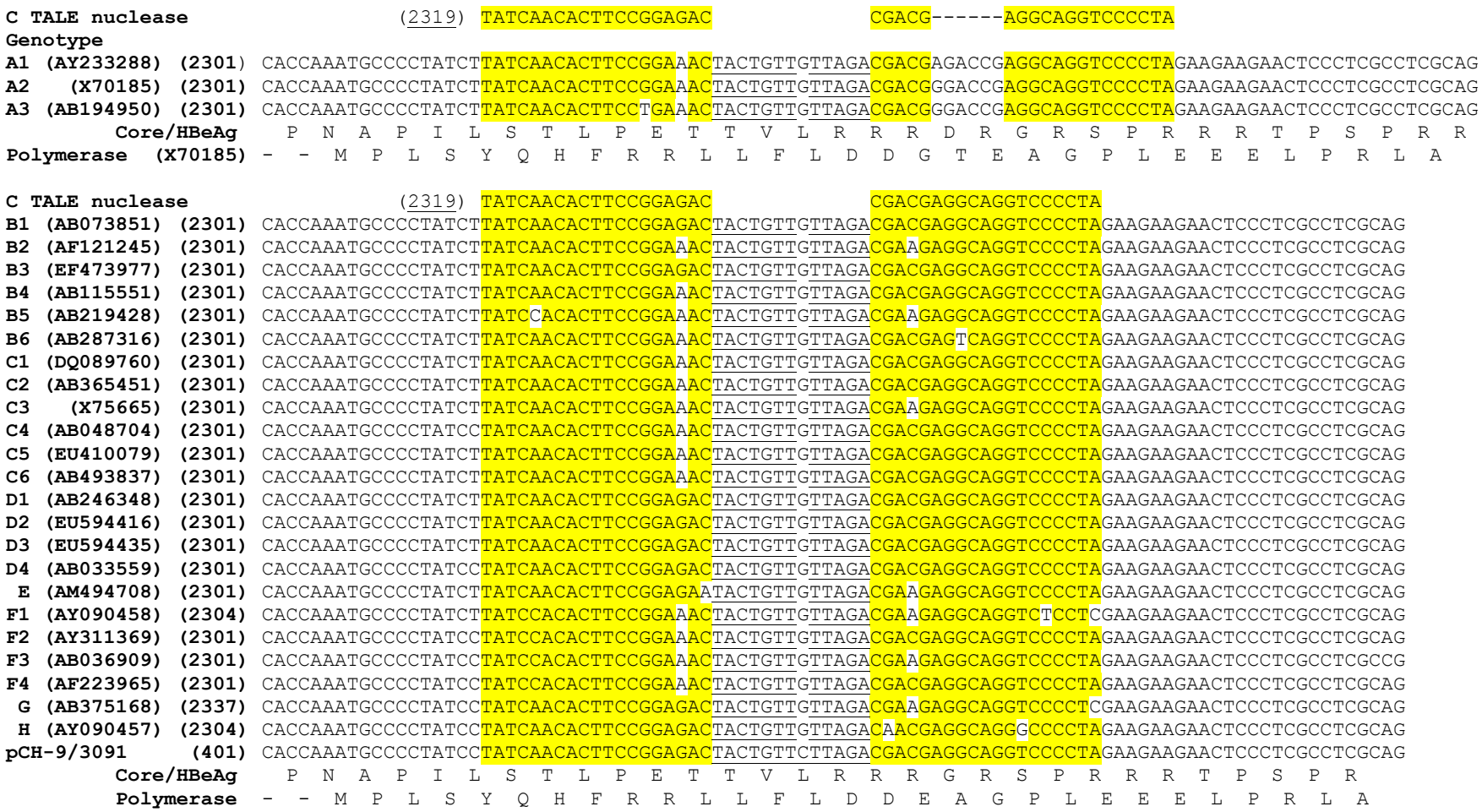

Figure 8.2.2: Comparison of HBV genotype sequences in the region targeted by the C TALEN. The sequences are depicted using a similar format to that described in Figure 8.2.1. HBV genotype A isolates have an additional 6 nucleotides in the in the sequence targeted by the right TALEN subunit.

```
P1 TALE nuclease                    (1144) TACCCCGTTGCCCGGCAAC          CCAAGTGTTTGCTGACGCA
Genotype
A1 (AY233288) (1119) TCTGAGTAAACAGTATATGAACCTTTACCCCGTTGCCCGGCAACGGCCTGGTCTGTGCCAAGTGTTTGCTGACGCAACCCCCACTGGCTGGGGCTTGGCT
A2   (X70185) (1119) TCTAAGTAAACAGTACATGAACCTTTACCCCGTTGCTCGGCAACGGCCTGGTCTGTGCCAAGTGTTTGCTGACGCAACCCCCACTGGCTGGGGCTTGGCC
A3 (AB194950) (1119) TCTAAGTAAACAGTATATGAACCTTTACCCCGTTGCCCGGCAACGGCCTGGTCTATGCCAAGTGTTTGCTGACGCAACCCCCACTGGCTGGGGCTTGGCC
B1 (AB073851) (1119) TCTAAGTAAACAGTATATGACCCTTTACCCCGTTGCTCGGCAACGGCCTGGTCTGTGCCAAGTGTTTGCTGACGCAACCCCCACTGGTTGGGGCTTGGCC
B2 (AF121245) (1119) TTTAAGTAAACAGTATCTGAACCTTTACCCCGTTGCTCGGCAACGGCCTGGTCTGTGCCAAGTGTTTGCTGACGCAACCCCCACTGGTTGGGGCTTGGCC
B3 (EF473977) (1119) TCTAAGCAAACAATATCTGAACCTTTACCCCGTTGCGCGGCAACGGCCAGGTCTGTGCCAAGTGTTTGCTGACGCAACCCCCACTGGCTGGGGCTTGGCC
B4 (AB115551) (1119) TTTAAGTAAACAGTATCTGAACCTTTACCCCGTTGCTCGGCAACGGCCTGGTCTATGCCAAGTGTTTGCTGACGCAACCCCCACTGGTTGGGGCTTGGCC
B5 (AB219428) (1119) TCTACACAAACAGTATTTGAACCTTTACCCCGTTGCTCGGCAACGGCCAGGTCTGTGCCAAGTGTTTGCTGACGCAACCCCCACTGGCTGGGGCTTGGCC
B6 (AB287316) (1119) TCTAAACAAACAATATCTGAACCTTTACCCCGTTACTCGGCAACGGCCAGGTCTGTGCCAAGTGTTTGCTGACGCAACCCCCACTGGCTGGGGCTTGGCT
C1 (DQ089760) (1119) TCTGTGTAAACAATATCAGAACCTTTACCCCGTTGCTCGGCAACGGTCAGGTCTTTGCCAAGTGTTTGCTGACGCAACCCCCACTGGTTGGGGCTTGGCC
C2 (AB365451) (1119) TCTGTGTCAACAATACCTGCACCTTTACCCCGTTGCCCGGCAACGGTCAGGCCTCTGCCAAGTGTTTGCTGACGCAACCCCCACTGGATGGGGCTTGGCC
C3   (X75665) (1119) TCTGTGTAAACAATATCTGAACCTTTACCCCGTTGCCCGGCAACGGTCTGGTCTTTGCCAAGTGTTTGCTGACGCAACCCCCACTGGCTGGGGCTTGGCC
C4 (AB048704) (1119) TCTGTGTAAACAATATCTGAACCTTTACCCCGTTGCCCGGCAACGGGCTGGTCTCTGCCAAGTGTTTGCTGACGCAACCCCCACTGGTTGGGGCTTGGCC
C5 (EU410079) (1119) TCTGTGTAAACAATATTTGACCCTTTATCCCGTTGCTCGGCAACGGCCAGGTCTATGCCAAGTGTTTGCTGATGCAACCCCCACTGGTTGGGGCTTGGCC
C6 (AB493837) (1119) TCTGTGTCAACAATATTTGCACCTTTACCCCGTTGCCCGGCAACGGTCTGGTCTTTGCCAAGTGTTTGCTGACGCAACCCCCACTGGCTGGGGCTTGGCA
D1 (AB246348) (1119) TCTGTGTAAACAATACATGACCCTTTACCCCGTTGCCCGGCAACGGCCAGGTCTGTGCCAAGTGTTTGCTGACGCAACCCCCACTGGCTGGGGCTTGGCC
D2 (EU594416) (1119) TCTGTGTAAACAATATCTGAACCTTTACCCCGTTGCCCGGCAACGGCCAGGTCTGTGCCAAGTGTTTGCTGACGCAACCCCCACTGGCTGGGGCTTGGTT
D3 (EU594435) (1119) TCTGTATAAACAATACCTGAACCTTTACCCCGTTGCCCGGCAACGGCCAGGTCTGTGCCAAGTGTTTGCTGACGCAACCCCCACTGGCTGGGGCTTGGTC
D4 (AB033559) (1119) TCTGTGTAAACAATACCTGAACCTTTACCCCGTTGCCAGGCAACGGCCAGGTCTGTGCCAAGTGTTTGCTGATGCAACCCCCACTGGGTGGGGCTTGGTC
 E (AM494708) (1119) TCTGTGTAAACAATACCTGAACCTTTACCCCGTTGCCCGGCAACGGCCCGGTCTGTGCCAAGTGTTTGCTGATGCAACCCCCACTGGCTGGGGCTTGGCC
F1 (AY090458) (1122) TCTATGTCAACAATACATGAACCTTTACCCCGTTGCTCGGCAACGGCCAGGCCTGTGCCAAGTGTTTGCTGACGCAACCCCCACTGGTTGGGGCTTGGCC
F2 (AY311369) (1119) TCTGTGTAAACAATACATGAACCTTTACCCCGTTGCTCGGCAACGGCCAGGCCTGTGCCAAGTGTTTGCTGACGCAACCCCCACTGGTTGGGGCTTGGCC
F3 (AB036909) (1119) TCTCTGTAAACAATACATGAACCTTTACCCCGTTGCTCGGCAACGGCCAGGCCTGTGCCAAGTGTTTGCTGACGCAACCCCCACTGGTTGGGGCTTGGCC
F4 (AF223965) (1119) TCTCTGTAAACAGTACATGAACCTTTACCCCGTTGCTCGGCAACGGCCAGGCCTGTGCCAAGTGTTTGCTGACGCAACCCCCACTGGTTGGGGCTTGGCC
 G (AB375168) (1119) TCTCTGTAAACAATACATGAACCTTTACCCCGTTGCTAGGCAACGGCCCGGTCTGTGCCAAGTGTTTGCTGACGCAACCCCCACTGGTTGGGGCTTGGCC
 H (AY090457) (1122) TCTCTGTAAACAATACATGAACCTTTACCCCGTTGCTCGGCAACGGCCAGGCCTTTGCCAAGTGTTTGCTGACGCAACCCCCACTGGCTGGGGCTTGGCG
pCH-9/3091    (2401) TCTGTGTAAACAATACCTGAACCTTTACCCCGTTGCCCGGCAACGGCCAGGTCTGTGCCAAGTGTTTGCTGACGCAACCCCCACTGGCTGGGGCTTGGTC
         Polymerase   L  C  K  Q  Y  L  N  L  Y  P  V  A  R  Q  R  P  G  L  C  Q  V  F  A  D  A  T  P  T  G  W  G  L  V
```

Figure 8.2.3: Comparison of HBV genotype sequences in the region targeted by the P1 TALEN. The sequences are depicted using a similar format to that described in Figure 8.2.1

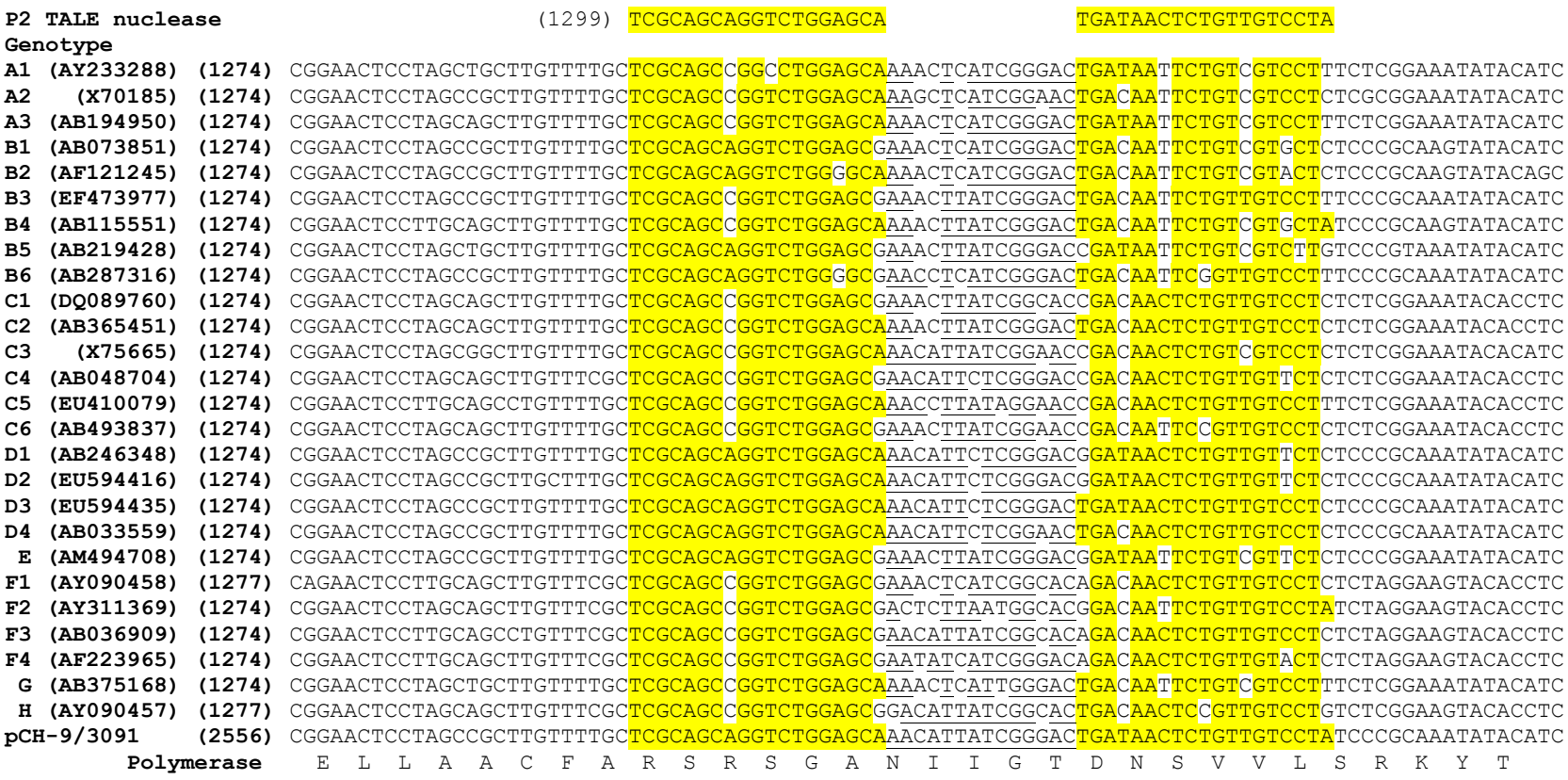

Figure 8.2.4: Comparison of HBV genotype sequences in the region targeted by the P2 TALEN. The sequences are depicted using a similar format to that described in Figure 8.2.1.

8.3 Data from *in vitro* and *in vivo* analysis of anti-HBV TALEN and rTALE efficiency

Table 8.3.1 Spectrophotometric assessment of MTT-based cell viability in Huh7 cell cultures

	Normalised OD ratio at 570/690 nm (±SEM, n = 5)
No DNA	1.000 (± 0.0384)
Stuffer DNA (No TALEN)	1.054 (± 0.0432)
S TALEN	1.082 (± 0.0310)
C TALEN	0.985 (± 0.0377)
P1 TALEN	1.085 (± 0.0671)
P2 TALEN	1.075 (± 0.0312)

Table 8.3.2: Quantification of HBsAg concentrations in Huh7 cell culture supernatants by ELISA

	HBsAg normalised relative OD ratio of 450/620 nm (±SEM, n = 3)	
	Day 2	**Day 3**
No TALEN	1.000 (± 0.1672)	1.000 (± 0.0695)
S TALEN	0.159 (± 0.0243)	0.179 (± 0.028)
C TALEN	1.029 (± 0.1568)	1.213 (± 0.0999)
P1 TALEN	0.314 (± 0.0563)	0.486 (± 0.0470)
P2 TALEN	0.618 (± 0.0188)	0.804 (± 0.0206)

Table 8.3.3: HBsAg concentrations in Huh7 cells following S or P1 TALEN subunit transfections

	HBsAg normalised relative OD ratio of 450/620 nm (±SEM, n = 3)
No TALEN	1.000 (± 0.0222)
SL TALEN subunit	1.036 (± 0.1532)
SR TALEN subunit	0.814 (± 0.0475)
S TALEN	0.4197 (0.0769)
No TALEN	1.000 (± 0.1054)
P1L TALEN subunit	0.608 (± 0.1580)
P1R TALEN subunit	0.432 (± 0.1255)
P1 TALEN	0.455 (± 0.2000)

8.4 Animal Ethics clearance certificate

AESC3

STRICTLY CONFIDENTIAL

ANIMAL ETHICS SCREENING COMMITTEE (AESC)

CLEARANCE CERTIFICATE NO. 2012/47/04

APPLICANT: **Mrs. K Bloom**

DEPARTMENT: **Molecular Medicine and Haematology**

PROJECT TITLE: **Targeted inactivation of Hepatitis B virus (HBV) DNA using Transcription Activator like effector Nucleases (TALENs) and repressor-like effectors (rTALEs) in the mouse liver.**

Number and Species

70 mice (strain NMRI)

Approval was given for to the use of animals for the project described above at an AESC meeting held on **30 October 2012**. This approval remains valid until **31 October 2014**.

The use of these animals is subject to AESC guidelines for the use and care of animals, is limited to the procedures described in the application and to the following additional conditions:

Conditions:

- Professor. P Arbuthnot must sign for the Isofor (Dr Abdullah does not have the appropriate qualification to do this.)

Signed: _____ (Chairperson, AESC) Date: 21/11/2012

I am satisfied that the persons listed in this application are competent to perform the procedures therein, in terms of Section 23 (1) (c) of the Veterinary and Para-Veterinary Professions Act (19 of 1982)

Signed: _____ (Registered Veterinarian) Date: 21/11/12

cc: Supervisor:
Director: CAS

CHAPTER 9 – REFERENCES

Aagaard, L. and Rossi, J.J., 2007. RNAi therapeutics: principles, prospects and challenges. Adv Drug Deliv Rev 59, 75-86.

Abramoff, M.D., Magelhaes, P.J., Ram, S.J., 2004. Image Processing with ImageJ. Biophotonics International 11, 36-42.

Altschul, S.F., Gish, W., Miller, W., Myers, E.W. and Lipman, D.J., 1990. Basic local alignment search tool. J Mol Biol 215, 403-10.

Ansai, S., Sakuma, T., Yamamoto, T., Ariga, H., Uemura, N., Takahashi, R. and Kinoshita, M., 2013. Efficient targeted mutagenesis in medaka using custom-designed transcription activator-like effector nucleases. Genetics 193, 739-49.

Antonucci, T.K. and Rutter, W.J., 1989. Hepatitis B virus (HBV) promoters are regulated by the HBV enhancer in a tissue-specific manner. J Virol 63, 579-83.

Arbuthnot, P., Capovilla, A. and Kew, M., 2000. Putative role of hepatitis B virus X protein in hepatocarcinogenesis: effects on apoptosis, DNA repair, mitogen-activated protein kinase and JAK/STAT pathways. J Gastroenterol Hepatol 15, 357-68.

Ayer, D.E., Laherty, C.D., Lawrence, Q.A., Armstrong, A.P. and Eisenman, R.N., 1996. Mad proteins contain a dominant transcription repression domain. Mol Cell Biol 16, 5772-81.

Bar-Yishay, I., Shaul, Y. and Shlomai, A., 2011. Hepatocyte metabolic signalling pathways and regulation of hepatitis B virus expression. Liver Int 31, 282-90.

Bedell, V.M., Wang, Y., Campbell, J.M., Poshusta, T.L., Starker, C.G., Krug, R.G., 2nd, Tan, W., Penheiter, S.G., Ma, A.C., Leung, A.Y., Fahrenkrug, S.C., Carlson, D.F., Voytas, D.F., Clark, K.J., Essner, J.J. and Ekker, S.C., 2012. In vivo genome editing using a high-efficiency TALEN system. Nature 491, 114-8.

Bellefroid, E.J., Poncelet, D.A., Lecocq, P.J., Revelant, O. and Martial, J.A., 1991. The evolutionarily conserved Kruppel-associated box domain defines a subfamily of eukaryotic multifingered proteins. Proc Natl Acad Sci U S A 88, 3608-12.

Belloni, L., Pollicino, T., De Nicola, F., Guerrieri, F., Raffa, G., Fanciulli, M., Raimondo, G. and Levrero, M., 2009. Nuclear HBx binds the HBV minichromosome and modifies the epigenetic regulation of cccDNA function. Proc Natl Acad Sci U S A 106, 19975-9.

Benson, D.A., Cavanaugh, M., Clark, K., Karsch-Mizrachi, I., Lipman, D.J., Ostell, J. and Sayers, E.W., 2013. GenBank. Nucleic Acids Res 41, D36-42.

Bernstein, K.A. and Rothstein, R., 2009. At loose ends: resecting a double-strand break. Cell 137, 807-10.

Bhakta, M.S. and Segal, D.J., 2010. The generation of zinc finger proteins by modular assembly. Methods Mol Biol 649, 3-30.

Bitinaite, J., Wah, D.A., Aggarwal, A.K. and Schildkraut, I., 1998. FokI dimerization is required for DNA cleavage. Proc Natl Acad Sci U S A 95, 10570-5.

Block, T.M., Guo, H. and Guo, J.T., 2007. Molecular virology of hepatitis B virus for clinicians. Clin Liver Dis 11, 685-706, vii.

Blum, H.E., Gerok, W. and Vyas, G.N., 1989. The molecular biology of hepatitis B virus. Trends Genet 5, 154-8.

Boch, J. and Bonas, U., 2009. Xanthomonas AvrBs3 family-type III effectors: discovery and function. Annu Rev Phytopathol 48, 419-36.

Boch, J., Scholze, H., Schornack, S., Landgraf, A., Hahn, S., Kay, S., Lahaye, T., Nickstadt, A. and Bonas, U., 2009. Breaking the code of DNA binding specificity of TAL-type III effectors. Science 326, 1509-12.

Bock, C.T., Kubicka, S., Manns, M.P. and Trautwein, C., 1999. Two control elements in the hepatitis B virus S-promoter are important for full promoter activity mediated by CCAAT-binding factor. Hepatology 29, 1236-47.

Bock, C.T., Schwinn, S., Locarnini, S., Fyfe, J., Manns, M.P., Trautwein, C. and Zentgraf, H., 2001. Structural organization of the hepatitis B virus minichromosome. J Mol Biol 307, 183-96.

Bree, R.T., Neary, C., Samali, A. and Lowndes, N.F., 2004. The switch from survival responses to apoptosis after chromosomal breaks. DNA Repair (Amst) 3, 989-95.

Briggs, A.W., Rios, X., Chari, R., Yang, L., Zhang, F., Mali, P. and Church, G.M., 2012. Iterative capped assembly: rapid and scalable synthesis of repeat-module DNA such as TAL effectors from individual monomers. Nucleic Acids Res 40, e117.

Brunetti-Pierri, N. and Ng, P., 2011. Helper-dependent adenoviral vectors for liver-directed gene therapy. Hum Mol Genet 20, R7-13.

Bultmann, S., Morbitzer, R., Schmidt, C.S., Thanisch, K., Spada, F., Elsaesser, J., Lahaye, T. and Leonhardt, H., 2012. Targeted transcriptional activation of silent oct4 pluripotency gene by combining designer TALEs and inhibition of epigenetic modifiers. Nucleic Acids Res 40, 5368-77.

Buttner, D. and Bonas, U., 2010. Regulation and secretion of Xanthomonas virulence factors. FEMS Microbiol Rev 34, 107-33.

Cade, L., Reyon, D., Hwang, W.Y., Tsai, S.Q., Patel, S., Khayter, C., Joung, J.K., Sander, J.D., Peterson, R.T. and Yeh, J.R., 2012. Highly efficient generation of heritable zebrafish gene mutations using homo- and heterodimeric TALENs. Nucleic Acids Res 40, 8001-10.

Carlson, D.F., Tan, W., Lillico, S.G., Stverakova, D., Proudfoot, C., Christian, M., Voytas, D.F., Long, C.R., Whitelaw, C.B. and Fahrenkrug, S.C., 2012. Efficient TALEN-mediated gene knockout in livestock. Proc Natl Acad Sci U S A 109, 17382-7.

Carmona, S., Ely, A., Crowther, C., Moolla, N., Salazar, F.H., Marion, P.L., Ferry, N., Weinberg, M.S. and Arbuthnot, P., 2006. Effective inhibition of HBV replication in vivo by anti-HBx short hairpin RNAs. Mol Ther 13, 411-21.

Caruntu, F.A. and Molagic, V., 2005. CccDNA persistence during natural evolution of chronic VHB infection. Rom J Gastroenterol 14, 373-7.

Cattaneo, R., Will, H., Hernandez, N. and Schaller, H., 1983. Signals regulating hepatitis B surface antigen transcription. Nature 305, 336-8.

Cermak, T., Doyle, E.L., Christian, M., Wang, L., Zhang, Y., Schmidt, C., Baller, J.A., Somia, N.V., Bogdanove, A.J. and Voytas, D.F., 2011. Efficient design and assembly of custom TALEN and other TAL effector-based constructs for DNA targeting. Nucleic Acids Res 39, e82.

Chan, H.L., Heathcote, E.J., Marcellin, P., Lai, C.L., Cho, M., Moon, Y.M., Chao, Y.C., Myers, R.P., Minuk, G.Y., Jeffers, L., Sievert, W., Bzowej, N., Harb, G., Kaiser, R., Qiao, X.J.

and Brown, N.A., 2007. Treatment of hepatitis B e antigen positive chronic hepatitis with telbivudine or adefovir: a randomized trial. Ann Intern Med 147, 745-54.

Chang, T.T., Gish, R.G., de Man, R., Gadano, A., Sollano, J., Chao, Y.C., Lok, A.S., Han, K.H., Goodman, Z., Zhu, J., Cross, A., DeHertogh, D., Wilber, R., Colonno, R. and Apelian, D., 2006. A comparison of entecavir and lamivudine for HBeAg-positive chronic hepatitis B. N Engl J Med 354, 1001-10.

Chang, T.T., Lai, C.L., Kew Yoon, S., Lee, S.S., Coelho, H.S., Carrilho, F.J., Poordad, F., Halota, W., Horsmans, Y., Tsai, N., Zhang, H., Tenney, D.J., Tamez, R. and Iloeje, U., 2010a. Entecavir treatment for up to 5 years in patients with hepatitis B e antigen-positive chronic hepatitis B. Hepatology 51, 422-30.

Chang, T.T., Liaw, Y.F., Wu, S.S., Schiff, E., Han, K.H., Lai, C.L., Safadi, R., Lee, S.S., Halota, W., Goodman, Z., Chi, Y.C., Zhang, H., Hindes, R., Iloeje, U., Beebe, S. and Kreter, B., 2010b. Long-term entecavir therapy results in the reversal of fibrosis/cirrhosis and continued histological improvement in patients with chronic hepatitis B. Hepatology 52, 886-93.

Chattopadhyay, S., Ely, A., Bloom, K., Weinberg, M.S. and Arbuthnot, P., 2009. Inhibition of hepatitis B virus replication with linear DNA sequences expressing antiviral micro-RNA shuttles. Biochem Biophys Res Commun 389, 484-9.

Chen, D.S., 2009. Hepatitis B vaccination: The key towards elimination and eradication of hepatitis B. J Hepatol 50, 805-16.

Chen, M. and Ou, J.H., 1995. Cell type-dependent regulation of the activity of the negative regulatory element of the hepatitis B virus core promoter. Virology 214, 198-206.

Chen, Y., Sze, J. and He, M.L., 2004. HBV cccDNA in patients' sera as an indicator for HBV reactivation and an early signal of liver damage. World J Gastroenterol 10, 82-5.

Chevalier, B.S., Kortemme, T., Chadsey, M.S., Baker, D., Monnat, R.J. and Stoddard, B.L., 2002. Design, activity, and structure of a highly specific artificial endonuclease. Mol Cell 10, 895-905.

Chisari, F.V. and Ferrari, C., 1995. Hepatitis B virus immunopathogenesis. Annu Rev Immunol 13, 29-60.

Cho, S.W., Kim, S., Kim, J.M. and Kim, J.S., 2013. Targeted genome engineering in human cells with the Cas9 RNA-guided endonuclease. Nat Biotechnol 31, 230-2.

Christian, M., Cermak, T., Doyle, E.L., Schmidt, C., Zhang, F., Hummel, A., Bogdanove, A.J. and Voytas, D.F., 2010. Targeting DNA double-strand breaks with TAL effector nucleases. Genetics 186, 757-61.

Christian, M.L., Demorest, Z.L., Starker, C.G., Osborn, M.J., Nyquist, M.D., Zhang, Y., Carlson, D.F., Bradley, P., Bogdanove, A.J. and Voytas, D.F., 2012. Targeting G with TAL effectors: a comparison of activities of TALENs constructed with NN and NK repeat variable di-residues. PLoS One 7, e45383.

Chudy, M., Hanschmann, K.M., Kress, J., Nick, S., Campos, R., Wend, U., Gerlich, W. and Nubling, C.M., 2012. First WHO International Reference Panel containing hepatitis B virus genotypes A-G for assays of the viral DNA. J Clin Virol 55, 303-9.

Cong, L., Ran, F.A., Cox, D., Lin, S., Barretto, R., Habib, N., Hsu, P.D., Wu, X., Jiang, W., Marraffini, L.A. and Zhang, F., 2013. Multiplex genome engineering using CRISPR/Cas systems. Science 339, 819-23.

Cong, L., Zhou, R., Kuo, Y.C., Cunniff, M. and Zhang, F., 2012. Comprehensive interrogation of natural TALE DNA-binding modules and transcriptional repressor domains. Nat Commun 3, 968.

Cooksley, W.G., Piratvisuth, T., Lee, S.D., Mahachai, V., Chao, Y.C., Tanwandee, T., Chutaputti, A., Chang, W.Y., Zahm, F.E. and Pluck, N., 2003. Peginterferon alpha-2a (40 kDa): an advance in the treatment of hepatitis B e antigen-positive chronic hepatitis B. J Viral Hepat 10, 298-305.

Cooper, A. and Shaul, Y., 2006. Clathrin-mediated endocytosis and lysosomal cleavage of hepatitis B virus capsid-like core particles. J Biol Chem 281, 16563-9.

Cradick, T.J., Keck, K., Bradshaw, S., Jamieson, A.C. and McCaffrey, A.P., 2010. Zinc-finger nucleases as a novel therapeutic strategy for targeting hepatitis B virus DNAs. Mol Ther 18, 947-54.

Custer, B., Sullivan, S.D., Hazlet, T.K., Iloeje, U., Veenstra, D.L. and Kowdley, K.V., 2004. Global epidemiology of hepatitis B virus. J Clin Gastroenterol 38, S158-68.

D'Ugo, E., Argentini, C., Giuseppetti, R., Canitano, A., Catone, S. and Rapicetta, M., 2010. The woodchuck hepatitis B virus infection model for the evaluation of HBV therapies and vaccine therapies. Expert Opin Drug Discov 5, 1153-62.

Dandri, M. and Locarnini, S., 2012. New insight in the pathobiology of hepatitis B virus infection. Gut 61 Suppl 1, i6-17.

Dane, D.S., Cameron, C.H. and Briggs, M., 1970. Virus-like particles in serum of patients with Australia-antigen-associated hepatitis. Lancet 1, 695-8.

de Franchis, R., Hadengue, A., Lau, G., Lavanchy, D., Lok, A., McIntyre, N., Mele, A., Paumgartner, G., Pietrangelo, A., Rodes, J., Rosenberg, W. and Valla, D., 2003. EASL International Consensus Conference on Hepatitis B. 13-14 September, 2002 Geneva, Switzerland. Consensus statement (long version). J Hepatol 39 Suppl 1, S3-25.

de Martel, C., Ferlay, J., Franceschi, S., Vignat, J., Bray, F., Forman, D. and Plummer, M., 2012. Global burden of cancers attributable to infections in 2008: a review and synthetic analysis. Lancet Oncol 13, 607-15.

Delaney, W.E.t., Ray, A.S., Yang, H., Qi, X., Xiong, S., Zhu, Y. and Miller, M.D., 2006. Intracellular metabolism and in vitro activity of tenofovir against hepatitis B virus. Antimicrob Agents Chemother 50, 2471-7.

Di Bisceglie, A.M., 2009. Hepatitis B and hepatocellular carcinoma. Hepatology 49, S56-60.

Dienstag, J.L., Goldin, R.D., Heathcote, E.J., Hann, H.W., Woessner, M., Stephenson, S.L., Gardner, S., Gray, D.F. and Schiff, E.R., 2003. Histological outcome during long-term lamivudine therapy. Gastroenterology 124, 105-17.

Ding, D., Lou, X., Hua, D., Yu, W., Li, L., Wang, J., Gao, F., Zhao, N., Ren, G. and Lin, B., 2012. Recurrent targeted genes of hepatitis B virus in the liver cancer genomes identified by a next-generation sequencing-based approach. PLoS Genet 8, e1003065.

Ding, Q., Lee, Y.K., Schaefer, E.A., Peters, D.T., Veres, A., Kim, K., Kuperwasser, N., Motola, D.L., Meissner, T.B., Hendriks, W.T., Trevisan, M., Gupta, R.M., Moisan, A., Banks, E., Friesen, M., Schinzel, R.T., Xia, F., Tang, A., Xia, Y., Figueroa, E., Wann, A., Ahfeldt, T., Daheron, L., Zhang, F., Rubin, L.L., Peng, L.F., Chung, R.T., Musunuru, K. and Cowan, C.A., 2013. A TALEN Genome-Editing System for Generating Human Stem Cell-Based Disease Models. Cell Stem Cell 12, 238-51.

Doyle, E.L., Booher, N.J., Standage, D.S., Voytas, D.F., Brendel, V.P., Vandyk, J.K. and Bogdanove, A.J., 2012. TAL Effector-Nucleotide Targeter (TALE-NT) 2.0: tools for TAL effector design and target prediction. Nucleic Acids Res 40, W117-22.

Doyon, Y., Choi, V.M., Xia, D.F., Vo, T.D., Gregory, P.D. and Holmes, M.C., 2010. Transient cold shock enhances zinc-finger nuclease-mediated gene disruption. Nat Methods 7, 459-60.

EASL, 2009. EASL Clinical Practice Guidelines: management of chronic hepatitis B. J Hepatol 50, 227-42.

Ely, A. and Arbuthnot, P. 2010. Advances in the Use of RNAi to Treat Chronic Hepatitis B Virus Infection. In: M.Á. Martínez (Ed), Rna Interference and Viruses: Current Innovations and Future Trends, Horizon Scientific Press, pp. 143.

Ely, A., Naidoo, T., Mufamadi, S., Crowther, C. and Arbuthnot, P., 2008. Expressed anti-HBV primary microRNA shuttles inhibit viral replication efficiently in vitro and in vivo. Mol Ther 16, 1105-12.

Engler, C., Gruetzner, R., Kandzia, R. and Marillonnet, S., 2009. Golden gate shuffling: a one-pot DNA shuffling method based on type IIs restriction enzymes. PLoS One 4, e5553.

Engler, C., Kandzia, R. and Marillonnet, S., 2008. A one pot, one step, precision cloning method with high throughput capability. PLoS One 3, e3647.

Epinat, J.C., Arnould, S., Chames, P., Rochaix, P., Desfontaines, D., Puzin, C., Patin, A., Zanghellini, A., Paques, F. and Lacroix, E., 2003. A novel engineered meganuclease induces homologous recombination in yeast and mammalian cells. Nucleic Acids Res 31, 2952-62.

Erhardt, A., Reineke, U., Blondin, D., Gerlich, W.H., Adams, O., Heintges, T., Niederau, C. and Haussinger, D., 2000. Mutations of the core promoter and response to interferon treatment in chronic replicative hepatitis B. Hepatology 31, 716-25.

Fattovich, G., Bortolotti, F. and Donato, F., 2008. Natural history of chronic hepatitis B: special emphasis on disease progression and prognostic factors. J Hepatol 48, 335-52.

Feitelson, M.A., 1998. The pathogenesis of chronic hepatitis B virus infection. Bulletin de l'Institut Pasteur 96, 227-236.

Firnhaber, C., Viana, R., Reyneke, A., Schultze, D., Malope, B., Maskew, M., Di Bisceglie, A., MacPhail, P., Sanne, I. and Kew, M., 2009. Occult hepatitis B virus infection in patients with isolated core antibody and HIV co-infection in an urban clinic in Johannesburg, South Africa. Int J Infect Dis 13, 488-92.

Fischer, K.P., Gutfreund, K.S. and Tyrrell, D.L., 2001. Lamivudine resistance in hepatitis B: mechanisms and clinical implications. Drug Resist Updat 4, 118-28.

Fisher, E.J., Chaloner, K., Cohn, D.L., Grant, L.B., Alston, B., Brosgart, C.L., Schmetter, B., El-Sadr, W.M. and Sampson, J., 2001. The safety and efficacy of adefovir dipivoxil in patients with advanced HIV disease: a randomized, placebo-controlled trial. AIDS 15, 1695-700.

Fisicaro, P., Valdatta, C., Boni, C., Massari, M., Mori, C., Zerbini, A., Orlandini, A., Sacchelli, L., Missale, G. and Ferrari, C., 2009. Early kinetics of innate and adaptive immune responses during hepatitis B virus infection. Gut 58, 974-82.

Franceschi, S. and Raza, S.A., 2008. Epidemiology and prevention of hepatocellular carcinoma. Cancer Lett.

Fukai, K., Takada, S., Yokosuka, O., Saisho, H., Omata, M. and Koike, K., 1997. Characterization of a specific region in the hepatitis B virus enhancer I for the efficient expression of X gene in the hepatic cell. Virology 236, 279-87.

Fung, H.B., Stone, E.A. and Piacenti, F.J., 2002. Tenofovir disoproxil fumarate: a nucleotide reverse transcriptase inhibitor for the treatment of HIV infection. Clin Ther 24, 1515-48.

Galibert, F., Chen, T.N. and Mandart, E., 1982. Nucleotide sequence of a cloned woodchuck hepatitis virus genome: comparison with the hepatitis B virus sequence. J Virol 41, 51-65.

Gane, E.J., Wang, Y., Liaw, Y.F., Hou, J., Thongsawat, S., Wan, M., Moon, Y.M., Jia, J., Chao, Y.C., Niu, J., Leung, N., Samuel, D., Hsu, C.W., Bao, W., Lopez, P. and Avila, C., 2011. Efficacy and safety of prolonged 3-year telbivudine treatment in patients with chronic hepatitis B. Liver Int 31, 676-84.

Garg, A., Lohmueller, J.J., Silver, P.A. and Armel, T.Z., 2012. Engineering synthetic TAL effectors with orthogonal target sites. Nucleic Acids Res 40, 7584-95.

Gearhart, T.L. and Bouchard, M.J., 2011. The hepatitis B virus HBx protein modulates cell cycle regulatory proteins in cultured primary human hepatocytes. Virus Res 155, 363-7.

Geissler, R., Scholze, H., Hahn, S., Streubel, J., Bonas, U., Behrens, S.E. and Boch, J., 2011. Transcriptional activators of human genes with programmable DNA-specificity. PLoS One 6, e19509.

Gerin, J.L., Tennant, B.C., Ponzetto, A., Purcell, R.H. and Tyeryar, F.J., 1983. The woodchuck animal model of hepatitis B-like virus infection and disease. Prog Clin Biol Res 143, 23-8.

Geurts, A.M., Cost, G.J., Freyvert, Y., Zeitler, B., Miller, J.C., Choi, V.M., Jenkins, S.S., Wood, A., Cui, X., Meng, X., Vincent, A., Lam, S., Michalkiewicz, M., Schilling, R., Foeckler, J., Kalloway, S., Weiler, H., Menoret, S., Anegon, I., Davis, G.D., Zhang, L., Rebar, E.J., Gregory, P.D., Urnov, F.D., Jacob, H.J. and Buelow, R., 2009. Knockout rats via embryo microinjection of zinc-finger nucleases. Science 325, 433.

Giacca, M. and Zacchigna, S., 2012. Virus-mediated gene delivery for human gene therapy. J Control Release 161, 377-88.

Glebe, D. and Urban, S., 2007. Viral and cellular determinants involved in hepadnaviral entry. World J Gastroenterol 13, 22-38.

Grizot, S., Epinat, J.C., Thomas, S., Duclert, A., Rolland, S., Paques, F. and Duchateau, P., 2009. Generation of redesigned homing endonucleases comprising DNA-binding domains derived from two different scaffolds. Nucleic Acids Res 38, 2006-18.

Grosse, S., Huot, N., Mahiet, C., Arnould, S., Barradeau, S., Clerre, D.L., Chion-Sotinel, I., Jacqmarcq, C., Chapellier, B., Ergani, A., Desseaux, C., Cedrone, F., Conseiller, E., Paques, F., Labetoulle, M. and Smith, J., 2011. Meganuclease-mediated Inhibition of HSV1 Infection in Cultured Cells. Mol Ther 19, 694-702.

Guidotti, L.G., Matzke, B., Schaller, H. and Chisari, F.V., 1995. High-level hepatitis B virus replication in transgenic mice. J Virol 69, 6158-69.

Guidotti, L.G., Rochford, R., Chung, J., Shapiro, M., Purcell, R. and Chisari, F.V., 1999. Viral clearance without destruction of infected cells during acute HBV infection. Science 284, 825-9.

Guo, W.T., Bell, K.D. and Ou, J.H., 1991. Characterization of the hepatitis B virus EnhI enhancer and X promoter complex. J Virol 65, 6686-92.

Guo, Y., Guo, H., Zhang, L., Xie, H., Zhao, X., Wang, F., Li, Z., Wang, Y., Ma, S., Tao, J., Wang, W., Zhou, Y., Yang, W. and Cheng, J., 2005. Genomic analysis of anti-hepatitis B virus (HBV) activity by small interfering RNA and lamivudine in stable HBV-producing cells. J Virol 79, 14392-403.

Hadziyannis, S.J., Tassopoulos, N.C., Heathcote, E.J., Chang, T.T., Kitis, G., Rizzetto, M., Marcellin, P., Lim, S.G., Goodman, Z., Ma, J., Arterburn, S., Xiong, S., Currie, G. and Brosgart, C.L., 2005. Long-term therapy with adefovir dipivoxil for HBeAg-negative chronic hepatitis B. N Engl J Med 352, 2673-81.

Hainaut, P. and Boyle, P., 2008. Curbing the liver cancer epidemic in Africa. Lancet 371, 367-8.

Hammond, S.M., Caudy, A.A. and Hannon, G.J., 2001. Post-transcriptional gene silencing by double-stranded RNA. Nat Rev Genet 2, 110-9.

Heermann, K.H., Goldmann, U., Schwartz, W., Seyffarth, T., Baumgarten, H. and Gerlich, W.H., 1984. Large surface proteins of hepatitis B virus containing the pre-s sequence. J Virol 52, 396-402.

Hockemeyer, D., Soldner, F., Beard, C., Gao, Q., Mitalipova, M., DeKelver, R.C., Katibah, G.E., Amora, R., Boydston, E.A., Zeitler, B., Meng, X., Miller, J.C., Zhang, L., Rebar, E.J., Gregory, P.D., Urnov, F.D. and Jaenisch, R., 2009. Efficient targeting of expressed and silent genes in human ESCs and iPSCs using zinc-finger nucleases. Nat Biotechnol 27, 851-7.

Hockemeyer, D., Wang, H., Kiani, S., Lai, C.S., Gao, Q., Cassady, J.P., Cost, G.J., Zhang, L., Santiago, Y., Miller, J.C., Zeitler, B., Cherone, J.M., Meng, X., Hinkley, S.J., Rebar, E.J., Gregory, P.D., Urnov, F.D. and Jaenisch, R., 2011. Genetic engineering of human pluripotent cells using TALE nucleases. Nat Biotechnol 29, 731-4.

Hoffmann, C.J. and Thio, C.L., 2007. Clinical implications of HIV and hepatitis B co-infection in Asia and Africa. Lancet Infect Dis 7, 402-9.

Holkers, M., Maggio, I., Liu, J., Janssen, J.M., Miselli, F., Mussolino, C., Recchia, A., Cathomen, T. and Goncalves, M.A., 2013. Differential integrity of TALE nuclease genes following adenoviral and lentiviral vector gene transfer into human cells. Nucleic Acids Res 41, e63.

Hosaka, T., Suzuki, F., Kobayashi, M., Seko, Y., Kawamura, Y., Sezaki, H., Akuta, N., Suzuki, Y., Saitoh, S., Arase, Y., Ikeda, K. and Kumada, H., 2012. Long-term entecavir treatment reduces hepatocellular carcinoma incidence in patients with hepatitis B virus infection. Hepatology.

Hou, J., Yin, Y.K., Xu, D., Tan, D., Niu, J., Zhou, X., Wang, Y., Zhu, L., He, Y., Ren, H., Wan, M., Chen, C., Wu, S., Chen, Y., Xu, J., Wang, Q., Wei, L., Chao, G., Constance, B.F., Harb, G., Brown, N.A. and Jia, J., 2008. Telbivudine versus lamivudine in Chinese patients with chronic hepatitis B: Results at 1 year of a randomized, double-blind trial. Hepatology 47, 447-54.

Huang, P., Xiao, A., Zhou, M., Zhu, Z., Lin, S. and Zhang, B., 2011. Heritable gene targeting in zebrafish using customized TALENs. Nat Biotechnol 29, 699-700.

Huang, S.N., Millman, I., O'Connell, A., Aronoff, A., Gault, H. and Blumberg, B.S., 1972. Virus-like particles in Australia antigen-associated hepatitis. An immunoelectron microscopic study of human liver. Am J Pathol 67, 453-70.

Huertas, P., 2010. DNA resection in eukaryotes: deciding how to fix the break. Nat Struct Mol Biol 17, 11-6.

Hurlin, P.J., Queva, C., Koskinen, P.J., Steingrimsson, E., Ayer, D.E., Copeland, N.G., Jenkins, N.A. and Eisenman, R.N., 1996. Mad3 and Mad4: novel Max-interacting transcriptional repressors that suppress c-myc dependent transformation and are expressed during neural and epidermal differentiation. EMBO J 15, 2030.

Hwang, W.Y., Fu, Y., Reyon, D., Maeder, M.L., Tsai, S.Q., Sander, J.D., Peterson, R.T., Yeh, J.R. and Joung, J.K., 2013. Efficient genome editing in zebrafish using a CRISPR-Cas system. Nat Biotechnol 31, 227-9.

Ishibashi, S., Cliffe, R. and Amaya, E., 2013. Highly efficient bi-allelic mutation rates using TALENs in Xenopus tropicalis. Biol Open 1, 1273-6.

Jacquier, A. and Dujon, B., 1985. An intron-encoded protein is active in a gene conversion process that spreads an intron into a mitochondrial gene. Cell 41, 383-94.

Jamieson, A.C., Miller, J.C. and Pabo, C.O., 2003. Drug discovery with engineered zinc-finger proteins. Nat Rev Drug Discov 2, 361-8.

Janssen, H.L., van Zonneveld, M., Senturk, H., Zeuzem, S., Akarca, U.S., Cakaloglu, Y., Simon, C., So, T.M., Gerken, G., de Man, R.A., Niesters, H.G., Zondervan, P., Hansen, B. and Schalm, S.W., 2005. Pegylated interferon alfa-2b alone or in combination with lamivudine for HBeAg-positive chronic hepatitis B: a randomised trial. Lancet 365, 123-9.

Jazwa, A., Florczyk, U., Jozkowicz, A. and Dulak, J., 2013. Gene therapy on demand: Site specific regulation of gene therapy. Gene http://dx.doi.org/10.1016/j.gene.2013.03.093.

Jiang, Z., Jhunjhunwala, S., Liu, J., Haverty, P.M., Kennemer, M.I., Guan, Y., Lee, W., Carnevali, P., Stinson, J., Johnson, S., Diao, J., Yeung, S., Jubb, A., Ye, W., Wu, T.D., Kapadia, S.B., de Sauvage, F.J., Gentleman, R.C., Stern, H.M., Seshagiri, S., Pant, K.P., Modrusan, Z., Ballinger, D.G. and Zhang, Z., 2012. The effects of hepatitis B virus

integration into the genomes of hepatocellular carcinoma patients. Genome Res 22, 593-601.

Jinek, M., Chylinski, K., Fonfara, I., Hauer, M., Doudna, J.A. and Charpentier, E., 2012. A programmable dual-RNA-guided DNA endonuclease in adaptive bacterial immunity. Science 337, 816-21.

Jinek, M., East, A., Cheng, A., Lin, S., Ma, E. and Doudna, J., 2013. RNA-programmed genome editing in human cells. Elife 2, e00471.

Jung, M.C. and Pape, G.R., 2002. Immunology of hepatitis B infection. Lancet Infect Dis 2, 43-50.

Kay, M.A., Glorioso, J.C. and Naldini, L., 2001. Viral vectors for gene therapy: the art of turning infectious agents into vehicles of therapeutics. Nat Med 7, 33-40.

Kay, S., Hahn, S., Marois, E., Hause, G. and Bonas, U., 2007. A bacterial effector acts as a plant transcription factor and induces a cell size regulator. Science 318, 648-51.

Kayhan, H., Karatayli, E., Turkyilmaz, A.R., Sahin, F., Yurdaydin, C. and Bozdayi, A.M., 2007. Inhibition of hepatitis B virus replication by shRNAs in stably HBV expressed HEPG2 2.2.15 cell lines. Arch Virol 152, 871-9.

Kew, M.C., 2008. Hepatitis B virus infection: the burden of disease in South Africa. The Southern African Journal of Epidemiology and Infection 23, 4-8.

Kim, H., Um, E., Cho, S.R., Jung, C. and Kim, J.S., 2011. Surrogate reporters for enrichment of cells with nuclease-induced mutations. Nat Methods 8, 941-3.

Kim, Y., Kweon, J., Kim, A., Chon, J.K., Yoo, J.Y., Kim, H.J., Kim, S., Lee, C., Jeong, E., Chung, E., Kim, D., Lee, M.S., Go, E.M., Song, H.J., Kim, H., Cho, N., Bang, D. and Kim, J.S., 2013a. A library of TAL effector nucleases spanning the human genome. Nat Biotechnol.

Kim, Y., Kweon, J. and Kim, J.S., 2013b. TALENs and ZFNs are associated with different mutation signatures. Nat Methods 10, 185.

Kim, Y.G., Cha, J. and Chandrasegaran, S., 1996. Hybrid restriction enzymes: zinc finger fusions to Fok I cleavage domain. Proc Natl Acad Sci U S A 93, 1156-60.

Klug, A., 2010. The discovery of zinc fingers and their applications in gene regulation and genome manipulation. Annu Rev Biochem 79, 213-31.

Konishi, M., Wu, C.H. and Wu, G.Y., 2003. Inhibition of HBV replication by siRNA in a stable HBV-producing cell line. Hepatology 38, 842-50.

Kostriken, R., Strathern, J.N., Klar, A.J., Hicks, J.B. and Heffron, F., 1983. A site-specific endonuclease essential for mating-type switching in Saccharomyces cerevisiae. Cell 35, 167-74.

Kramvis, A. and Kew, M.C., 2007. Epidemiology of hepatitis B virus in Africa, its genotypes and clinical associations of genotypes. Hepatol Res 37, S9-S19.

Krastev, Z.A., 2006. The "return" of hepatitis B. World J Gastroenterol 12, 7081-6.

Kurbanov, F., Tanaka, Y. and Mizokami, M., 2010. Geographical and genetic diversity of the human hepatitis B virus. Hepatol Res 40, 14-30.

Lai, C.L., Chien, R.N., Leung, N.W., Chang, T.T., Guan, R., Tai, D.I., Ng, K.Y., Wu, P.C., Dent, J.C., Barber, J., Stephenson, S.L. and Gray, D.F., 1998. A one-year trial of lamivudine for chronic hepatitis B. Asia Hepatitis Lamivudine Study Group. N Engl J Med 339, 61-8.

Lai, C.L., Dienstag, J., Schiff, E., Leung, N.W., Atkins, M., Hunt, C., Brown, N., Woessner, M., Boehme, R. and Condreay, L., 2003. Prevalence and clinical correlates of YMDD variants during lamivudine therapy for patients with chronic hepatitis B. Clin Infect Dis 36, 687-96.

Lai, C.L., Gane, E., Liaw, Y.F., Hsu, C.W., Thongsawat, S., Wang, Y., Chen, Y., Heathcote, E.J., Rasenack, J., Bzowej, N., Naoumov, N.V., Di Bisceglie, A.M., Zeuzem, S., Moon, Y.M., Goodman, Z., Chao, G., Constance, B.F. and Brown, N.A., 2007. Telbivudine versus lamivudine in patients with chronic hepatitis B. N Engl J Med 357, 2576-88.

Lai, C.L., Shouval, D., Lok, A.S., Chang, T.T., Cheinquer, H., Goodman, Z., DeHertogh, D., Wilber, R., Zink, R.C., Cross, A., Colonno, R. and Fernandes, L., 2006. Entecavir versus lamivudine for patients with HBeAg-negative chronic hepatitis B. N Engl J Med 354, 1011-20.

Laras, A., Koskinas, J., Dimou, E., Kostamena, A. and Hadziyannis, S.J., 2006. Intrahepatic levels and replicative activity of covalently closed circular hepatitis B virus DNA in chronically infected patients. Hepatology 44, 694-702.

Lavanchy, D., 2004. Hepatitis B virus epidemiology, disease burden, treatment, and current and emerging prevention and control measures. J Viral Hepat 11, 97-107.

Lee, C.M., Flynn, R., Hollywood, J.A., Scallan, M.F. and Harrison, P.T., 2013. Correction of the DeltaF508 Mutation in the Cystic Fibrosis Transmembrane Conductance Regulator Gene by Zinc-Finger Nuclease Homology-Directed Repair. Biores Open Access 1, 99-108.

Lee, J.M., Kim, H.J., Park, J.Y., Lee, C.K., Kim do, Y., Kim, J.K., Lee, H.W., Paik, Y.H., Lee, K.S., Han, K.H., Chon, C.Y., Hong, S.P., Nguyen, T. and Ahn, S.H., 2009. Rescue

monotherapy in lamivudine-resistant hepatitis B e antigen-positive chronic hepatitis B: adefovir versus entecavir. Antivir Ther 14, 705-12.

Lei, Y., Guo, X., Liu, Y., Cao, Y., Deng, Y., Chen, X., Cheng, C.H., Dawid, I.B., Chen, Y. and Zhao, H., 2012. Efficient targeted gene disruption in Xenopus embryos using engineered transcription activator-like effector nucleases (TALENs). Proc Natl Acad Sci U S A 109, 17484-9.

Levrero, M., Pollicino, T., Petersen, J., Belloni, L., Raimondo, G. and Dandri, M., 2009. Control of cccDNA function in hepatitis B virus infection. J Hepatol 51, 581-92.

Li, G.Q., Gu, H.X., Li, D. and Xu, W.Z., 2007. Inhibition of Hepatitis B virus cccDNA replication by siRNA. Biochem Biophys Res Commun 355, 404-8.

Li, G.Q., Yu, D.M., Lu, J., Chen, S.L., Zhao, J.Y. and Wang, Y.C., 2011a. Study of the efficacy of combination therapy of SiRNAs in HepG2.2.15 cells. Hepatogastroenterology 58, 570-4.

Li, T., Huang, S., Jiang, W.Z., Wright, D., Spalding, M.H., Weeks, D.P. and Yang, B., 2010. TAL nucleases (TALNs): hybrid proteins composed of TAL effectors and FokI DNA-cleavage domain. Nucleic Acids Res 39, 359-72.

Li, T., Huang, S., Zhao, X., Wright, D.A., Carpenter, S., Spalding, M.H., Weeks, D.P. and Yang, B., 2011b. Modularly assembled designer TAL effector nucleases for targeted gene knockout and gene replacement in eukaryotes. Nucleic Acids Res 39, 6315-25.

Li, T., Liu, B., Spalding, M.H., Weeks, D.P. and Yang, B., 2012. High-efficiency TALEN-based gene editing produces disease-resistant rice. Nat Biotechnol 30, 390-2.

Lieber, M.R., 2010. The mechanism of double-strand DNA break repair by the nonhomologous DNA end-joining pathway. Annu Rev Biochem 79, 181-211.

Lin, C.L. and Kao, J.H., 2011. The clinical implications of hepatitis B virus genotype: Recent advances. J Gastroenterol Hepatol 26 Suppl 1, 123-30.

Liu, F., Song, Y. and Liu, D., 1999. Hydrodynamics-based transfection in animals by systemic administration of plasmid DNA. Gene Ther 6, 1258-66.

Liu, J., Guo, Y., Xue, C.F., Li, Y.H., Huang, Y.X., Ding, J., Gong, W.D. and Zhao, Y., 2004. Effect of vector-expressed siRNA on HBV replication in hepatoblastoma cells. World J Gastroenterol 10, 1898-901.

Liu, J., Li, C., Yu, Z., Huang, P., Wu, H., Wei, C., Zhu, N., Shen, Y., Chen, Y., Zhang, B., Deng, W.M. and Jiao, R., 2012. Efficient and specific modifications of the Drosophila genome by means of an easy TALEN strategy. J Genet Genomics 39, 209-15.

Low, E., Cox, A., Atkins, M. and Nelson, M., 2009. Telbivudine has activity against HIV-1. AIDS 23, 546-7.

Maeder, M.L., Thibodeau-Beganny, S., Sander, J.D., Voytas, D.F. and Joung, J.K., 2009. Oligomerized pool engineering (OPEN): an 'open-source' protocol for making customized zinc-finger arrays. Nat Protoc 4, 1471-501.

Maier, D.A., Brennan, A.L., Jiang, S., Binder-Scholl, G.K., Lee, G., Plesa, G., Zheng, Z., Cotte, J., Carpenito, C., Wood, T., Spratt, S.K., Ando, D., Gregory, P., Holmes, M.C., Perez, E.E., Riley, J.L., Carroll, R.G., June, C.H. and Levine, B.L., 2013. Efficient Clinical Scale Gene Modification via Zinc Finger Nuclease-Targeted Disruption of the HIV Co-receptor CCR5. Hum Gene Ther 24, 245-58.

Mak, A.N., Bradley, P., Cernadas, R.A., Bogdanove, A.J. and Stoddard, B.L., 2012. The crystal structure of TAL effector PthXo1 bound to its DNA target. Science 335, 716-9.

Mali, P., Yang, L., Esvelt, K.M., Aach, J., Guell, M., DiCarlo, J.E., Norville, J.E. and Church, G.M., 2013. RNA-guided human genome engineering via Cas9. Science 339, 823-6.

Mancini-Bourgine, M., Bayard, F., Soussan, P., Deng, Q., Lone, Y.C., Kremsdorf, D. and Michel, M.L., 2007. Hepatitis B virus splice-generated protein induces T-cell responses in HLA-transgenic mice and hepatitis B virus-infected patients. J Virol 81, 4963-72.

Marcellin, P., Chang, T.T., Lim, S.G., Sievert, W., Tong, M., Arterburn, S., Borroto-Esoda, K., Frederick, D. and Rousseau, F., 2008. Long-term efficacy and safety of adefovir dipivoxil for the treatment of hepatitis B e antigen-positive chronic hepatitis B. Hepatology 48, 750-8.

Marcellin, P., Lau, G.K., Bonino, F., Farci, P., Hadziyannis, S., Jin, R., Lu, Z.M., Piratvisuth, T., Germanidis, G., Yurdaydin, C., Diago, M., Gurel, S., Lai, M.Y., Button, P. and Pluck, N., 2004. Peginterferon alfa-2a alone, lamivudine alone, and the two in combination in patients with HBeAg-negative chronic hepatitis B. N Engl J Med 351, 1206-17.

Margolis, H.S., 1998. Hepatitis B virus infection. Bull World Health Organ 76 Suppl 2, 152-3.

Mason, W.S., Litwin, S., Xu, C. and Jilbert, A.R., 2007. Hepatocyte turnover in transient and chronic hepadnavirus infections. J Viral Hepat 14 Suppl 1, 22-8.

McVey, M. and Lee, S.E., 2008. MMEJ repair of double-strand breaks (director's cut): deleted sequences and alternative endings. Trends Genet 24, 529-38.

Menne, S. and Cote, P.J., 2007. The woodchuck as an animal model for pathogenesis and therapy of chronic hepatitis B virus infection. World J Gastroenterol 13, 104-24.

Meuleman, P. and Leroux-Roels, G., 2008. The human liver-uPA-SCID mouse: a model for the evaluation of antiviral compounds against HBV and HCV. Antiviral Res 80, 231-8.

Meuleman, P., Libbrecht, L., De Vos, R., de Hemptinne, B., Gevaert, K., Vandekerckhove, J., Roskams, T. and Leroux-Roels, G., 2005. Morphological and biochemical characterization of a human liver in a uPA-SCID mouse chimera. Hepatology 41, 847-56.

Miller, J.C., Tan, S., Qiao, G., Barlow, K.A., Wang, J., Xia, D.F., Meng, X., Paschon, D.E., Leung, E., Hinkley, S.J., Dulay, G.P., Hua, K.L., Ankoudinova, I., Cost, G.J., Urnov, F.D., Zhang, H.S., Holmes, M.C., Zhang, L., Gregory, P.D. and Rebar, E.J., 2011. A TALE nuclease architecture for efficient genome editing. Nat Biotechnol 29, 143-8.

Modi, A.A. and Feld, J.J., 2007. Viral hepatitis and HIV in Africa. AIDS Rev 9, 25-39.

Moehle, E.A., Rock, J.M., Lee, Y.L., Jouvenot, Y., DeKelver, R.C., Gregory, P.D., Urnov, F.D. and Holmes, M.C., 2007. Targeted gene addition into a specified location in the human genome using designed zinc finger nucleases. Proc Natl Acad Sci U S A 104, 3055-60.

Moolla, N., Kew, M. and Arbuthnot, P., 2002. Regulatory elements of hepatitis B virus transcription. J Viral Hepat 9, 323-31.

Morbitzer, R., Elsaesser, J., Hausner, J. and Lahaye, T., 2011. Assembly of custom TALE-type DNA binding domains by modular cloning. Nucleic Acids Res 39, 5790-9.

Morbitzer, R., Romer, P., Boch, J. and Lahaye, T., 2010. Regulation of selected genome loci using de novo-engineered transcription activator-like effector (TALE)-type transcription factors. Proc Natl Acad Sci U S A 107, 21617-22.

Moscou, M.J. and Bogdanove, A.J., 2009. A simple cipher governs DNA recognition by TAL effectors. Science 326, 1501.

Mowa, M.B., Crowther, C. and Arbuthnot, P., 2010. Therapeutic potential of adenoviral vectors for delivery of expressed RNAi activators. Expert Opin Drug Deliv 7, 1373-85.

Mulrooney-Cousins, P.M. and Michalak, T.I., 2007. Persistent occult hepatitis B virus infection: experimental findings and clinical implications. World J Gastroenterol 13, 5682-6.

Murakami, Y., Saigo, K., Takashima, H., Minami, M., Okanoue, T., Brechot, C. and Paterlini-Brechot, P., 2005. Large scaled analysis of hepatitis B virus (HBV) DNA integration in HBV related hepatocellular carcinomas. Gut 54, 1162-8.

Mussolino, C., Morbitzer, R., Lutge, F., Dannemann, N., Lahaye, T. and Cathomen, T., 2011. A novel TALE nuclease scaffold enables high genome editing activity in combination with low toxicity. Nucleic Acids Res 39, 9283-93.

Nassal, M., 1992. The arginine-rich domain of the hepatitis B virus core protein is required for pregenome encapsidation and productive viral positive-strand DNA synthesis but not for virus assembly. J Virol 66, 4107-16.

Nassal, M., 2008. Hepatitis B viruses: reverse transcription a different way. Virus Res 134, 235-49.

Neff, K.L., Argue, D.P., Ma, A.C., Lee, H.B., Clark, K.J. and Ekker, S.C., 2013. Mojo Hand, a TALEN design tool for genome editing applications. BMC Bioinformatics 14, 1.

Neurath, A.R., Strick, N. and Sproul, P., 1992. Search for hepatitis B virus cell receptors reveals binding sites for interleukin 6 on the virus envelope protein. J Exp Med 175, 461-9.

Newbold, J.E., Xin, H., Tencza, M., Sherman, G., Dean, J., Bowden, S. and Locarnini, S., 1995. The covalently closed duplex form of the hepadnavirus genome exists in situ as a heterogeneous population of viral minichromosomes. J Virol 69, 3350-7.

Olinger, C.M., Jutavijittum, P., Hubschen, J.M., Yousukh, A., Samountry, B., Thammavong, T., Toriyama, K. and Muller, C.P., 2008. Possible new hepatitis B virus genotype, southeast Asia. Emerg Infect Dis 14, 1777-80.

Ono-Nita, S.K., Kato, N., Shiratori, Y., Lan, K.H., Yoshida, H., Carrilho, F.J. and Omata, M., 1999. Susceptibility of lamivudine-resistant hepatitis B virus to other reverse transcriptase inhibitors. J Clin Invest 103, 1635-40.

Osborn, M.K., 2009. Safety and efficacy of telbivudine for the treatment of chronic hepatitis B. Ther Clin Risk Manag 5, 789-98.

Ott, J.J., Stevens, G.A. and Wiersma, S.T., 2012. The risk of perinatal hepatitis B virus transmission: hepatitis B e antigen (HBeAg) prevalence estimates for all world regions. BMC Infect Dis 12, 131.

Parkin, D.M., 2006. The global health burden of infection-associated cancers in the year 2002. Int J Cancer 118, 3030-44.

Paronetto, F. and Tennant, B.C., 1990. Woodchuck hepatitis virus infection: a model of human hepatic diseases and hepatocellular carcinoma. Prog Liver Dis 9, 463-83.

Pattanayak, V., Ramirez, C.L., Joung, J.K. and Liu, D.R., 2011. Revealing off-target cleavage specificities of zinc-finger nucleases by in vitro selection. Nat Methods 8, 765-70.

Perez-Pinera, P., Ousterout, D.G., Brunger, J.M., Farin, A.M., Glass, K.A., Guilak, F., Crawford, G.E., Hartemink, A.J. and Gersbach, C.A., 2013. Synergistic and tunable human gene activation by combinations of synthetic transcription factors. Nat Methods 10, 239-42.

Perrillo, R.P., Schiff, E.R., Davis, G.L., Bodenheimer, H.C., Jr., Lindsay, K., Payne, J., Dienstag, J.L., O'Brien, C., Tamburro, C., Jacobson, I.M. and et al., 1990. A randomized, controlled trial of interferon alfa-2b alone and after prednisone withdrawal for the treatment of chronic hepatitis B. The Hepatitis Interventional Therapy Group. N Engl J Med 323, 295-301.

Perz, J.F., Armstrong, G.L., Farrington, L.A., Hutin, Y.J. and Bell, B.P., 2006. The contributions of hepatitis B virus and hepatitis C virus infections to cirrhosis and primary liver cancer worldwide. J Hepatol 45, 529-38.

Pollicino, T., Belloni, L., Raffa, G., Pediconi, N., Squadrito, G., Raimondo, G. and Levrero, M., 2006. Hepatitis B virus replication is regulated by the acetylation status of hepatitis B virus cccDNA-bound H3 and H4 histones. Gastroenterology 130, 823-37.

Porteus, M.H., 2006. Mammalian gene targeting with designed zinc finger nucleases. Mol Ther 13, 438-46.

Porteus, M.H. and Baltimore, D., 2003. Chimeric nucleases stimulate gene targeting in human cells. Science 300, 763.

Qi, L.S., Larson, M.H., Gilbert, L.A., Doudna, J.A., Weissman, J.S., Arkin, A.P. and Lim, W.A., 2013. Repurposing CRISPR as an RNA-guided platform for sequence-specific control of gene expression. Cell 152, 1173-83.

Quasdorff, M. and Protzer, U., 2010. Control of hepatitis B virus at the level of transcription. J Viral Hepat 17, 527-36.

Rabe, B., Glebe, D. and Kann, M., 2006. Lipid-mediated introduction of hepatitis B virus capsids into nonsusceptible cells allows highly efficient replication and facilitates the study of early infection events. J Virol 80, 5465-73.

Rahman, S.H., Maeder, M.L., Joung, J.K. and Cathomen, T., 2011. Zinc-finger nucleases for somatic gene therapy: the next frontier. Hum Gene Ther 22, 925-33.

Ramirez, C.L., Foley, J.E., Wright, D.A., Muller-Lerch, F., Rahman, S.H., Cornu, T.I., Winfrey, R.J., Sander, J.D., Fu, F., Townsend, J.A., Cathomen, T., Voytas, D.F. and Joung, J.K., 2008. Unexpected failure rates for modular assembly of engineered zinc fingers. Nat Methods 5, 374-5.

Rehermann, B., Ferrari, C., Pasquinelli, C. and Chisari, F.V., 1996. The hepatitis B virus persists for decades after patients' recovery from acute viral hepatitis despite active maintenance of a cytotoxic T-lymphocyte response. Nat Med 2, 1104-8.

Revill, P. and Yuan, Z., 2013. New insights into how HBV manipulates the innate immune response to establish acute and persistent infection. Antivir Ther 18, 1-15.

Reyon, D., Tsai, S.Q., Khayter, C., Foden, J.A., Sander, J.D. and Joung, J.K., 2012. FLASH assembly of TALENs for high-throughput genome editing. Nat Biotechnol 30, 460-5.

Richardson, C. and Jasin, M., 2000. Frequent chromosomal translocations induced by DNA double-strand breaks. Nature 405, 697-700.

Richman, D.D., Little, S.J., Smith, D.M., Wrin, T., Petropoulos, C. and Wong, J.K., 2004. HIV evolution and escape. Trans Am Clin Climatol Assoc 115, 289-303.

Robbins, P.D. and Ghivizzani, S.C., 1998. Viral vectors for gene therapy. Pharmacol Ther 80, 35-47.

Robinson, W.S., 1977. The genome of hepatitis B virus. Annu Rev Microbiol 31, 357-77.

Robinson, W.S., Clayton, D.A. and Greenman, R.L., 1974. DNA of a human hepatitis B virus candidate. J Virol 14, 384-91.

Roggendorf, M. and Tolle, T.K., 1995. The woodchuck: an animal model for hepatitis B virus infection in man. Intervirology 38, 100-12.

Romer, P., Hahn, S., Jordan, T., Strauss, T., Bonas, U. and Lahaye, T., 2007. Plant pathogen recognition mediated by promoter activation of the pepper Bs3 resistance gene. Science 318, 645-8.

Roos, W.P. and Kaina, B., 2006. DNA damage-induced cell death by apoptosis. Trends Mol Med 12, 440-50.

Rosen, L.E., Morrison, H.A., Masri, S., Brown, M.J., Springstubb, B., Sussman, D., Stoddard, B.L. and Seligman, L.M., 2006. Homing endonuclease I-CreI derivatives with novel DNA target specificities. Nucleic Acids Res 34, 4791-800.

Sajwan, S., Takasu, Y., Tamura, T., Uchino, K., Sezutsu, H. and Zurovec, M., 2012. Efficient disruption of endogenous Bombyx gene by TAL effector nucleases. Insect Biochem Mol Biol 43, 17-23.

Sander, J.D., Cade, L., Khayter, C., Reyon, D., Peterson, R.T., Joung, J.K. and Yeh, J.R., 2011. Targeted gene disruption in somatic zebrafish cells using engineered TALENs. Nat Biotechnol 29, 697-8.

Sander, J.D., Dahlborg, E.J., Goodwin, M.J., Cade, L., Zhang, F., Cifuentes, D., Curtin, S.J., Blackburn, J.S., Thibodeau-Beganny, S., Qi, Y., Pierick, C.J., Hoffman, E., Maeder, M.L., Khayter, C., Reyon, D., Dobbs, D., Langenau, D.M., Stupar, R.M., Giraldez, A.J.,

Voytas, D.F., Peterson, R.T., Yeh, J.R. and Joung, J.K., 2010a. Selection-free zinc-finger-nuclease engineering by context-dependent assembly (CoDA). Nat Methods 8, 67-9.

Sander, J.D., Maeder, M.L., Reyon, D., Voytas, D.F., Joung, J.K. and Dobbs, D., 2010b. ZiFiT (Zinc Finger Targeter): an updated zinc finger engineering tool. Nucleic Acids Res 38, W462-8.

Sander, J.D., Zaback, P., Joung, J.K., Voytas, D.F. and Dobbs, D., 2007. Zinc Finger Targeter (ZiFiT): an engineered zinc finger/target site design tool. Nucleic Acids Res 35, W599-605.

Schiffer, J.T., Aubert, M., Weber, N.D., Mintzer, E., Stone, D. and Jerome, K.R., 2012. Targeted DNA mutagenesis for the cure of chronic viral infections. J Virol 86, 8920-36.

Schmid-Burgk, J.L., Schmidt, T., Kaiser, V., Honing, K. and Hornung, V., 2012. A ligation-independent cloning technique for high-throughput assembly of transcription activator-like effector genes. Nat Biotechnol 31, 76-81.

Schmitz, A., Schwarz, A., Foss, M., Zhou, L., Rabe, B., Hoellenriegel, J., Stoeber, M., Pante, N. and Kann, M., 2010. Nucleoporin 153 arrests the nuclear import of hepatitis B virus capsids in the nuclear basket. PLoS Pathog 6, e1000741.

Schreier, H., 1994. The new frontier: gene and oligonucleotide therapy. Pharm Acta Helv 68, 145-59.

Schultz, D.C., Ayyanathan, K., Negorev, D., Maul, G.G. and Rauscher, F.J., 3rd, 2002. SETDB1: a novel KAP-1-associated histone H3, lysine 9-specific methyltransferase that contributes to HP1-mediated silencing of euchromatic genes by KRAB zinc-finger proteins. Genes Dev 16, 919-32.

Seeger, C. and Mason, W.S., 2000. Hepatitis B virus biology. Microbiol Mol Biol Rev 64, 51-68.

Seligman, L.M., Chisholm, K.M., Chevalier, B.S., Chadsey, M.S., Edwards, S.T., Savage, J.H. and Veillet, A.L., 2002. Mutations altering the cleavage specificity of a homing endonuclease. Nucleic Acids Res 30, 3870-9.

Sells, M.A., Chen, M.L. and Acs, G., 1987. Production of hepatitis B virus particles in Hep G2 cells transfected with cloned hepatitis B virus DNA. Proc Natl Acad Sci U S A 84, 1005-9.

Sells, M.A., Zelent, A.Z., Shvartsman, M. and Acs, G., 1988. Replicative intermediates of hepatitis B virus in HepG2 cells that produce infectious virions. J Virol 62, 2836-44.

Shi, H., Lu, L., Zhang, N.P., Zhang, S.C. and Shen, X.Z., 2012. Effect of interferon-gamma and tumor necrosis factor-alpha on hepatitis B virus following lamivudine treatment. World J Gastroenterol 18, 3617-22.

Smith, J., Grizot, S., Arnould, S., Duclert, A., Epinat, J.C., Chames, P., Prieto, J., Redondo, P., Blanco, F.J., Bravo, J., Montoya, G., Paques, F. and Duchateau, P., 2006. A combinatorial approach to create artificial homing endonucleases cleaving chosen sequences. Nucleic Acids Res 34, e149.

Soriano, V., Puoti, M., Peters, M., Benhamou, Y., Sulkowski, M., Zoulim, F., Mauss, S. and Rockstroh, J., 2008. Care of HIV patients with chronic hepatitis B: updated recommendations from the HIV-Hepatitis B Virus International Panel. AIDS 22, 1399-410.

Soussan, P., Tuveri, R., Nalpas, B., Garreau, F., Zavala, F., Masson, A., Pol, S., Brechot, C. and Kremsdorf, D., 2003. The expression of hepatitis B spliced protein (HBSP) encoded

by a spliced hepatitis B virus RNA is associated with viral replication and liver fibrosis. J Hepatol 38, 343-8.

Starkey, J.L., Chiari, E.F. and Isom, H.C., 2009. Hepatitis B virus (HBV)-specific short hairpin RNA is capable of reducing the formation of HBV covalently closed circular (CCC) DNA but has no effect on established CCC DNA in vitro. J Gen Virol 90, 115-26.

Streubel, J., Blucher, C., Landgraf, A. and Boch, J., 2012. TAL effector RVD specificities and efficiencies. Nat Biotechnol 30, 593-5.

Stroud, D.A., Formosa, L.E., Wijeyeratne, X.W., Nguyen, T.N. and Ryan, M.T., 2013. Gene knockout using transcription activator-like effector nucleases (TALENs) reveals that human NDUFA9 protein is essential for stabilizing the junction between membrane and matrix arms of complex I. J Biol Chem 288, 1685-90.

Su, H. and Yee, J.K., 1992. Regulation of hepatitis B virus gene expression by its two enhancers. Proc Natl Acad Sci U S A 89, 2708-12.

Summers, J., Jilbert, A.R., Yang, W., Aldrich, C.E., Saputelli, J., Litwin, S., Toll, E. and Mason, W.S., 2003. Hepatocyte turnover during resolution of a transient hepadnaviral infection. Proc Natl Acad Sci U S A 100, 11652-9.

Summers, J., O'Connell, A. and Millman, I., 1975. Genome of hepatitis B virus: restriction enzyme cleavage and structure of DNA extracted from Dane particles. Proc Natl Acad Sci U S A 72, 4597-601.

Sun, N., Liang, J., Abil, Z. and Zhao, H., 2012. Optimized TAL effector nucleases (TALENs) for use in treatment of sickle cell disease. Mol Biosyst 8, 1255-63.

Sung, W.K., Zheng, H., Li, S., Chen, R., Liu, X., Li, Y., Lee, N.P., Lee, W.H., Ariyaratne, P.N., Tennakoon, C., Mulawadi, F.H., Wong, K.F., Liu, A.M., Poon, R.T., Fan, S.T., Chan, K.L., Gong, Z., Hu, Y., Lin, Z., Wang, G., Zhang, Q., Barber, T.D., Chou, W.C., Aggarwal, A., Hao, K., Zhou, W., Zhang, C., Hardwick, J., Buser, C., Xu, J., Kan, Z., Dai, H., Mao, M., Reinhard, C., Wang, J. and Luk, J.M., 2012. Genome-wide survey of recurrent HBV integration in hepatocellular carcinoma. Nat Genet 44, 765-9.

Sung, Y.H., Baek, I.J., Kim, D.H., Jeon, J., Lee, J., Lee, K., Jeong, D., Kim, J.S. and Lee, H.W., 2013. Knockout mice created by TALEN-mediated gene targeting. Nat Biotechnol 31, 23-4.

Tenney, D.J., Rose, R.E., Baldick, C.J., Pokornowski, K.A., Eggers, B.J., Fang, J., Wichroski, M.J., Xu, D., Yang, J., Wilber, R.B. and Colonno, R.J., 2009. Long-term monitoring shows hepatitis B virus resistance to entecavir in nucleoside-naive patients is rare through 5 years of therapy. Hepatology 49, 1503-14.

Tesson, L., Usal, C., Menoret, S., Leung, E., Niles, B.J., Remy, S., Santiago, Y., Vincent, A.I., Meng, X., Zhang, L., Gregory, P.D., Anegon, I. and Cost, G.J., 2011. Knockout rats generated by embryo microinjection of TALENs. Nat Biotechnol 29, 695-6.

Thierry, A. and Dujon, B., 1992. Nested chromosomal fragmentation in yeast using the meganuclease I-Sce I: a new method for physical mapping of eukaryotic genomes. Nucleic Acids Res 20, 5625-31.

Thimme, R., Wieland, S., Steiger, C., Ghrayeb, J., Reimann, K.A., Purcell, R.H. and Chisari, F.V., 2003. CD8(+) T cells mediate viral clearance and disease pathogenesis during acute hepatitis B virus infection. J Virol 77, 68-76.

Tiollais, P., Pourcel, C. and Dejean, A., 1985. The hepatitis B virus. Nature 317, 489-95.

Toh, S.T., Jin, Y., Liu, L., Wang, J., Babrzadeh, F., Gharizadeh, B., Ronaghi, M., Toh, H.C., Chow, P.K., Chung, A.Y., Ooi, L.L. and Lee, C.G., 2013. Deep sequencing of the hepatitis B virus in hepatocellular carcinoma patients reveals enriched integration events, structural alterations and sequence variations. Carcinogenesis 34, 787-98.

Tong, C., Huang, G., Ashton, C., Wu, H., Yan, H. and Ying, Q.L., 2012. Rapid and cost-effective gene targeting in rat embryonic stem cells by TALENs. J Genet Genomics 39, 275-80.

Tran, T.T., Trinh, T.N. and Abe, K., 2008. New complex recombinant genotype of hepatitis B virus identified in Vietnam. J Virol 82, 5657-63.

Tremblay, J.P., Chapdelaine, P., Coulombe, Z. and Rousseau, J., 2012. Transcription activator-like effector proteins induce the expression of the frataxin gene. Hum Gene Ther 23, 883-90.

Trippler, M., Meyer zum Buschenfelde, K.H. and Gerken, G., 1999. HBV viral load within subpopulations of peripheral blood mononuclear cells in HBV infection using limiting dilution PCR. J Virol Methods 78, 129-47.

Tuttleman, J.S., Pourcel, C. and Summers, J., 1986. Formation of the pool of covalently closed circular viral DNA in hepadnavirus-infected cells. Cell 47, 451-60.

UNAIDS. 2012. Global Report: UNAIDS Report on the global AIDS epidemic, www.unaids.org/en/resources/campaigns/20121120_globalreport2012/globalreport/, WHO Library Cataloguing-in-Publication Data, ISBN 978-92-9173-592-1

Urnov, F.D., Miller, J.C., Lee, Y.L., Beausejour, C.M., Rock, J.M., Augustus, S., Jamieson, A.C., Porteus, M.H., Gregory, P.D. and Holmes, M.C., 2005. Highly efficient endogenous human gene correction using designed zinc-finger nucleases. Nature 435, 646-51.

Valton, J., Dupuy, A., Daboussi, F., Thomas, S., Marechal, A., Macmaster, R., Melliand, K., Juillerat, A. and Duchateau, P., 2012. Overcoming transcription activator-like effector (TALE) DNA binding domain sensitivity to cytosine methylation. J Biol Chem 287, 38427-32.

Vanwolleghem, T., Libbrecht, L., Hansen, B.E., Desombere, I., Roskams, T., Meuleman, P. and Leroux-Roels, G., 2010. Factors determining successful engraftment of hepatocytes and susceptibility to hepatitis B and C virus infection in uPA-SCID mice. J Hepatol 53, 468-76.

Vivekanandan, P., Kannangai, R., Ray, S.C., Thomas, D.L. and Torbenson, M., 2008. Comprehensive genetic and epigenetic analysis of occult hepatitis B from liver tissue samples. Clin Infect Dis 46, 1227-36.

Wah, D.A., Hirsch, J.A., Dorner, L.F., Schildkraut, I. and Aggarwal, A.K., 1997. Structure of the multimodular endonuclease FokI bound to DNA. Nature 388, 97-100.

Wang, L., Wang, H., Bell, P., McCarter, R.J., He, J., Calcedo, R., Vandenberghe, L.H., Morizono, H., Batshaw, M.L. and Wilson, J.M., 2010. Systematic evaluation of AAV vectors for liver directed gene transfer in murine models. Mol Ther 18, 118-25.

Watanabe, T., Ochiai, H., Sakuma, T., Horch, H.W., Hamaguchi, N., Nakamura, T., Bando, T., Ohuchi, H., Yamamoto, T., Noji, S. and Mito, T., 2012. Non-transgenic genome modifications in a hemimetabolous insect using zinc-finger and TAL effector nucleases. Nat Commun 3, 1017.

Weber, E., Engler, C., Gruetzner, R., Werner, S. and Marillonnet, S., 2011. A modular cloning system for standardized assembly of multigene constructs. PLoS One 6, e16765.

Wiedenheft, B., Sternberg, S.H. and Doudna, J.A., 2012. RNA-guided genetic silencing systems in bacteria and archaea. Nature 482, 331-8.

Wiens, A., Lenzi, L., Venson, R., Correr, C.J., Rotta, I., Pedroso, M.L. and Pontarolo, R., 2013. Comparative efficacy of oral nucleoside or nucleotide analog monotherapy used in chronic hepatitis B: a mixed-treatment comparison meta-analysis. Pharmacotherapy 33, 144-51.

Wong, D.K., Cheung, A.M., O'Rourke, K., Naylor, C.D., Detsky, A.S. and Heathcote, J., 1993. Effect of alpha-interferon treatment in patients with hepatitis B e antigen-positive chronic hepatitis B. A meta-analysis. Ann Intern Med 119, 312-23.

Wong, D.K., Yuen, M.F., Yuan, H., Sum, S.S., Hui, C.K., Hall, J. and Lai, C.L., 2004. Quantitation of covalently closed circular hepatitis B virus DNA in chronic hepatitis B patients. Hepatology 40, 727-37.

Wood, A.J., Lo, T.W., Zeitler, B., Pickle, C.S., Ralston, E.J., Lee, A.H., Amora, R., Miller, J.C., Leung, E., Meng, X., Zhang, L., Rebar, E.J., Gregory, P.D., Urnov, F.D. and Meyer, B.J., 2011. Targeted genome editing across species using ZFNs and TALENs. Science 333, 307.

Wu, K., Mu, Y., Hu, J., Lu, L., Zhang, X., Yang, Y., Li, Y., Liu, F., Song, D., Zhu, Y. and Wu, J., 2007. Simultaneously inhibition of HIV and HBV replication through a dual small interfering RNA expression system. Antiviral Res 74, 142-9.

Wu, Y.H., Hao, B.J., Cao, H.C., Xu, W., Li, Y.J. and Li, L.J., 2012. Anti-hepatitis B virus effect and possible mechanism of action of 3,4-o-dicaffeoylquinic Acid in vitro and in vivo. Evid Based Complement Alternat Med 2012, 356806.

Xin, X.M., Li, G.Q., Jin, Y.Y., Zhuang, M. and Li, D., 2008. Combination of small interfering RNAs mediates greater suppression on hepatitis B virus cccDNA in HepG2.2.15 cells. World J Gastroenterol 14, 3849-54.

Yang, P.L., Althage, A., Chung, J. and Chisari, F.V., 2002. Hydrodynamic injection of viral DNA: a mouse model of acute hepatitis B virus infection. Proc Natl Acad Sci U S A 99, 13825-30.

Yuen, M.F., Wong, D.K., Sum, S.S., Yuan, H.J., Yuen, J.C., Chan, A.O., Wong, B.C. and Lai, C.L., 2005. Effect of lamivudine therapy on the serum covalently closed-circular (ccc) DNA of chronic hepatitis B infection. Am J Gastroenterol 100, 1099-103.

Zhang, F., Cong, L., Lodato, S., Kosuri, S., Church, G.M. and Arlotta, P., 2011. Efficient construction of sequence-specific TAL effectors for modulating mammalian transcription. Nat Biotechnol 29, 149-53.

Zhang, X., Zoulim, F., Habersetzer, F., Xiong, S. and Trepo, C., 1996. Analysis of hepatitis B virus genotypes and pre-core region variability during interferon treatment of HBe antigen negative chronic hepatitis B. J Med Virol 48, 8-16.

Zhang, X.S., Jin, R., Zhang, S.B. and Tao, M.L., 2008. Clinical features of adverse reactions associated with telbivudine. World J Gastroenterol 14, 3549-53.

Zhang, Y., Satterlee, A. and Huang, L., 2012. In vivo gene delivery by nonviral vectors: overcoming hurdles? Mol Ther 20, 1298-304.

Zhou, D.X. and Yen, T.S., 1991. The hepatitis B virus S promoter comprises A CCAAT motif and two initiation regions. J Biol Chem 266, 23416-21.

Zimmerman, K.A., Fischer, K.P., Joyce, M.A. and Tyrrell, D.L., 2008. Zinc finger proteins designed to specifically target duck hepatitis B virus covalently closed circular DNA inhibit viral transcription in tissue culture. J Virol 82, 8013-21.

Zou, J., Sweeney, C.L., Chou, B.K., Choi, U., Pan, J., Wang, H., Dowey, S.N., Cheng, L. and Malech, H.L., 2011. Oxidase-deficient neutrophils from X-linked chronic granulomatous disease iPS cells: functional correction by zinc finger nuclease-mediated safe harbor targeting. Blood 117, 5561-72.

Zoulim, F., 2004. Antiviral therapy of chronic hepatitis B: can we clear the virus and prevent drug resistance? Antivir Chem Chemother 15, 299-305.

Zoulim, F., 2005. New insight on hepatitis B virus persistence from the study of intrahepatic viral cccDNA. J Hepatol 42, 302-8.

Zoulim, F. and Locarnini, S., 2012. Management of treatment failure in chronic hepatitis B. J Hepatol 56 Suppl 1, S112-22.

Zu, Y., Tong, X., Wang, Z., Liu, D., Pan, R., Li, Z., Hu, Y., Luo, Z., Huang, P., Wu, Q., Zhu, Z., Zhang, B. and Lin, S., 2013. TALEN-mediated precise genome modification by homologous recombination in zebrafish. Nat Methods.